SAND81-7067
UNLIMITED RELEASE
CATEGORY UC-66c

EVALUATION OF CAVIJET® CAVITATING JETS FOR DEEP-HOLE ROCK CUTTING

Andrew F. Conn, Virgil E. Johnson, Jr.,
Han-Lieh Liu, Gary S. Frederick

Prepared by Sandia Laboratories, Albuquerque, New Mexico 87185 and Livermore, California 94550 for the United States Department of Energy under Contract DE-AC04-76DP00789.

May 1981

Work performed under Sandia National Laboratories Contract No. 07-7067 for the U.S. Department of Energy, Division of Geothermal Energy. Technical direction was provided by Sandia National Laboratories Division 4751, with Mr. D. A. Glowka as the Technical Project Officer.

Sandia National Laboratories

Issued by Sandia National Laboratories, operated for the United States Department of Energy by Sandia Corporation.

Printed in the United States of America
Available from:
National Technical Information Service
U. S. Department of Commerce
5285 Port Royal Road
Springfield, VA 22161
Price: Printed Copy $7.75; Microfiche $3.00

SAND81-7067
UNLIMITED RELEASE
PRINTED MAY 1981

Category UC-66c

SAND--81-7067

DE81 025015

EVALUATION OF CAVIJET® CAVITATING JETS FOR DEEP-HOLE ROCK CUTTING*

Andrew F. Conn
Virgil E. Johnson, Jr.,
Han-Lieh Liu
Gary S. Frederick

HYDRONAUTICS, Incorporated
Laurel, Maryland

ABSTRACT

Increasing deep-hole drilling rig costs are motivating efforts to increase rates of penetration (ROP), particularly as ever deeper holes are needed to locate new geothermal and fossil energy supplies. A feasibility study has shown that the CAVIJET cavitating fluid jet method should be capable of successfully augmenting the cutting action of mechanical bits under deep-hole conditions. Increased rock cutting rates by existing cavitating jet nozzles can be anticipated with conventional rig pressures for hole depths of at least 1,200 m (4,000 ft) and possibly deeper. Improved ROP's, based on preliminary laboratory roller bit tests, should be achieved by simply substituting CAVIJET nozzles absorbing equivalent hydraulic power for conventional roller bit nozzles.

*Work performed under Sandia National Laboratories Contract No. 07-7067 for the U.S. Department of Energy, Division of Geothermal Energy.

FOREWORD

The study described in this report was conducted by HYDRONAUTICS, Incorporated, Howard County, Laurel, Maryland. Portions of the experimental program were conducted under subcontracts, within the Drilling Research Laboratory (DRL) at Terra Tek, Inc., Salt Lake City, Utah; and in the laboratory of Professor Albert T. Ellis, University of California, La Jolla, California. This program was supported by the U.S. Department of Energy, Division of Geothermal Energy, under Sandia National Laboratories Contract No. 07-7067; and portions of the costs were shared by NL/Hycalog, Houston, Texas. Specific contributions from NL/Hycalog included the CAVIJET® cavitating fluid jet nozzles and the roller bits used in these tests, as well as a portion of the DRL rental.

The CAVIJET® cavitating fluid jet technology used in this program has been patented by HYDRONAUTICS, Incorporated* and is currently being developed for a variety of commercial applications.

Technical direction was provided by Sandia National Laboratories Division 4751, with Mr. D. A. Glowka as the Technical Project Officer.

---

* U.S. Patent Nos. 3,528,704; 3,713,699; and 3,807,632. Other U.S. and Foreign patents are pending or have been granted. CAVIJET is a registered trademark of HYDRONAUTICS, Incorporated.

ACKNOWLEDGMENTS

The successful completion of this program involved a number of people and organizations. The authors would like to express their sincere appreciation, and acknowledge the contributions of:

- Sandia Laboratories - - Dr. Samuel G. Varnado, Mr. Jon H. Barnette, and Mr. David A. Glowka, for the continuous support, encouragement, and advice during their monitoring of this program.
- NL/Hycalog - - for their cost sharing contributions, and Mr. Robert P. Radtke, without whose unstinting efforts this program would neither have begun, nor have carried through to its present status.
- Terra Tek/Drilling Research Laboratory - - for efforts beyond the call of duty during our tests, especially by Mr. Alan D. Black, Mr. John Sandstrom, Mr. Earl Miller, and Mr. Robert Attridge.
- University of California, San Diego - - Professor Albert T. Ellis and Mr. J. E. ("Skip") Starrett, for the creative adaptations of their flow measuring techniques to our program.
- NL/Baroid - - Mr. William Carnicom and Mr. Ed Ingram, for teaching us how to handle the mud.
- at HYDRONAUTICS - - advice, counsel, design, and data reduction involving many people, especially: Dr. James Duncan, Mr. Herbert Hickey, Mr. Fon-Chen Lee, Mr. Stephen L. Van Doren, and the late S. Lee Rudy.
- and: Mr. Clifton Carwile, Department of Energy, Division of Geothermal Energy, for the initial encouragement and support which allowed this program to happen.

CONTENTS

Chapter		Page
SUMMARY		13
I	INTRODUCTION	17
	A. Background	17
	B. The Cavitation Number	20
	C. Outline of the Program	20
	D. Scope of This Report	21
II	THE CAVIJET CAVITATING FLUID JET TECHNOLOGY	23
	A. The CAVIJET Cavitating Fluid Jet Concept	23
	B. The CAVIJET Cavitating Fluid Jet Test Facility	25
III	STATIONARY NOZZLE CUTTING TESTS AT DRL	33
	A. The Wellbore Simulator	33
	B. Test Configuration and Procedures	36
	C. Discussion of Results	49
IV	STATIONARY AND SLOT CUTTING TESTS AT HYDRONAUTICS	63
	A. Test Objectives and Procedures	63
	B. Stationary-Nozzle Rock Cutting Tests	67
	C. Slot Cutting Test Results	74
V	FLOW STUDIES OF SUBMERGED CAVITATING JETS	77
	A. Test Configuration and Procedures	77
	B. Cavitation Inception and Desinence Results	79
VI	DRILL BIT TESTS AT DRL	87
	A. Objectives of These Tests	87
	B. Test Configuration and Procedures	88
	C. Test Results	92

CONTENTS (Continued)

Chapter		Page
VII	GENERAL DISCUSSION OF RESULTS	101
	A. Effect of Depth on Cutting Rates	101
	B. Cavitation Inception and Peak Cavitation	103
	C. Prediction of CAVIJET Nozzle Performance	109
	D. Extrapolation of Granite Cutting Results	114
VIII	CONCLUSIONS AND RECOMMENDATIONS	119
	REFERENCES	121
	APPENDIX A -- Results from Stationary-Nozzle Tests at DRL	125
	APPENDIX B -- Results from Stationary-Nozzle and Slot Cutting Tests at Hydronautics	181
	APPENDIX C -- Results from Drill Bit Tests at DRL	193

ILLUSTRATIONS

Figure		
1	Typical CAVIJET Cavitating Fluid Jet Nozzle Configurations	24
2	Schematic of CAVIJET Cavitating Water Jet Test Facility	26
3	CAVIJET Cavitating Fluid Jet Facility with Elevated Ambient Pressure and Mud Testing Modifications	27
4	New Pressure Cell for Elevated Ambient Pressure Studies of CAVIJET Nozzles	29
5a	Overall View of Pressure Cell: for elevated ambient pressure tests of CAVIJET nozzles	30
5b	Close Up of Pressure Cell: Showing floating valve ("choke") used to control the ambient pressure in the cell	31
6	The Wellbore Simulator at the Drilling Research Laboratory	34
7	Configuration for Stationary-Nozzle Tests at D.R.L	37
8a	Drawing of the Four-Nozzle Tool: used for stationary-nozzle testing at D.R.L.	38
8b	The Four-Nozzle Tool: used for stationary-nozzle rock cutting at D.R.L. after a test	39

ILLUSTRATIONS (Continued)

Figure		Page
9	Specimen for Four-Nozzle Stationary Cutting Tests	41
10a	Four-Nozzle Stationary Cutting Test Specimen: sawed in half after the test	42
10b	Close-Up of Four-Nozzle Specimen: Indiana limestone specimen No. 5	43
11	Schematic of the Leach and Walker Nozzle Configuration	46
12	Definition of Parameters Measured in Stationary-Nozzle Tests at D.R.L.	48
13	Typical Results from Stationary-Nozzle Testing with Mud; Plain, 6.4 mm (0.25 in.) CAVIJET Nozzle; Standoff: 1.6 cm (0.62 in.)	50
14	Dependence of Cutting Rate on Nozzle Pressure in Stationary-Nozzle Tests with Mud	51
15	Scaling the Stationary-Nozzle Test Results: for plain CAVIJET nozzle	53
16	Comparison of Various Nozzles Tested at D.R.L.: Stationary-Nozzle Tests with Four-Nozzle Tool	54
17	Comparing Water versus Mud: Effect on Cutting Rate Effectiveness; mud density: 1.1 gm/cm^3 (9.3 ppg)	57
18	Comparing Water versus Mud: Effect on Volume Removal Effectiveness; mud density: 1.1 gm/cm^3 (9.3 ppg)	58
19a	Effect of Standoff Distance on Cutting Rate Effectiveness	59
19b	Effect of Standoff Distance on Volume Removal Effectiveness	60
20a	Typical Stationary-Nozzle Specimen: Indiana limestone	64
20b	Typical Slot Cutting Specimen: Indiana limestone	65
21	Stationary-Nozzle Rock Cutting Results: Tests in pressure cell at Hydronautics on Indiana limestone	68
22	Exponential Curve Fitting to Stationary-Nozzle Test Results	69
23	The Equivalence Principle for Comparing Results from Stationary and Slot Cutting Tests	71
24	Comparison of Stationary-Nozzle Cutting Results for Three Rock Types	73
25	Exponential Curve Fitting to Slot Cutting Test Results	75

ILLUSTRATIONS (Continued)

Figure		Page
26	Blow-Down Water Tunnel Facility at University of California, San Diego	78
27	Results from Flow Studies at University of California, San Diego	80
28	Standoff Distance and Cavitation Inception: From flow studies at the University of California, San Diego	82
29	Dependence of Optimum Standoff on Cavitation Number	84
30	Observation of Submerged CAVIJET Nozzle Flow: Ultra-high-speed photography by A.T. Ellis	86
31a	View of Bottom of Two-Cone Roller Bit: Showing two extended nozzles on same diameter of rotation	89
31b	Side View of Two-Cone Roller Bit: Showing extra extensions for two extended CAVIJET nozzles	90
32	Schematic of Two-Cone Roller Bit Used in Preliminary Tests at D.R.L.	91
33	Comparison of Penetration Rates in Colton Sandstone	95
34	Comparison of Penetration Rates in Indiana Limestone	96
35	Comparison of Specific Penetration Rates in Colton Sandstone	98
36	Comparison of Specific Penetration Rates in Indiana Limestone	99
37	Derivation of Dependence of Cavitation Number on Hole Depth	102
38	Effect of Depth on CAVIJET Stationary Cutting Rate	104
39	Dependence of Cavitation Number on Reynolds Number for Submerged Cavitating Jets	108
40	Prediction of Slot Cutting: Depth versus translation velocity	111
41	Prediction of Slot Cutting: Depth versus ambient pressure	112
42	Effect of Pressure on Slot Cutting of Granite with a CAVIJET Nozzle	116

TABLES

Table		Page
1	Summary of Nozzles Used in Stationary Cutting Tests at Drilling Research Laboratory	44
2	Results from Flow Studies at University of California, San Diego (Ref. 28)	81
3	Summary of Roller Bit Tests at DRL	93
4	Submerged Cavitating Jet Studies	107

SUMMARY

A feasibility study has been completed, which had the objective of evaluating whether the cavitation erosion caused by submerged cavitating jets could be effective in either cutting or weakening rocks so that increased rates of penetration might be achieved by rotary mechanical bits. The ultimate objective of this program, dependent on successful results from the feasibility phase discussed in this report, is the development of new deep-hole drilling bits which would incorporate CAVIJET nozzles (nozzles designed to enhance the cavitation erosion potential of the jet), using drilling mud as the working fluid, to augment the mechanical cutting action of the bit.

Specific questions related to the performance of submerged cavitating jets were answered in this study, which demonstrated that CAVIJET nozzles have the potential for augmenting the performance of either roller or diamond bits. The approach used to gain these answers was experimental, combining observations from rock cutting tests with single nozzles, preliminary laboratory drilling tests using roller bits to examine the effect on penetration rates of replacing the conventional bit nozzles with CAVIJET nozzles, and flow studies of submerged cavitating nozzles that provided initial insights into some of the basic fluid dynamic mechanisms involved in this process.

These experiments yielded a number of empirical relationships which showed how the cutting action of various nozzles is affected by pressure drop across the nozzle, Δp, ambient pressure, p_a, and the velocity of translation of the jet across the surface of the rock, v. Tests on limestone, sandstone, and granite indicated the influence of rock properties on this erosive process.

Some of the specific aspects of this study which served to answer these feasibility questions are:

- Effect of nozzle design: Single nozzle tests confirmed that submerged jets are more erosive when they cavitate and that jets from CAVIJET nozzles designed to increase the degree of cavitation are more erosive than jets issuing from conventional nozzles.
- Effect of drilling mud: Single nozzle tests revealed that no adverse influence on CAVIJET nozzle rock cutting was seen when muds having densities up to 1.4 gm/cm^3 (12 lb/gal) were substituted for water; in fact the use of mud increased the erosivity of the jet cutting.
- Effect of nozzle pressure drop (Δp): Single nozzle tests revealed that the cutting rates of cavitating jets vary approximately as the cube of the nozzle pressure drop over the entire range of cavitation numbers tested.
- Effect of ambient pressure (p_a): The effect of ambient pressure is characterized for all values of Δp by the cavitation number, $\sigma = p_a/\Delta p$. Single nozzle tests revealed that the cutting rate for all nozzles tested increased substantially from noncavitating conditions ($\sigma \approx 1$ to 2) to a maximum occurring at approximately $\sigma = 0.4$, and then decreasing with further reduction in the cavitation number. Thus for pump pressures of 13.8 MPa (2000 psi), cavitation will substantially increase the cutting rate of the nozzles tested at hole depths less than about 1220 m (4000 ft). This maximum depth is directly proportional to the pressure drop (2440 m (8000 ft) for Δp = 27.6 MPa (4000 psi)) and can be further increased for a given pressure drop by improving the nozzle design so as to further stimulate cavitation.

- Effect of nozzle design on roller bit cutting rates: Tests were conducted on two roller bits under simulated downhole conditions with conventional nozzles and with CAVIJET nozzles. Since these tests were conducted using nozzles of the same diameter rather than nozzles of equivalent discharge a direct comparison is not possible. However, the results indicate that if CAVIJET nozzles are sized to give equivalent discharges when substituted for conventional nozzles, a modest improvement in drilling rate should result. If future studies evolve nozzle designs which further enhance cavitation then these nozzles should further increase the drilling rate when substituted for conventional nozzles.

The experimental observations made during this phase, and the empirical relationships derived from these results, were sufficient to successfully answer the feasibility questions. However, to achieve maximum gains during any future optimization efforts, basic understanding of the mechanisms contributing to these experimental relations should be sought. Thus, of primary importance to this optimization is a continuation of the examination of parameters which affect the erosive process, both with respect to nozzle designs and the jet-to-rock interaction. Specific objectives include seeking ways to increase the point of cavitation inception, and hence the effective depth for cavitation erosion, and how to best utilize the available hydraulic power to weaken the rock for improving the cutting action of both roller and diamond bit types.

I. INTRODUCTION

A. Background

Historically, improved control of the fluid dynamics of the drilling mud has consistently contributed to increased performance of oil well drill bits. The perfect cleaning theory proposed by Maurer (1) for roller bits emphasized the importance of hydraulic chip removal for maximizing the drilling rate. The performance of diamond drill bits also depends on suitable fluid flow to clean the bit face efficiently.

Nozzles were first tested in roller bits in 1949. By 1955 the use of nozzles to direct the flow of the drilling mud was a standard feature in roller bit design. As a result, there was a marked increase in roller bit penetration rates. In recent years, extended nozzles in roller bits have created more efficient use of available hydraulic horsepower. Drilling rates in weak formations have been increased by up to 25 percent over the rates for similar bits without nozzles.

Diamond drill bits with jet nozzles have been tested experimentally since the mid 1950s. The advent of the General Electric Stratapax drill blank has led to the development of new bit designs which incorporate nozzles to clean cuttings from the bit face. More efficient use of hydraulic energy at the bit face has consistently resulted in major improvements in drill bit performance (2).

The use of fluid jets to augment the cutting action of various mechanical devices for drilling, tunneling, and mining applications is now being actively studied by investigators throughout the world (3,4,5,6). The reason for this wide interest in the exploitation of jets is the inherent power delivery advantage over a purely mechanical device. As described by Maurer (2) and Bobo (7), because of material strength limitations, a typical

rotary drill (20 cm dia.) can deliver only about 19 to 75 kw (25 to 100 hp) to the rock. The power deliverable via a fluid jet is governed only by practical questions of system costs and the pressure limits on key components for any particular application. Thus, water jets up to 414 MPa (60,000 psi) are now being operated in many commercial installations (3,4,5,6).

Drilling tests with fluid (water, drilling mud) jets, either alone or in conjunction with roller or diamond cutting surfaces (8,9,10) have proven that, at sufficiently high pump pressures, dramatic increases in drilling rates can be achieved. For instance, Maurer (8) and Pols (9), each using high-pressure conventional fluid jets to assist the action of mechanical bits, were able to drill two to three times faster than the rates achieved by ordinary bits in the same formations. Pressures in these tests have, however, typically been in the range of 69 MPa to 103 MPa (10,000 to 15,000 psi). Thus, the pressures which have been used in these conventional jet drilling studies are well above the currently available mud pump pressures on rigs now in operation. These are typically 14 to 21 MPa (2,000 to 3,000 psi), with a few off-shore rigs using up to 31 MPa (4,500 psi). Reliable and safe pumps and supporting components could readily be introduced to provide pressures up to 52 MPa (7,500 psi) at many rigs, if sufficient increases in the rate of penetration could be demonstrated.

In a preliminary feasibility study (11) the possibility of using CAVIJET cavitating fluid jet nozzles for rock cutting under elevated ambient conditions was examined. These tests, with water as the working fluid, demonstrated that the erosive action of a 6.4 mm (0.25 in.) CAVIJET nozzle continued to be observed up to ambient pressures of 20.7 MPa (3,000 psi). In comparative

tests with a "Leach & Walker" nozzle (12), the CAVIJET nozzle showed a higher volume removal efficiency under elevated ambient pressures. Specimens of Berea sandstone and Indiana limestone were used, with pressure drops across the nozzles ranging from 6.9 to 17.2 MPa (1,000 to 2,500 psi). The success of this preliminary study provided the basis for this first phase of a new program, which is described in this report.

The CAVIJET cavitating fluid jet technology (see Chapter II), is being successfully developed for a variety of commercial cleaning and cutting applications. These include removal of marine fouling (13,14), cutting coal (15,16), cleaning explosives and propellants from munitions (17,18), and rock cutting (19,20). However, in all of these applications the working fluid was water and the ambient pressure surrounding the jet was essentially atmospheric.

Thus, this study of the feasibility of using the CAVIJET cavitating jet technology to augment the drilling action of deep-hole geothermal drill bits, so as to increase the rates of penetration, was initiated to answer the following questions:

a. Will there be sufficient erosion by cavitation from CAVIJET nozzles, when operated under the elevated ambient pressures down-hole, to increase mechanical drill bit penetration rates?

b. What is the effect of substituting drilling mud for the ordinary water which has been the working fluid for all previous CAVIJET cavitating jet operations?

c. How can the CAVIJET nozzles be introduced into drill bits, so as to effectively augment the mechanical cutting action, and also satisfy the requirements for bit cooling and chip removal?

This report summarizes the first phase of a program, which has been planned to include a systematic series of laboratory and field trials, to provide answers to these questions.

B. The Cavitation Number

The dimensionless number which has been developed to describe cavitation phenomena is known as the cavitation number, σ. This parameter usually has the form:

$$\sigma = \frac{p_a - p_v}{\frac{1}{2}\rho v_o^2} \qquad [1]$$

where:

p_a is the local value of ambient pressure,

v_o is a characteristic velocity of the fluid,

p_v is the vapor pressure of the fluid, and

ρ is the density of the fluid.

For the purposes of this study of submerged cavitating jets, where p_a is much larger than p_v; and Δp, the pressure drop across the nozzle closely approximates $\frac{1}{2}\rho v_o^2$, (where v_o is the jet exit velocity), we will define and hereafter use the following definition for the cavitation number:

$$\sigma = \frac{p_a}{\Delta p} \qquad [2]$$

C. Outline of the Program

The ultimate objective of this program is the development of improved deep-hole drilling bits, suitable for geothermal energy acquisition, which incorporate the CAVIJET cavitating fluid jet technology. The program has been divided into three phases, having the following objectives:

PHASE I - Feasibility

Objective: To determine the effect of drilling mud, at elevated ambient pressures, on the rock cutting performance of existing CAVIJET nozzle designs. This initial effort is focused on the use of existing or readily available mud pump pressures, namely below 52 MPa (7,500 psi).

PHASE II - Optimization

Objective: To develop optimum design and operating parameters for deep-hole mechanical drill bits which are augmented by improved CAVIJET nozzle configurations. If warranted to provide increased rates of penetration in very hard formations, then pressures above 52 MPa (7,500 psi) may be considered.

PHASE III - Field Trials

Objective: To validate and improve the design and operating parameters by testing bits under actual operating field conditions.

D. Scope of This Report

All of the work performed under Phase I of this program has been summarized in this report. In the main text only selected typical examples of the experimental results have been presented, to allow a less cluttered development of this feasibility study. However, all of the data which were obtained are tabulated and/or presented in figures in the several appendices.

Individual chapters have been devoted to first describing the CAVIJET cavitating jet technology (Chapter II), and then to each of the four types of testing which were conducted: Chapter III - Stationary nozzle tests in the Drilling Research

Laboratory, which permited a wide range of both ambient and nozzle pressures, but wherein slot cutting tests could not practically be made; Chapter IV - Tests at HYDRONAUTICS, which were conducted within a new pressure cell that was developed for this program, to allow both stationary and slot cutting studies of an individual CAVIJET nozzle - to provide results to supplement the DRL tests, and allow development of scaling relationships for all relevant parameters; Chapter V - Flow visualization studies of submerged nozzles at the University of California at San Diego - the first high speed photography and cavitation inception studies of a CAVIJET nozzle; and Chapter VI - Preliminary roller bit tests at DRL, using a two cone bit, to compare the penetration rates with either CAVIJET or conventional nozzles.

Chapter VII presents a general discussion of the results, describing how the various types of test results can be related, and how these results demonstrate the feasibility of deep-hole rock cutting by CAVIJET cavitating jets. Conclusions and recommendations are listed in Chapter VIII.

II. THE CAVIJET CAVITATING FLUID JET TECHNOLOGY

A. The CAVIJET Cavitating Fluid Jet Concept

The CAVIJET is a turbulent jet in which vapor and gas cavities are deliberately stimulated to enhance the erosive action of a relatively low velocity liquid jet. Thus, although the destructive action of cavitation is well known, often to the despair of designers and users of pumps, propellers, and other hydraulic components, CAVIJET is one of the few useful applications of this phenomenon. In contrast to noncavitating jets, the cutting or drilling is achieved by the energy from collapsing cavitation bubbles. The pressure from these imploding bubbles is extremely high, and is focused at many small areas on the eroding surface.

In materials such as rocks, which are prone to cracking, the extremely localized pressure amplifications from cavitation cause rapid fracturing which greatly enhances the erosive mechanisms. It is this process of amplifying the local pressure, and focusing the energy delivered to the rock surface, which provides the CAVIJET with a basic advantage over jets discharging from nozzles not designed to maximize cavitation erosion when operating at the same pump pressure and flow rate.

Although CAVIJET nozzle designs are proprietary, some typical configurations are shown schematically in Figure 1. The objective of these designs is to maximize the pressure reduction at the center of vortices created within the jet or on its periphery and hence induce the growth of vapor or gas cavities in the fluid. While specific applications (drilling, cutting, or cleaning) each require nozzles tailored to the particular material and operating mode, we generally find that the centerbody configuration is best for in-air situations. For operation on submerged surfaces, as in deep-hole drilling or underwater removal of fouling from ship hulls, either the turning vane or "plain" (without vanes or centerbody) CAVIJET nozzle designs usually provide better results, namely, greater volume removal and area cleaning rates.

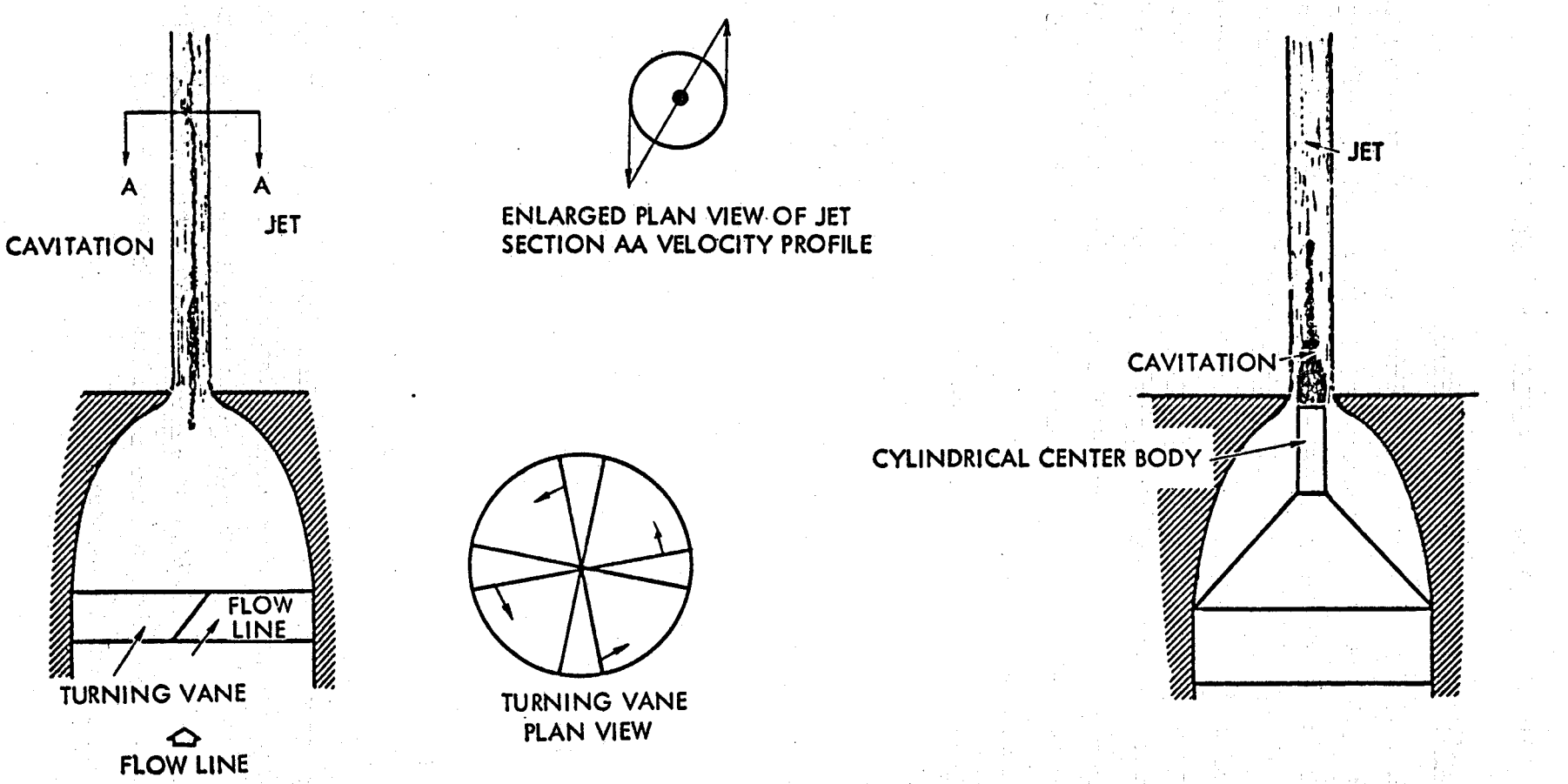

NOZZLE SYSTEM TO INDUCE ROTATIONAL VORTEX CAVITATION

NOZZLE SYSTEM TO INDUCE CAVITATION BY FLOW SEPARATION

FIGURE 1 - TYPICAL CAVIJET® CAVITATING FLUID JET NOZZLE CONFIGURATIONS

Further details about both the CAVIJET concept and the laboratory test and evaluation facility used for the atmospheric pressure flow calibrations discussed in the next section may be found in References 13 through 22.

B. The CAVIJET Cavitating Fluid Jet Test Facility

An experimental facility was designed and built at HYDRONAUTICS, Incorporated for studying and developing practical devices which utilize the cavitating fluid jet principle. This facility, shown schematically in Figure 2, was used during this program to calibrate the flow of the various nozzles which were tested both at HYDRONAUTICS and at the Terra Tek Drilling Research Laboratory. The four-nozzle tool, described in Chapter III, was mounted within the test chamber as seen in Figure 2 for these flow calibrations. By plugging the other three openings in the four-nozzle tool, one nozzle at a time could be flow calibrated. The chamber contains a fluid level indicator so that, over timed intervals, the flow through a nozzle at a given nozzle pressure drop can be accurately determined.

For the elevated ambient pressure rock cutting tests described in Chapter IV, the facility seen in Figure 2 was completely modified. These modifications were necessary in order to be able to utilize drilling mud as the working fluid instead of water. A schematic drawing indicating these facility modifications is shown in Figure 3. It is seen that all filters and heat exchangers have been removed from the circuit. The mud makeup tank and reservoir, with capacity 950 l (250 gal), was a rectangular fiberglass tank. The mud in the tank was stirred with a 0.75 kw (1 hp) two-bladed mixer, Model No. G-11, purchased from the Philadelphia Gear Corporation, which was also used to provide constant agitation

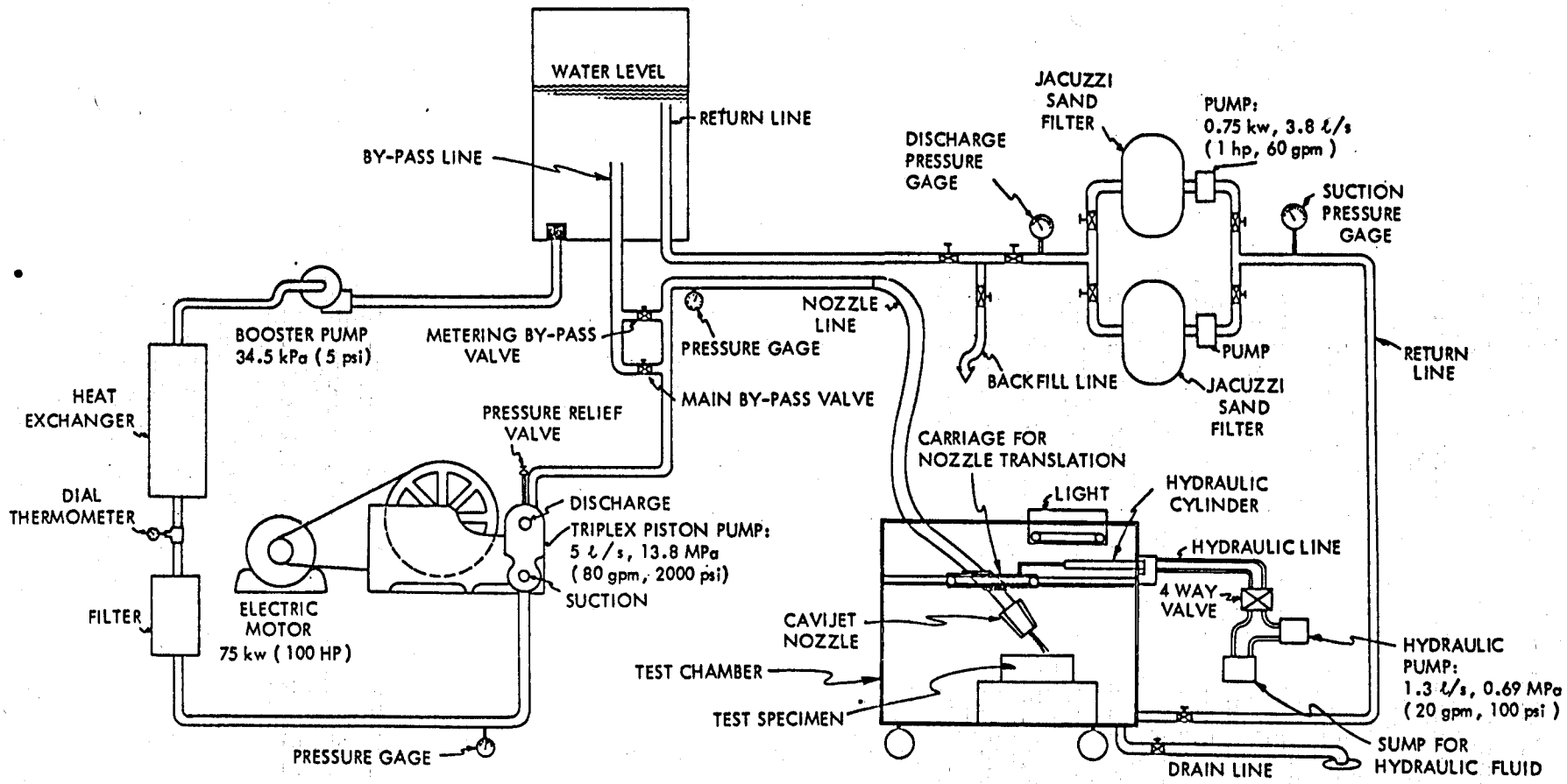

FIGURE 2 - SCHEMATIC OF CAVIJET® CAVITATING WATER JET TEST FACILITY

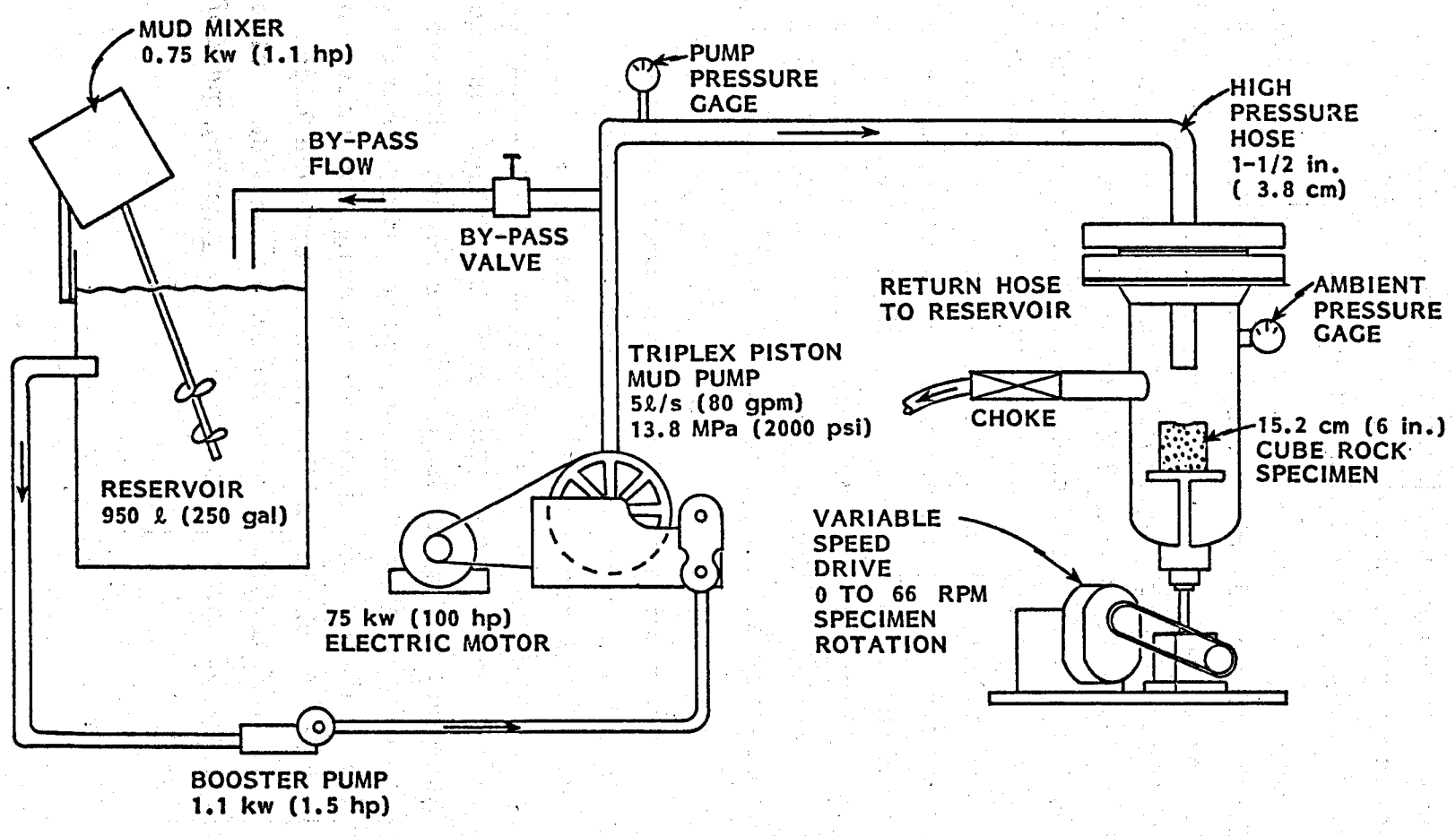

FIGURE 3 - CAVIJET® CAVITATING FLUID JET FACILITY WITH ELEVATED AMBIENT PRESSURE AND MUD TESTING MODIFICATIONS

of the mud throughout the testing. The existing Gardner-Denver triplex piston pump was used for the rock cutting tests with mud. A new booster pump and bypass valve were added to the system. The bypass valve had a replaceable stellite valve disk which experienced considerable wear during our tests.

The high pressure test cell was specially fabricated for these studies of the elevated ambient pressure performance of the CAVIJET cavitating fluid jet technology. A drawing of this new cell is shown in Figure 4 and photographs are seen in Figure 5. The cube-shaped rock specimens, 15.2 cm (6 in.) on a side, were clamped into a square holder, and then mounted on a turntable. The specimens could be rotated at any desired rate from 0 to 66 rpm by means of a gear box driven by an infinitely variable motor. The flow into the chamber entered through a removable lid which was bolted to the main chamber and sealed with an O-ring. A chain hoist was utilized to lift the lid free and by including a 3.7 m (12 ft) length of flexible hose in the input line it was therefore unnecessary to unfasten any high pressure fittings when removing the lid.

The ambient pressure within the cell was controlled by a "choke", a valve which used a "floating" double-ended piston with an area-ratio of 6.25:1 to regulate the pressure drop. The smaller end of the piston was exposed to the mud flow, and nitrogen gas pressure on the larger end was then adjusted until the desired valve opening, and hence pressure drop, was achieved. Due to the floating action of the double-ended piston, rock particles could escape without inflicting damage or jamming the valve open. All components within the choke which might experience high velocity mud flow were fabricated from sintered carbide. This choke performed very well throughout the entire testing period.

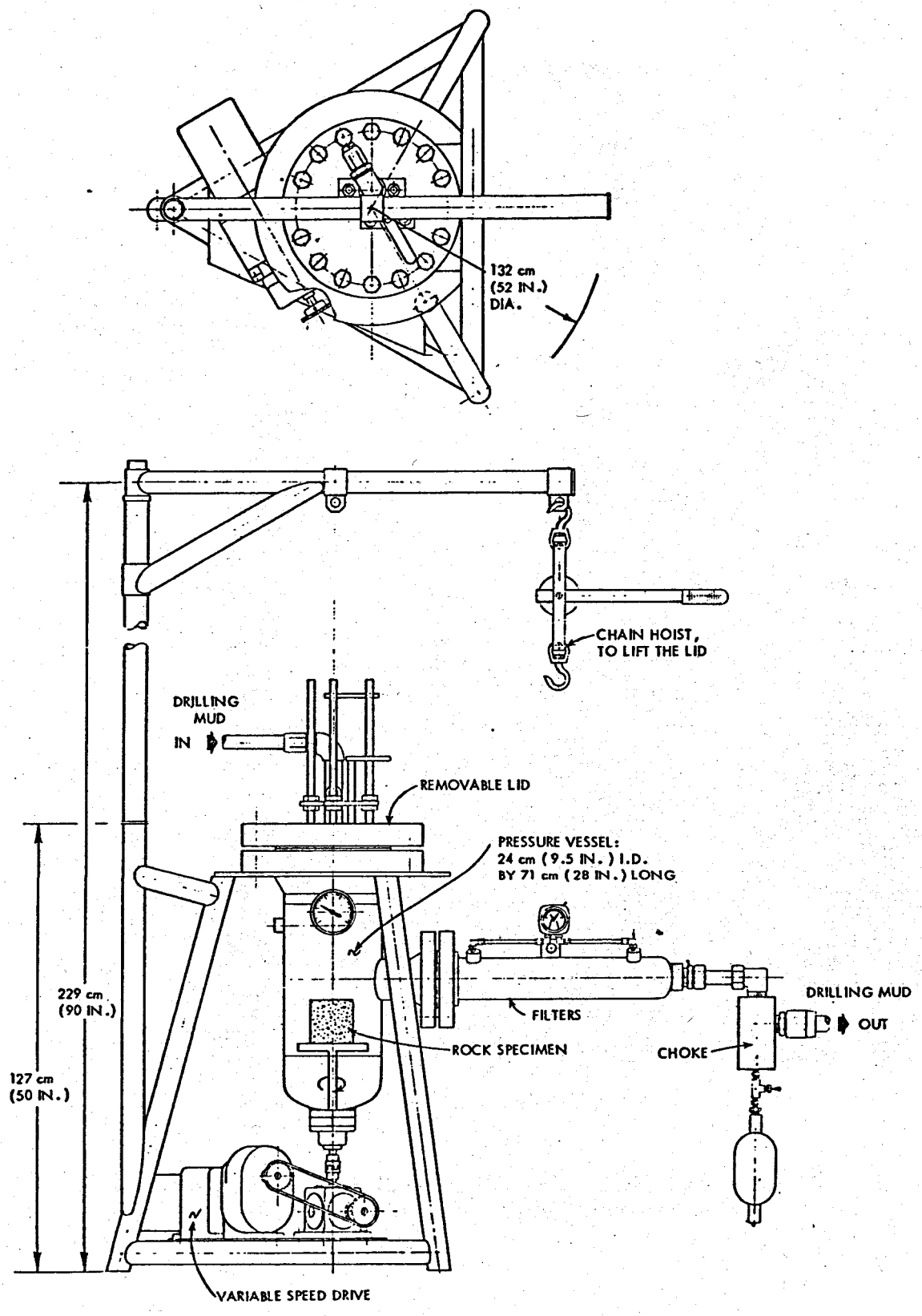

FIGURE 4 - NEW PRESSURE CELL FOR ELEVATED AMBIENT PRESSURE STUDIES OF CAVIJET® NOZZLES

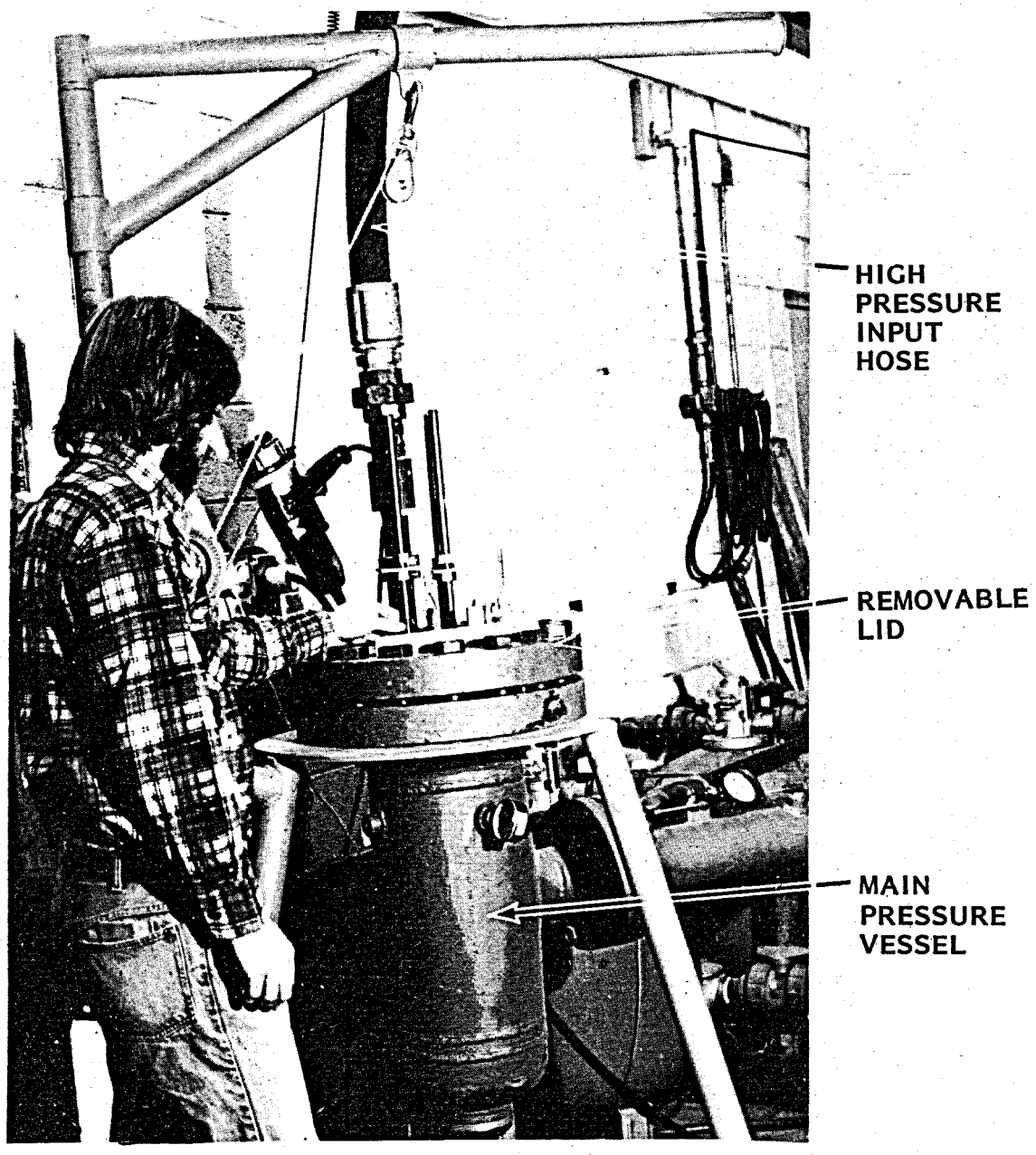

FIGURE 5a - OVERALL VIEW OF PRESSURE CELL: for elevated ambient pressure tests of CAVIJET® nozzles

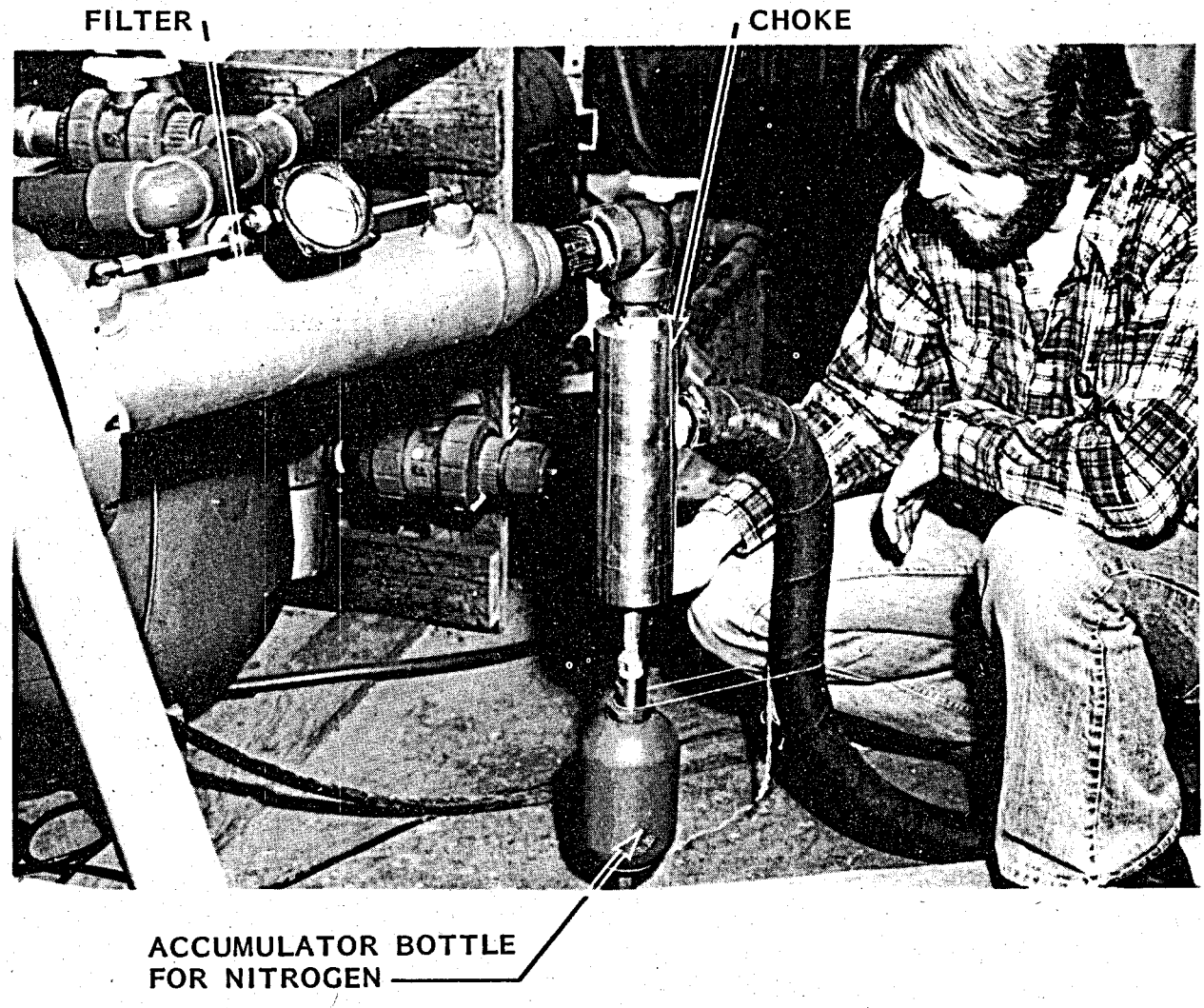

FIGURE 5b - CLOSE UP OF PRESSURE CELL: Showing floating valve ("choke") used to control the ambient pressure in the cell

The rated pressure capacity of the cell is 20.7 MPa (3,000 psi). It was fabricated from Schedule 80 steel pressure fittings. The standoff distance for the nozzle could be varied by sliding the input pipe vertically and clamping it into place at the desired setting. The test duration was controlled by a "shutter-plate", operated by a handle which extended thru the lid. A segment of sintered carbide was soldered to the plate to resist erosion. The plate was kept in place between the jet and the rock surface until all pressures were set. The handle was then actuated to move the plate out of the way for the desired duration of the test.

The outflow from the pressure cell was recirculated directly back to the mud reservoir. Any rock chips entrained in the mud flow apparently were able to settle to the bottom of the tank since no chip difficulties were encountered in recirculating the mud back through the main triplex pump. However, the 1.1 kw (1.5 hp) Teel centrifugal booster pump, which provided the input head to the main pump was found, due to overheating, to be too small for its task. Forced air cooling from fans provided a temporary solution that was adequate during the brief running times required for this part of the study. If longer runs are needed in the future, then this pump should be replaced.

III. STATIONARY NOZZLE CUTTING TESTS AT DRL

A. The Wellbore Simulator

The elevated ambient pressure testing described in this chapter was conducted within the wellbore simulator facility at the Drilling Research Laboratory (DRL) in Salt Lake City, Utah. Within this facility most of the stresses, pressures, and temperatures experienced by *in situ* rock formations can be simulated. These include confining and overburden pressures as well as the ambient or "downhole" pressure. The test chamber for the wellbore simulator at DRL is a converted, 58 cm (23 in.) diameter, 6.1 m (20 ft) long gun barrel with a removable cap and suitable flow controls to provide the desired values of pressure across the nozzles and inside the chamber. The ambient pressure within the chamber is controlled with a "choke" that is remotely actuated to throttle the outflow from the chamber. The pressure into the chamber is supplied by a triplex mud pump capable of providing flows up to 22.7 l/s (360 gpm) at pressures up to 37.9 MPa (5,500 psi). This pump is driven by two variable-speed electric motors, each rated for 670 kw (900 hp), which provide control of the flow into the test chamber.

The test specimens were 91.4 cm (36 in.) long with an outside diameter of 39.4 cm (15.5 in.). The confining pressure, imposed on the cylindrical surface of these rock specimens, was applied by pressurizing an inert fluid that surrounded the specimen. The overburden pressure on the rock is simulated by means of a ram which applies a load at the bottom surface of the specimen. The overburden and confining pressures are independently controlled to balance the principal stresses within the rock, thus minimizing the chance for fracturing of the specimen during the test. The photographs in Figure 6 show some of the features of this facility. One important parameter not simulated during either these stationary cutting tests or the full-scale bit tests described in Chapter VI of this report was the pore pressure within the rock. Due to practical problems

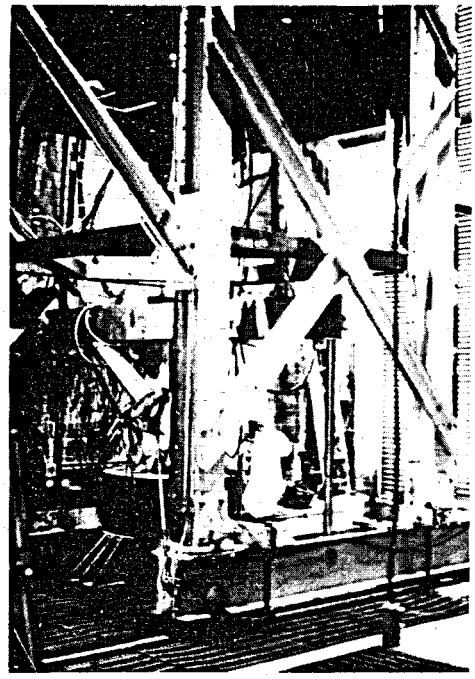

a. OVERALL VIEW OF THE DRILLING TOWER

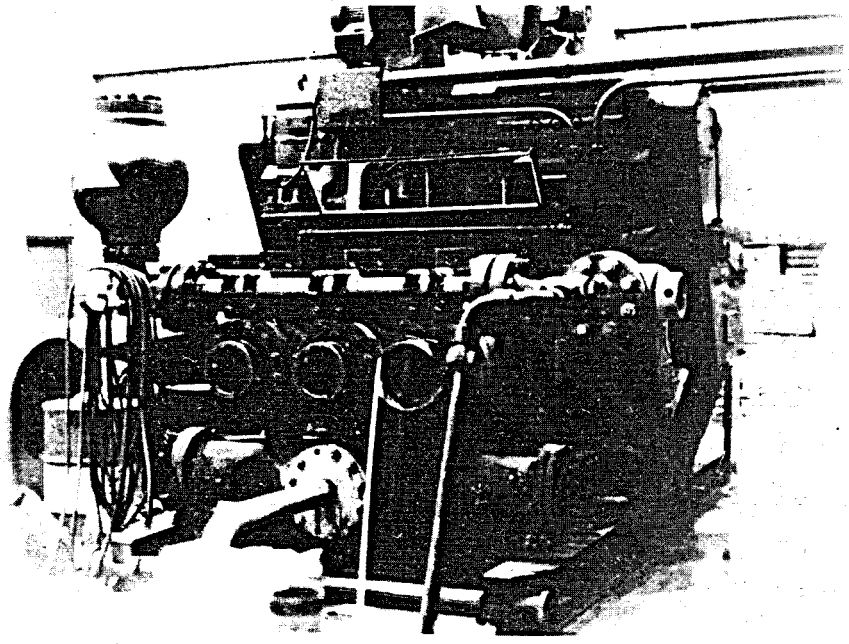

b. TRIPLEX MUD PUMP: 1340 kw (1800 hp), 22.7 ℓ/s (360 gpm) at 37.9 MPa (5,500 psi)

FIGURE 6 - THE WELLBORE SIMULATOR AT THE DRILLING RESEARCH LABORATORY

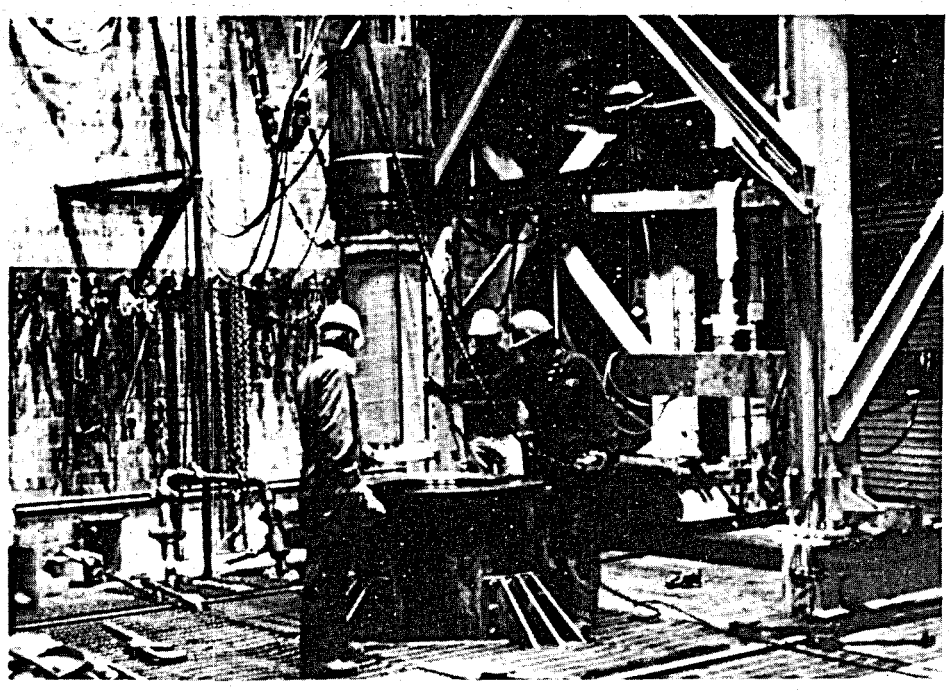

c. TEST SPECIMEN BEING INSERTED INTO THE PRESSURE CHAMBER

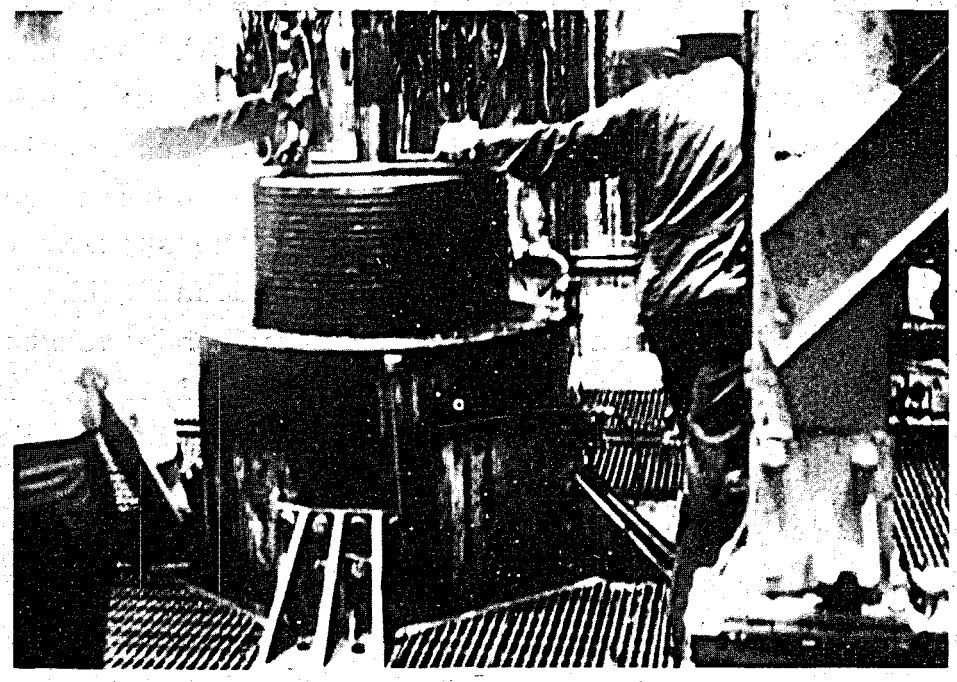

d. PRESSURE CAP BEING TIGHTENED ONTO THE CHAMBER

FIGURE 6 - CONCLUDED

related to saturating the rock specimens this pressure was not simulated in our tests and hence was considerably lower than would be encountered in the actual downhole situation. Thus the chip hold-down conditions were felt to be more severe in these laboratory tests in comparison to those encountered in the field.

All of the test parameters were remotely controlled, and recorded by means of a strip chart, an X-Y plotter, and an on-line computer. For these stationary rock cutting tests, the parameters were: mud flow rate, swivel pressure, ambient pressure, mud temperature, confining pressure, overburden pressure, and the time duration of each run. The pressure drop across the nozzles, Δp, was derived using:

$$\Delta p = p_{swivel} - p_{ambient} \qquad [3]$$

B. Test Configuration and Procedures

A unique test configuration was created to allow maximum data acquisition from each rock specimen, since only one of these tests could be run during an eight-hour shift. The set up, as shown schematically in Figure 7, allowed simultaneous testing of four different nozzles, with the ability to set each nozzle at an independent standoff distance (distance from the nozzle face to the rock). This was accomplished by means of the special tool seen in Figures 8a and 8b. This tool, designed and fabricated by NL/Hycalog in consultation with HYDRONAUTICS and the staff at DRL, was threaded onto a standard segment of drill pipe. The drill rig at DRL was modified for our tests by affixing an indexing mechanism to the drill pipe. This pneumatically-actuated device, which was controlled remotely, allowed the drill pipe to be indexed to any one of 24 equally spaced circumferential locations. The purpose for this indexing will become evident as we describe

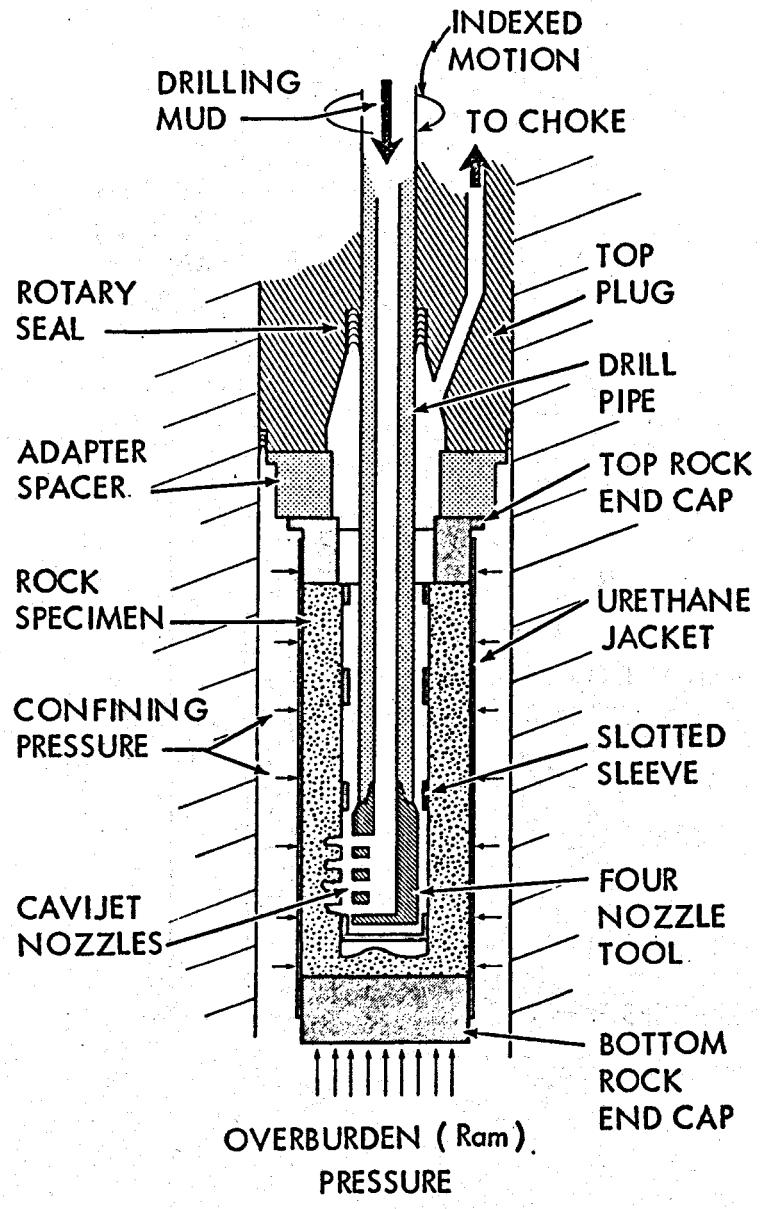

FIGURE 7 - CONFIGURATION FOR STATIONARY-NOZZLE TESTS AT D.R.L.

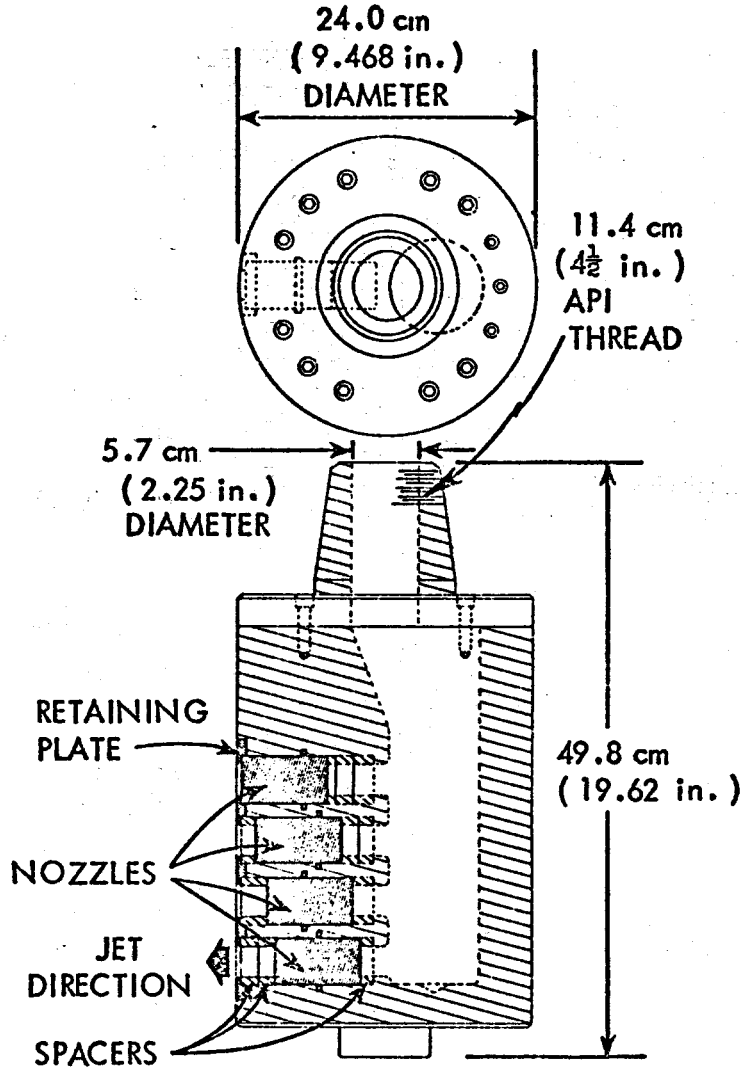

FIGURE 8a - DRAWING OF THE FOUR-NOZZLE TOOL: used for stationary-nozzle testing at D.R.L.

FIGURE 8b - THE FOUR-NOZZLE TOOL: used for stationary-nozzle rock cutting at D.R.L., after a test

the test specimen.

The specimens for all of our DRL tests had the standard outside dimensions given in the previous section. However for these stationary nozzle tests, the rock cylinders were prebored with a 25.1 cm (9.88 in.) diameter diamond drill bit. This prebored hole in the center of the specimen was 76.2 cm (30 in.) deep (see Figure 9a). Within this prebored hole a special slotted steel sleeve was inserted to fit snugly against the cylindrical inside surface of the rock. The sleeve (see Figure 9b) had a total of 36 slots arranged in three tiers each having 12 slots which were 2.5 cm (1 in.) wide. Thus at each tier there were a series of 3.8 cm (1.5 in.) wide strips of steel, alternating with the twelve slots. The test was begun with the nozzles impinging upon one of the strips of steel. When all of the pressures were properly adjusted, the run was initiated by indexing once, thus allowing the jets to begin to impinge directly upon the rock surface. At the completion of the required time for that run, another index was made to shift the orientation of the tool so that the jets were now impinging upon the next steel strip. With the jets again prevented from eroding the rock, the settings for the next run could be made. In this manner a potential of 144 holes (4 nozzles × 3 tiers × 12 slots per tier) could be perforated into each specimen. Typical results may be seen in Figures 10a and 10b.

All of the nozzles used in these tests had nominal orifice diameters of 6.4 mm (0.25 in.). A listing of the various types of nozzles used in each test is given in Table 1. The "plain" CAVIJET nozzle refers to the basic CAVIJET nozzle body configuration without added flow-conditioning inserts. The vane set tested here was a preliminary concept based on utilizing vortices shed from the tips of wing-shaped foils. Four pairs of these vanes were affixed within the flow. The "conventional"

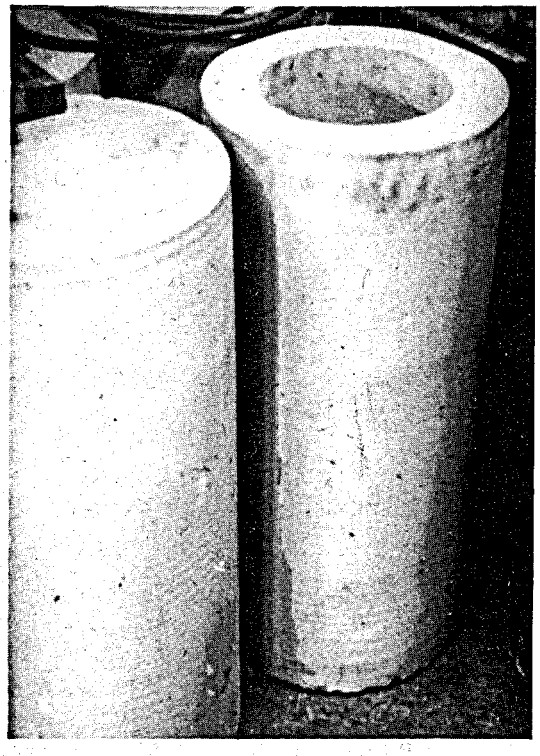

a. PRECORED SPECIMEN OF INDIANA LIMESTONE

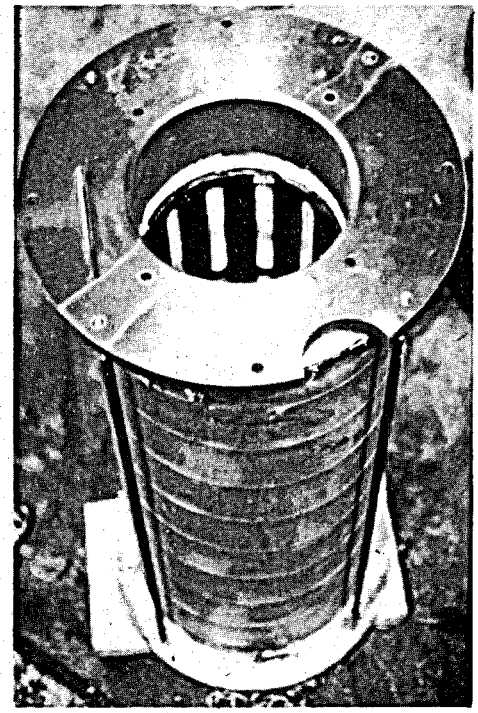

b. SPECIMEN READY FOR TESTING, WITH SLOTTED SLEEVE IN PLACE, AND WRAPPED IN PLASTIC JACKET

FIGURE 9 - SPECIMEN FOR FOUR-NOZZLE STATIONARY CUTTING TESTS

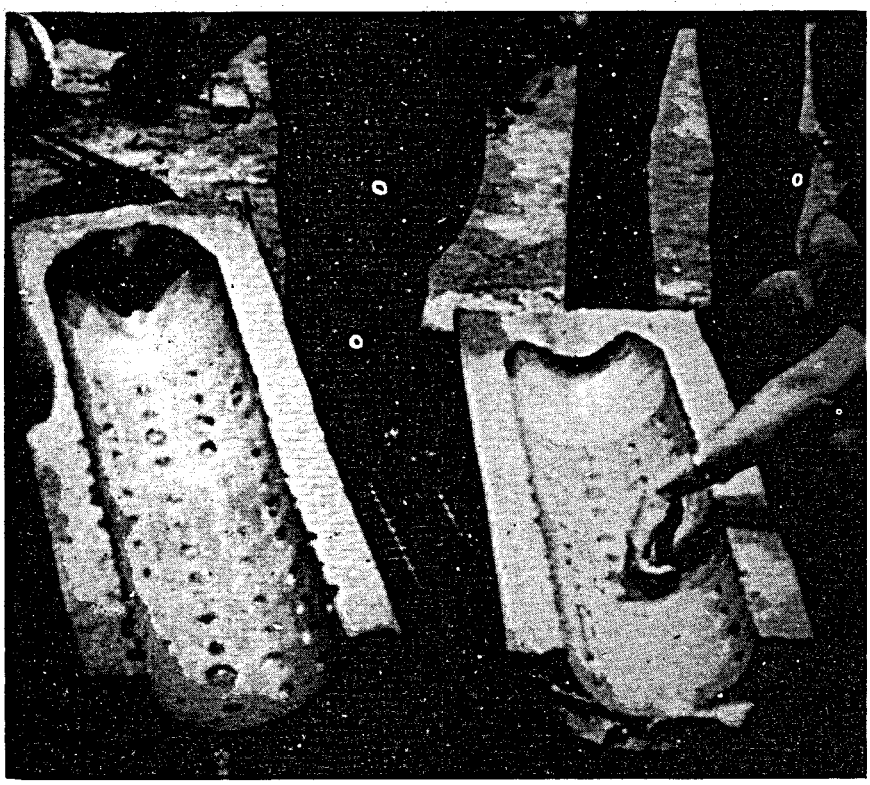

FIGURE 10a - FOUR-NOZZLE STATIONARY CUTTING TEST SPECIMEN: sawed in half after the test

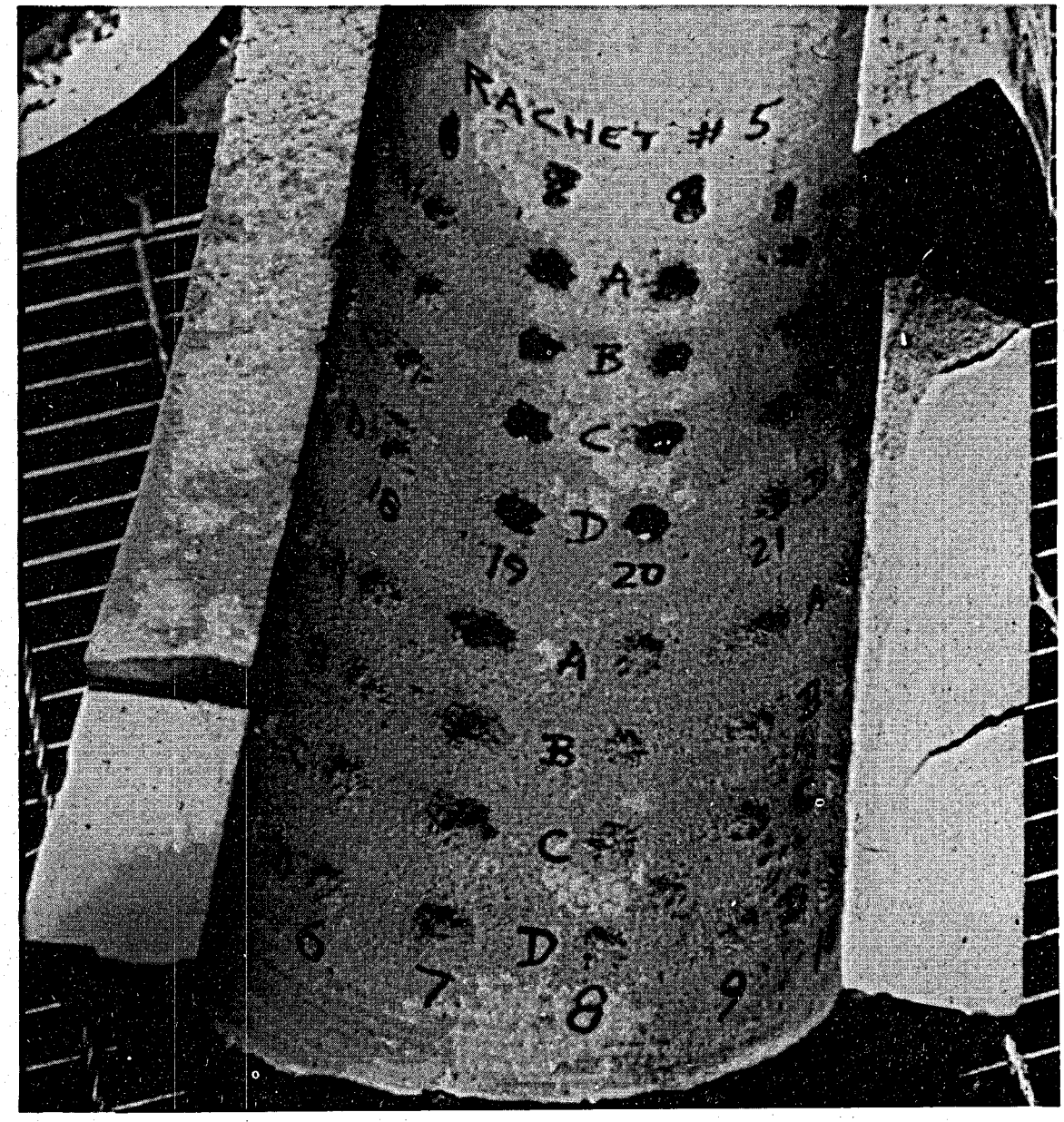

FIGURE 10b - CLOSE-UP OF FOUR-NOZZLE SPECIMEN:
Indiana limestone specimen NO.5

TABLE 1

Summary of Nozzles Used in Stationary Cutting Tests at Drilling Research Laboratory

Standoff distance: 1.6 cm (0.62 in.), except as noted

Rock: Indiana limestone

Nozzle orifice: 6.4 mm (0.25 in.) (nominal)

Specimen No.	Position in Four-Nozzle Tool			
	A	B	C	D
1	Plain CAVIJET	CAVIJET with 3.2 mm (0.125 in.) "conventional" cylindrical centerbody	CAVIJET with "tee-shaped" centerbody; shaft dia.: 3.2 mm (0.125 in.)	CAVIJET with vane set
2	Plain CAVIJET	CAVIJET with 3.2 mm (0.125 in.) cylindrical centerbody	CAVIJET with 3.2 mm (0.125 in.) cylin. centerbody, Standoff 2.9 cm (1.12 in.)	CAVIJET with vane set
3	Plain CAVIJET	Leach & Walker; stainless steel*	Plain CAVIJET, Standoff: 2.1 cm (0.81 in.)	CAVIJET with 3.2 mm (0.125 in.) cylin. centerbody
4	Plain CAVIJET	Plain CAVIJET, Standoff: 2.1 cm (0.81 in.)	CAVIJET with vane set	CAVIJET with 3.2 mm (0.125 in.) cylin. centerbody
5	Plain CAVIJET	CAVIJET with 3.2 cm (0.125 in.) cylin. centerbody	Plain CAVIJET	CAVIJET with 3.2 mm (0.125 in.) cylin. centerbody
6	Plain CAVIJET	Leach & Walker, carbide	Smith Tool Co., drill bit nozzle	CAVIJET with 3.2 mm (0.125 in.) cylin. centerbody

* All nozzles, with exception of this one, were fabricated with sintered carbide. This nozzle was severely eroded during the test.

centerbody CAVIJET consisted of a right circular cylinder having a diameter of 3.2 mm (0.125 in.). Also, in Specimen No. 1 a "tee-shaped" centerbody was tested. Unfortunately this centerbody was not fabricated from carbide, hence it was rapidly eroded so that at the end of the test its geometry resembled that of the conventional centerbody. The Leach & Walker (L&W) nozzle geometry is shown in Figure 11 (12). Also tested was a standard carbide 6.4 mm (0.25 in.) drill bit nozzle purchased from the Smith Tool Co. This nozzle was the same type as those used in the drill bit tests discussed in Chapter VI of this report. All of the nozzles used here, with the exception of the Smith Tool nozzle tested on Specimen No. 6 and the steel L&W nozzle tested on Specimen No. 3, were provided by NL/Hycalog under a subcontract to a sintered carbide component manufacturer.

The flow versus nozzle pressure drop calibrations for these nozzles were obtained, using water, within the laboratories at HYDRONAUTICS with the nozzles inserted into the four nozzle tool. By comparing these water calibrations with the total mud flows in these tests it was possible to determine the flow for each nozzle. The hydraulic power, P, delivered by each nozzle during the stationary cutting tests could then be calculated by using:

$$P = k \cdot \Delta p \cdot Q, \quad \text{kw (hp)} \qquad [4]$$

where:

$k = 1$, for Δp in MPa (megapascals), Q in l/s

($k = 5.834 \times 10^{-4}$, for Δp in psi, Q in gpm)

The ambient pressures, p_a, in the DRL tests were varied from about 0.9 to 27.2 MPa (130 to 3,950 psi). We were not able to run at atmospheric ambient pressures as this would have required

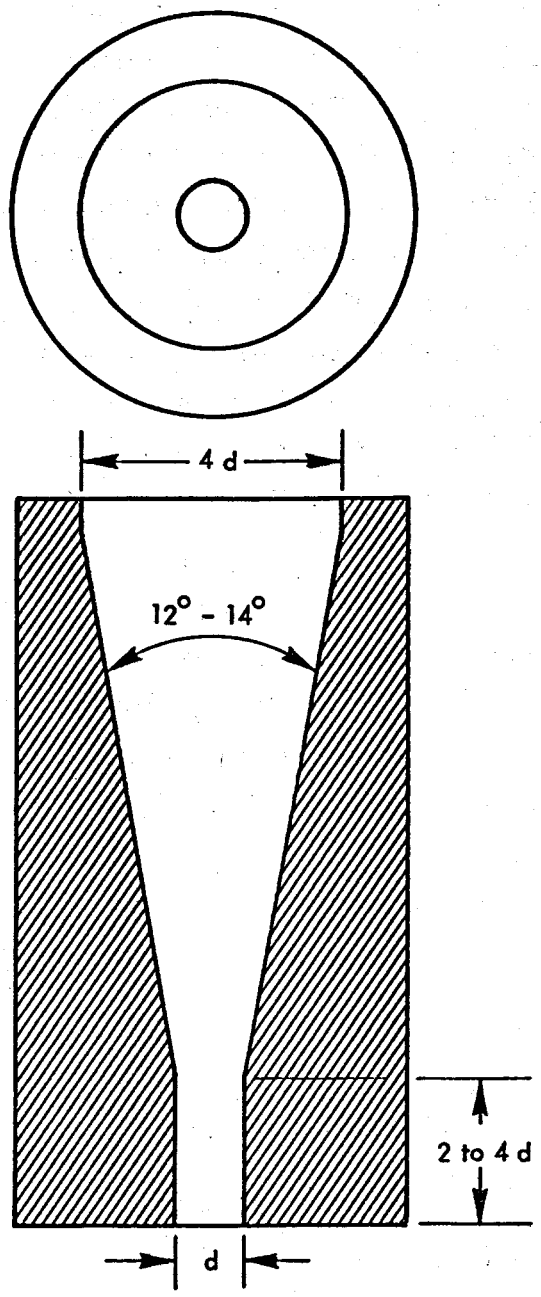

FIGURE 11 - SCHEMATIC OF THE LEACH AND WALKER NOZZLE CONFIGURATION (Ref. 12)

substantial changes to the facility. Also, the minimum pressure for a given run was a function of the swivel pressure and total flow for that run. For instance, the minimum ambient pressure at a flow of 18 l/s (285 gpm) was about 3.4 MPa (500 psi). These minimum pressure limitations were due to pressure drops along the flow path exiting from the chamber, even with the choke in its widest open position. The nozzle pressure drop, Δp, range was 6.2 to 26.9 MPa (900 to 3,900 psi). The simulated confining and overburden pressures on the rock, see Figure 7, were varied according to the following relations in order to balance the ambient pressure inside these hollow rock specimens:

$$\text{Confining pressure} = \text{Ambient pressure} + 1.4 \text{ MPa (200 psi)} \quad [5]$$

$$\text{Overburden pressure} = \text{Ambient pressure} + 4.1 \text{ MPa (600 psi)} \quad [6]$$

The mud used in all of these stationary nozzle tests was a water-based barite and bentonite mud with a nominal density of 1.1 gm/cm^3 (9.3 lb/gal); its apparent viscosity was controlled at about 10 to 11 cp. Mud properties were measured before and after each test. The yield point was found to vary from about 18 to 36 N (4 to 8 lb). No control for the temperature of the mud was available during these tests. This temperature was measured at the beginning and end of each of the runs on each specimen. The range for this parameter was from about 34 to 71°C (93 to 160°F).

In addition to the various flows and pressures cited above, the parameters measured on the rocks after the tests (see Figure 12) were: the eroded depths at the center of each hole, the volume removed, (utilizing a graduated syringe to determine the amount of water required to fill the hole), and the diameter of the eroded area at the surface. In the following section of the report, in order to describe the effects of pressure, nozzle configuration, and standoff distance, we will concentrate primarily on the hole depth parameter. However all of the data obtained from these

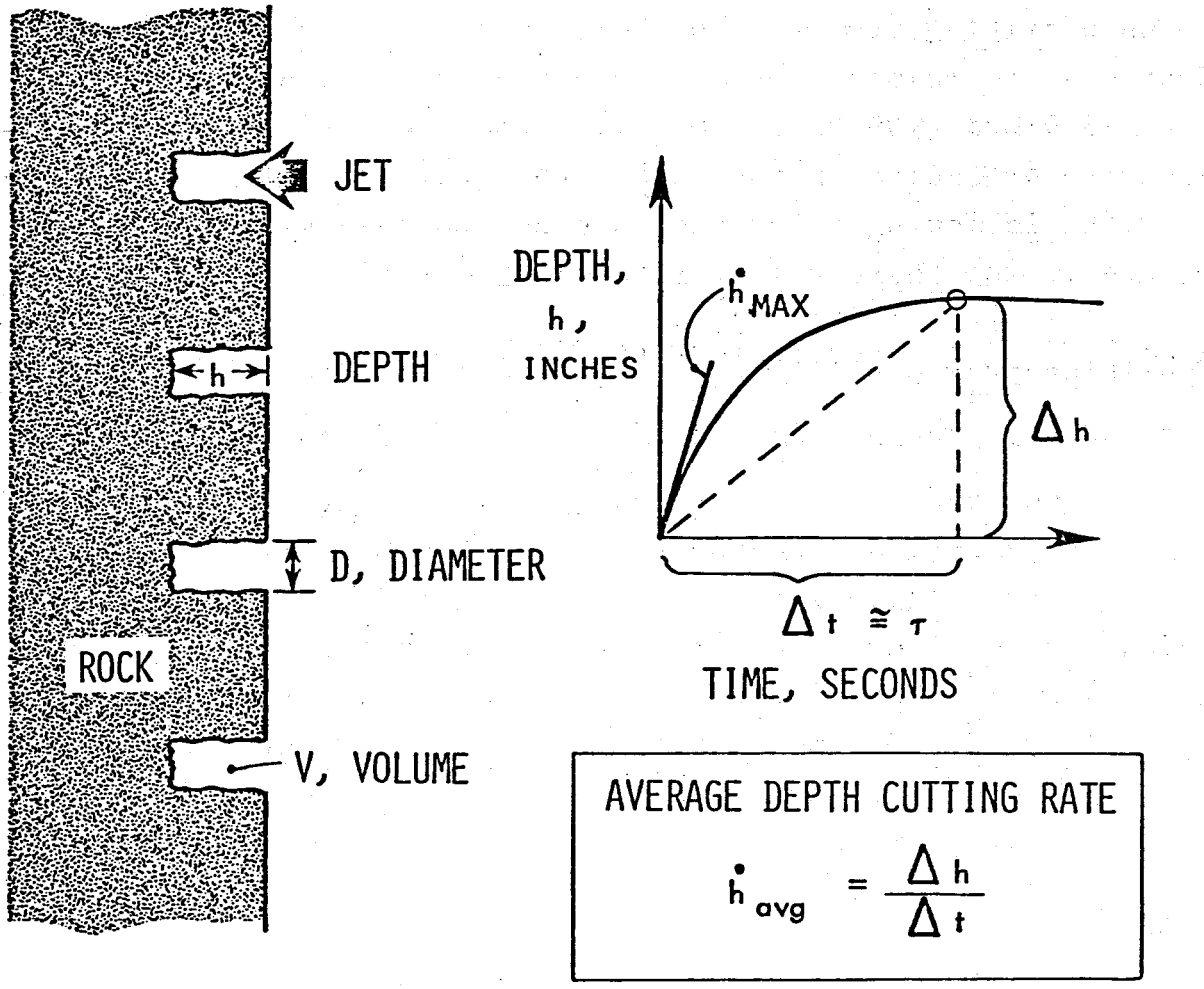

(See definitions of $\dot{h}_{avg}$ and τ in Figure 23)

FIGURE 12 - DEFINITION OF PARAMETERS MEASURED IN STATIONARY-NOZZLE TESTS AT D.R.L.

tests are listed within Appendix A.*

C. Discussion of Results

A typical set of data from these tests with the four nozzle tool is shown in Figure 13. We have plotted the parameter "average depth cutting rate", $\dot{h}_{avg}$, versus the ambient pressure, p_a for various fixed values of nozzle pressure drop, Δp. This $\dot{h}_{avg}$ is defined schematically in Figure 12 and 23. In Chapter IV, when empirical descriptions of complete depth versus time curves are discussed for the tests conducted within the new pressure cell at HYDRONAUTICS, it will be seen that the time increment, Δt, is related to the time constant, τ, for these exponential curves. Based on prior experience and with modifications on subsequent tests based on observations of prior hole depths, the Δt parameter was varied to insure that the hole depths were within a range of about 1.2 to 2.5 cm (0.5 to 1 in.). Thus for the lower intensity tests; i.e., those run either at low nozzle pressures and/or high ambient pressures, larger time increments were utilized relative to the more erosive tests. In this fashion, Δt was varied in accordance with the time constant, τ, as discussed in Chapter IV.

Although the data points in Figure 13 are from tests on a single rock specimen, the curves in this figure are the result of averaging all of the data for the particular nozzle type and standoff for each of the rock specimens. This averaging was done after these data had been normalized according to the scaling concepts which we will now discuss. To develop an understanding of the effect of the nozzle and ambient pressures the peak values of $\dot{h}_{avg}$, which will be denoted as $\dot{h}_{peak}$, for each curve of constant Δp as seen in Figure 13 were plotted versus the respective p_a. For the plain 6.4 mm (0.25 in.) CAVIJET nozzle the characteristic result seen in Figure 14 was obtained. This curve indicates that

*Since the hole diameters from these tests were all essentially the same (about 2.5 cm (1 in.) this parameter was not listed in Appendix A.

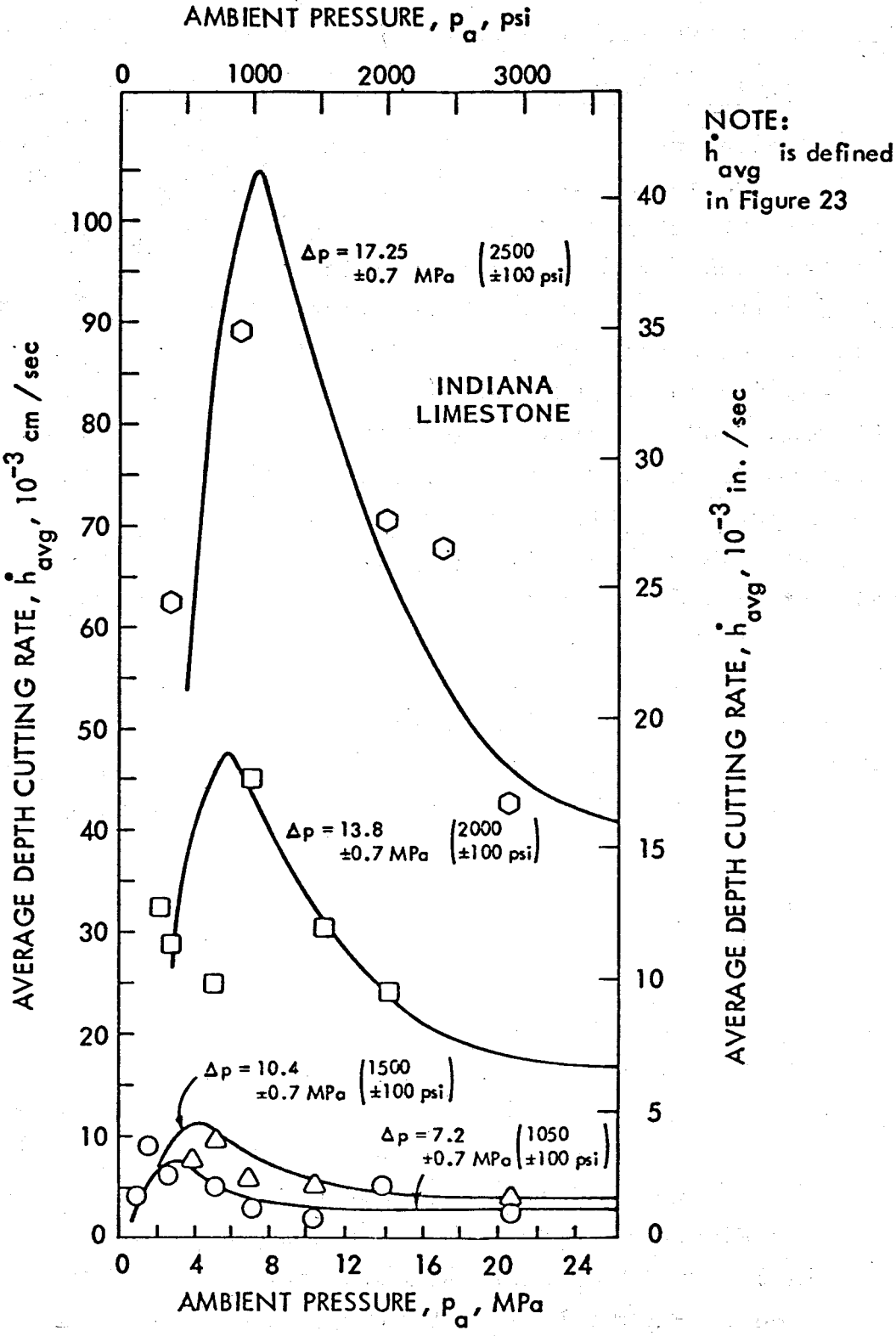

FIGURE 13 - TYPICAL RESULTS FROM STATIONARY-NOZZLE TESTING WITH MUD; PLAIN, 6.4 mm(0.25 in.) CAVIJET® NOZZLE; STANDOFF: 1.6 cm (0.62 in.)

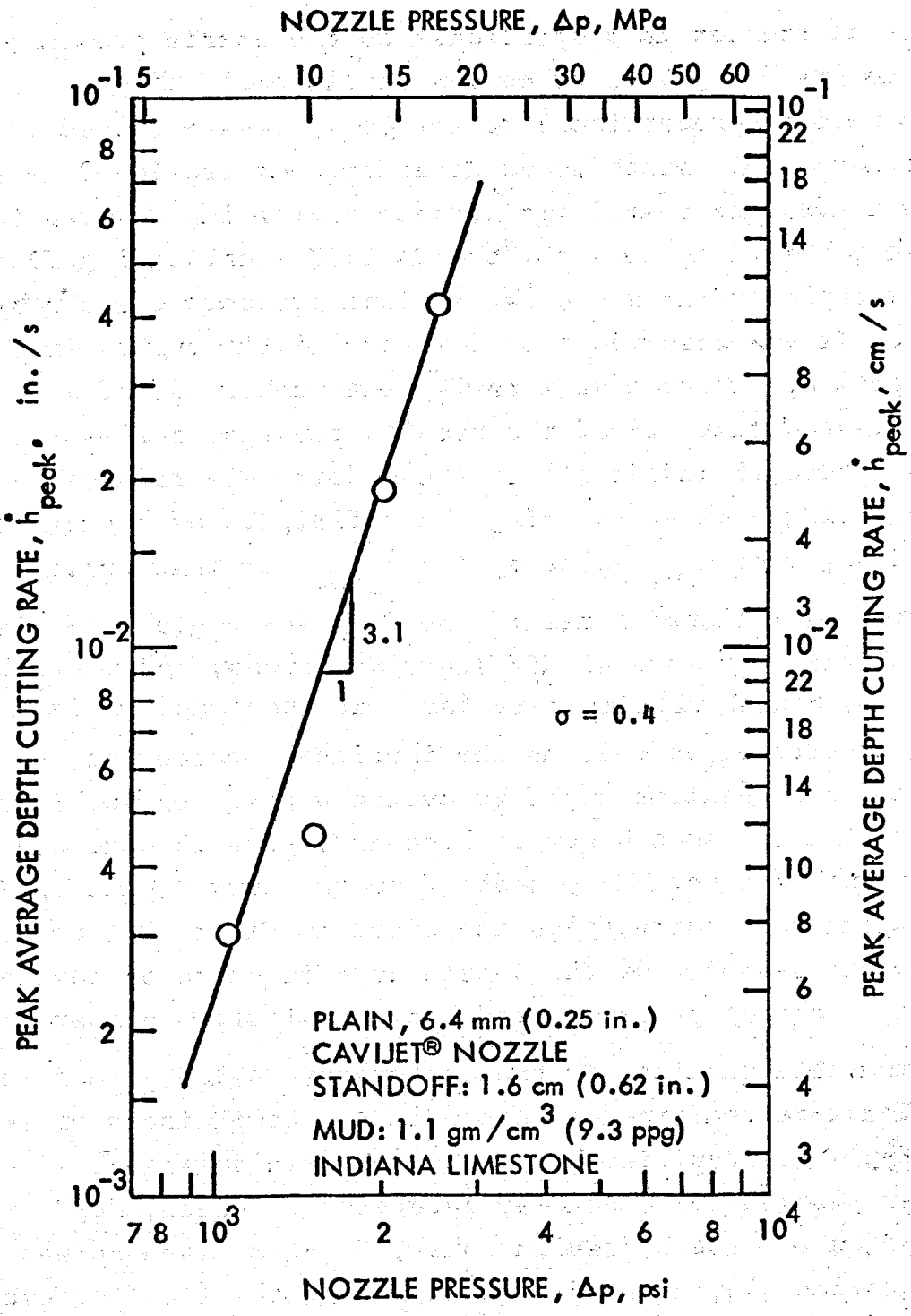

FIGURE 14 - DEPENDENCE OF CUTTING RATE ON NOZZLE PRESSURE IN STATIONARY-NOZZLE TESTS WITH MUD

the rate of erosion is proportional to the nozzle pressure drop raised to the 3.1 power, or approximately that this erosion rate is proportional to the jet velocity raised to the sixth power. This sixth power dependence of erosion rate on velocity is a familiar result for various cavitating devices (23) and has been observed as well for the CAVIJET cavitating fluid jet in other applications where the ambient pressure was atmospheric (19,22). It was observed that for each of the curves in Figure 13 the peaking occurred at a cavitation number, σ, of about 0.4. This suggested that all of the results could be scaled, and as seen in Figure 15 indeed all of these data were reduceable essentially to a single curve by using the definition of σ (Equation [2]) and dividing each $\dot{h}_{avg}$ value by the $\dot{h}_{peak}$ for that curve.

Thus, by collapsing all of the data for a given nozzle, although obtained on several different specimens, and normalizing in terms of each peak cutting rate for that specimen, variations in rock properties as well as the intrinsic scatter of the cavitation erosion mechanisms could be averaged out. Again, it is emphasized that the smooth curves seen in Figure 13 were the result of reversing this scaling process from the curve shown in Figure 15 and using that curve, plus the curve in Figure 14, to describe the complete behavior of the nozzle as a function of nozzle pressure drop, ambient pressure, and hence cavitation number.

Comparable results for the centerbody CAVIJET nozzle configurations are contained in Appendix A. Comparisons of several nozzle types are typified by the curves seen in Figure 16. The parameter plotted here, cutting rate effectiveness, "$e_{\dot{h}}$", is defined as $\dot{h}_{avg}/P$, where the hydraulic power, P, at a given Δp was derived using Equation [4], after determination of the flow for each nozzle. Using the plain CAVIJET nozzle for reference the relative

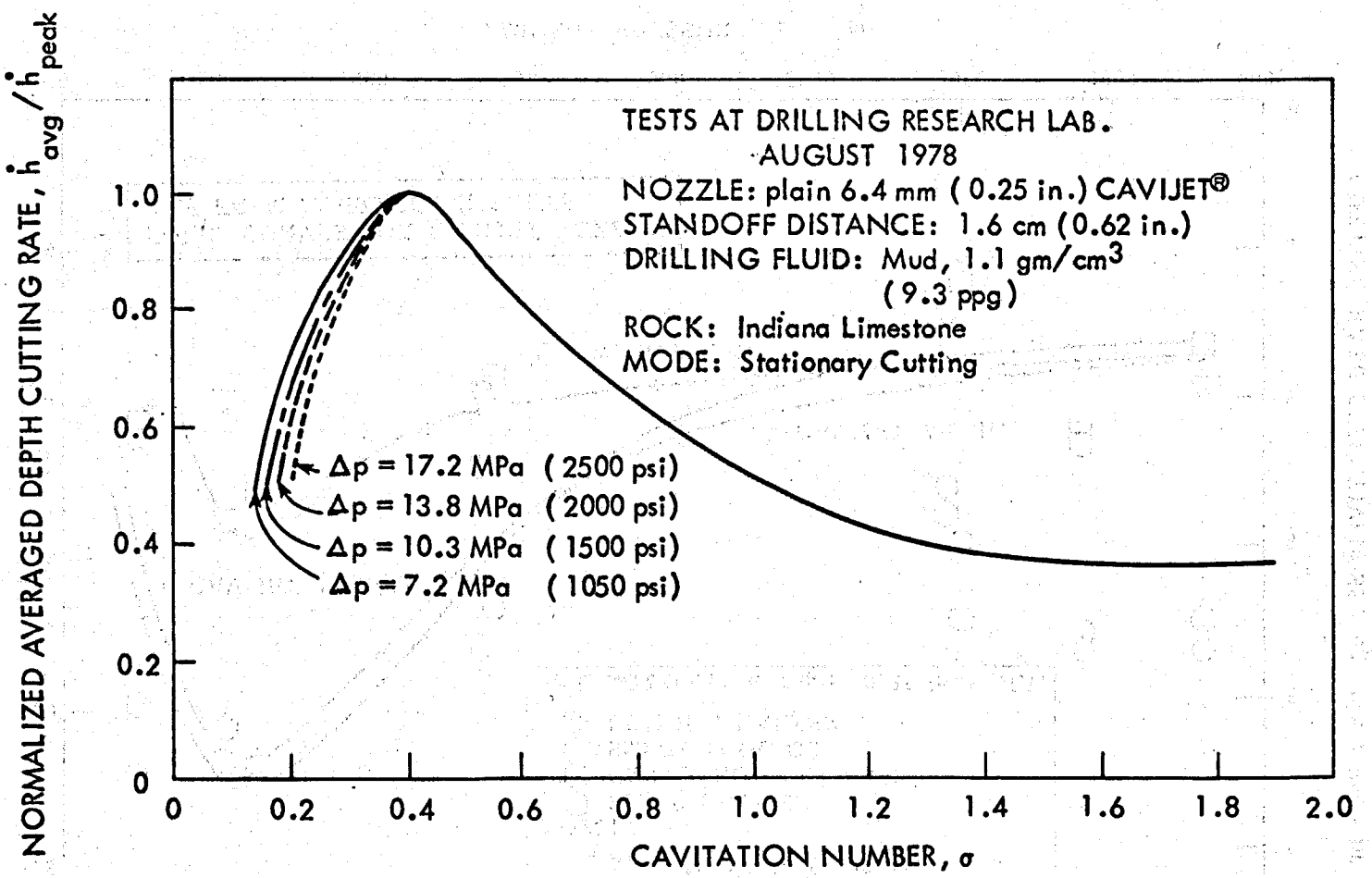

FIGURE 15 - SCALING THE STATIONARY-NOZZLE TEST RESULTS: for plain CAVIJET® nozzle

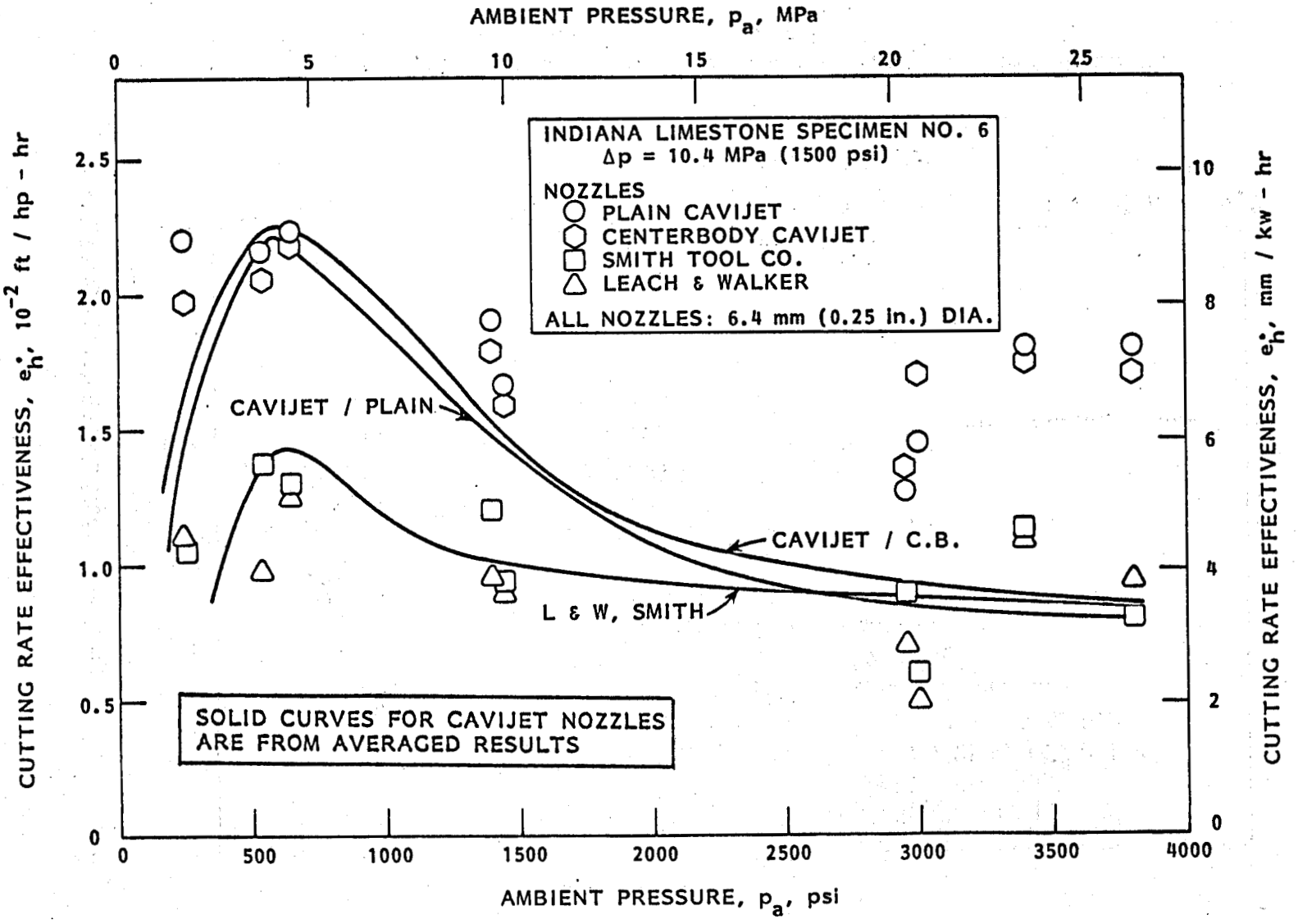

FIGURE 16 - COMPARISON OF VARIOUS NOZZLES TESTED AT D.R.L.:
Stationary-nozzle tests with four-nozzle tool

discharges of the four nozzles compared in Figure 16 are:

Plain CAVIJET nozzle	1
CAVIJET nozzle with cylindrical 3.2 mm (0.25 in.) centerbody	0.86
L&W nozzle	1.61
Smith Tool drill bit nozzle	1.39

As typified by Figure 16, the CAVIJET nozzles produced e_h values almost twice those of the conventional nozzles. Of interest in this figure is a result which was seen rather consistently in these tests, namely an increase in cutting rate and cutting rate effectiveness at higher values of ambient pressure. Indeed, very frequently at pressures just above about 20 MPa (3,000 psi), these increases were observed both during the stationary nozzle tests as well as in the drill bit tests described in Chapter VI. At this time we are not able to say whether this increased cutting at higher ambient pressures was a real effect related somehow to the cavitation phenomena or merely perhaps an anomaly related to the particular test configuration and testing procedures utilized at DRL. Perhaps these increased rates were due to the prolonged exposure of the rock at these higher pressure tests, which were typically of longer duration due to the lower anticipated cutting rates at these conditions. This extended exposure might tend to more fully saturate the rock, hence minimizing the excessive chip hold-down effect caused by incomplete simulation of the pore pressure.

One of the primary questions to be answered during this phase of our investigation was whether differences would be observed in comparing erosion with water versus drilling mud as the fluid to be cavitated, since all of our prior experience before this

study has been limited to the use of water as the operating fluid. Thus, a limited series of comparisons were made, and some typical results are summarized in Figures 17 and 18. It may be seen that for the lowest values of nozzle pressure the values of cutting rate effectiveness, as seen in Figure 17, were lower for water than for mud. As nozzle pressures of about 17.2 MPa (2,500 psi) were achieved, these data, within scatter, seem to converge. A comparable effectiveness based on the volume removal rate, $\dot{V}$, is plotted in Figure 18. This parameter, the "volume removal effectiveness", $e_{\dot{V}}$, is defined as $\dot{V}/P$, where the delivered hydraulic power, P, is based on the individual flows through each nozzle at the respective nozzle pressure drop for that run. Again for the $e_{\dot{V}}$ parameter the water results at the lower pressures are below those for the mud. We may conjecture that at the lower pressures the intrinsic erosiveness of the mud itself may have contributed to the observed differences, so that the lower Δp rates of erosion are equally due to both cavitation and to impingement erosion from the suspended particles within the mud. However, as higher jet velocities are reached, it may be that cavitation becomes the increasingly strong contribution to the erosion observed, thus outweighing the effects due to particle impingement.

The effect of standoff distance, that is, the distance between the face of the nozzle and the rock surface prior to the test, was also examined. This standoff parameter was varied over a range from 1.6 to 2.9 cm (0.62 to 1.12 in.). Typical results from these comparisons are indicated by the data in Figures 19a and 19b. It was determined that the optimum standoff occurred at the 1.6 cm (0.62 in.) value. Unfortunately the test configuration precluded standoffs smaller than the 1.6 cm (0.62 in.) value.

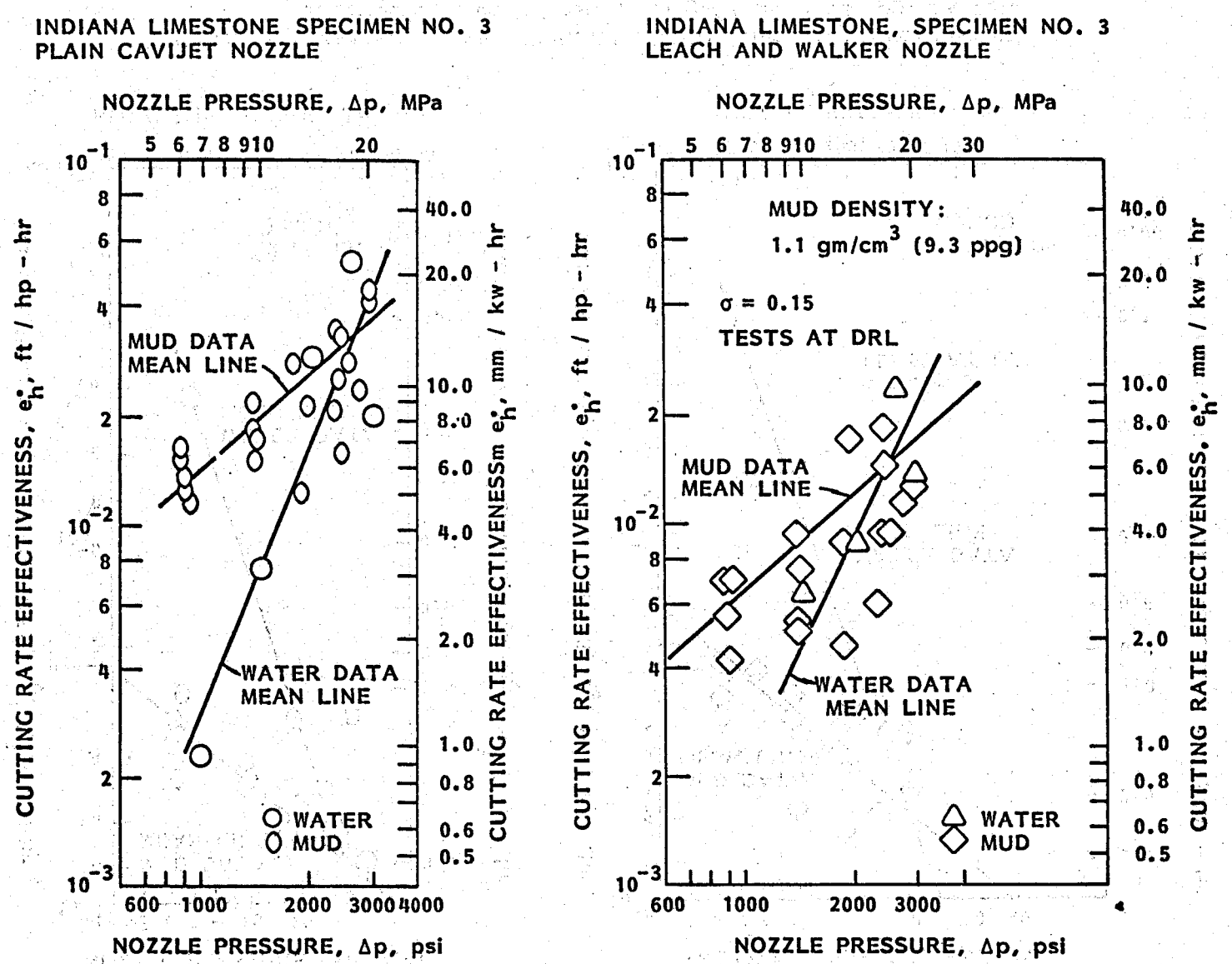

FIGURE 17 - COMPARING WATER VERSUS MUD: Effect on Cutting Rate Effectiveness; mud density: 1.1 gm / cm³ (9.3 ppg), σ = 0.15

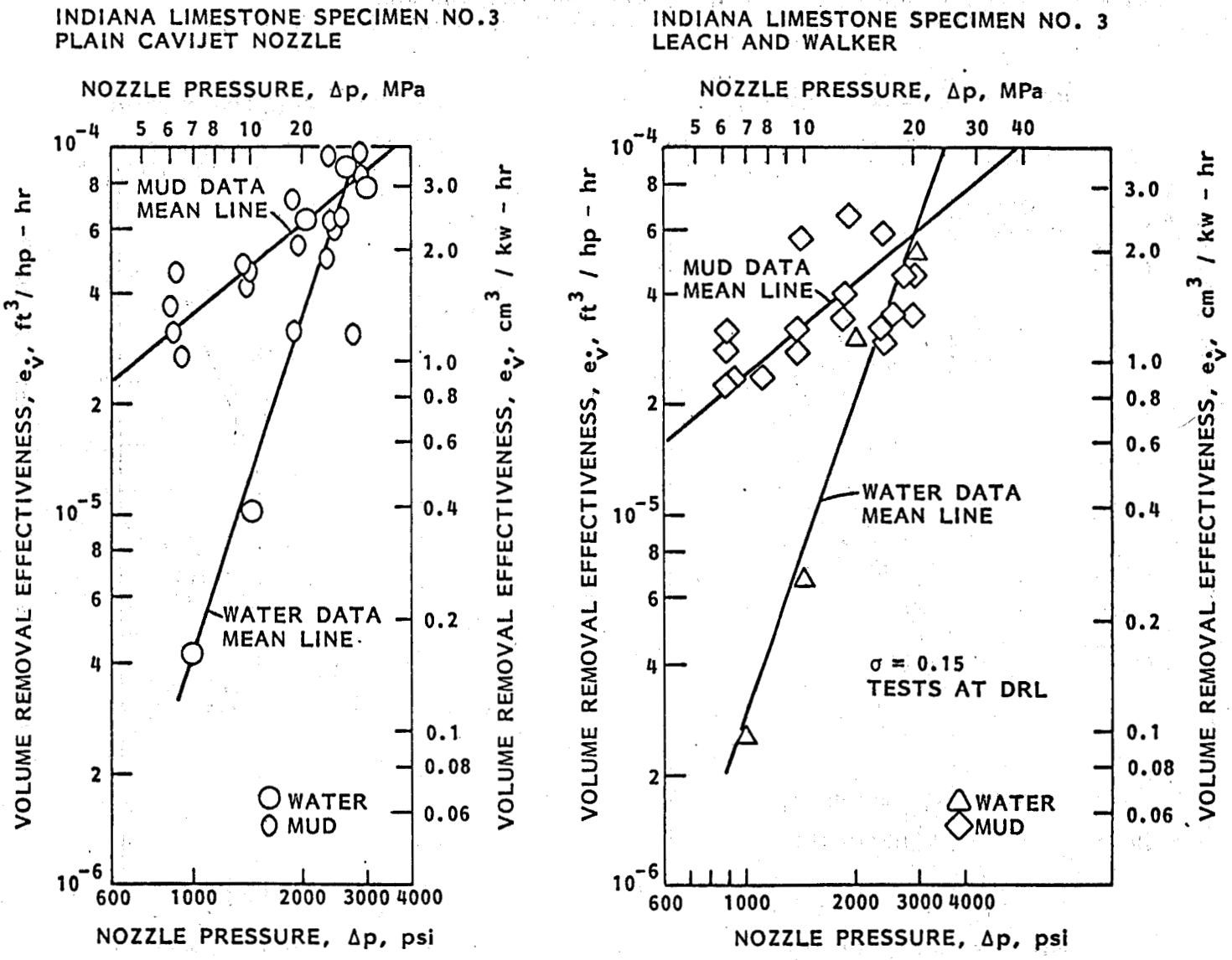

FIGURE 18 - COMPARING WATER VERSUS MUD: Effect on Volume Removal Effectiveness; mud density: 1.1 gm / cm^3 (9.3 ppg), σ = 0.15

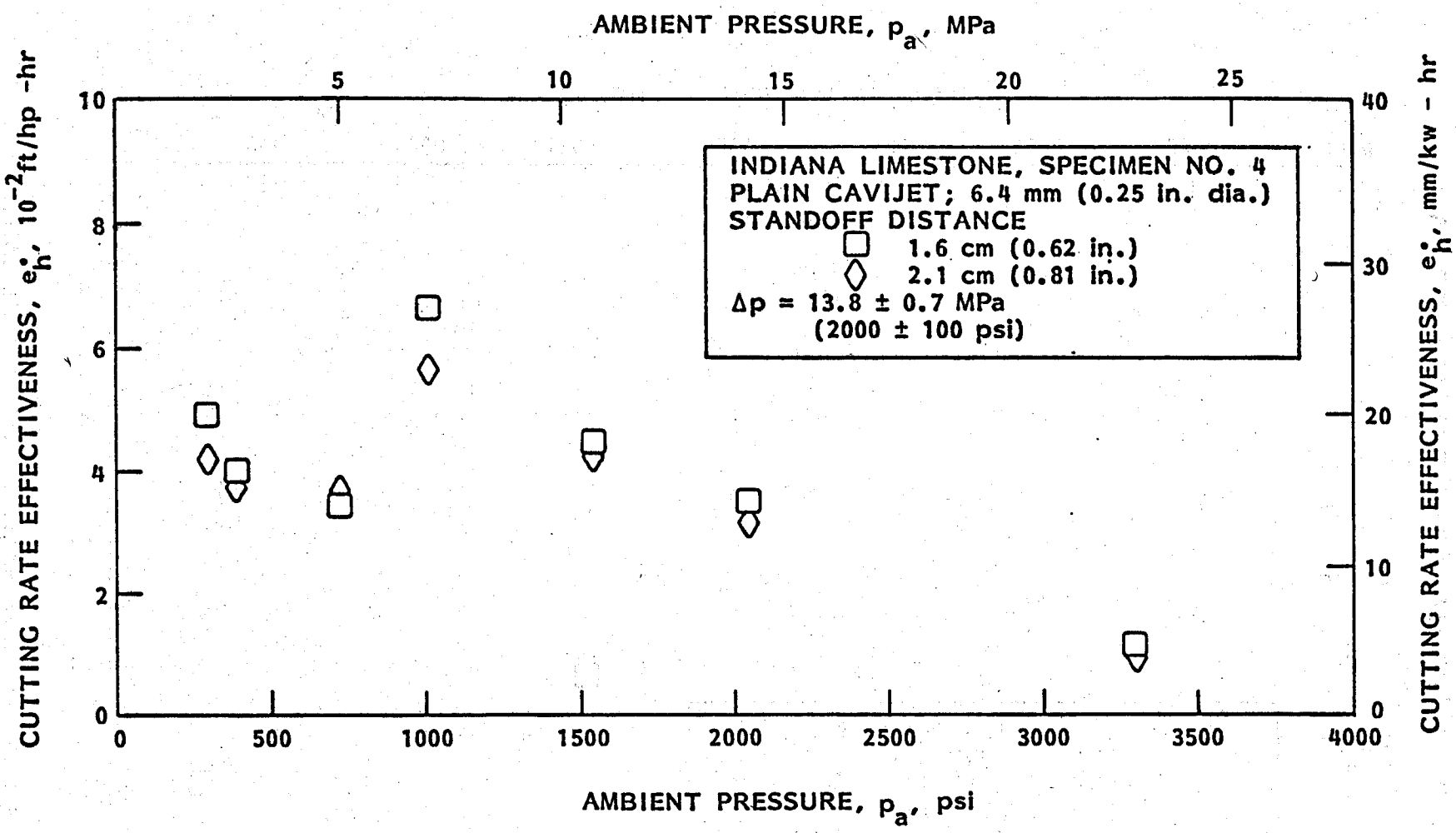

FIGURE 19a - EFFECT OF STANDOFF DISTANCE ON CUTTING RATE EFFECTIVENESS

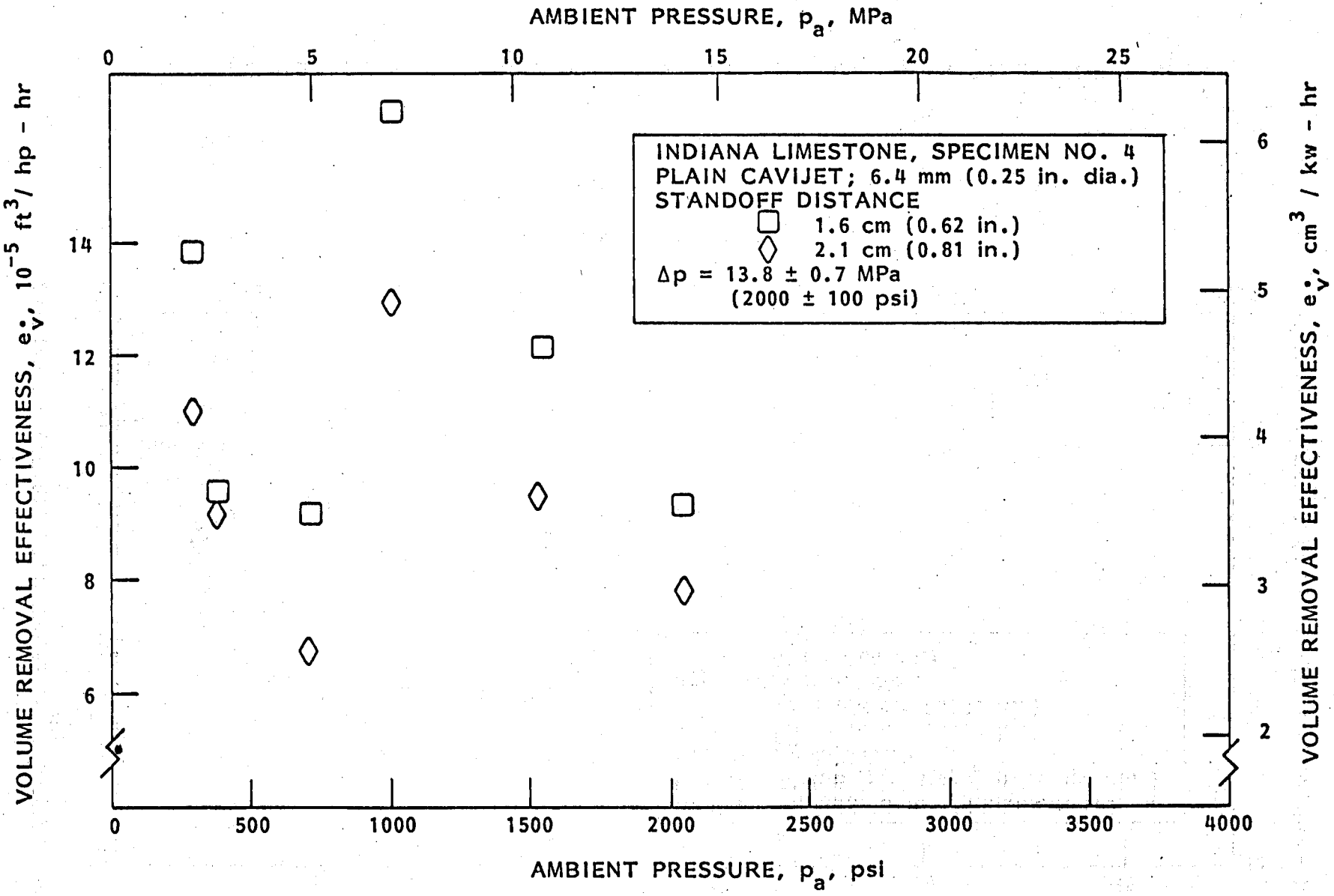

FIGURE 19b - EFFECT OF STANDOFF DISTANCE ON VOLUME REMOVAL EFFECTIVENESS

However, since there seemed to be a consistently higher cutting rate observed at the 1.6 cm (0.62 in.) standoff, this value was chosen for the majority of tests performed with this stationary nozzle mode as well as for the drill bit tests discussed in Chapter VI. It should be noted that this optimum standoff determination is consistent with our preliminary work (11) which suggested that the optimum standoff was between 1.3 and 2.5 cm (0.5 to 1.0 in.) for a 6.4 cm (0.25 in.) diameter plain CAVIJET. The standoff of 1.6 cm (0.62 in.) was also found to be optimum for the centerbody CAVIJET nozzle configuration.

IV. STATIONARY AND SLOT CUTTING TESTS AT HYDRONAUTICS

A. Test Objectives and Procedures

The tests conducted within the new pressure cell, described in Chapter II, were planned so as to complement the tests conducted within the well bore simulator at DRL (see Chapter III). While the tests at DRL could be conducted over a wide range of both ambient pressure and nozzle pressure, there were limitations in the type and amount of tests which could be run. The test configuration was such that only selected discrete time intervals could be examined for the stationary nozzle tests. Also, at DRL no provision for slot cutting tests was feasible within the time and cost limitations of this program. The program was therefore planned to allow a more extensive examination of both stationary and slot cutting tests, although within a more limited range of pressures, by creating the pressure cell at HYDRONAUTICS. Thus, by using the scaling laws which define the effects of pressure and cavitation number from the DRL tests, it was expected that the influence of time and velocity obtained in tests at HYDRONAUTICS could be combined to provide the desired understanding of all relevant parameters.

A specimen configuration to permit both slot cutting and stationary hole cutting was used. This specimen shape was a cube, 15.2 cm (6 in.) on a side to allow maximum use of each rock by testing on several surfaces (see Figures 20a and 20b). Preliminary testing showed that reproducible results could be obtained on any of the four "sides" which allowed jet impingement parallel to the bedding planes. However tests conducted on either the "top" or "bottom", i.e., on a surface which allowed the jet to impinge perpendicular to the bedding planes, achieved different results. Thus all tests were conducted on the sides of the specimens.

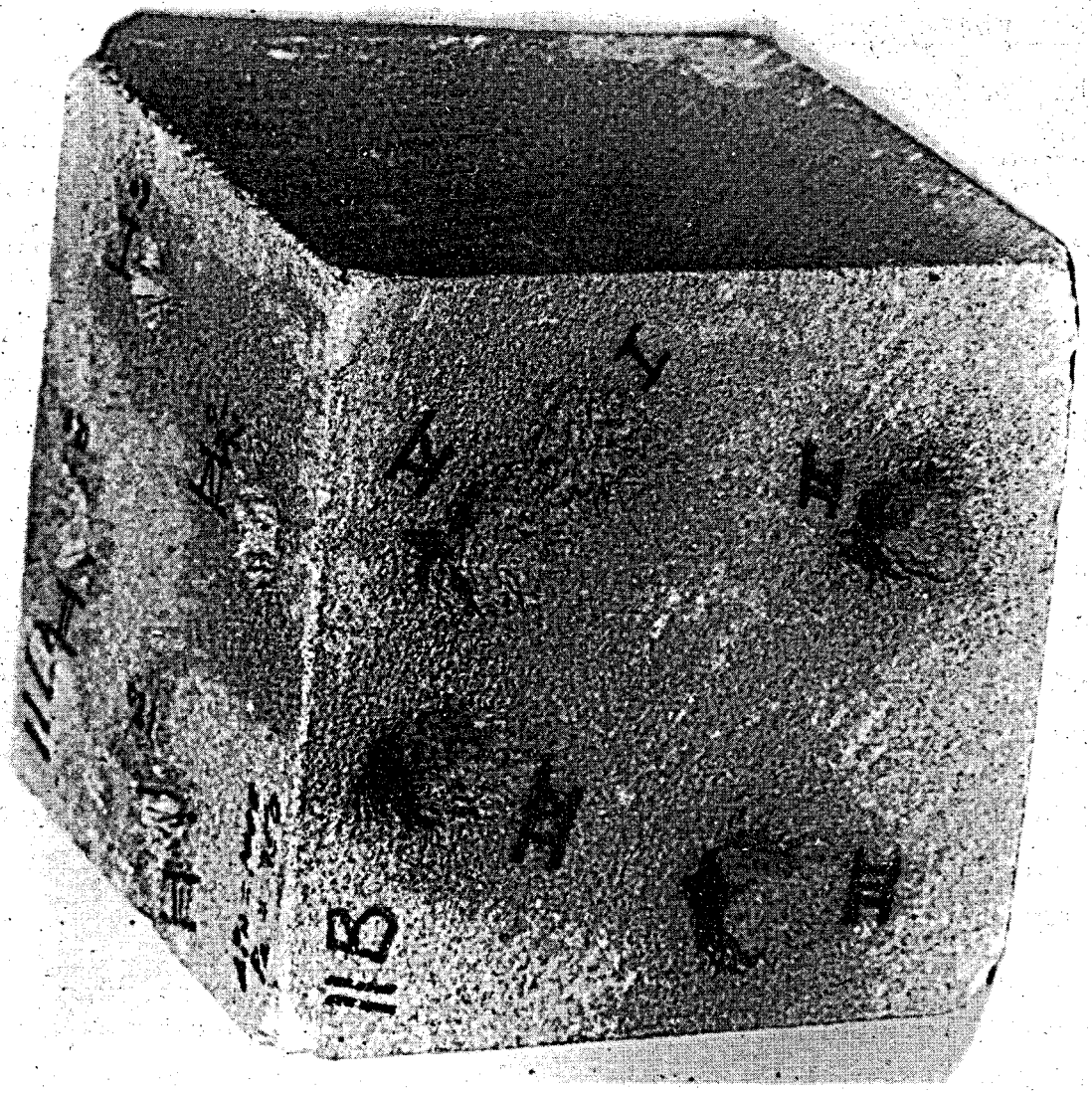

FIGURE 20a - TYPICAL STATIONARY-NOZZLE SPECIMEN: Indiana limestone; Test Conditions: Δp = 12.4 MPa (1,800 psi), p_a = 2.1 MPa (300 psi), σ = 0.17. I : 12 sec, V : 60 sec, II : 100 sec, III : 160 sec, IV : 200 sec; 6.4 mm (0.25 in.) dia. plain CAVIJET® nozzle; 1.1 gm /cm^3 (9.3 ppg) mud.

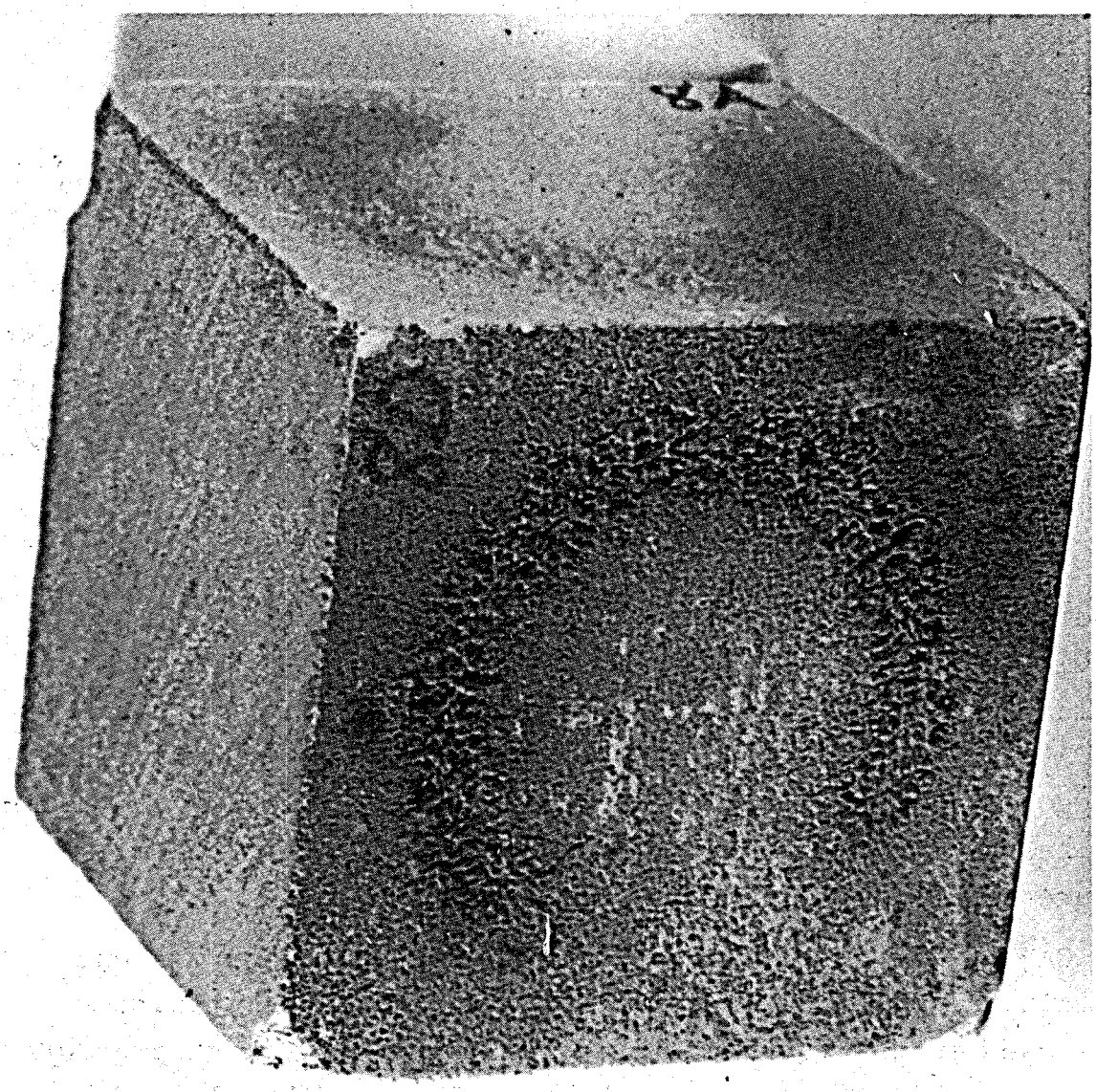

FIGURE 20b - TYPICAL SLOT CUTTING SPECIMEN: Indiana limestone; Test Conditions: Δp = 12.4 MPa (1,800 psi), p_a = 2.1 MPa (300 psi), σ = 0.17; 6.4 mm (0.25 in.) dia. plain CAVIJET® nozzle; 1.1 gm / cm^3 (9.3 ppg) mud; Translation rate 0.64 cm/sec (0.25 in./sec).

This testing orientation agreed with the orientation of the jets relative to the bedding planes in the large specimens tested with the four nozzle tool at DRL.

Three types of rocks were examined, with the majority of tests performed on specimens of Indiana limestone, in order to compare these results with the data obtained at DRL on this same rock. Limited tests were also performed on cubes of Berea sandstone and Georgia grey granite.

The mud used in these tests was the same type used in the tests at DRL, namely a water-based mud with density of 1.1 gm/cm^3 (9.3 ppg). This barite and bentonite mud, after a learning period, was easily controlled within the reservoir shown schematically in Figure 3. Details relating to the properties of this mud, as well as all of the data obtained during this part of the program, are given in Appendix B. A limited amount of testing was also conducted with heavier muds up to a density of 1.4 gm/cm^3 (12 ppg). No measurable differences in the erosion caused by the plain configuration of CAVIJET cavitating fluid jet nozzle were observed over this range of mud densities. The mud temperature was not controlled in these tests, and this temperature varied from ambient room temperature values up to about 46°C (115°F).

The CAVIJET nozzle used for all of these studies was one of the plain CAVIJET nozzles fabricated of sintered carbide which was used in the four nozzle tests at DRL. The high pressure test cell was fabricated so that this nozzle could be clamped into place in a manner comparable to that used in the four nozzle tool. The standoff distance could be varied by moving the entire input flow pipe in the vertical direction. However, a fixed standoff distance of 2.1 cm (0.81 in.) was used for all of these tests (the minimum achievable due to the "shutter-plate.")

B. Stationary-Nozzle Rock Cutting Tests

A series of tests were conducted with both the rock specimen and the nozzle stationary. Typical results are seen in Figure 20a, where it is seen that several tests were usually run on each side of the specimen, varying the time increment, and merely rotating the rock a fraction of a revolution between runs. This saved time by avoiding having to remove the rock from the cell between runs. In this fashion a considerable amount of information could be obtained in a relatively short period of time.

Typical data from this type of test are seen in Figure 21 for several combinations of ambient and nozzle pressure. These tests were all conducted on specimens of Indiana limestone. Note that Curve 4 in Figure 21 is substantially higher than would be expected for these values of Δp and σ. One would expect this curve to lie well below Curve 3, since these tests were run at the peak $\sigma = 0.4$ (see Figure 15) and at a higher $\Delta p = 8.3$ MPa (1,200 psi) relative to Curve 4. Thus, it might be conjectured that this particular portion of the rock was softer than average. This hypothesis that Curve 4 was too high was corroborated subsequently, as discussed below in conjunction with Figure 22.

To characterize the stationary rock cutting performance of the CAVIJET , in order to be able to utilize the pressure scaling ideas derived from the DRL testing, it was necessary to obtain an empirical description of these stationary cutting tests. As shown in Figure 22, these data could be described by means of an exponential curve of the form:

$$h = h_{max} \ (1 - e^{t/\tau}) \qquad [7]$$

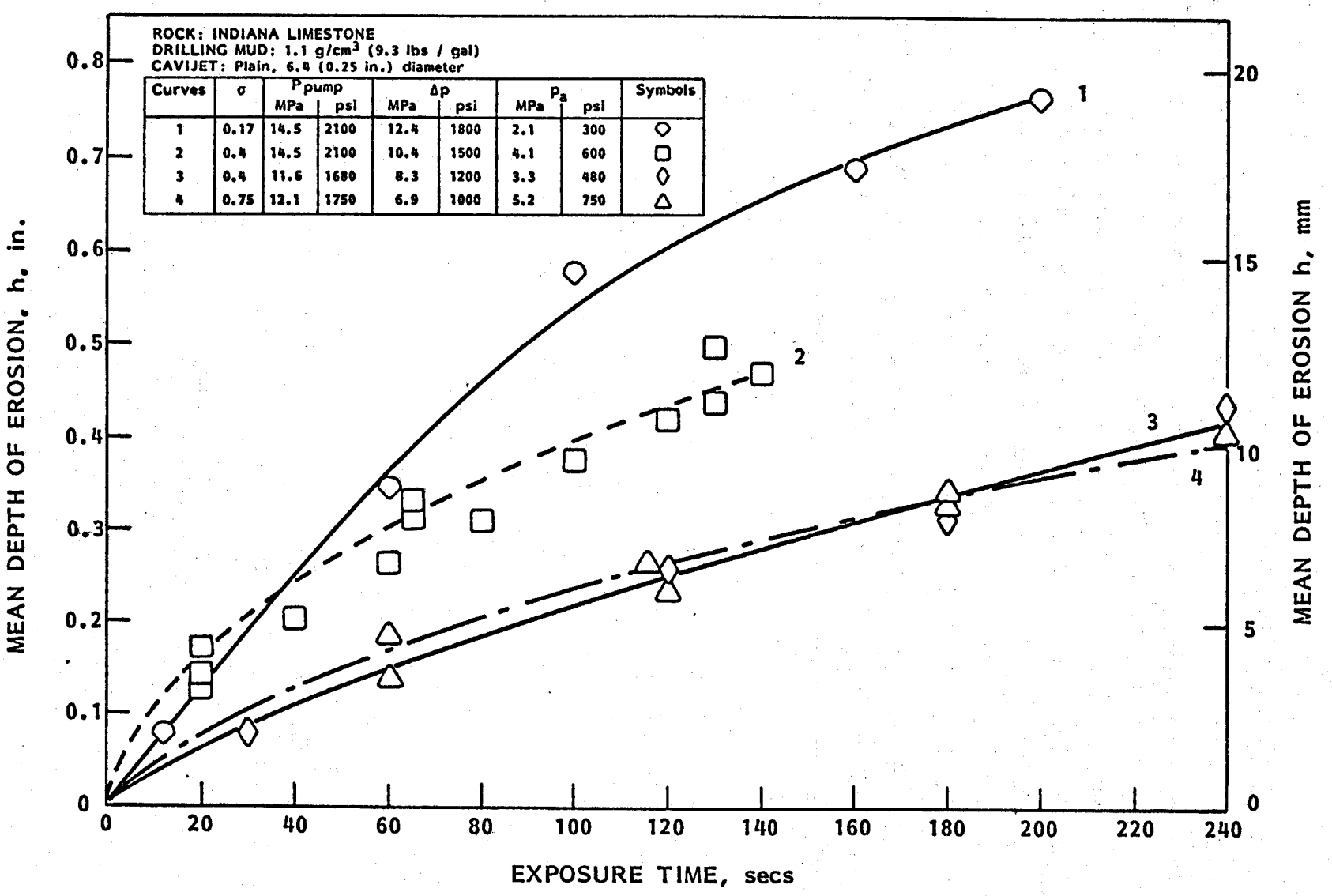

FIGURE 21 - STATIONARY-NOZZLE ROCK CUTTING RESULTS: Tests in pressure cell at HYDRONAUTICS on Indiana limestone

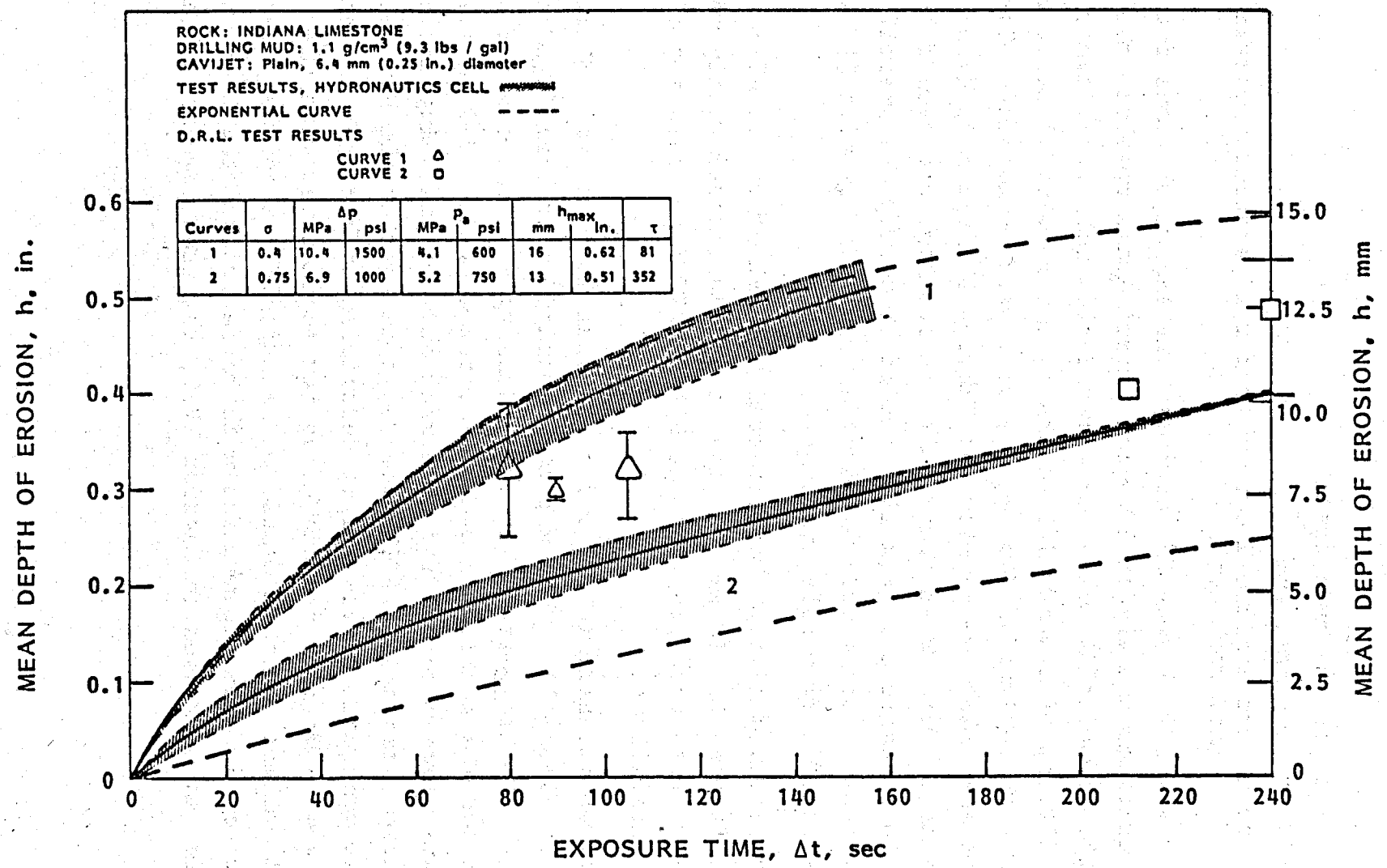

FIGURE 22 - EXPONENTIAL CURVE FITTING TO STATIONARY-NOZZLE TEST RESULTS

where:

h is the hole depth,

t is time, and

h_{max} and τ are empirical constants for a particular nozzle and rock type.

Note that, in Figure 22, although the empirical curve for Curve 1 quite accurately follows the experimental results, the comparable exponential curve for Curve 2 lies well below the data. Similar fitting of exponential curves to the results of tests run at other combinations of (Δp, p_a, σ) were very successful. Thus, the hypothesis that the results for Curve 4 in Figure 21 (which is the same as Curve 2 in Figure 22) are too high has been demonstrated to be correct. This also served to verify the overall effectiveness of using this exponential curve in Equation [7] to describe stationary-nozzle cutting data.

Some individual test results from the DRL study are also shown on Figure 22. It is seen that these data agree fairly well with the results from the tests at HYDRONAUTICS for each set of pressure conditions.

The two parameters h_{max} and τ, as seen in Equation [7], are defined in Figure 23. The original description of this "Equivalence Principle" (24) suggested that the values of h_{max} and τ would be the same for the stationary and slot cutting tests. Indeed for situations wherein relatively soft rock or coal was being cut by a very high intensity CAVIJET nozzle, this form of the Equivalance Principle was quite successful in describing either type of test results (24). However for the situation encountered with the elevated ambient pressure tests, at relatively low nozzle pressures, hence low cavitation intensities with harder rocks, the Equivalance Principle, as discussed in Section IV.C, required some modification.

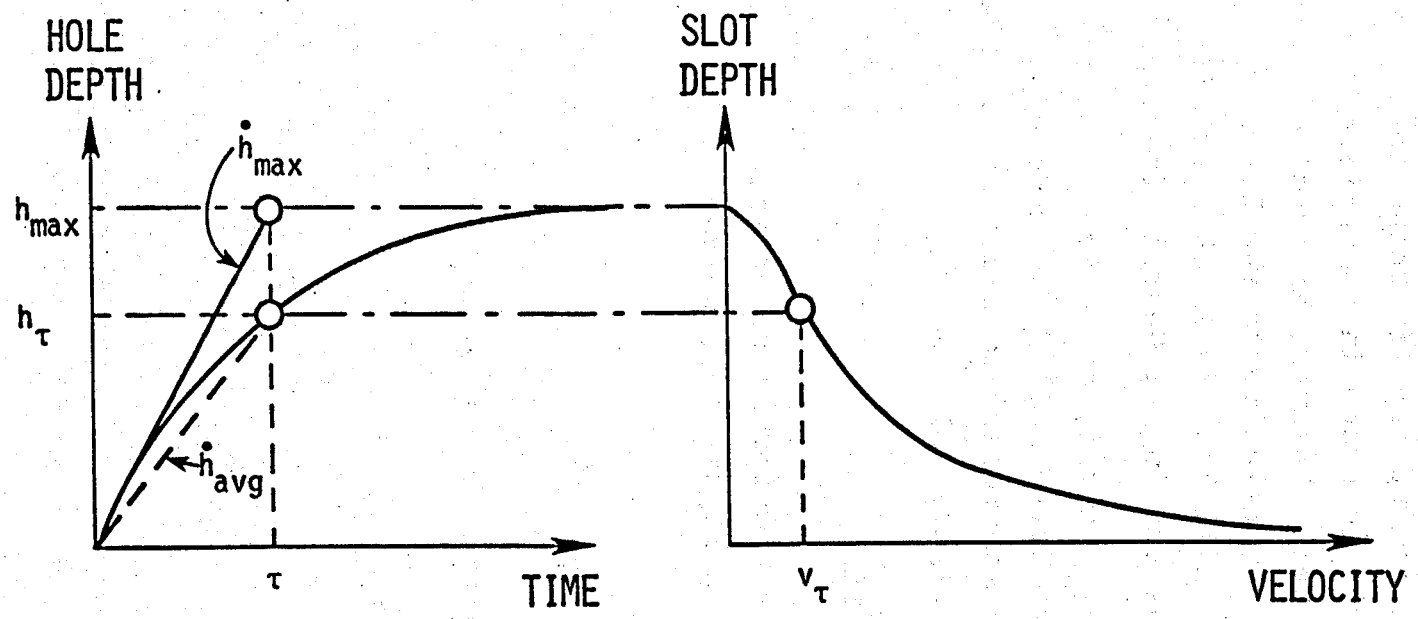

STATIONARY CUTTING	SLOT CUTTING
$h = h_{max}(1 - e^{-t/\tau})$	$h = h_{max}(1 - e^{-D/v\tau})$
AT $t = 0$: $\dot{h} = \dot{h}_{max} = h_{max}/\tau$	WHERE: D IS DIAMETER OF ZONE INFLUENCED BY THE JET
AT $t = \tau$: $\dot{h}_{avg} = h_\tau/\tau$; $h_\tau = h_{max}(1 - 1/e)$	
THUS: $\dot{h}_{avg} \propto h_{max}/\tau$	

FIGURE 23 - THE EQUIVALENCE PRINCIPLE FOR COMPARING RESULTS FROM STATIONARY AND SLOT CUTTING TESTS (Reference 24)

The stationary hole cutting results for the three rocks tested are compared by the typical data shown in Figure 24. In prior tests (11) the particular specimens of Indiana limestone then tested were relatively more difficult to erode in comparison to the Berea sandstone. It was found here, however, as seen in Figure 24, that the Indiana limestone, relative to the Berea sandstone, was easier to cut. More will be said in Chapter VII about the effects of pressure on the cutting of Georgia granite.

By comparing the parameters, h_{max} and τ, as derived from the stationary-nozzle tests conducted at HYDRONAUTICS, and the $\dot{h}_{avg}$ data obtained during the comparable stationary-nozzle tests at DRL, it was found that (as indicated in Figure 23):

$$\dot{h}_{avg} \propto \frac{h_{max}}{\tau} \qquad [8]$$

Therefore, by making use of the previously determined relation: $\dot{h}_{avg} \propto (\Delta p)^{3.1}$ (see Section III.C and Figure 14), we can use Equation [8] to conclude:

$$\dot{h}_{avg} \propto \frac{h_{max}}{\tau} \sim (\Delta p)^{3.1} \qquad [9]$$

The dependence of τ on Δp was empirically found to be:

$$\tau \propto \Delta p^{-\frac{1}{2}}, \qquad [10]$$

hence, combining [9] and [10]:

$$h_{max} \propto (\Delta p)^{2.6} \approx (\Delta p)^{5/2} \qquad [11]$$

Equations [10] and [11] were experimentally verified to be capable of predicting, at any fixed value of σ, the effect of Δp on the

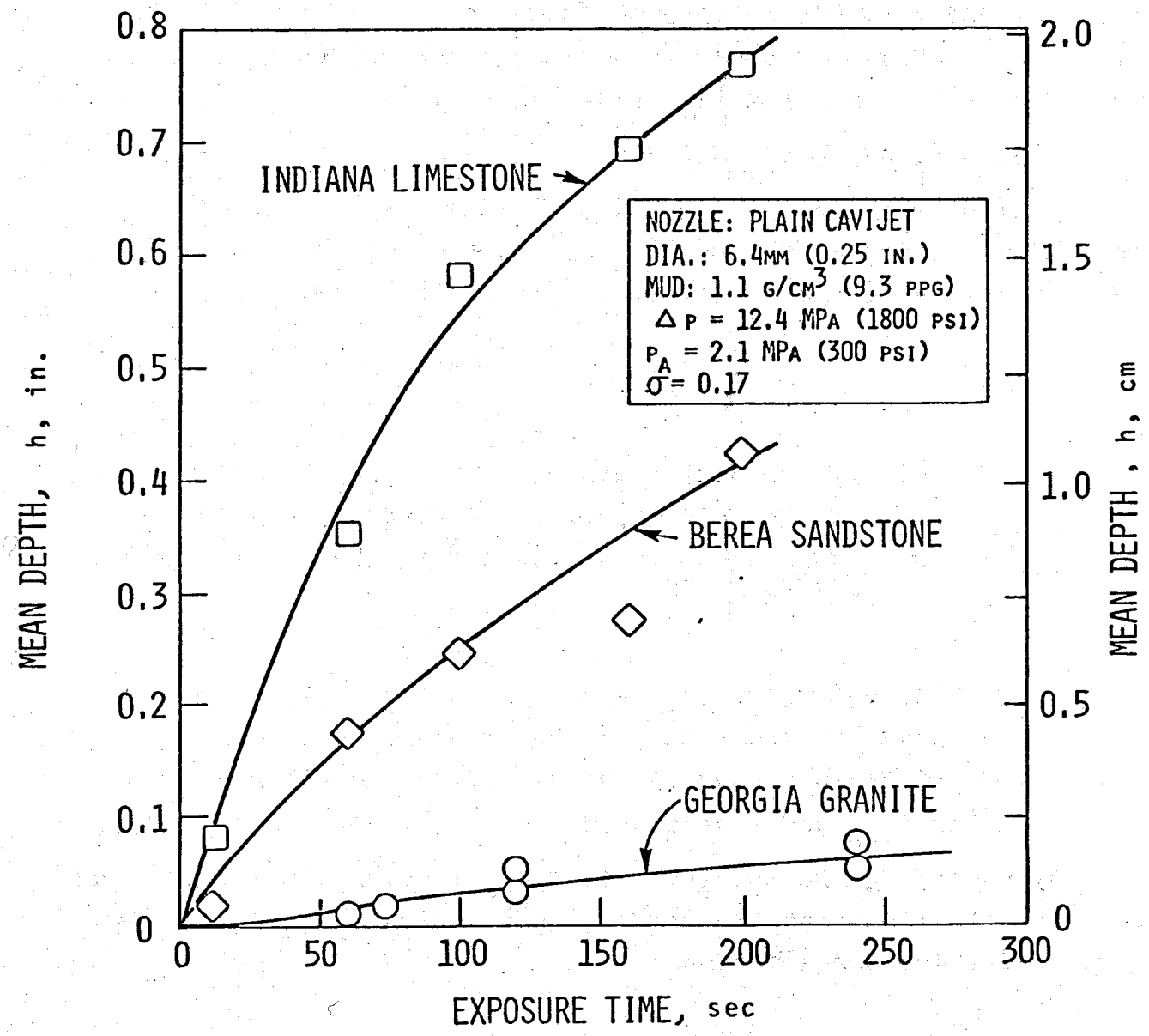

FIGURE 24 - COMPARISON OF STATIONARY-NOZZLE CUTTING RESULTS FOR THREE ROCK TYPES

stationary-nozzle cutting by this plain CAVIJET nozzle. The effect of varying σ is defined by the curve shown in Figure 15. Thus, the full definition which we have been seeking for predicting the stationary nozzle cutting performance of a plain, 6.4 mm (0.25 in.) CAVIJET nozzle on Indiana limestone is given by Equations [7], [10], and [11] plus Figure 15.

C. Slot Cutting Test Results

Typical results from the slot cutting tests at HYDRONAUTICS are shown in Figure 20b and 25. Fitted through the experimental data in Figure 25 are empirical curves of the form:

$$h' = h'_{max} \left(1 - e^{-D/v\tau'}\right) \qquad [12]$$

where:

h' is the slot depth,

v is the velocity of translation of the jet

h'_{max}, τ', D: are empirical constants for a particular nozzle and rock type

Note that these values of h'_{max} and τ' do not coincide with the parameters shown in Figure 23 for the original Equivalence Principle (24). Indeed, the h'_{max} and τ' values are much smaller than the corresponding h_{max} and τ stationary-nozzle parameters.

By comparing the results, under the same pressure conditions, from the stationary-nozzle testing, the following relations were derived for Indiana limestone:

$$h'_{max} = 0.060\ h_{max} \qquad [13]$$

$$\tau' = 0.021\ \tau, \qquad [14]$$

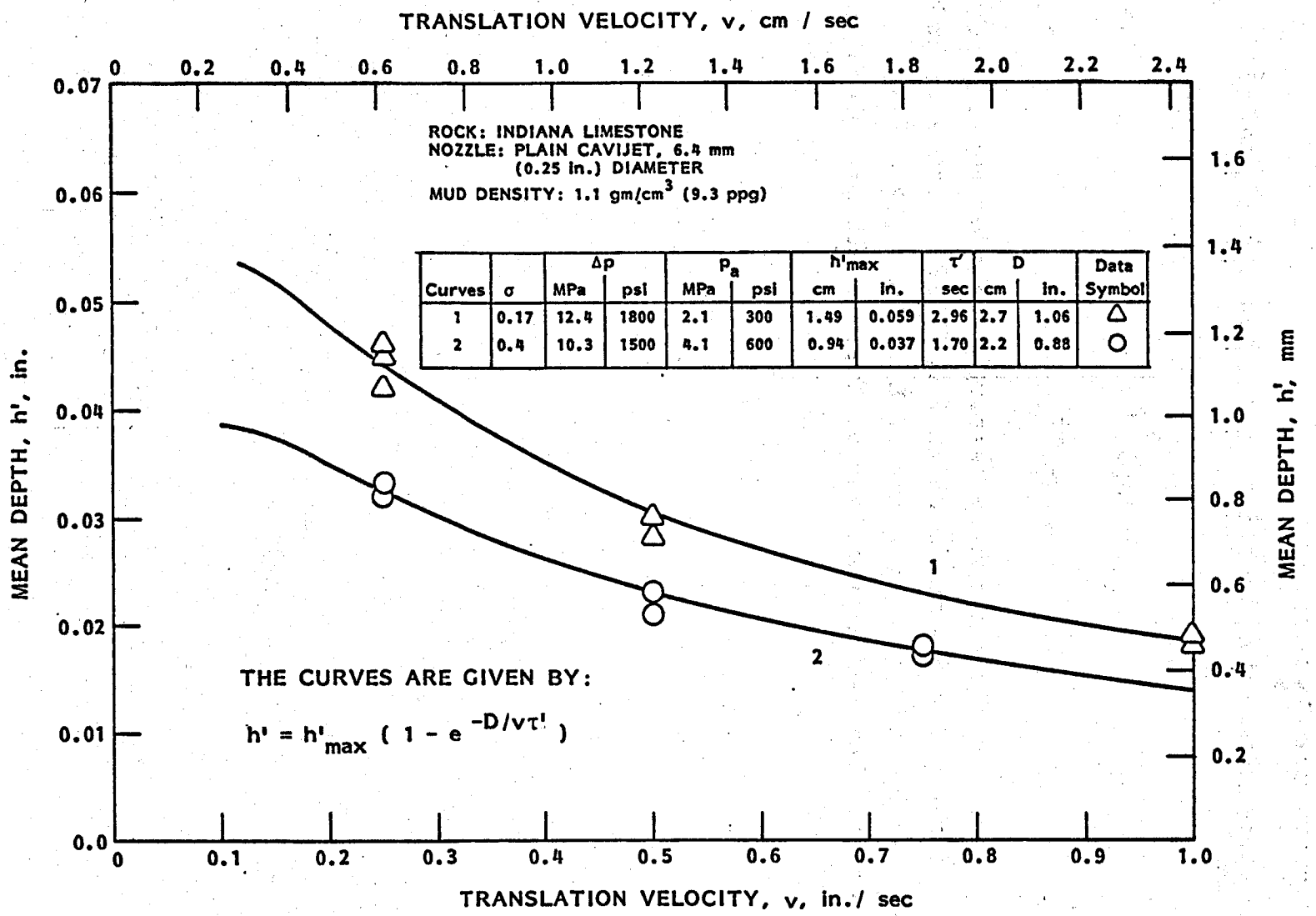

Curves	σ	Δp MPa	Δp psi	p_a MPa	p_a psi	h'max cm	h'max in.	τ' sec	D cm	D in.	Data Symbol
1	0.17	12.4	1800	2.1	300	1.49	0.059	2.96	2.7	1.06	△
2	0.4	10.3	1500	4.1	600	0.94	0.037	1.70	2.2	0.88	○

FIGURE 25 - EXPONENTIAL CURVE FITTING TO SLOT CUTTING TEST RESULTS

and, D, which may be considered to be the diameter of influence of the jet, was taken as: 2.5 cm (1 in.) based on the results from the stationary-nozzle testing.

Therefore, combining Equations [10], [11], [13], and [14], we obtain:

$$h'_{max} \propto (\Delta p)^{5/2}, \qquad [15]$$

$$\tau' \propto (\Delta p)^{-\frac{1}{2}}. \qquad [16]$$

Thus, analogous to the stationary testing, the slot cutting performance of the plain 6.4 mm (0.25 in.) CAVIJET nozzle on Indiana limestone can be predicted by means of Equations [12], [15], [16], and Figure 15. Further discussions of this result are given in Section VII.C.

V. FLOW STUDIES OF SUBMERGED CAVITATING JETS

A. Test Configuration and Procedures

The tests to be discussed in this section were performed in the laboratories of Professor Albert T. Ellis at the University of California, San Diego, in La Jolla (25). These studies were performed with 6.4 mm (0.25 in.) nozzles provided by HYDRONAUTICS. These nozzles were: (a) a plain configuration CAVIJET cavitating fluid jet nozzle and (b) a Leach and Walker nozzle (see Figure 11). As shown schematically in Figure 26, a blow-down water tunnel facility consisting of two large reservoirs was utilized. The upper pressurized reservoir was filled with water prior to the test and then pressurized to the desired value, while the lower tank, by means of a vacuum pump, was set at the desired reduced pressure. The upper tank may be pressurized over a range up to 0.69 MPa (100 psig) while the pressure in the lower reservoir can be reduced to 3.4 kPa (0.5 psig). The size of the system allows ample time for measurement of both inception and desinence of cavitation during the run.

The nozzles were mounted as shown in Figure 26 so that the distance to a "target" could be varied. This target had a flat surface, normal to the flow, which was circular and about 2.5 cm (1 in.) in diameter. Below the surface of the target a lithium niobate piezoelectric crystal was mounted to provide a signal for monitoring pressure pulses caused by cavitation from the nozzles.

In addition to this pressure indication of cavitation, an optical technique was also utilized. A He-Ne laser beam was oriented to pass across the flow just below the face of the nozzle. The presence or absence of cavitation was observed by using a photo-multiplier tube to detect light scattered from the laser beam.

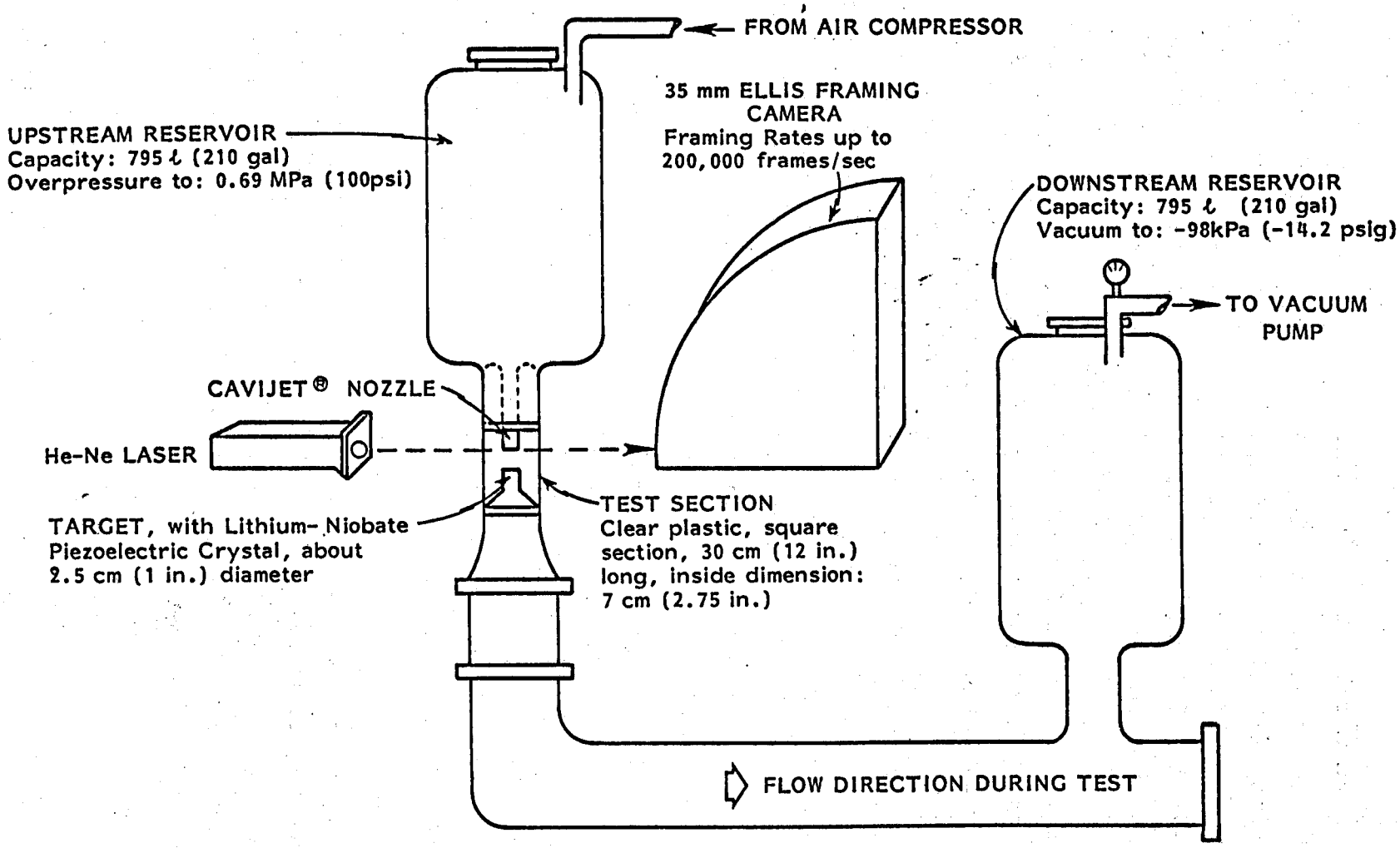

FIGURE 26 - BLOW-DOWN WATER TUNNEL FACILITY AT UNIVERSITY OF CALIFORNIA, SAN DIEGO

Both this optical detector and the crystal pressure readings were used to reconfirm the onset and cessation of cavitation. In addition, a unique high speed photographic technique capable of up to 200,000 frames per second, with extremely short exposure times, was also used to provide visualization of the cavitation in the flow issuing from the nozzles. This camera, which was developed by Professor Ellis, utilizes a laser light source and operates with a Kerr cell for shuttering.

B. Cavitation Inception and Desinence Results

The results of the measurements of cavitation with the CAVIJET cavitating fluid jet nozzle are summarized in Figure 27. These tests were run at three standoff distances, namely with 2, 5 and 10 nozzle diameters for the distance between the face of the nozzle and the target. These data are also summarized in Table 2. Although there is considerable scatter in these observations, it may be seen that for the standoff distances of 5 and 10 nozzle diameters there seems to be a general increasing trend for cavitation inception with increasing Reynolds number. However, at a standoff of two nozzle diameters this trend with Reynolds number does not appear to exist. Indeed, all of the inception measurements at this smallest standoff appear to be relatively constant over the range of Reynolds numbers examined, and to lie in a span of about 0.6 to 0.7.

If these cavitation inception measurements are plotted as in Figure 28, it is seen that there is a trend suggested where at smaller standoff distances larger values of σ_i, the cavitation inception number, are observed. The large bands to the left and right of each averaged point in Figure 28 are not completely due to data scatter, since the Reynolds number effect described in the previous paragraph is responsible for the variations in σ_i at

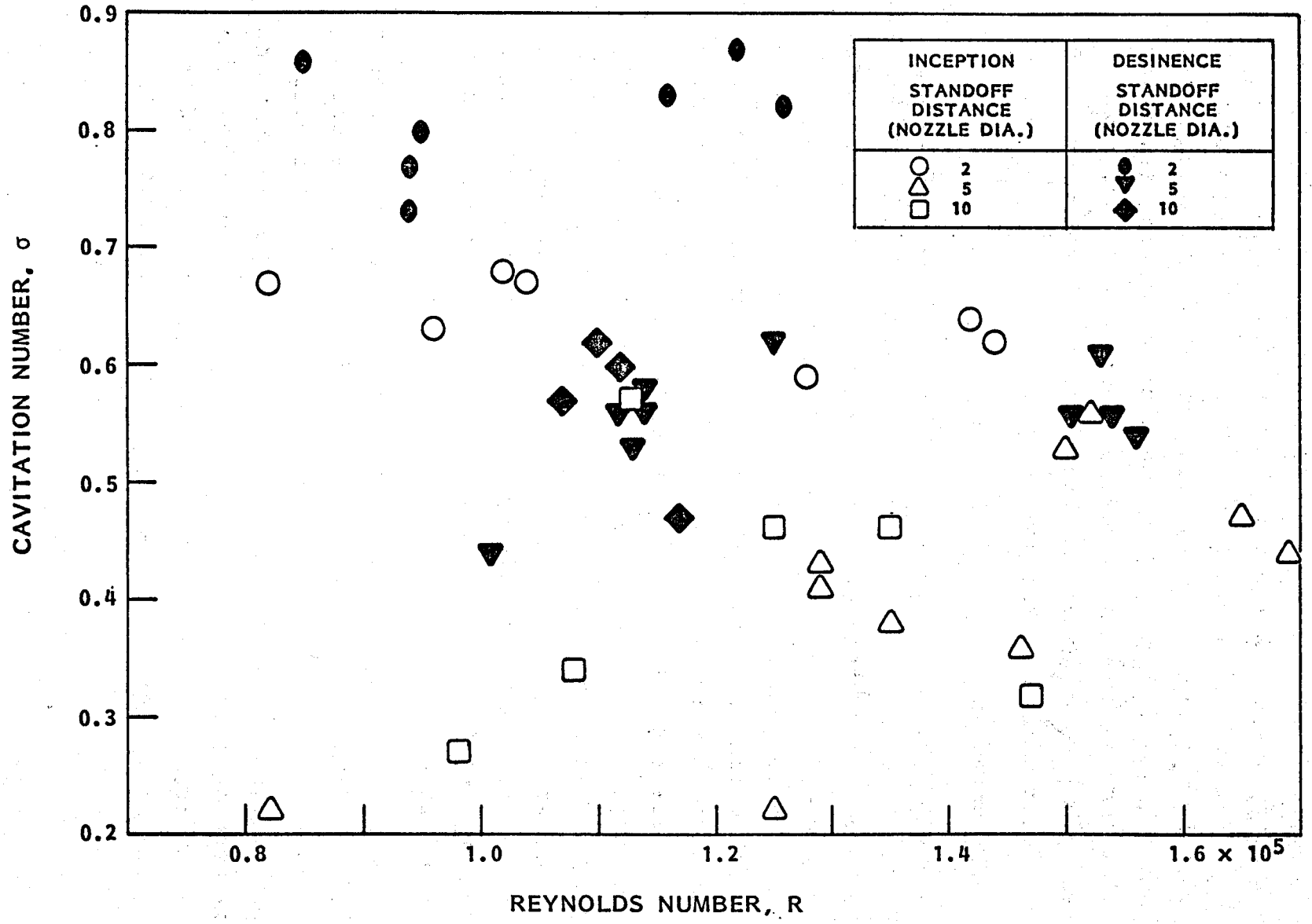

FIGURE 27 - RESULTS FROM FLOW STUDIES AT UNIVERSITY OF CALIFORNIA - SAN DIEGO (Ref. 25); For: plain, 6.4 mm (0.25 in.) CAVIJET® nozzle

TABLE 2

RESULTS FROM FLOW STUDIES AT UNIVERSITY OF CALIFORNIA - SAN DIEGO (REF. 28)

For: Plain, 6.4 mm (0.25 in.) CAVIJET® NOZZLE

INCEPTION			Standoff Distance (Nozzle Diameters)	DESINENCE		
Ambient Pressure (psig)	Reynolds Number	Cavitation Number		Cavitation Number	Reynolds Number	Ambient Pressure (psig)
-6.3	82,000	.67	2	.73	94,000	-3.0
-3.9	96,000	.63	2	.86	85,000	-3.2
-1.5	102,000	.68	2	.80	95,000	-1.5
-1.4	104,000	.67	2	.82	94,000	-1.3
2.8	128,000	.59	2	.83	116,000	6.0
8.7	142,000	.64	2	.82	126,000	9.1
8.5	144,000	.62	2	.87	122,000	9.0
-11.6	82,000	.22	5	.44	101,000	-6.2
-1.4	125,000	.22	5	.58	114,000	-0.8
-1.8	129,000	.41	5	.53	113,000	-2.0
-1.5	129,000	.43	5	.56	114,000	-1.7
-1.8	135,000	.38	5	.56	112,000	-1.6
-0.6	146,000	.36	5	.62	125,000	3.2
7.4	150,000	.53	5	.54	156,000	9.3
8.8	152,000	.56	5	.61	153,000	11.1
8.9	165,000	.47	5	.56	154,000	9.7
8.3	169,000	.44	5	.56	151,000	8.9
-9.6	98,000	.27	10	.57	107,000	-2.5
-7.1	108,000	.34	10	.47	117,000	-2.8
-1.3	113,000	.57	10	.60	112,000	-.9
-1.6	125,000	.46	10	.62	110,000	-.9
.9	135,000	.46	10	.62	110,000	-.9
-1.7	147,000	.32	10			

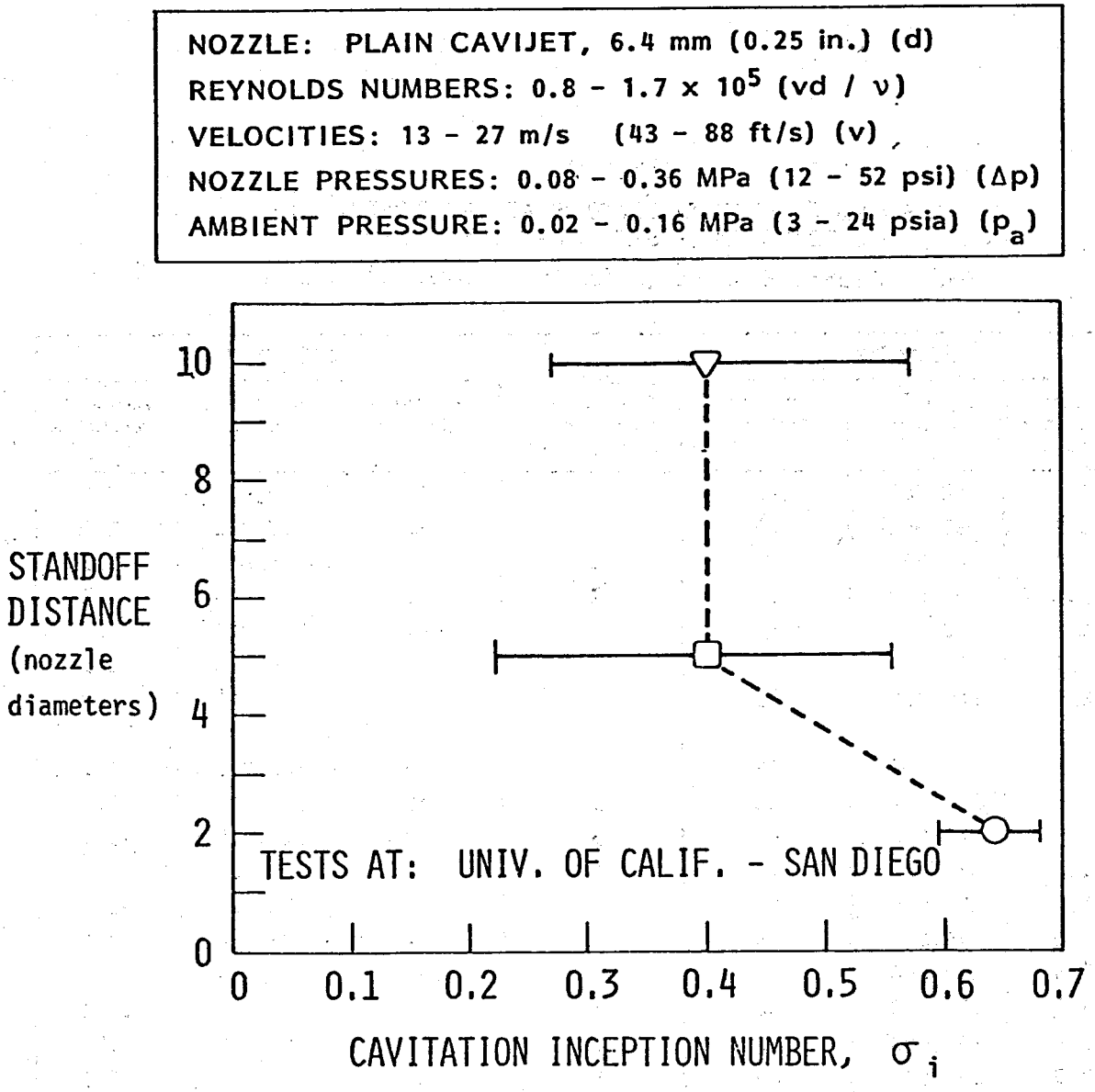

FIGURE 28 - STANDOFF DISTANCE AND CAVITATION INCEPTION: From flow studies at the University of California - San Diego (Ref. 25)

5 and 10 nozzle diameters standoff.

The trend for smaller standoffs at larger values of σ_i is not inconsistent with our, although limited, experience in the erosion measurements with the CAVIJET nozzles. As seen in Figure 29, the standoff for low σ (ambient pressure ≈ atmospheric) tests is about 14 nozzle diameters, while this standoff was reduced to about two to three diameters in the elevated ambient pressure tests. Although this trend was not fully defined by our CAVIJET tests, hence the dotted curve in Figure 29, there have been observations of this same effect in erosion studies of small cavitating jets of oil (26, 27). Although operating at much lower values of Reynolds number (see Section VII.B, and Figure 39), a smooth curve of decreasing standoff versus increasing values of the cavitation number at the point of peak rate of erosion was observed by both of these investigators.

Similar attempts were made to measure cavitation inception and desinence for the Leach & Walker nozzle. However, it was found that it was much more difficult to produce cavitation from this nozzle, since considerably lower cavitation numbers were required to cause cavitation in comparison to the CAVIJET nozzle. Indeed it was necessary to utilize degassed water with the Leach & Walker nozzle before any observations could be made since at the very low pressures required to cavitate this nozzle air bubbles in the flow would grow and obscure the observations with either the photomultiplier or the high speed photography. For this reason no systematic study of the Leach and Walker nozzle was performed, although it was estimated that an approximate inception point for this nozzle occurred at a Reynolds number of about 1.8×10^5 with $\sigma \approx 0.3$ for a standoff of two nozzle diameters.

The high speed photographic records of the CAVIJET nozzle produced visualizations of relatively well defined ring vortices

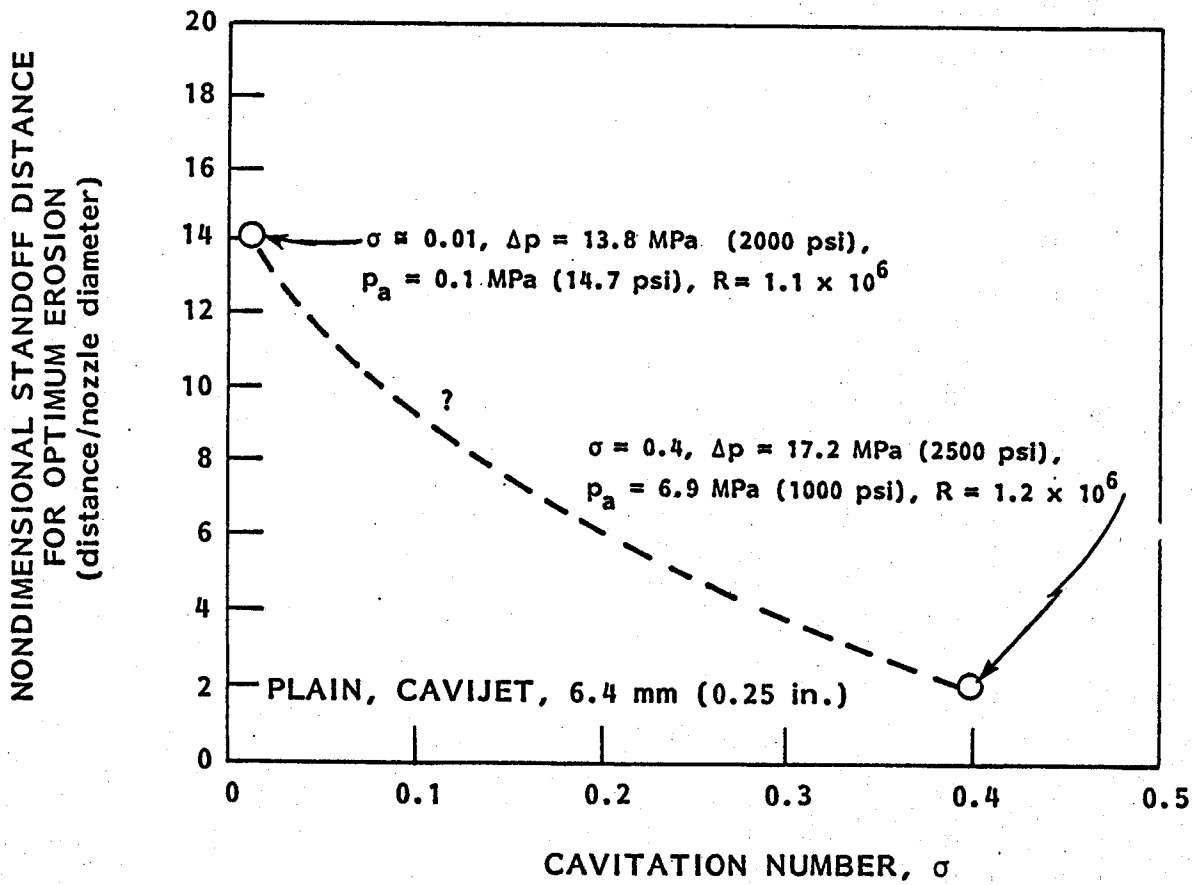

FIGURE 29 - DEPENDENCE OF OPTIMUM STANDOFF ON CAVITATION NUMBER

as indicated schematically in Figure 30. These vortices seemed quite periodic, with a spacing between as indicated by the wave length, λ, approximately equal to the nozzle diameter of 6.4 mm (0.25 in.). The frequency of shedding was also quite periodic and the velocity of these vorticies was approximately one-half that of the jet velocity. The appearance of these well defined ring vortices tends to confirm the appearance of the initially damaged region, namely an annulus with a rather undamaged central region. Lichtarowicz (27) also reports this ring-type of damage. Also, it should be noted that such vortices were not observed with the Leach & Walker nozzle until cavitation numbers well below one-half of those for the CAVIJET nozzle, and were not as well-defined as those from the CAVIJET nozzle. Thus the degree of cavitation at any given cavitation number for the Leach & Walker nozzle would be less than that of the CAVIJET nozzle.

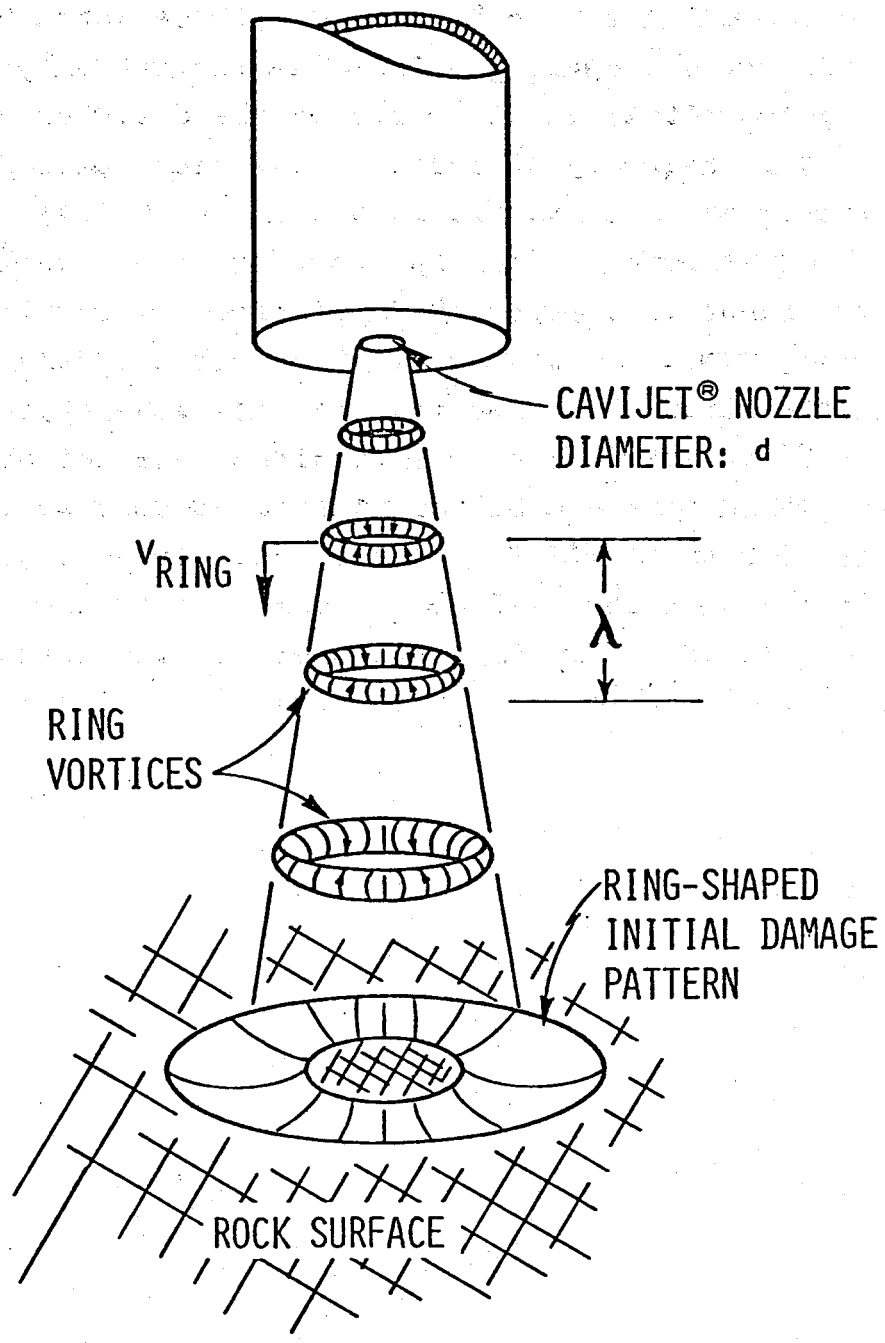

FIGURE 30 – OBSERVATION OF SUBMERGED CAVIJET® NOZZLE FLOW: Ultrahigh speed photography by A.T. Ellis (Ref. 25)

VI. DRILL BIT TESTS AT DRL

A. Objectives of These Tests

Detailed tests with CAVIJET augmented drill bits were not originally planned for the first phase of this program, but it was felt that a limited amount of such tests would provide valuable insights into the performance of CAVIJET nozzles in this situation and would assist in guiding the design efforts during later phases of this study. As discussed in the introduction to this report, testing and analysis with the motivation of optimizing the design of a set of CAVIJET nozzles into various mechanical bit configurations is one of the objectives for the second phase of this program.

The roller bit used in these preliminary tests was selected, not because it presented an optimum configuration for the utilization of the CAVIJET nozzles, but because it was readily available, required minimum modification to accept the available CAVIJET nozzles which had been fabricated of sintered carbide for the stationary nozzle tests describe in Chapter III, and this particular roller bit could be tested within the DRL well bore simulator without modifications to their equipment. Thus, this bit design was such that both of the extended nozzles were located on the same diameter of rotation, 14.3 cm (5.62 in.)(see Figure 31a). This would probably not be desirable for a bit which was specifically designed to utilize the erosive action of CAVIJET nozzles to assist the mechanical cutting by weakening the rock. This weakening of the rock would be best accomplished by, at least, placing two or more nozzles on different circles of rotation. Also optimization studies in Phase II may suggest that the jets should be oriented other than at the perpendicular angle of impingement to the rock face while parallel to the axis of rotation which was

the only possible configuration that could be used with the preliminary bit tests described in this chapter without making major modifications to the bit.

B. Test Configuration and Procedures

These preliminary drill bit tests represent a somewhat more conventional use of the DRL wellbore simulator. A two-cone, extended nozzle roller bit, manufactured by the Smith Tool Co. (28) was adapted for these tests. The configuration of this bit may be seen from the photographs in Figures 31a and 31b and the schematic drawing Figure 32 (this figure is reproduced from Reference 28, courtesy of the author). It may be seen that this bit utilizes three nozzles, the center nozzle has a converging-diverging configuration, designed to clean the intermesh area of the two tungsten carbide studded roller cones. As discussed in Reference 28, this nozzle was observed to experience cavitation in its venturi-like throat region. Thus its discharge coefficient is affected by not only the pressure drop across the nozzle but also the ambient pressure for a given test. This fact was unknown to us when our tests were conducted. However by analysis of the total flow as a function of ambient and nozzle pressure drops, using our prior flow calibrations for the two extended nozzles, we were able to derive the same results measured by Baker for this center nozzle (28).

The only modification to this 20 cm (7-7/8 in.) diameter bit was with regard to the two extended outer nozzles. The normal standoff distance for these nozzles is 3.8 cm (1.5 in.). Extra extensions were provided so that this standoff could be reduced to 1.6 cm (0.62 in.).

The test specimens were solid cylindrical rock specimens with the same outside dimensions as those used in the stationary nozzle

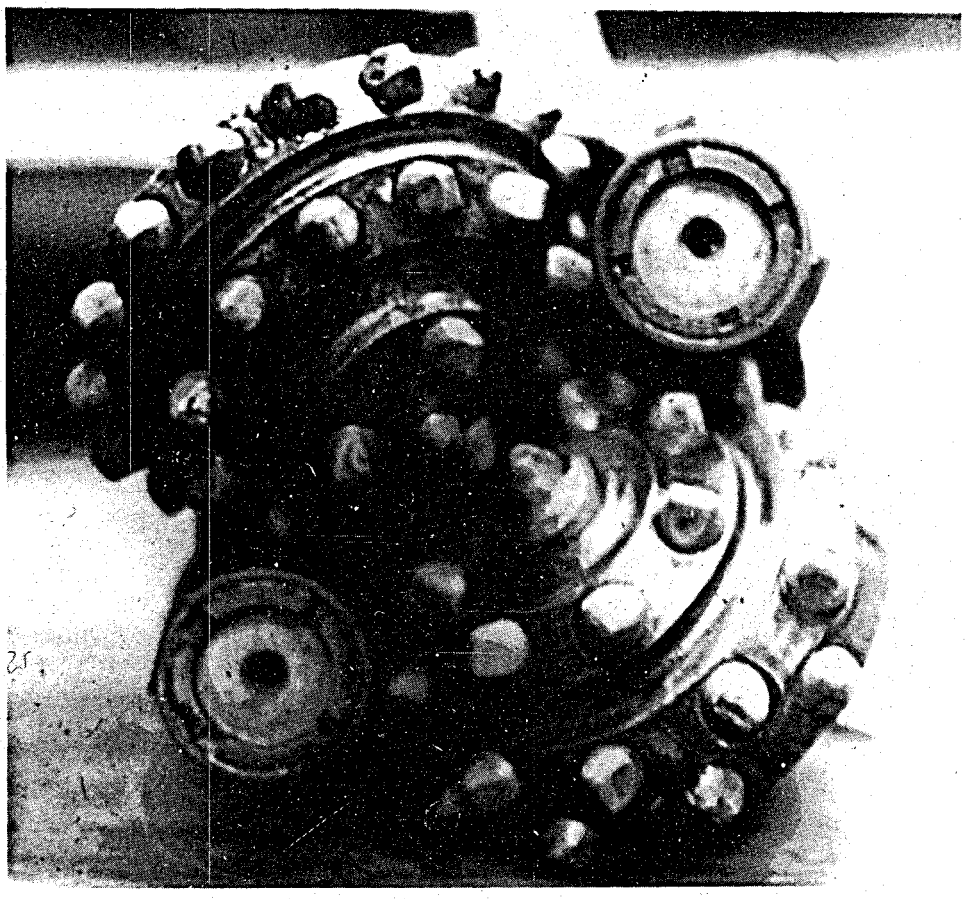

FIGURE 31a - VIEW OF BOTTOM OF TWO CONE ROLLER BIT: Showing two extended nozzles on same diameter of rotation

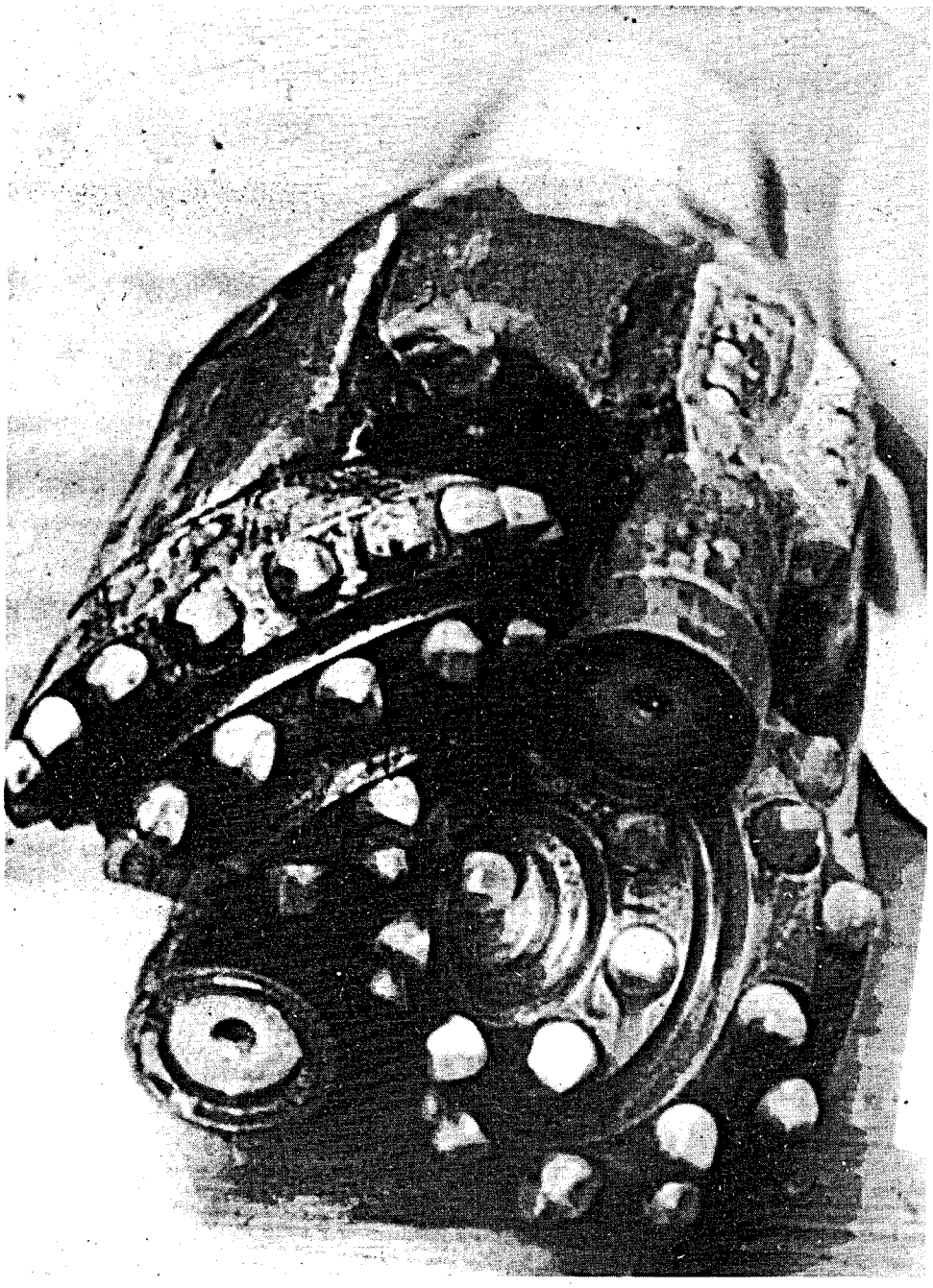

FIGURE 31b – SIDE VIEW OF TWO-CONE ROLLER BIT:
Showing extra extensions for two extended CAVIJET® nozzles

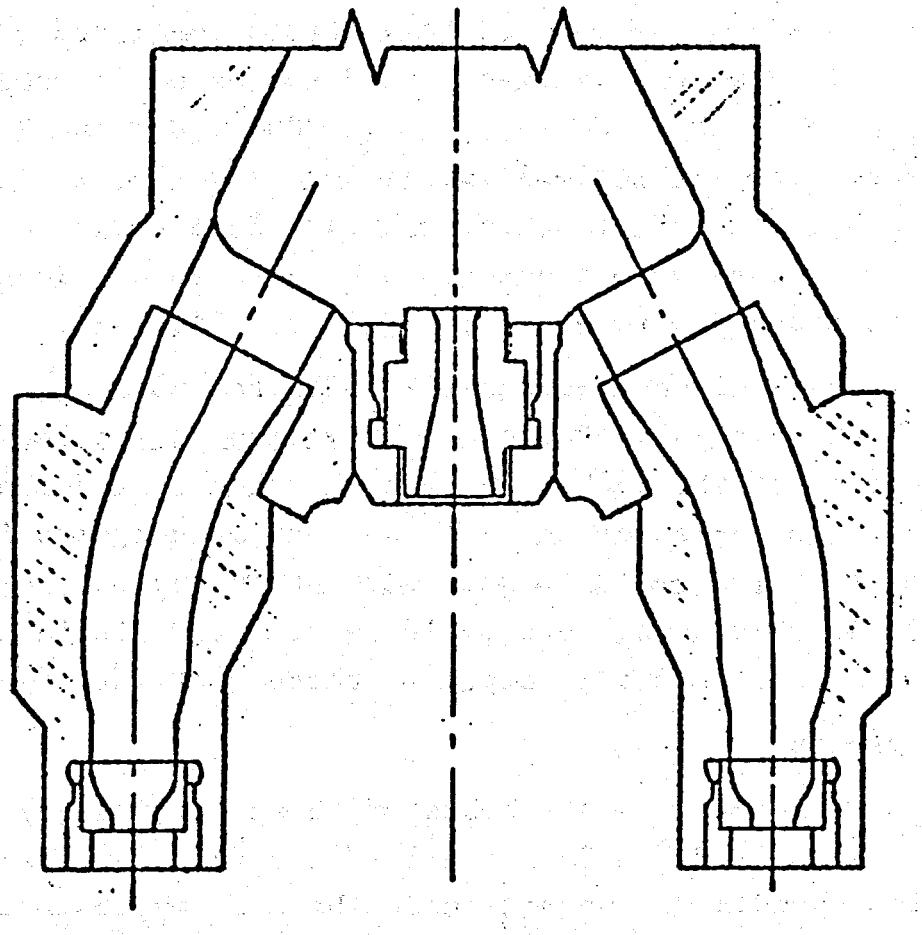

FIGURE 32 - SCHEMATIC OF TWO-CONE ROLLER BIT USED IN PRELIMINARY TESTS AT D.R.L. (Ref. 28)

cutting tests, namely, a length of 91.4 cm (36 in.) and a diameter of 39.4 cm (15.5 in.). Two rock types were used, Colton sandstone and Indiana limestone. During the tests, readings of the rate of penetration, rate of revolution of the bit, and bit weight were recorded as well as the pressures and flow rates as described in Chapter III. The test matrix for these tests consisted of making a series of drilling runs at three fixed values of the nozzle pressure drop, 8.3, 12.4 and 16.5 MPa (1,200, 1,800 and 2,400 psi). Although these were the nominal values for each run, individual tests did show variations in these values. Each series of fixed nozzle pressure drops were conducted over a range of ambient pressures of from about 3.4 to 20.7 MPa (500 to 3,000 psi).

The test on a given specimen was initiated by a slow spud-in to establish the bit in a stable configuration within the first few centimeters of the rock. The bit was then raised about 10 cm (4 in.) above the bottom of the hole so that adjustments in pressure for the next run could be made without "using up rock". In this fashion as many as 21 runs could be achieved within less than the 91.4 cm (36 in.) overall length of these rock specimens.

C. Test Results

A complete summary of the tests of these preliminary drill bits is outlined in Table 3, and all of the data for these tests are given in Appendix C. We will describe some typical results in this section. The first series of tests were run in Colton sandstone, a rock which had been previously examined in the wellbore simulator by the staff at DRL (29). This provided guidance for planning our test parameters. All of the tests on the Colton sandstone as well as the Indiana limestone were run at the same rotary rate of 60 rpm. However for the relatively harder Colton sandstone the bit weight was 44.4 kN (10,000 lb.). The second series, conducted on Indiana limestone, was run with a bit weight

TABLE 3

SUMMARY OF ROLLER BIT* TESTS AT DRL

Test Series	Test No.	Center** Nozzle	Extended*** Nozzle	Standoff Distance		Type of Rock	No. of Successful Runs
				cm	in.		
2	1	A	Smith	3.8	1.5	Colton Sandstone	0
2	2	A	Smith	3.8	1.5	Colton Sandstone	0
3	3	A	Smith	1.6	0.62	Colton Sandstone	15
3	4	A	Plain CAVIJET	1.6	0.62	Colton Sandstone	16
3	5	A	Plain CAVIJET	1.6	0.62	Colton Sandstone	15
3	6	A	Centerbody CAVIJET	1.6	0.62	Colton Sandstone	0
4	1	B	Smith	1.6	0.62	Indiana Limestone	15
4	2	B	Smith	3.8	1.5	Indiana Limestone	16
4	3	B	Plain CAVIJET	1.6	0.62	Indiana Limestone	19
4	4	B	Centerbody CAVIJET	1.6	0.62	Indiana Limestone	21

* Bit Type: 20 cm (7-7/8 in.) diameter, Smith Tool Company, two-cone roller bit with two extended nozzles

** Center Nozzle: TYPE A: 0.79 cm (0.31 in.) diameter center nozzle
TYPE B: 0.64 cm (0.25 in.) diameter center nozzle

*** All extended nozzles had a nominal orifice diameter of 6.4 mm (0.25 in.)

of one-half of that for the Colton sandstone, i.e., 22.2 kN (5,000 lb.). Comparing the raw data penetration rates seen in Figures 33 and 34 it is seen that, under the same conditions at a nozzle pressure drop of 16.5 MPa (2,400 psi), despite the higher bit weight for the Colton sandstone considerably lower rates of penetration were achieved relative to those for the Indiana limestone. It is seen from these figures that in the Colton sandstone rates of penetration of about 1.5 to 3 m/hr (about 5 to 9 ft per hr.) were measured. This should be compared to the rates with the Indiana limestone which, under the same Δp value, were about 3.5 to 7 m/hr (about 12 to 24 ft/hr). The three successful tests with the Colton sandstone were all conducted with the standoff distance for the two extended nozzles set at the 1.6 cm (0.62 in.) value. One run was made with the standard Smith Tool Co. 6.4 mm (0.25 in.) nozzles in the extended locations and the other two tests were run with plain 6.4 mm (0.25 in.) CAVIJET nozzles replacing the Smith nozzles. A feel for the scatter in the measurement of penetration rates may be gained by comparing the data for the two CAVIJET nozzles in Figure 33. For the second series of tests conducted on the Indiana limestone a comparison was made of the performance of the standard Smith Tool nozzles when located either at the original design standoff of 3.8 cm (1.5 in.) versus the added extension standoff distance of 1.6 cm (0.62 in.). As seen in Figure 34 moving these nozzles closer to the rock surface seems to measureably improve the rate of penetration. Consistently in these tests the smaller standoff distance provided higher rates of penetration.

A comparison was also made in these tests on the Indiana limestone of the performance of plain CAVIJET nozzles versus CAVIJET nozzles provided with a 3.2 mm (0.125 in.) conventional centerbody. Results shown in Figure 34 with regard to the rate

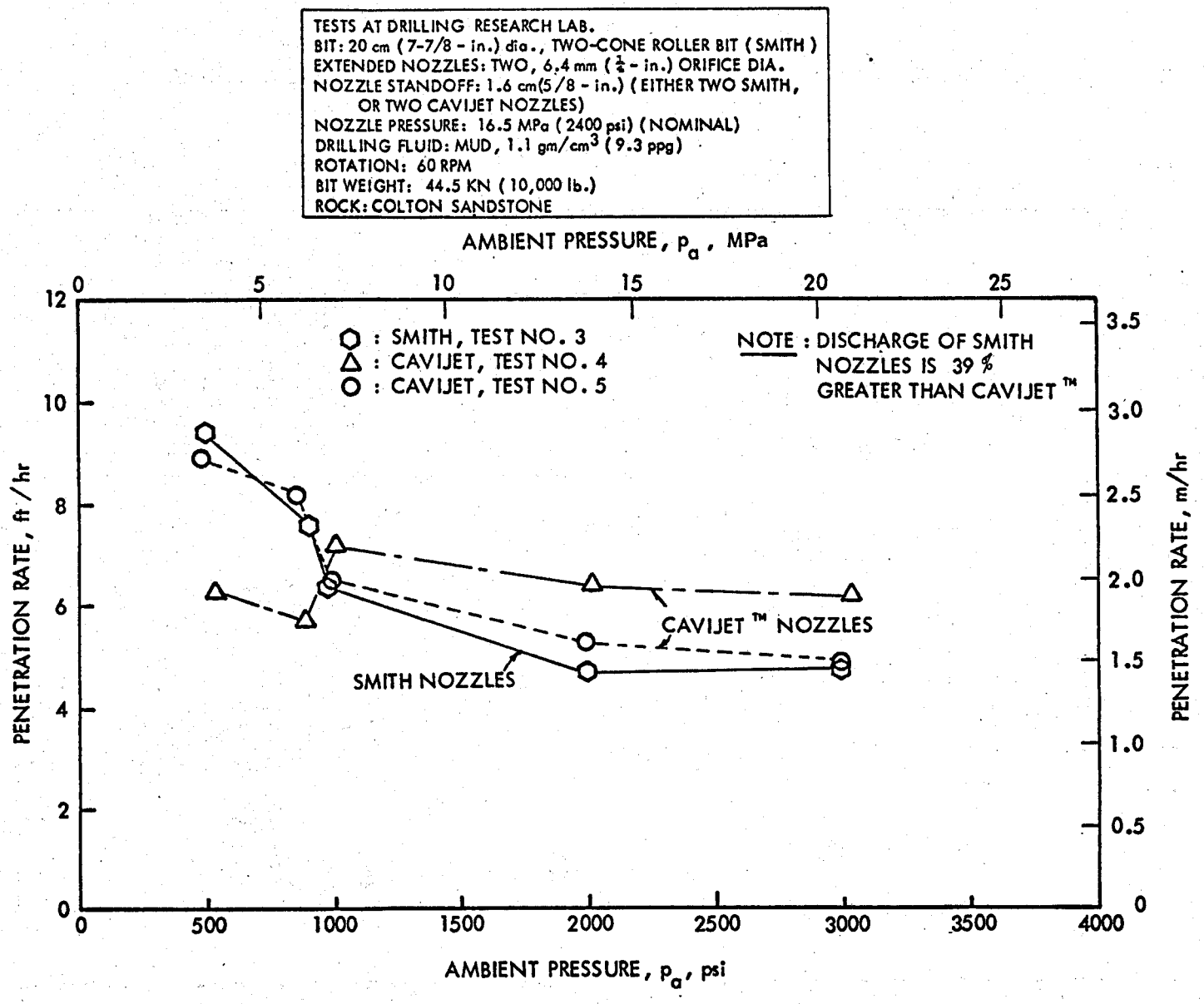

FIGURE 33 - COMPARISON OF PENETRATION RATES IN COLTON SANDSTONE, Δp = 16.5 MPa (2,400 psi)

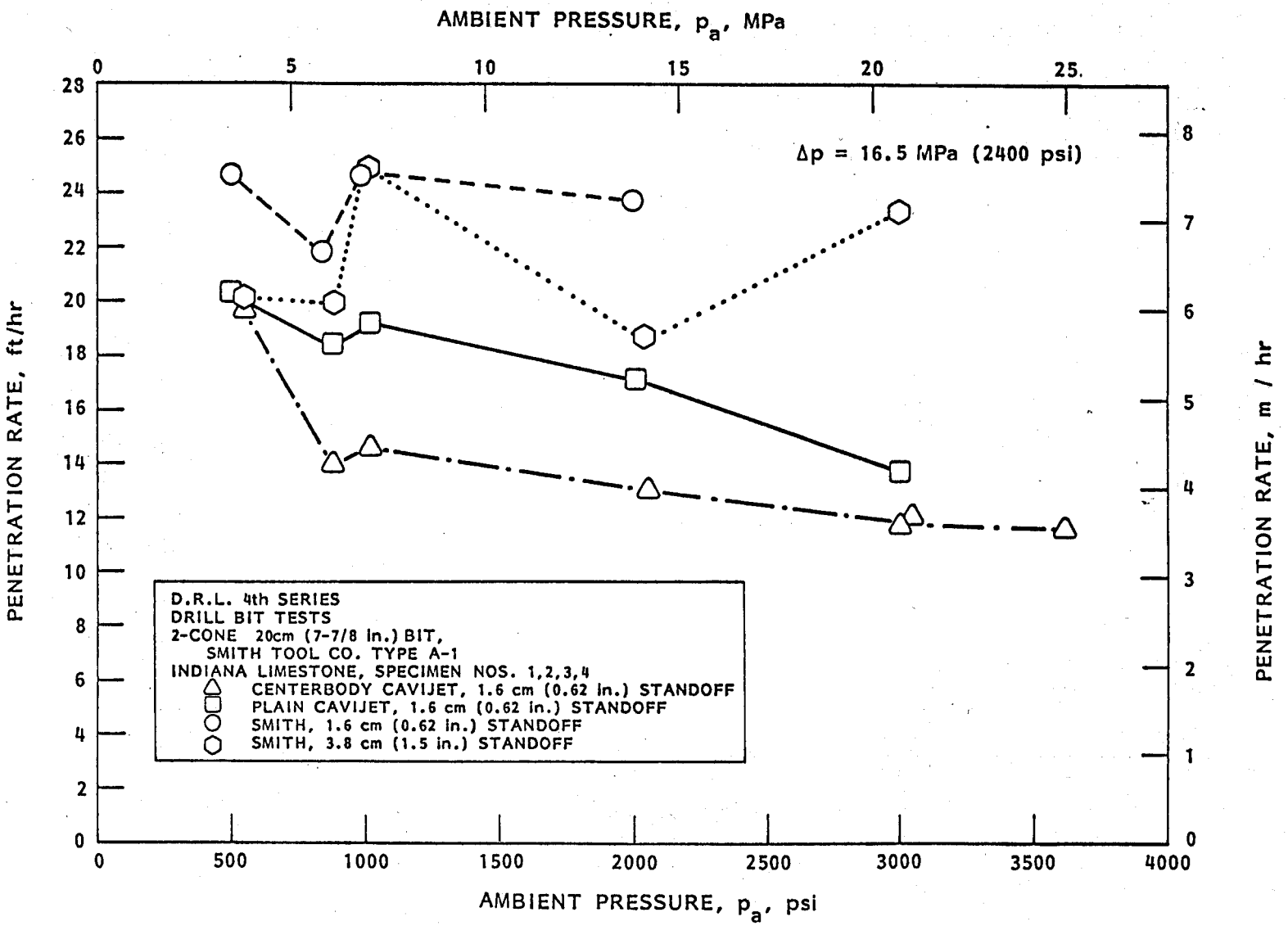

FIGURE 34 - COMPARISON OF PENETRATION RATES IN INDIANA LIMESTONE, Δp = 16.5 MPa (2,400 psi)

of penetration were not considered necessarily typical since, as may be observed by examining the raw data in Appendix C, at lower values of nozzle pressure the centerbody CAVIJET configuration seemed to provide either higher or comparable rates of penetration. These variances in the rates of penetration may indeed be considered to be within the scatter of the data, and hence should not be considered conclusive based on these minimal tests.

To attempt to account for the different discharge coefficients of the CAVIJET nozzles and the Smith Tool Company bit nozzles these rate of penetration data were normalized as seen in Figures 35 and 36. Here we have plotted a "specific penetration rate" derived by dividing each rate of penetration by the actual hydraulic power delivered by only the two extended nozzles for each test. This particular normalization of the raw data was motivated by the usual practice of attempting to determine the proper hydraulic power in terms of the area of hole bottom created by the bit. Thus, although this bit contained three nozzles, the role of the center diffuser nozzle is to clean the cones (28) with little if any contribution either to clearing chips from the rock surface or weakening the formation by erosion. Hence, it was decided to exclude the hydraulic power delivered by the center nozzle from the derivation of "specific penetration rate." It may be seen that when the greater discharge of the Smith Tool Company nozzles is thus accounted for, a significantly more effective drilling efficiency is observed for the CAVIJET nozzles in both the Colton sandstone and the Indiana limestone. In future tests, nozzle sizes should be adjusted so that the same actual flow rates of mud would be utilized at a given nozzle pressure to allow direct comparisons of penetration rates.

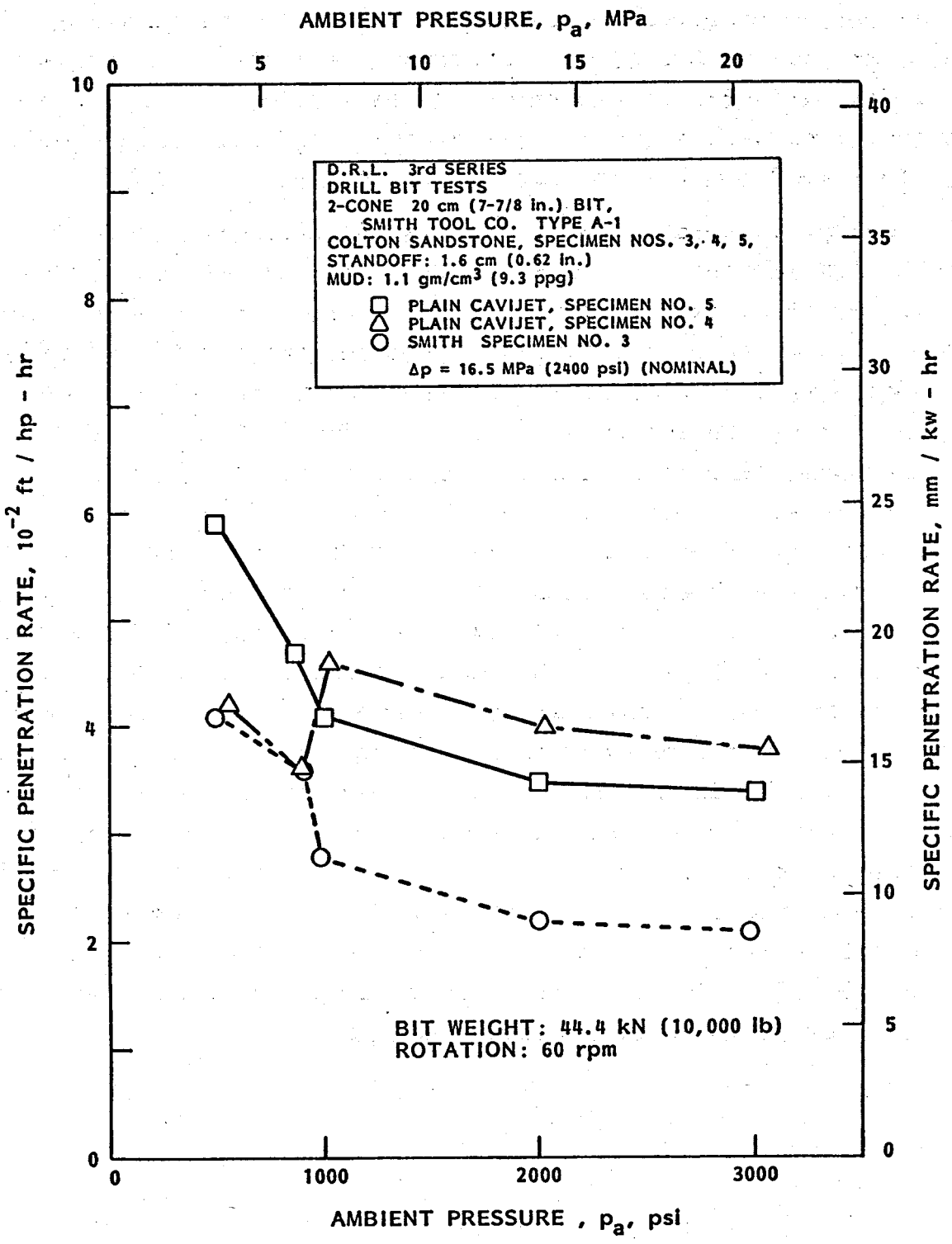

FIGURE 35 - COMPARISON OF SPECIFIC PENETRATION RATES IN COLTON SANDSTONE; Δp = 16.5 MPa, (2400 psi); rotation: 60 rpm; bit weight: 44.4 kN (10,000 lb)

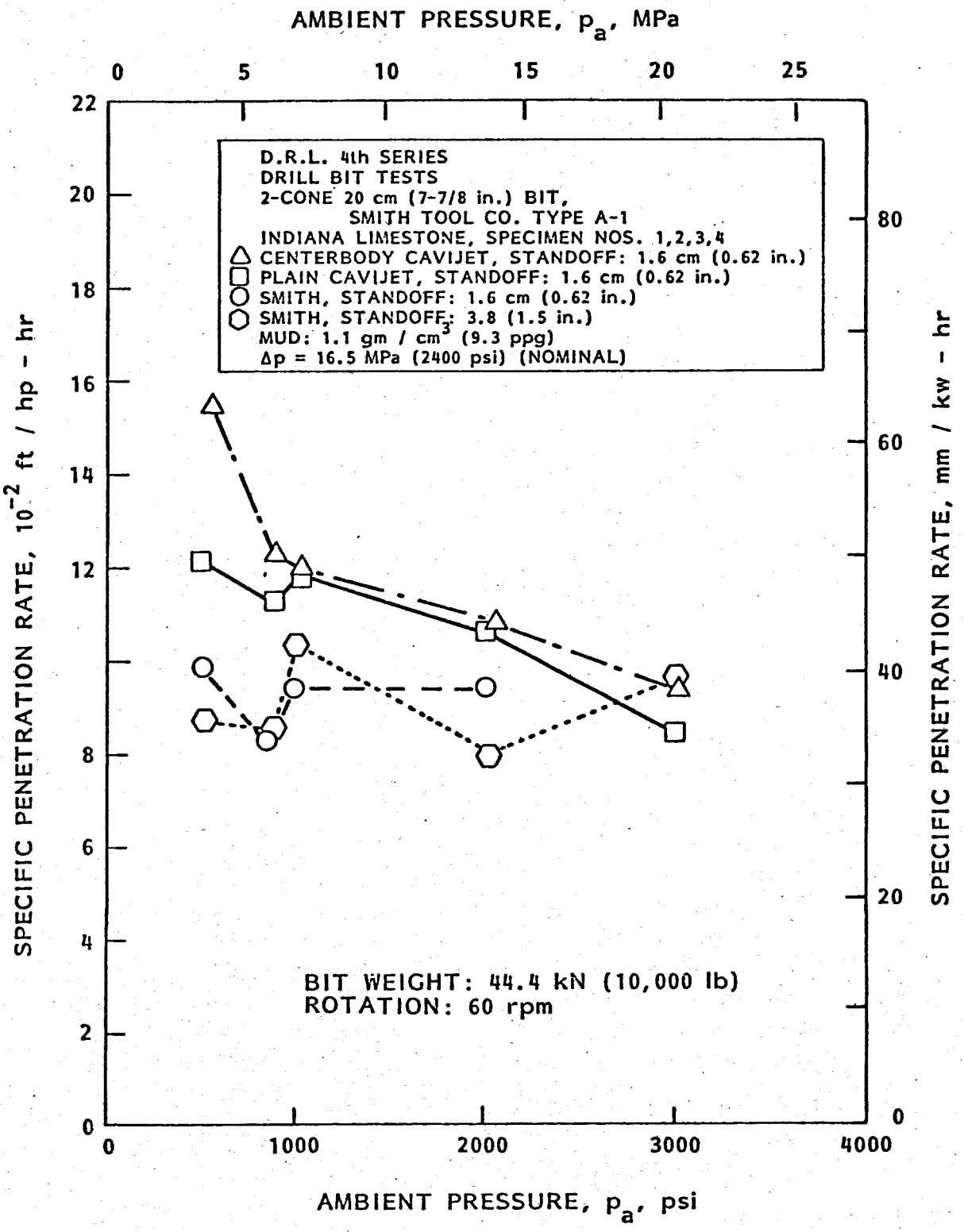

FIGURE 36 - COMPARISON OF SPECIFIC PENETRATION RATES IN INDIANA LIMESTONE; Δp = 16.5 MPa (2,400 psi) rotation: 60 rpm; bit weight: 22.2 kN (5,000 lb)

VII. GENERAL DISCUSSION OF RESULTS

In this chapter, discussions will be provided of the various experimental results obtained during this program. Relationships among these results will be examined, as well as descriptions of how these tests have served to define the feasibility of using the CAVIJET cavitating fluid jet method to augment deep hole mechanical drill bits.

A. Effect of Depth on Cutting Rates

The experimental results from the stationary nozzle rock cutting tests conducted at DRL (see Chapter III) were used to derive an empirical description of the effect of cavitation number on the averaged depth cutting rate. This dependence on σ is typified by the curve in Figure 15 for the plain 6.4 mm (0.25 in.) CAVIJET nozzle. However, it is of interest to also provide a direct estimate of the effect of ambient pressure in terms of hole depth.

To derive an estimate of CAVIJET nozzle cutting as a function of depth, it was first necessary to select a typical set of conditions as the basis for describing the relation between cavitation number and depth. As indicated schematically in Figure 37, these conditions were:

Mud Pump: Swivel pressure: 19.3 MPa (2,800 psi)
Mud flow rate: 17.7 l/s (280 gpm)

Bit: Two cone, roller bit; 20 cm (7-7/8 in.) diameter

Drill pipe: 11.4 cm (4½ in.)

Liner: 20 cm (7-7/8 in.), from surface down to 450 m (1,500 ft)

Drill collar: 16.5 cm (6½ in.), length: 140 m (450 ft)

Mud: 1.1 gm/cm^3 (9.3 ppg), water based, 10cp apparent viscosity

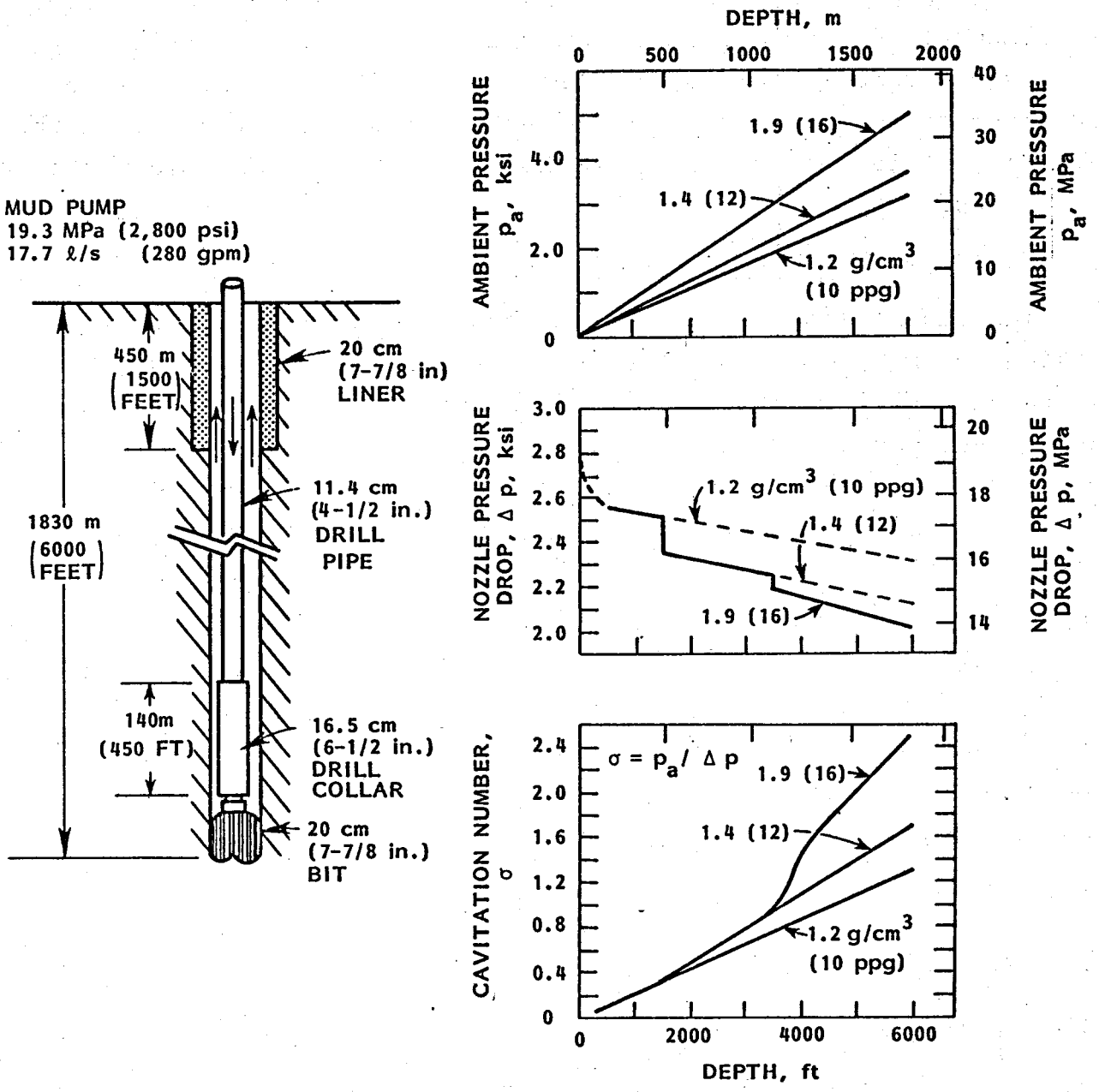

FIGURE 37 - DERIVATION OF DEPENDENCE OF CAVITATION NUMBER ON HOLE DEPTH

Using this hypothetical drill string, the pressure losses in the system were estimated, and used to derive the net pressure drop available across the bit nozzles as a function of depth. Using these Δp-values, with the ambient pressure head, p_a, the cavitation number (defined by Equation [2]) was obtained as indicated in Figure 37 for various mud weights as a function of depth. Note that even with 1.9 gm/cm^3 (16 ppg) mud, a Δp of over 13.8 MPa (2,000 psi) would still be available at 1,830 m (6,000 ft) under these conditions.

To provide the estimate of depth effect, a constant Δp of 13.8 MPa (2,000 psi) was used, with a constant mud density of 1.1 gm/cm^3 (9.3 ppg) since these two approximations have offsetting effects. Thus, the curve in Figure 13, for Δp = 13.8 MPa (2,000 psi) was used to directly derive the depth dependence shown in Figure 38.

It should be emphasized that this curve in Figure 38 tends to underestimate cutting rates at the shallow depths, since nozzle pressures well above the assumed constant value of 13.8 MPa (2,000 psi) are available in many actual drilling rigs. Also this curve tends to overestimate the roll-off in cutting rate with depths down to 1,830 m (6,000 ft) since the use of the constant Δp tends to exaggerate the increase of σ with depth. However, despite these deliberately conservative assumptions, this estimate of depth effects suggests that enhanced cutting rates by a CAVIJET nozzle can be anticipated, relative to surface rates (atmospheric ambient pressure), until depths of at least 1,200 m (4,000 ft) and possibly deeper.

B. Cavitation Inception and Peak Cavitation

As discussed in the Introduction, the scaling parameter known as the cavitation number, σ, can be used to describe the

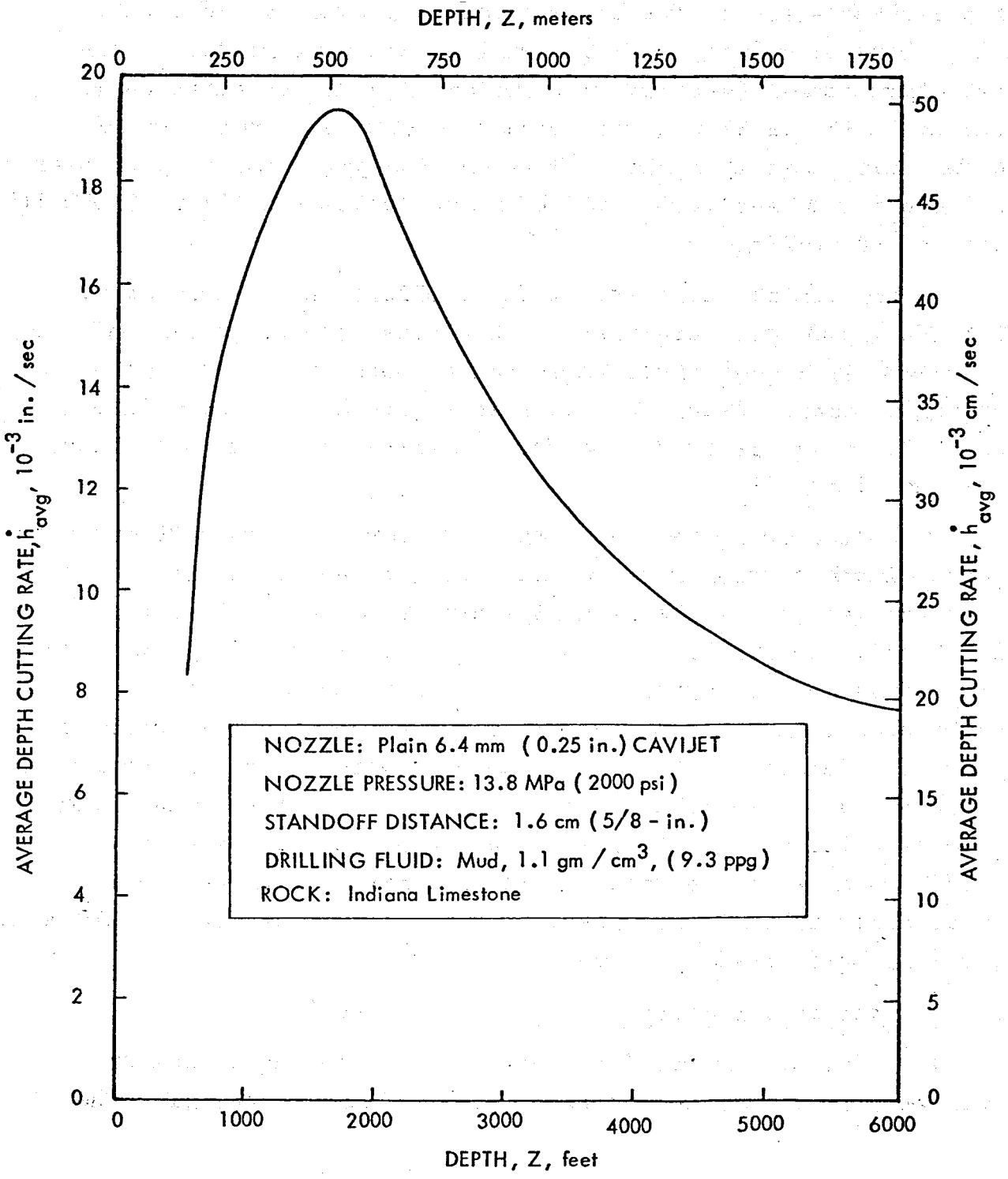

FIGURE 38 - EFFECT OF DEPTH ON CAVIJET®. STATIONARY CUTTING RATE

degree of cavitation, and hence the erosive potential in any fluid dynamics situation. For understanding the potential effectiveness of the CAVIJET method in cutting rocks downhole, σ is thus the parameter which we can use to interrelate experiments conducted under a variety of conditions both under this program and by other investigators. The definition for the cavitation number, as given in Equation [2] will be used in this section, where, as indicated by Equation [3] , the pressure drop across the nozzle is calculated by taking the difference between upstream and downstream pressure measurements.

It will be seen from the following discussion that the concept of scaling by means of σ, and the Reynolds number R:

$$R = \frac{v_j \, d}{\nu} \qquad [17]$$

where:

v_j = is the jet velocity, estimated from: $v_j = \sqrt{2 \quad \Delta p / \rho}$,
ρ = fluid density, Δp = pressure drop across the nozzle or orifice,

d = is the nozzle or orifice diameter (corrected, where possible, for differences in discharge coefficient), and

ν = is the kinematic viscosity of fluid,

can provide a consistent picture of the behavior of submerged cavitating jets.

Let σ_i be the value of cavitation number describing a ratio of p_a and Δp which allows the inception of cavitation in a submerged jet, i.e., for values of σ larger than σ_i no cavitation bubbles can be seen (or heard). Thus, for downhole applications, below some depth σ would exceed σ_i and hence erosive effects from cavitation should no longer be expected. The curves as shown typically in Figure 15 suggest that σ_i is about 1.8 to 2.0 for

the plain 6.4 mm (0.25 in.) CAVIJET used in the tests at DRL. The Reynolds number in these tests is about 1.2×10^6. If we let σ_p represent the value of σ where curves of the type seen in Figure 15 reach a peak rate of cutting, then $\sigma_p \approx 0.4$ appears to be the value for this nozzle. The purpose of the following discussion is to show that these values of σ_i and σ_p are consistent both with the observations made at UCSD (see Figure 27), as well as measurements reported by Rouse (30), Ball (31), Jorgensen (32), Lienhard & Stephenson (33), Kleinbreuer (26), and Lichtarowicz (27).

These studies, as seen in the summary in Table 4, cover a range of almost three orders of magnitude in R and over two orders of magnitude in σ. However, when plotted, as in Figure 39, a well-defined trend is seen. The straight lines in this figure are plotted so that the relation between σ and R is:

$$\sigma \propto R^{2/3}. \qquad [18]$$

Equation [18] is comparable to the relation:

$$\sigma_i \propto d^{2/3} \qquad [19]$$

reported by Lienhard & Stephenson (33). However we found that by including estimates of the jet velocities (and viscosities, but since all of these studies considered by Lienhard & Stephenson were in water, this was not a variable) a somewhat improved trend was derived.

Thus, within rather large bands of uncertainty based on the necessity to estimate pressure drops (and the derived jet velocities) the orifices tend to have larger values of σ_i relative to the conventional nozzles which are constructed with long, gradually

TABLE 4

SUBMERGED CAVITATING JET STUDIES

Source	Diameter cm	Jet Velocity, 10^3 cm/s	Reynolds Number, R	Cavitation No.
CAVITATION INCEPTION (WATER, ν = 1 cs), NOZZLES				
Rouse (Ref.30)	3.81	1.5 - 2.6	$5.8 - 9.8 \times 10^5$	0.55 - 0.60
Ball (Ref.31)	3.39	2.0 - 2.3	$6.9 - 7.8 \times 10^6$	0.7 - 1.2
Jorgensen (Ref.32)	0.95	2.4 - 3.6	$2.2 - 3.5 \times 10^5$	0.2 - 0.4
	1.91	2.1 - 2.7	$4.0 - 5.2 \times 10^5$	0.3 - 0.5
	1.91	1.8	3.5×10^5	0.4 - 0.5
	3.81	1.6	6.0×10^5	0.75 - 0.9
Lienhard & Stephenson (Ref.33)	0.32	≈3.4	$\approx 1.1 \times 10^5$	0.24
Ellis & Starrett (Ref.25)	0.64 CAVIJET® Nozzle	1.9 - 2.5	$1.2 - 1.6 \times 10^5$	0.3 - 0.6
	0.64 Leach & Walker Nozzle	≈2.8	$\approx 1.8 \times 10^5$	≈ 0.3
CAVITATION INCEPTION (WATER, ν = 1 cs), ORIFICES				
Ball (Ref.31)	3.18	2.0 - 2.9	$6.4 - 7.3 \times 10^5$	1.0
	4.45	2.0 - 2.9	$9.0 - 10.2 \times 10^5$	1.2
	6.03	2.0 - 2.9	$1.2 - 1.4 \times 10^6$	1.4
Lienhard & Stephenson Ref.33)	0.16	≈3.4	$\approx 5.4 \times 10^4$	0.12
	0.32	≈3.4	$\approx 1.1 \times 10^5$	0.2
	0.64	≈3.4	$\approx 2.1 \times 10^5$	0.58
PEAK-EROSION CAVITATION NUMBER, NOZZLES				
Kleinbreuer (Ref.26) Oil; ν = 50 cs	0.045	22.4	2×10^3	0.005
Lichtarowicz (Ref.27) Oil; $\nu \approx 2$ cs	0.0477	13.9 - 22.0	$3.3 - 5.2 \times 10^4$	0.02
CAVIJET® Water, ν = 1 cs Mud, ν = 10 cs	0.64	16.8	1.2×10^6	0.4

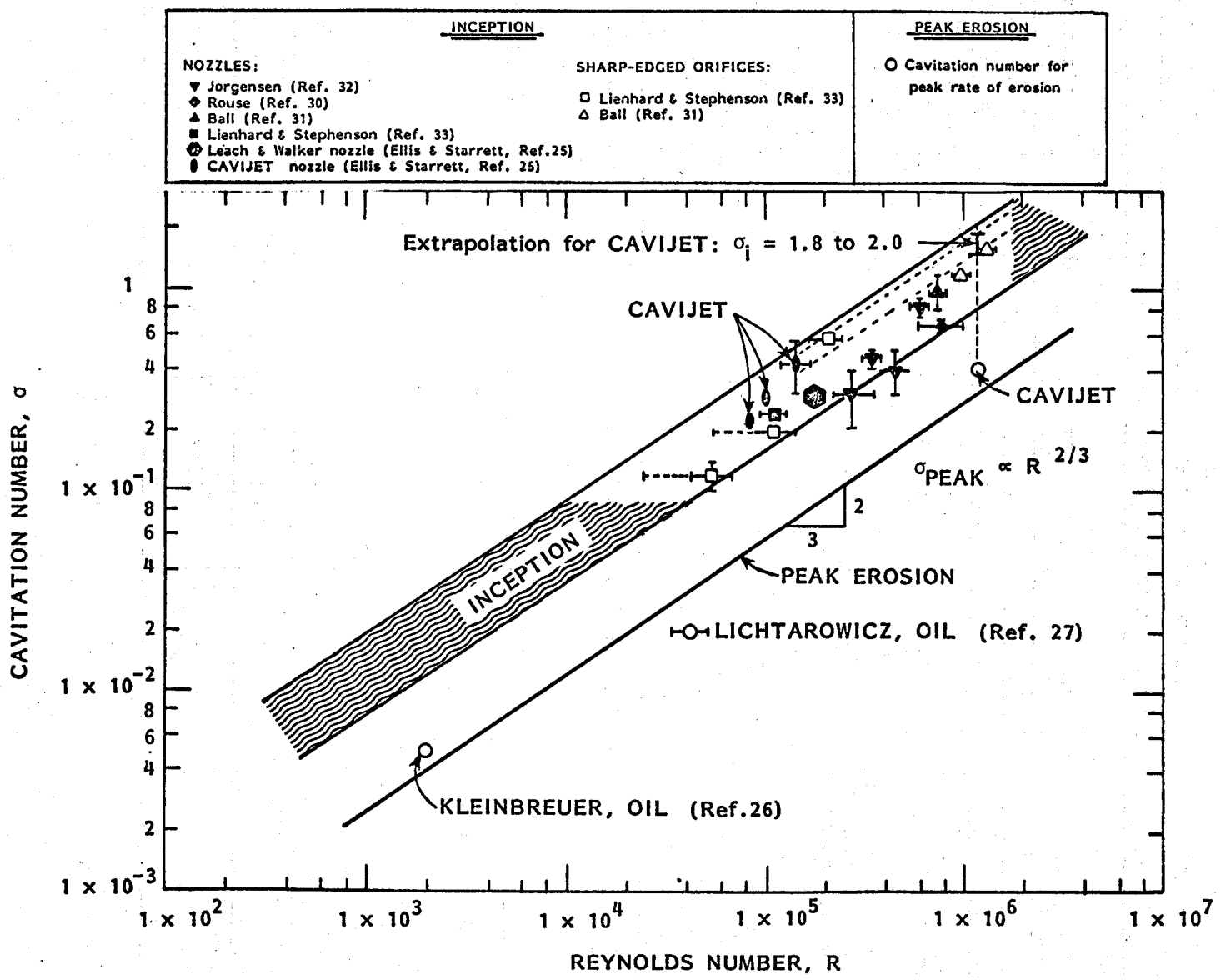

FIGURE 39 - DEPENDENCE OF CAVITATION NUMBER ON REYNOLDS NUMBER FOR SUBMERGED CAVITATING JETS

tapering exits. Inception for the plain CAVIJET nozzle, as measured by Ellis & Starrett (25) is, as expected, more nearly allied with the orifice inceptions. This is because, as shown schematically in Figure 1, the plain CAVIJET nozzle has a rapidly converging bore and a short, orifice-like exit geometry.

Although the capabilities of the UCSD blow-down facility limited their σ_i measurements to a range of Reynolds numbers about an order of magnitude lower than in the erosion tests at DRL, the curves in Figure 39 suggest how these σ_i results could be extrapolated. As seen in Figure 39, this extrapolation results in predicted σ_i's of about 1.8 to 2.0, the same inception suggested (see Figure 15) by our stationary-nozzle rock cutting experiments. Further tests, at full scale Reynolds numbers within the new pressure cell at HYDRONAUTICS (modified to allow observation of the inception) should be conducted to confirm this analysis. However, this model of the effects of the various relevant fluid dynamics and nozzle parameters (Equation [18]) should serve as a useful guide to future optimizations of new CAVIJET nozzle configurations that are to be specially designed to increase σ_i for deep-hole utilizations.

C. Prediction of CAVIJET Nozzle Performance

The experimental results from the stationary-nozzle rock cutting tests at DRL (Chapter III), plus the stationary-nozzle and slot cutting results from the tests conducted in the pressure cell at HYDRONAUTICS (Chapter IV), have provided a complete empirical description of how the plain and centerbody CAVIJET nozzle types are affected by:

i) ambient pressure, p_a

ii) nozzle pressure drop, Δp

iii) velocity of translation of the jet, v.

In summary, the slot cutting depth, h', of these CAVIJET nozzles was found to to empirically predicted by the equation:

$$h' = h'_{max} \left(1 - e^{\frac{-D}{V\tau'}}\right) \qquad [12]$$

where: h'_{max}, τ', and D are experimentally determined constants, which depend on both the nozzle type and the erosion strength of the rock. With cavitation number fixed, h'_{max} and τ' vary with changes in Δp in accordance with:

$$h'_{max} \propto (\Delta p)^{5/2} \qquad [15]$$

$$\tau' \propto (\Delta p)^{-\frac{1}{2}} \qquad [16]$$

and, as discussed in Chapter IV, h'_{max} and τ' can be derived directly from the h_{max} and τ values for the stationary-nozzle rock cutting tests. To include the effect of changing the cavitation number, these parameters can be scaled as shown by a curve of the type shown in Figure 15. Thus, once h' and τ' are known at $\sigma_p = 0.4$, for the plain CAVIJET nozzle, values of these two parameters at any other σ can be scaled down as a percentage of the peak value by using a curve as in Figure 15.

For instance, as shown in Figure 40, the effect of varying Δp can be predicted for a given cavitation number. Alternatively, at any given translation velocity, as shown in Figure 41, the effects of varying the ambient pressure at a fixed or varying Δp can be examined to explore, for instance, how the slot depth can be expected to change as the bit moves down-hole. Thus, from a sequence of stationary nozzle tests, sufficient only to define the dependence of h_{max} and τ on p_a, Δp, and σ, and a single series

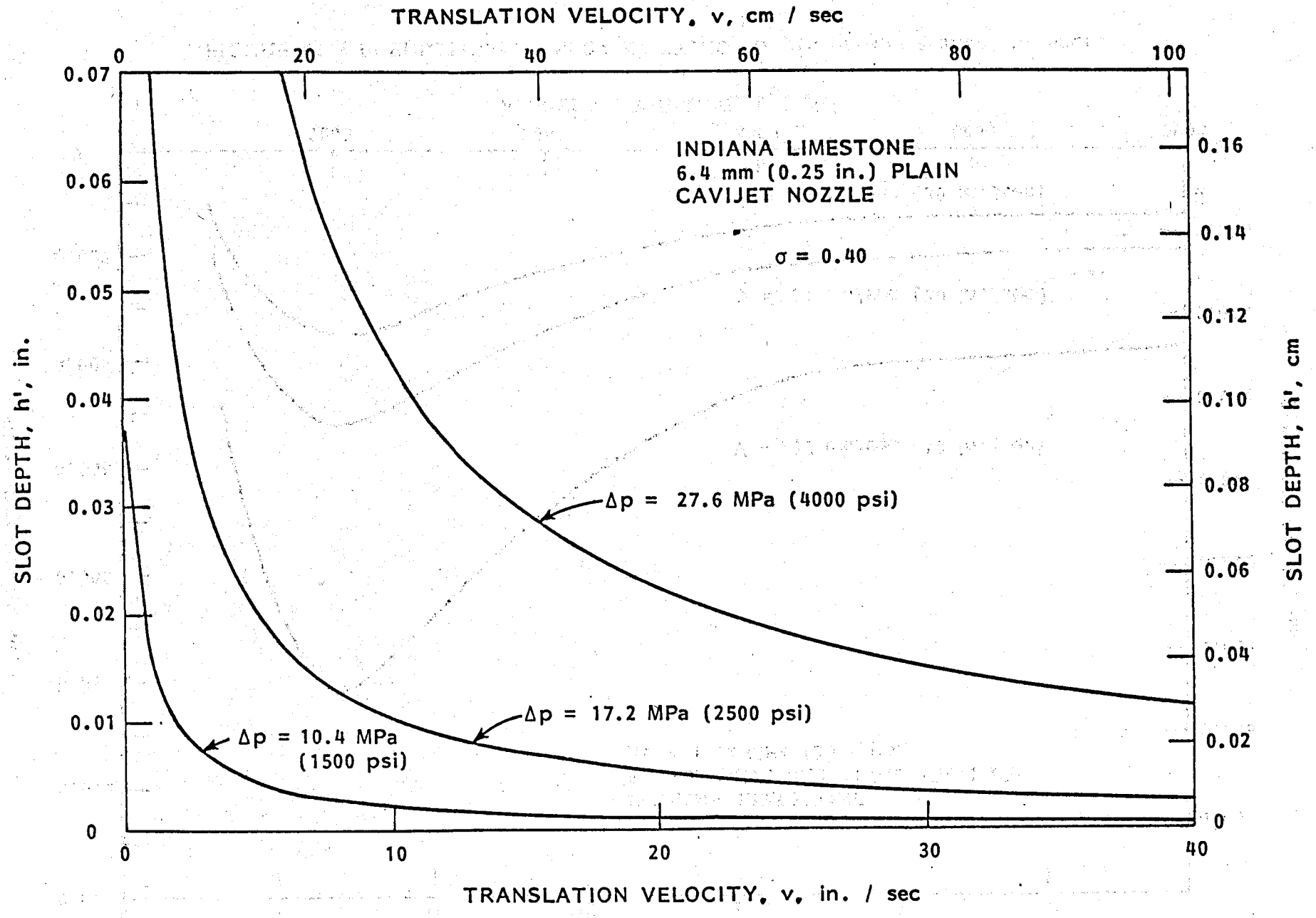

FIGURE 40 - PREDICTION OF SLOT CUTTING: Depth versus translation velocity

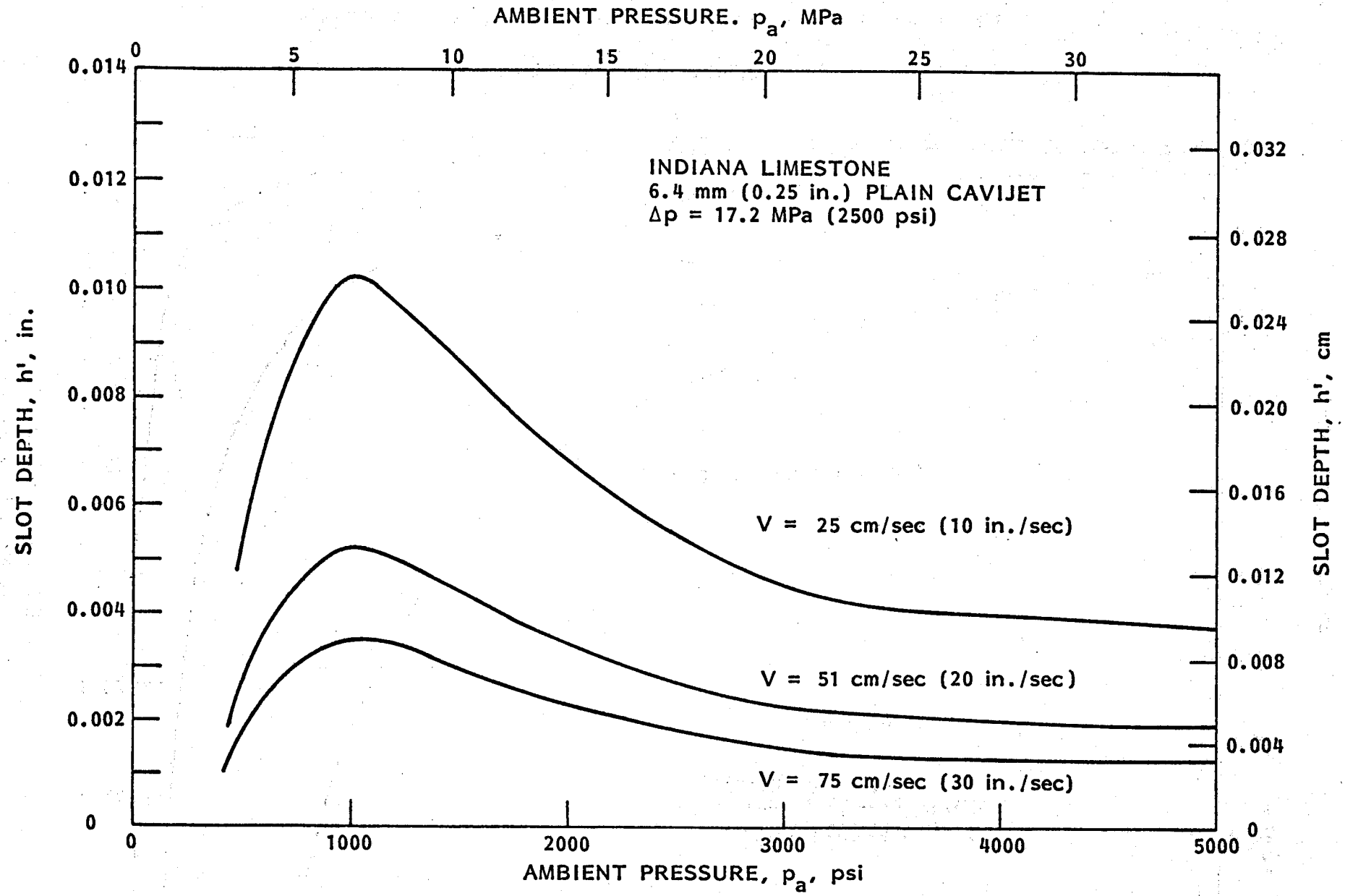

FIGURE 41 - PREDICTION OF SLOT CUTTING: Depth versus ambient pressure

of slot cutting tests at one value of (p_a, Δp), a complete slot cutting description can be derived.

The translation velocity of the nozzle is determined, in a rotating bit, by the rotation rate and the diameter of the circle of rotation of the nozzle. For instance, on the two-cone roller bit used for the tests discussed in Chapter VI, the two extended nozzles were located on a 14.3 cm (5.62 in.) diameter circle. Thus, at the 60 rpm used in these tests, the translation velocity was about 45 cm/s (18 in/s). From Figure 40, for a Δp = 16.5 MPa (2,400 psi), the slot depth in Indiana limestone at this velocity should be about 0.15 mm (0.006 in.), for σ = 0.4. For this Δp, the rates of penetration for this bit (see Figure 34) were about 4.3 to 5.5 m/hr (14 to 18 ft/hr). Thus, at 60 rpm, the depth cut by this bit on each revolution was about 1.3 to 1.5 mm/rev (0.05 to 0.06 in./rev). The predicted slot depth for each of the two plain CAVIJET nozzles was therefore only about 1/10th of this depth per revolution. This may explain why, under these conditions, the raw data for the CAVIJET nozzles (with their lower delivered hydraulic power) fell below that of the standard Smith Tool Co. nozzles as shown in Figure 34.

Although basic stationary nozzle information was not obtained for the Colton sandstone, this same type of arguement may also be the reason for the observation that the CAVIJET -augmented bit provided, in comparison to the standard nozzles, slightly higher rates of penetration in this slower drilling rock (see Figure 33), and substantially higher specific penetration rates (see Figure 35). Here, since the penetration rate is only about 2m/hr (7 ft/hr) under the same conditions, the depth cut per revolution is only about 0.64 mm/rev. (0.025 in./rev.). Thus, in this case, with the CAVIJET nozzles each possibly cutting about 1/4 of this amount,

substantial weakening of the rock could have been occurring -- if we can correctly assume that the Colton sandstone exhibits a comparable basic erosion behavior to that determined for Indiana limestone.

D. Extrapolation of Granite Cutting Results

The pressure limitations of the system developed at HYDRONAUTICS for elevated ambient pressure testing precluded effective single pass slot cutting of granite. As seen in Figure 24, stationary nozzle testing showed that the Georgia granite was about 20 times more resistant to erosion than the Indiana limestone. In the latter part of the previous section it was seen that, for a Δp = 16.5 MPa (2,400 psi), substantial specific penetration rate improvement was provided by CAVIJET nozzle augmented bits, where the depth cut per revolution was about 0.64 mm/rev. (0.025 in./rev.) (60 rpm, ROP = 2m/hr (7 ft/hr)). The question to be explored here is: what pressure drop across the same 6.4 mm (0.25 in.) plain CAVIJET nozzle would be required to produce sufficient slot depths in granite to provide comparable improved penetration rates?

One approach would be to merely assume that the same relationship between cutting rate and Δp, as experimentally determined for Indiana limestone, also holds true for Georgia granite. Thus, the factor of 20 between the erosion resistances of these two rocks would be balanced by raising the pressure from Δp = 16.5 MPa (2,400 psi) to Δp_2 in accordance with Equation [9]:

$$\left(\frac{\Delta p_2}{16.5 \text{ MPa}}\right)^{3.1} = 20, \text{ or } \Delta p_2 = 43.5 \text{ MPa (6,300 psi)}.$$

It should be noted that, since this type of power law dependence

for erosion rate, with even higher values for the exponent, has frequently been observed for CAVIJET nozzles and other cavitating devices under a variety of situations, the assumption that $\dot{h} \propto (\Delta p)^{3.1}$ holds for elevated ambient pressure CAVIJET nozzle cutting of granite has a good chance of being valid.

An alternate approach to estimating an effective Δp for granite, and one which further supports the assumption that $\dot{h} \propto (\Delta p)^n$ for $n \geq 3$ is valid, stems from data obtained during another investigation now on-going at HYDRONAUTICS (20). Several shales and slates, plus a granite, have been subjected to in-air slot cutting with a small, centerbody configuration CAVIJET nozzle, to determine whether the CAVIJET method can augment the cutting action of mining machines which remove rock layers adjacent to coal seams.

The results of such tests on a California black granite are summarized in Figure 42. Thus, at a translation velocity of 0.64 cm/s (0.25 in./s), a Δp of 43.5 MPa (6,300 psi) produced a slot depth of about 0.76 mm (0.03 in.) with a 2.2 mm (0.086 in.) diameter, centerbody CAVIJET nozzle in air. Neglecting the fact that submerged operation of the CAVIJET nozzles generally increases the intensity of cavitation, we will only account for the nozzle diameter difference by utilizing the relation:

$$h' \propto d^{3/2} \qquad [20]$$

for scaling the slot depth, h', for increases in the nozzle diameter d. Equation [20] was derived during slot cutting trials in coal (16). Thus, scaling up from the 2.2 mm (0.086 in.) diameter of the nozzle used to produce the data in Figure 42, to the 6.4 mm (0.25 in.) CAVIJET nozzle used in the present study, a factor of $(6.4/2.2)^{3/2} = 5$ is obtained. Applied to the observed

ROCK: CALIFORNIA BLACK GRANITE
NOZZLE: 2.2 mm (0.086 in.) WITH CENTER BODY
MODE: IN-AIR; STANDOFF: 2.2 cm (0.88 in.)
TRANSLATION VELOCITY: 6.4 mm/sec (0.25 in./sec)
FLUID: WATER

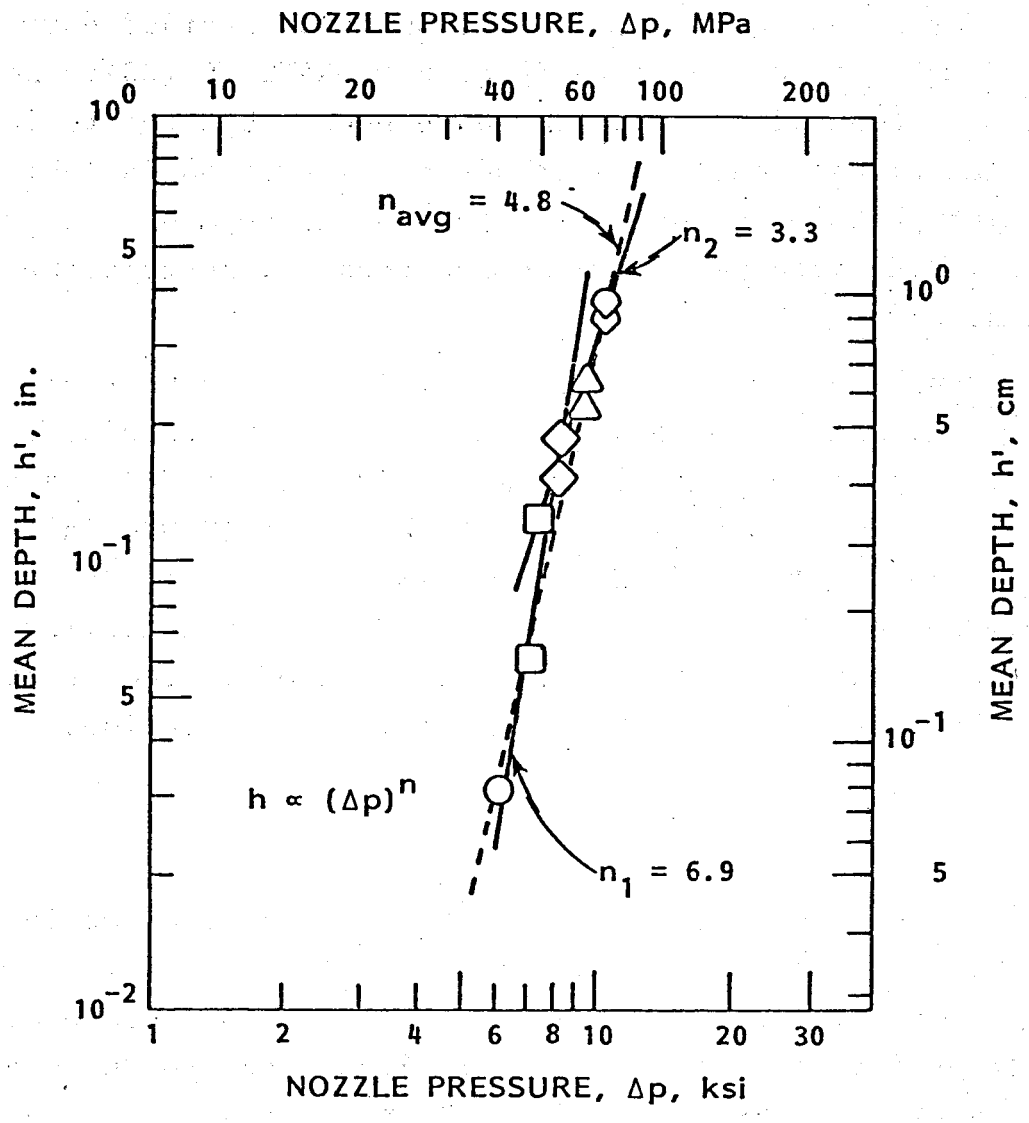

FIGURE 42 - EFFECT OF PRESSURE ON SLOT CUTTING OF GRANITE WITH A CAVIJET® NOZZLE

h' = 0.76 mm (0.03 in.) depth in Figure 42, a slot depth of 3.8 mm (0.15 in.) is predicted for the 6.4 mm (0.25 in.) plain CAVIJET nozzle at a Δp = 43.5 MPa (6,300 psi), with a translation velocity: v = 0.64 cm/s (0.25 in./s).

One last step remains, namely to estimate what slot depth would be anticipated for v = 45 cm/s (18 in./s), the translation velocity of the two extended nozzles in the bit tests, as discussed in the previous section. This estimate can be made by using the types of curves given in Figure 40. Since the curves for lower Δp's show steeper roll-offs with respect to increases in translation velocity, a conservative estimate of what may happen in granite at a Δp = 43.5 MPa (6,300 psi) will be derived if we use the Δp = 10.4 MPa (1,500 psi) curve in Figure 40. Thus, comparing the slot depths at v = 0.64 and 45 cm/s (0.25 and 18 in./s), a slot depth decrease factor of about 32:1 is predicted. Finally, using this factor of 32 to reduce the h = 3.8 mm (0.15 in.) depth at the lower velocity, a slot having a depth: h' = 0.12 mm (0.005 in.) is predicted for the granite at v = 45 cm/s (18 in./s).

Compare this depth with the estimated depth: h' = 0.15 mm (0.006 in.)*, found to be an effective value for the Δp = 16.5 MPa (2,400 psi) drill bit tests in Colton sandstone at an ROP of about 2 m/hr (7 ft/hr). Thus it is seen that this estimate for granite produced a comparable slot depth prediction, at the same RPM and nozzle location, but with Δp = 43.5 MPa (6,300 psi). This was an admittedly circuitous derivation, based on an independent set of experiments, and requiring scaling the effects of nozzle size and translation velocity. Hence, achieving essentially the same results as the simple $(\Delta p)^{3.1}$ scaling approach, would seem to enforce a feeling for the validity of the various assumptions which had to be made.

This type of derivation should be verified with suitable

*See Page 46.

full-scale testing in hard rocks before final conclusions can be drawn. It must also be emphasized that these performance extrapolations were based upon a number of empirically derived relations. Thus, although these relations were sufficient to meet the objectives of this phase of the program, namely to determine the feasibility of effectively using cavitation erosion in submerged jets operating under high ambient pressures, much remains to be learned about the basic mechanisms which are contributing to these experimental observations. A full understanding of both nozzle design parameters and the jet-rock interaction process must be sought if maximum gains are to be made from this attempt to exploit cavitation erosion for deep hole drilling. However, the experimental results already obtained, plus the foregoing extrapolations, strongly suggest that moderate pressure increases in Δp can allow the CAVIJET cavitating fluid jet method to achieve sufficient erosive intensity to improve drilling rates in hard, geothermal-well rock formations.

VIII. CONCLUSIONS AND RECOMMENDATIONS

From the experimental results and analyses performed during this program, it may be concluded that the CAVIJET cavitating fluid jet method can successfully augment the cutting action of mechanical bits under deep-hole conditions. This general conclusion is based on the following specific conclusions drawn from this study:

a. Elevated ambient pressure can enhance the erosive action of CAVIJET cavitating fluid jet nozzles. For instance (see Figure 38), at a nozzle pressure drop Δp = 13.8 MPa (2,000 psi), increased cutting rates, relative to atmospheric pressure results, can be anticipated until hole depths of at least 1,200 m (4,000 ft) and possibly deeper. Nozzle size and configuration, as well as jet velocity (or Δp) and fluid properties, affect cavitation inception (see Figure 39), and hence the effective ambient pressure (or hole depth) range for this increased rate of erosion.

b. The CAVIJET cavitating jet erosive cutting performance is not adversely affected by substituting a water-based drilling mud for the working fluid instead of water, for mud densities up to 1.4 gm/cm^3 (12 lb/gal).

c. The same strong dependence on nozzle pressure for CAVIJET cavitating jet erosive cutting rates, seen in atmospheric ambient testing (21, 22), was also observed under elevated ambient pressures (see Figure 14). Thus, increases in Δp tend to produce proportionately larger increases in the cutting rate, $\dot{h}$, since $\dot{h} \propto (\Delta p)^{3.1}$ has been observed for a plain CAVIJET nozzle.

d. CAVIJET nozzles, at elevated ambient pressures, produce more effective rock cutting in comparison to conventional

nozzles operated under the same conditions (see Figure 16); this has also been observed under atmospheric ambient pressures (see, for instance References 16, 17, 21).

e. The optimum standoff distance for CAVIJET nozzles decreases with increases in ambient pressure. At pressures above about 3.5 MPa (500 psi), this standoff should be about two to three nozzle diameters (see Figure 29) to maximize the cutting rate. This result simplifies the design of diamond bits which are to be augmented with CAVIJET nozzles, but may create design difficulties with roller bits.

f. Improved rates of penetration should be achieved by substituting CAVIJET nozzles of the type tested for conventional nozzles in roller bits (see Figures 33 through 36) if the nozzle sizes are selected so as to absorb equal hydraulic power. Centerbody CAVIJET nozzles produce a greater improvement than plain CAVIJET nozzles.

g. Pressures in the range of Δp = 43.5 MPa (6,300 psi) were extrapolated to be sufficient to allow CAVIJET nozzles to improve the drilling rates of mechanical bits in hard (granite) rocks. (See Chapter VII, Section D.)

As a result of the success of this feasibility phase, it is recommended that an optimization effort should be initiated, with the following objectives:

a. Development of CAVIJET cavitating fluid jet nozzle configurations which are optimized for deep-hole rock erosion, and are compatible with mechanical bit designs. Both rock cutting and flow visualization studies should be used to reach this objective.

b. Optimization of CAVIJET nozzle augmented bit configurations, both roller and diamond bits, by means of laboratory and field trials of various experimental bit concepts.

REFERENCES

1. Maurer, W.C., "The 'Perfect-Cleaning' Theory of Rotary Drilling", Journal of Petroleum Technology, Vol. 14, No. 11 pp. 1270 ff, November 1962.

2. Maurer, W.C., Novel Drilling Techniques, Pergamon Press, Oxford, 1968.

3. Proceedings, First International Symposium on Jet Cutting Technology, Coventry, England, BHRA Fluid Engineering, April 1972.

4. Proceedings, Second International Symposium on Jet Cutting Technology, Cambridge, England, BHRA Fluid Engineering, April 1974.

5. Proceedings, Third International Symposium on Jet Cutting Technology, Chicago, Illinois, BHRA Fluid Engineering, May 1976.

6. Proceedings, Fourth International Symposium on Jet Cutting Technology, Canterbury, England, BHRA Fluid Engineering, April 1978.

7. Wylie, M.R.J., "Jetted Particle Drilling", 8th World Petroleum Congress, Special Paper No. 6, Moscow, June 1971.

8. Maurer, W.C., Heilhecker, J.K. and Love, W.W., "High-Pressure Drilling", J. Petroleum Technology, Vol. 255, pp. 851-859, July 1973, (also see Proc., 2nd Int'l. Sympos. on Jet Cutting Technology, pp. X80-X89, April 1974).

9. Pols, A.C., "Hard-Rock Jetting", The Oil and Gas Journal, Part 1: pp. 134-144, Jan. 31, 1977; Part 2: pp. 71-75, Feb. 7, 1977.

10. Summers, D.A., et al., "Environmental Effects on a High Pressure Jet Drill", paper presented at the ASME Petroleum Mechanical Engineering Conference, Mexico City, Sept. 1976.

11. Conn, A.F., and Radtke, R. P., "Cavitating Bit Jets Promise Faster Drilling for Deep-Hole Operations", The Oil and Gas Journal, pp. 129-146, October 31, 1977 (also see: Trans. ASME, J. Pressure Vessel Tech., Vol. 100, pp. 52-59, 1978).

12. Leach, S.J. and Walker, G.L., "Some Aspects of Rock Cutting by High Speed Water Jets", Phil. Trans. Royal Soc., Vol. 260, pp. 295-308, 1966.

13. Conn, A.F., and Rudy, S.L., "A Cavitating Water Jet for Fouling Removal", Proceedings, Fourth International Congress on Marine Corrosion and Fouling, Juan-les-Pins, France, pp. 97-103, June, 1976.

14. Conn, A.F., "Application of a CAVIJET® System for Removing Marine Fouling and Rust", Proceedings, 19th American Towing Tank Conference, Vol. Two, pp. 415-428, August, 1977.

15. Conn, A.F., and Rudy, S.L., "Cutting Coal with the CAVIJET® Cavitating Water Jet Method", Paper D8 in Ref. 5, May 1976.

16. Conn, A.F. and Rudy, S.L., "Parametric Study of Coal Cutting with the CAVIJET® Cavitating Water Jet Method", HYDRONAUTICS, Incorporated Technical Report 7511-1, September 1976 (NTIS No. PB 266-060/AS).

17. Conn, A.F., and Rudy, S.L., "Using Cavitating Water Jets for Demilitarization", Proceedings, Symposium on Demilitarization of Conventional Munitions, ADPA, April 1976.

18. Conn, A.F., Krajkowski, E.A. and Shapira, N. I., "Using the CAVIJET® Process to Remove Explosives from Army Munitions", Proceedings, Second Demilitarization and Disposal Technology Conference, ADPA, pp. 38-40, April 1979.

19. Johnson, V.E., Jr., et al., "Tunnelling, Fracturing, Drilling, and Mining with High Speed Water Jets Utilizing Cavitation Damage", Paper A3 in Reference 3, April 1972.

20. Conn, A.F., et al., "Evaluation of Coal-Associated Rock Cutting by the CAVIJET® Cavitating Fluid Jet Process", HYDRONAUTICS, Incorporated Technical Report 7774-1, (in preparation).

21. Conn, A.F., and Johnson, V.E., Jr., "Further Application on the CAVIJET® (Cavitating Water Jet) Method", pp. D2-7 - D2-20 in Ref. 4, April 1974.

22. Conn, A.F., Mehta, G.D., and Sundaram, T.R., "Cavitating Water Jets, I. Review and Application", Proceedings, Cavitation and Polyphase Flow Forum - 1976, ASME, pp. 12-15, March 1976.

23. Knapp, R.T., Daily, J.W., and Hammitt, F.G., Cavitation, McGraw-Hill Book Co., New York, 1970.

24. Sundaram, T.R., and Liu, H.-L., "On the Equivalence Between Stationary and Nonstationary Modes of Operation of Water Jets", pp. F2-17 - F2-30 in Reference 6, April 1978.

25. Ellis, A.T., and Starrett, J.E., Jr., "Report on CAVIJET® Studies", University of California - San Diego Technical Report, April 1979.

26. Kleinbreuer, W., "Werkstoffzerstörung durch Kavitation in ölhydraulischen Systemen," Industrie-Anzeiger, Vol. 98, No. 61, pp. 1096-1100, July 28, 1976.

27. Lichtarowicz, A., "Cavitating Jet Apparatus for Cavitation Erosion Testing", Erosion: Prevention and Useful Applications, ASTM STP664, pp. 530-549, 1979; also, with P.J. Scott, "Erosion Testing with Cavitating Jet", Proceedings, Fifth International Symposium on Erosion by Liquid and Solid Impact (in preparation).

28. Baker, W., "Extended Nozzle Bits Require Precise Nozzle Sizing", The Oil and Gas Journal, pp. 88-97, March 19, 1979.

29. Black, A.D., "Laboratory Simulation of Deep Well Drilling", Petroleum Engineer International, pp. 40-48, March 1978 (also: presented at the ASME Energy Conference, Houston, Texas, September 1977).

30. Rouse, H., "Cavitation in the Mixing Zone of a Submerged Jet", La Houille Blanche, pp. 9-19, Jan.-Feb. 1953.

31. Ball, J.W. discussion of paper (by Numachi, F., et al., "Cavitation Effect on the Discharge Coefficient of the Sharp-Edged Orifice Plate", J. of Basic Engineering, Trans. ASME, Series D, Vol. 82, pp. 1-11, 1960), pp. 6-10 of Volume 82.

32. Jorgensen, D.W., "Noise from Cavitating Submerged Water Jets", J. Acoustical Soc. of America, Vol. 33, pp. 1334-1338, October 1961.

33. Lienhard, J.H. and Stephenson, J.M., "Temperature and Scale Effects Upon Cavitation and Flashing in Free and Submerged Jets", J. of Basic Engineering, Trans. ASME, Series D, Vol. 88, pp. 525-532, 1966.

APPENDIX A

RESULTS FROM STATIONARY-NOZZLE TESTS AT DRL

TABLE A-1

PEAK VALUES USED FOR NORMALIZATIONS[a]

Figure No.	CAVIJET Nozzle Type[b]	Parameter	Peak Value	
A-1	Plain	Average cutting rate	4.6×10^{-2} cm/sec	1.8×10^{-2} in./sec
A-2		Volume removal rate	2.8×10^{-4} m^3/hr	1.0×10^{-2} ft^3/hr
A-3		Cutting rate effectiveness	2.0 cm/kw-hr	5.0×10^{-2} ft/hp-hr
A-4		Volume removal effectiveness	3.1 cm^3/kw-hr	8.2×10^{-5} ft^3/hp-hr
A-7	Centerbody[c]	Average cutting rate	4.1×10^{-2} cm/sec	1.6×10^{-2} in./sec
A-8		Volume removal rate	1.8×10^{-4} m^3/hr	6.4×10^{-3} ft^3/hr
A-9		Cutting rate effectiveness	2.0 cm/kw-hr	5.0×10^{-2} ft/hp hr
A-10		Volume removal effectiveness	2.8 cm^3/kw-hr	7.5×10^{-5} ft^3/hp-hr

[a]To derive the curves for the figures listed in this table. These peak values are from the stationary-nozzle tests at the nozzle pressure: Δp = 17.2 MPa (2,500 psi), conducted on Indiana limestone at D.R.L.

[b]These nozzles had an orifice diameter of 6.4 mm (0.25 in.)

[c]The centerbody for this nozzle had a diameter of 3.2 mm (0.125 in.)

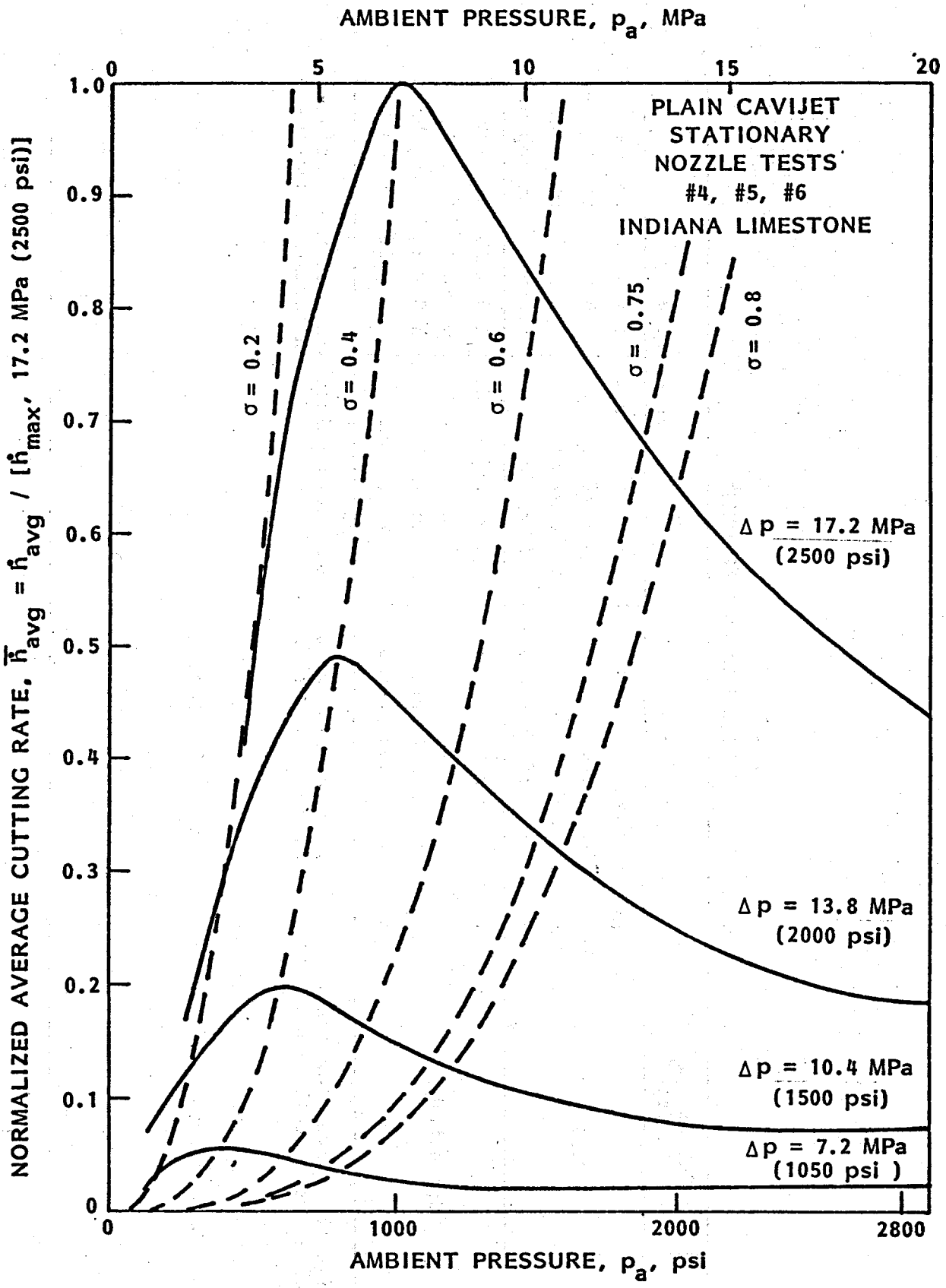

FIGURE A-1 - NORMALIZED AVERAGE CUTTING RATES FOR PLAIN CAVIJET® NOZZLE

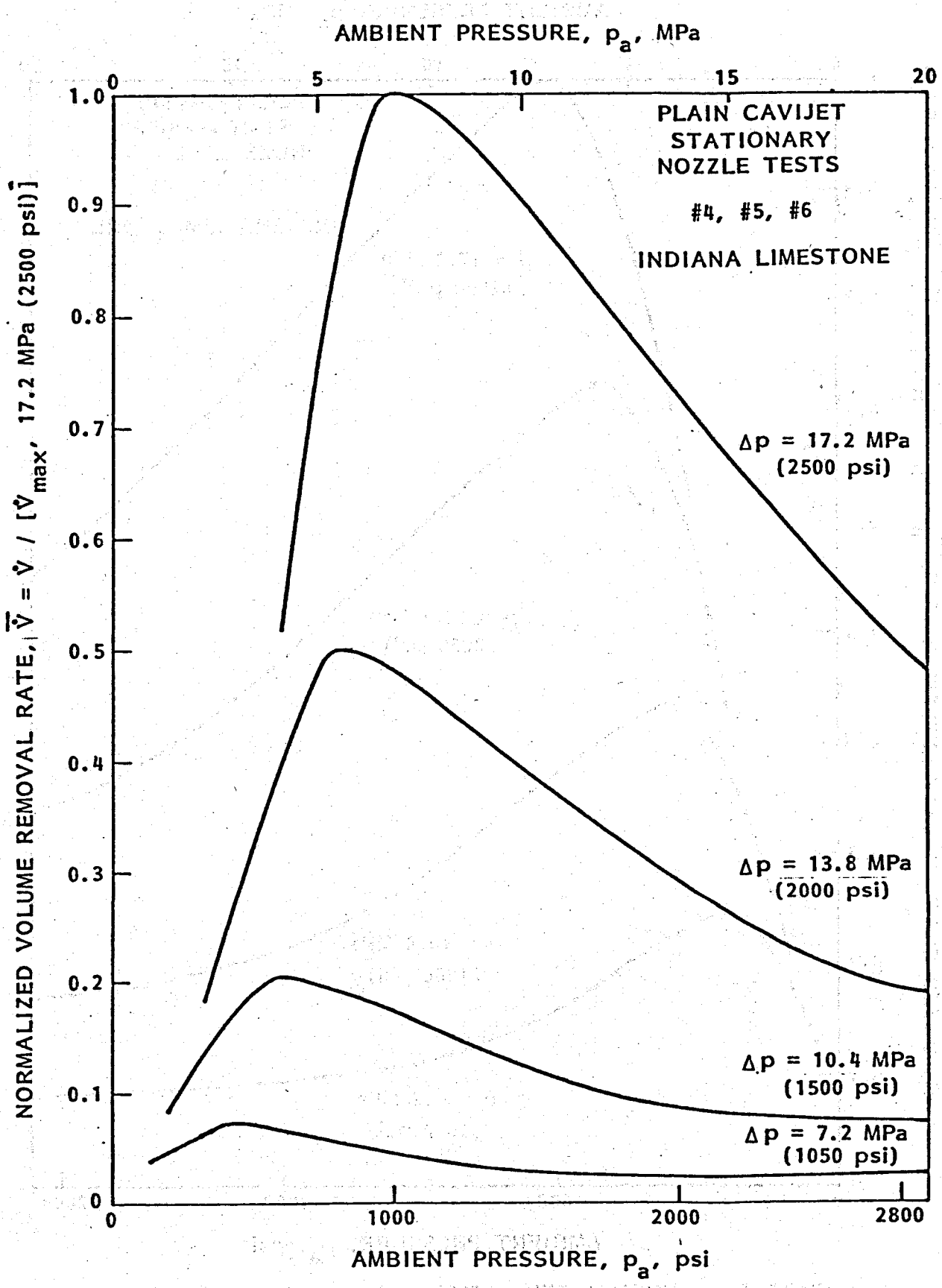

FIGURE A-2 - NORMALIZED VOLUME REMOVAL RATES FOR PLAIN CAVIJET® NOZZLE

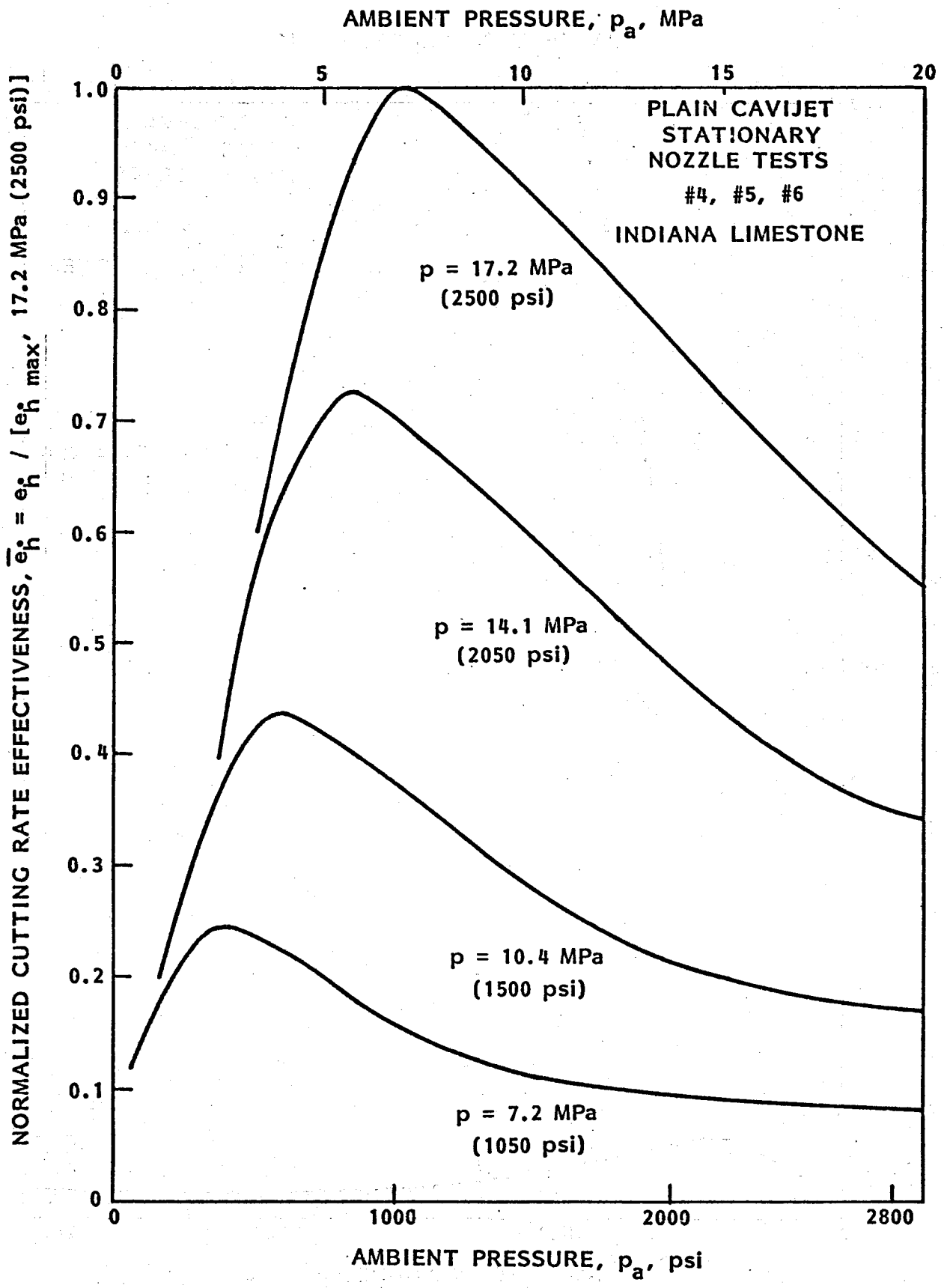

FIGURE A-3 - NORMALIZED CUTTING RATE EFFECTIVENESSES FOR PLAIN CAVIJET® NOZZLE

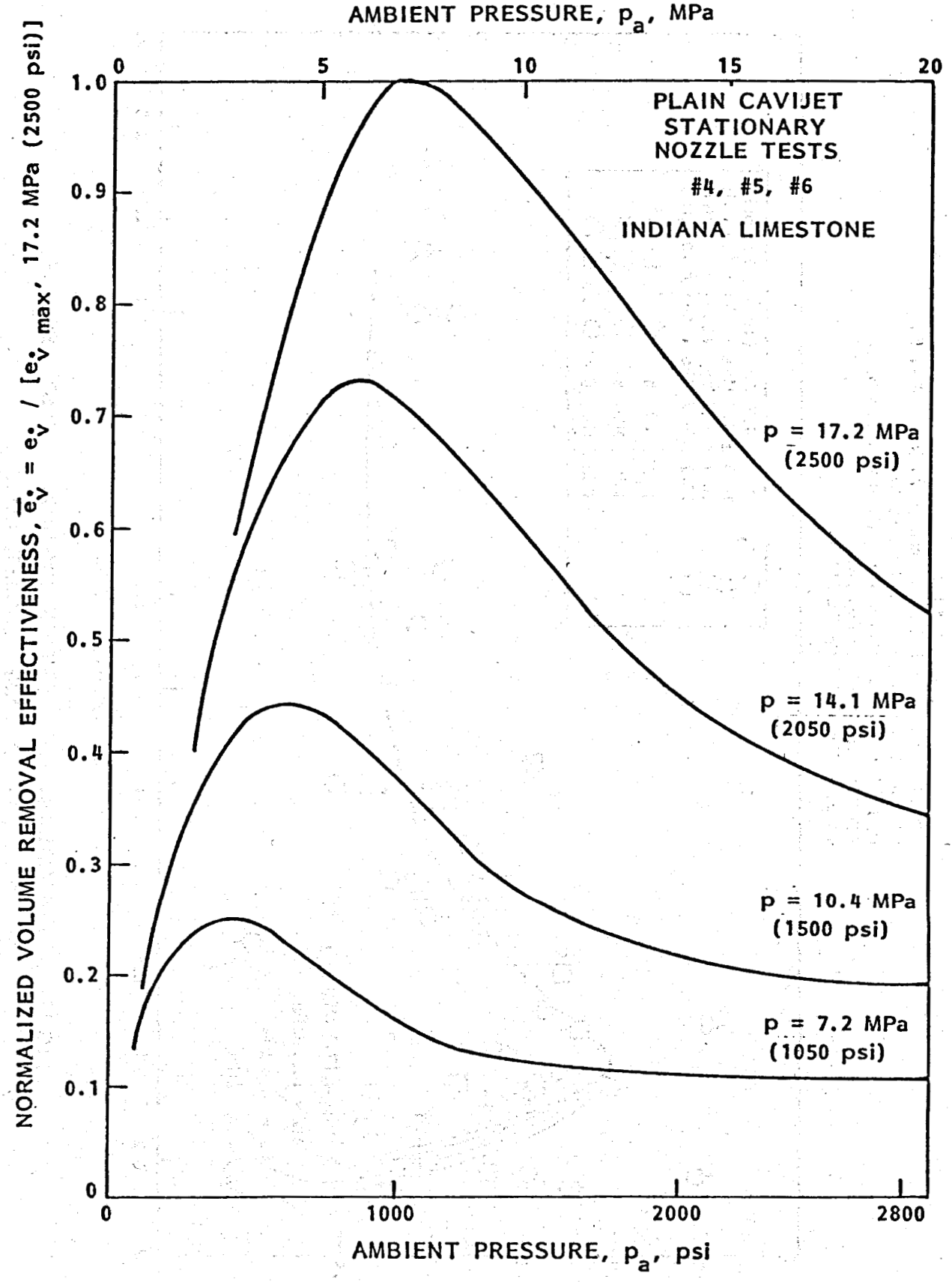

FIGURE A-4 - NORMALIZED VOLUME REMOVAL EFFECTIVENESSES FOR PLAIN CAVIJET® NOZZLE

TEST AT DRILLING RESEARCH LAB.
AUGUST 1978
NOZZLE: CENTERBODY 6.4 mm (0.25 in.) CAVIJET
STANDOFF DISTANCE: 1.6 cm (0.62 in.)
DRILLING FLUID: MUD, 1.1 gm / cm^3 (9.3 ppg)
ROCK: INDIANA LIMESTONE
MODE: STATIONARY CUTTING

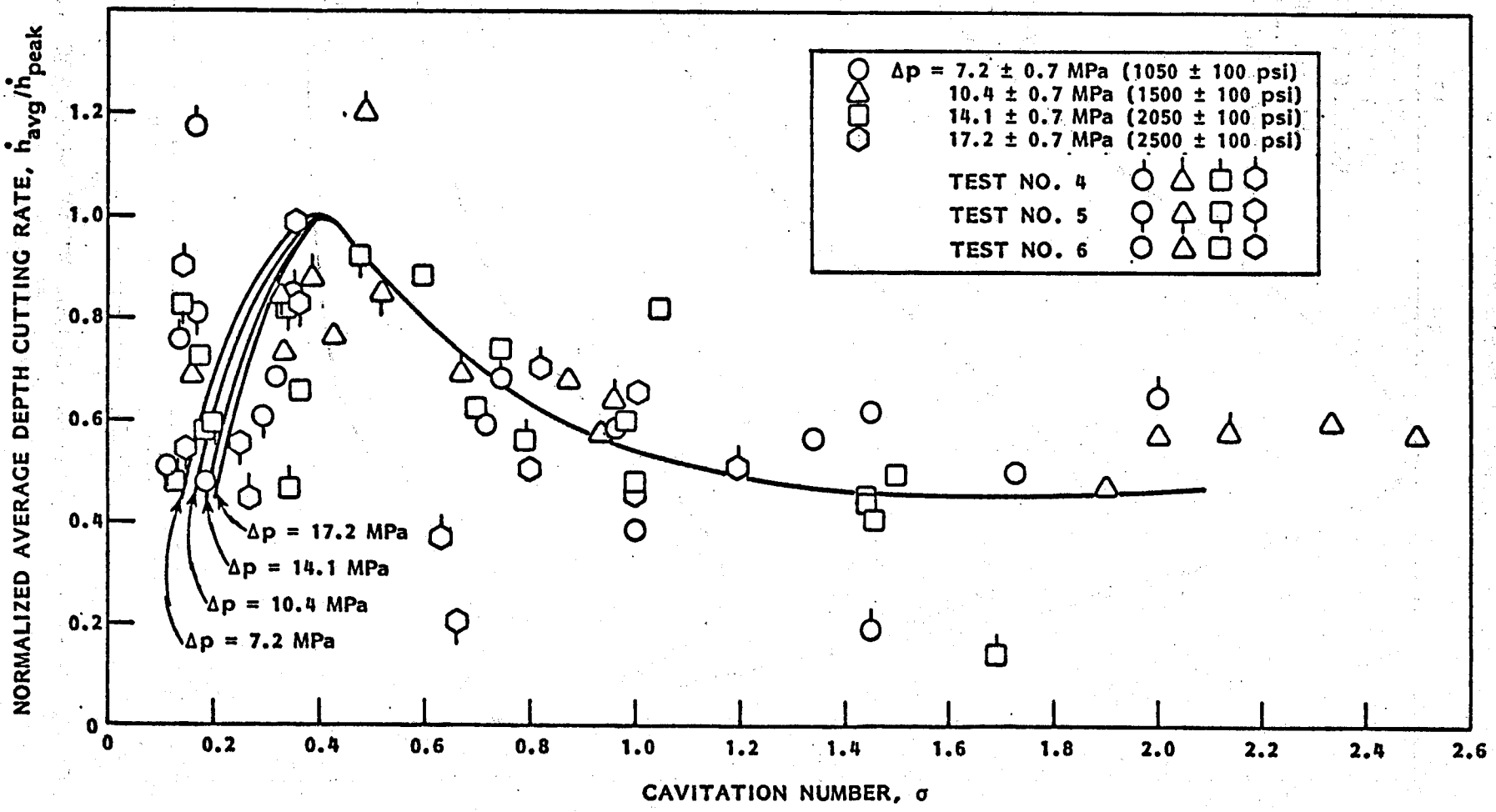

FIGURE A-5 - SCALING THE STATIONARY-NOZZLE TEST RESULTS FOR CENTERBODY CAVIJET NOZZLE

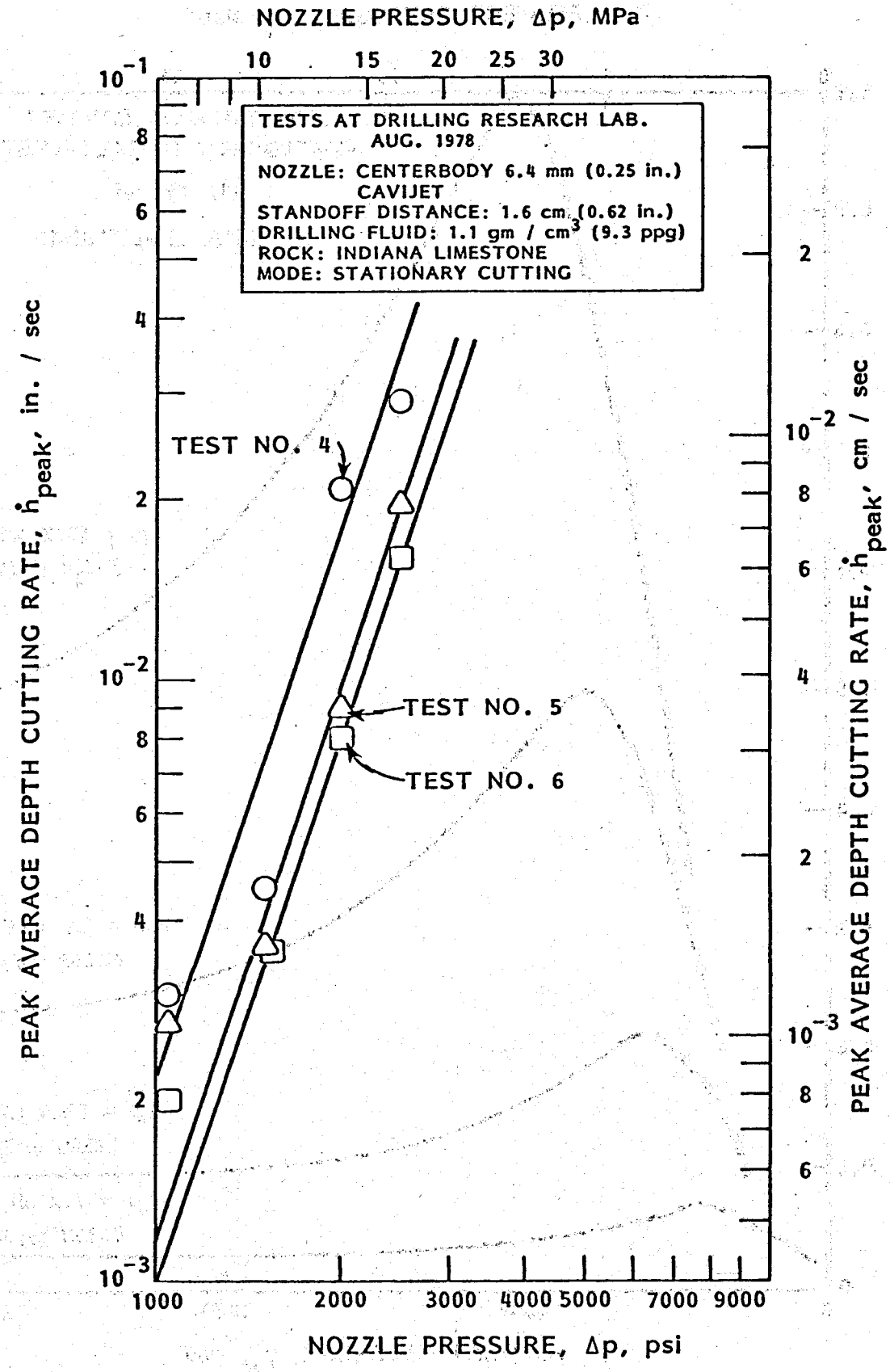

FIGURE A-6 - DEPENDENCE OF CUTTING RATE ON NOZZLE PRESSURE FOR CENTERBODY CAVIJET® NOZZLE

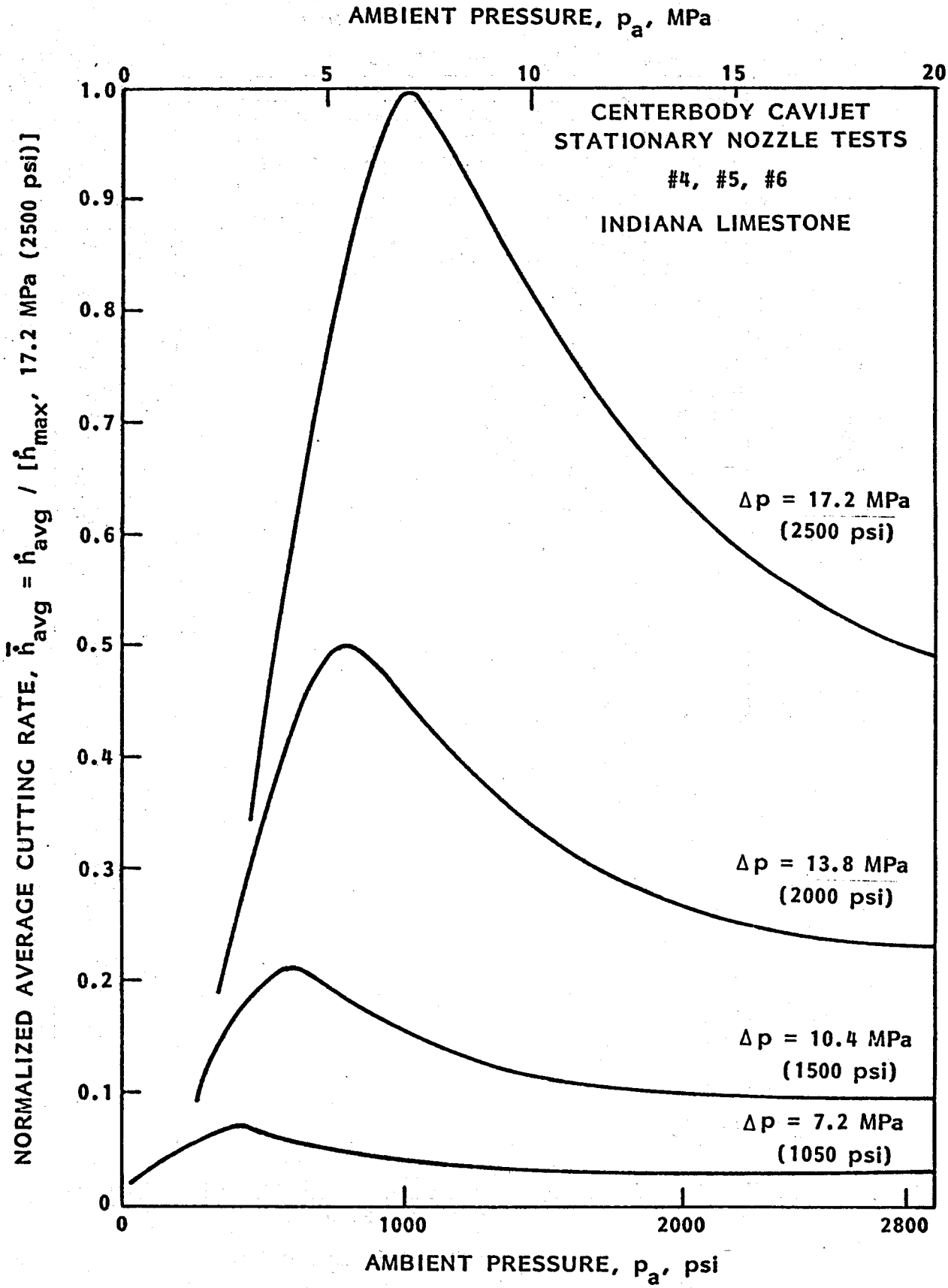

FIGURE A-7 - NORMALIZED AVERAGE CUTTING RATES FOR CENTERBODY CAVIJET® NOZZLE

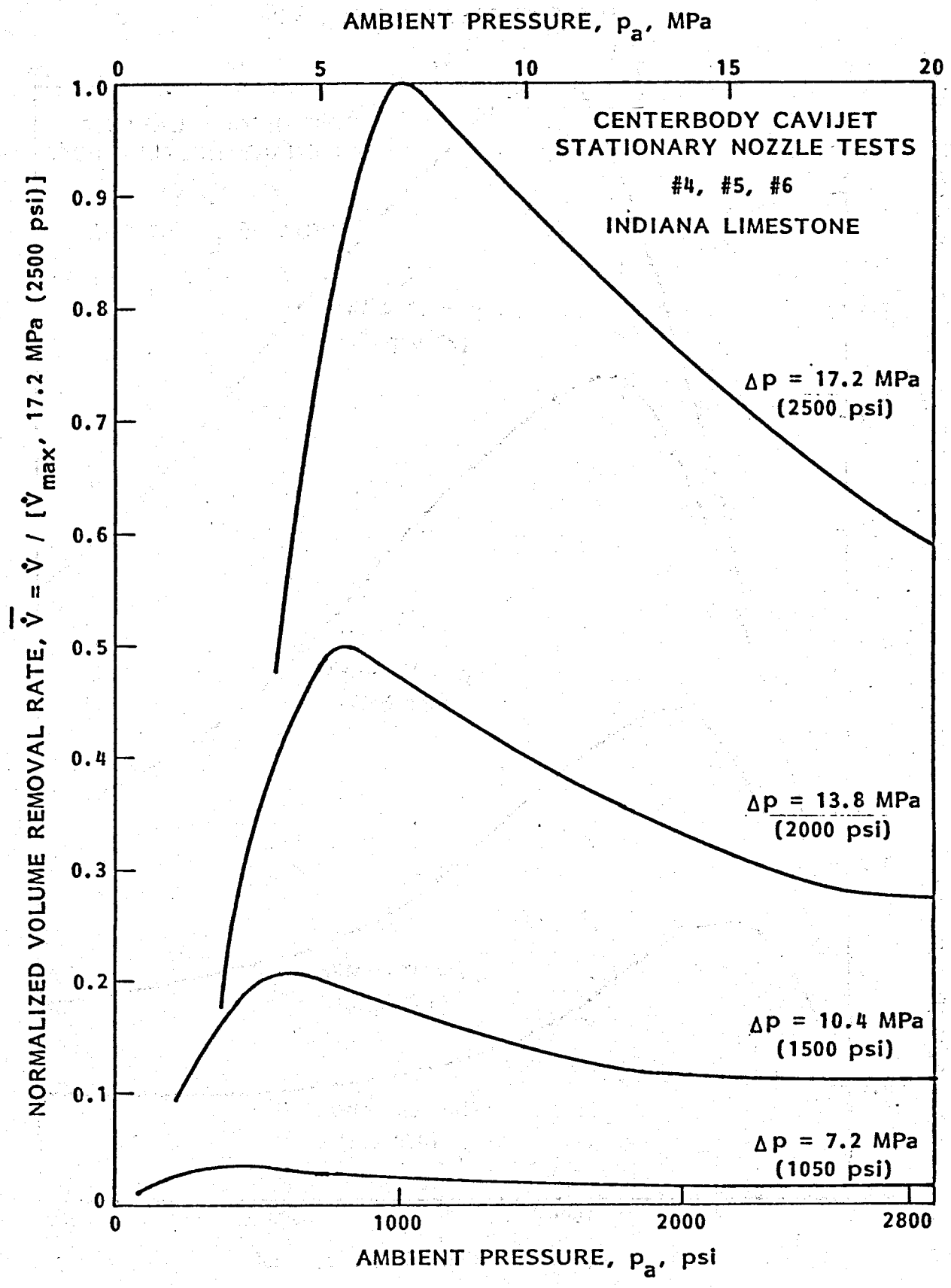

FIGURE A-8 - NORMALIZED VOLUME REMOVAL RATES FOR CENTERBODY CAVIJET® NOZZLE

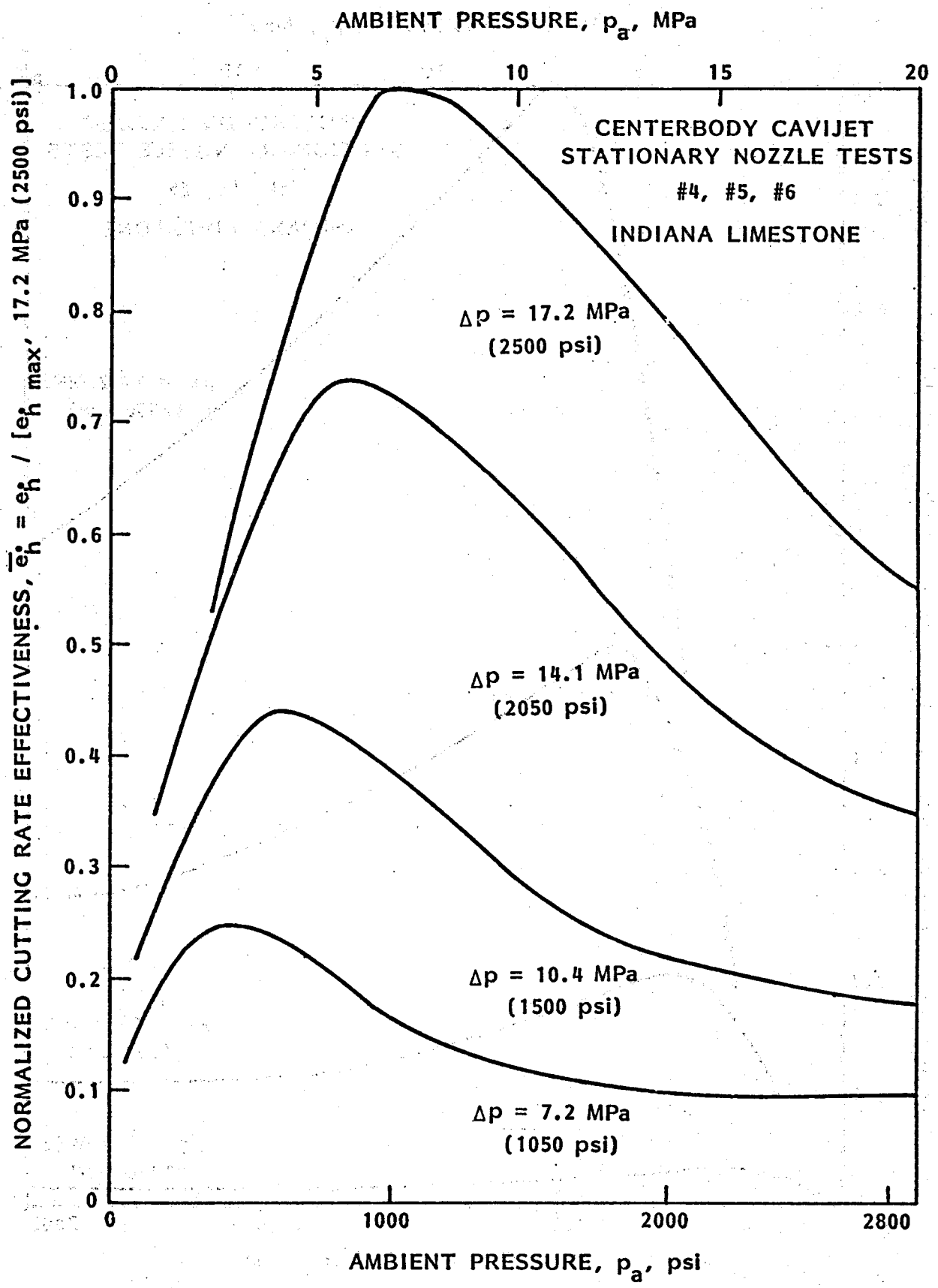

FIGURE A-9 - NORMALIZED CUTTING RATE EFFECTIVENESSES FOR CENTERBODY CAVIJET® NOZZLE

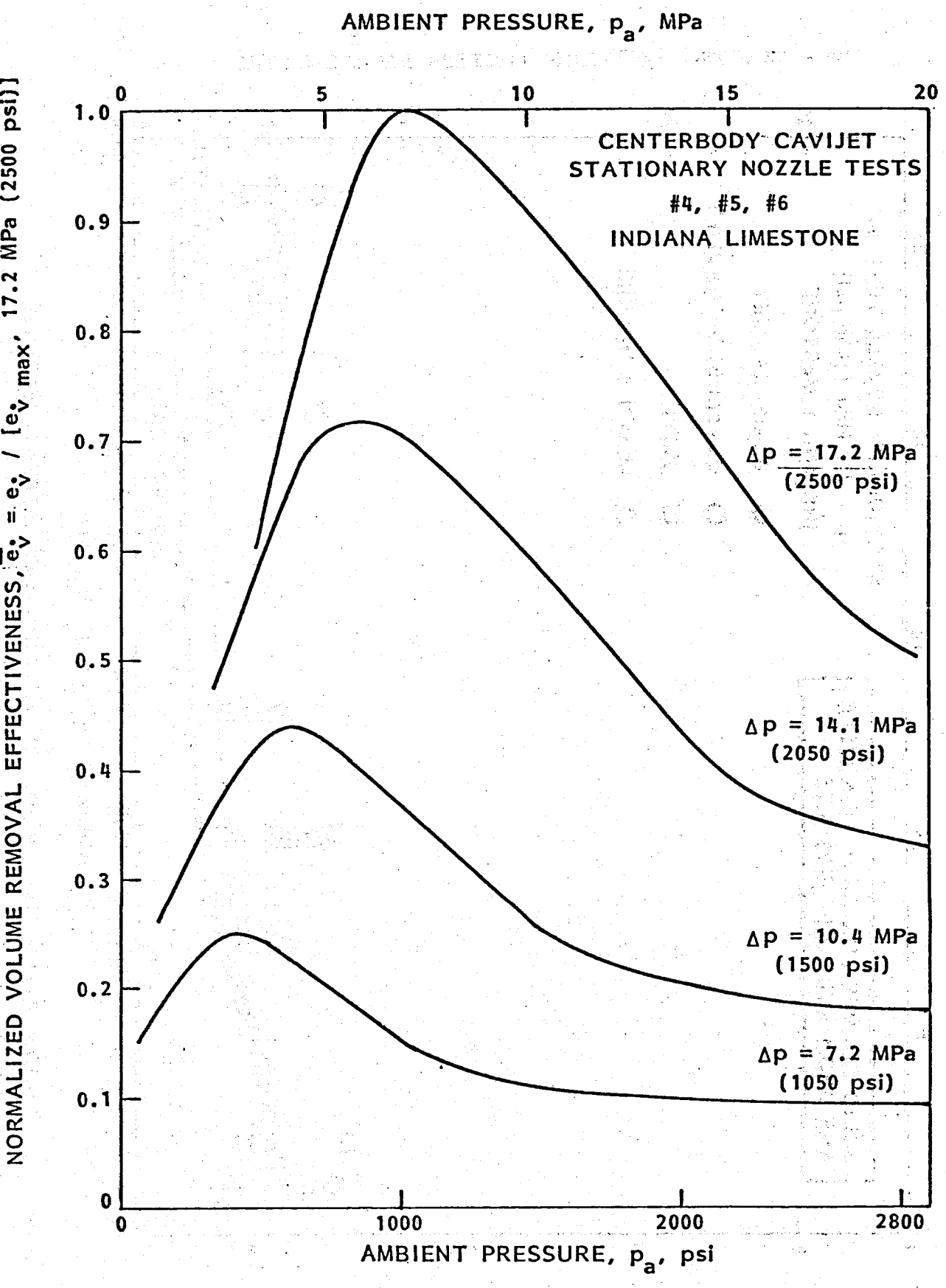

FIGURE A-10- NORMALIZED VOLUME REMOVAL EFFECTIVENESSES FOR CENTERBODY CAVIJET® NOZZLE

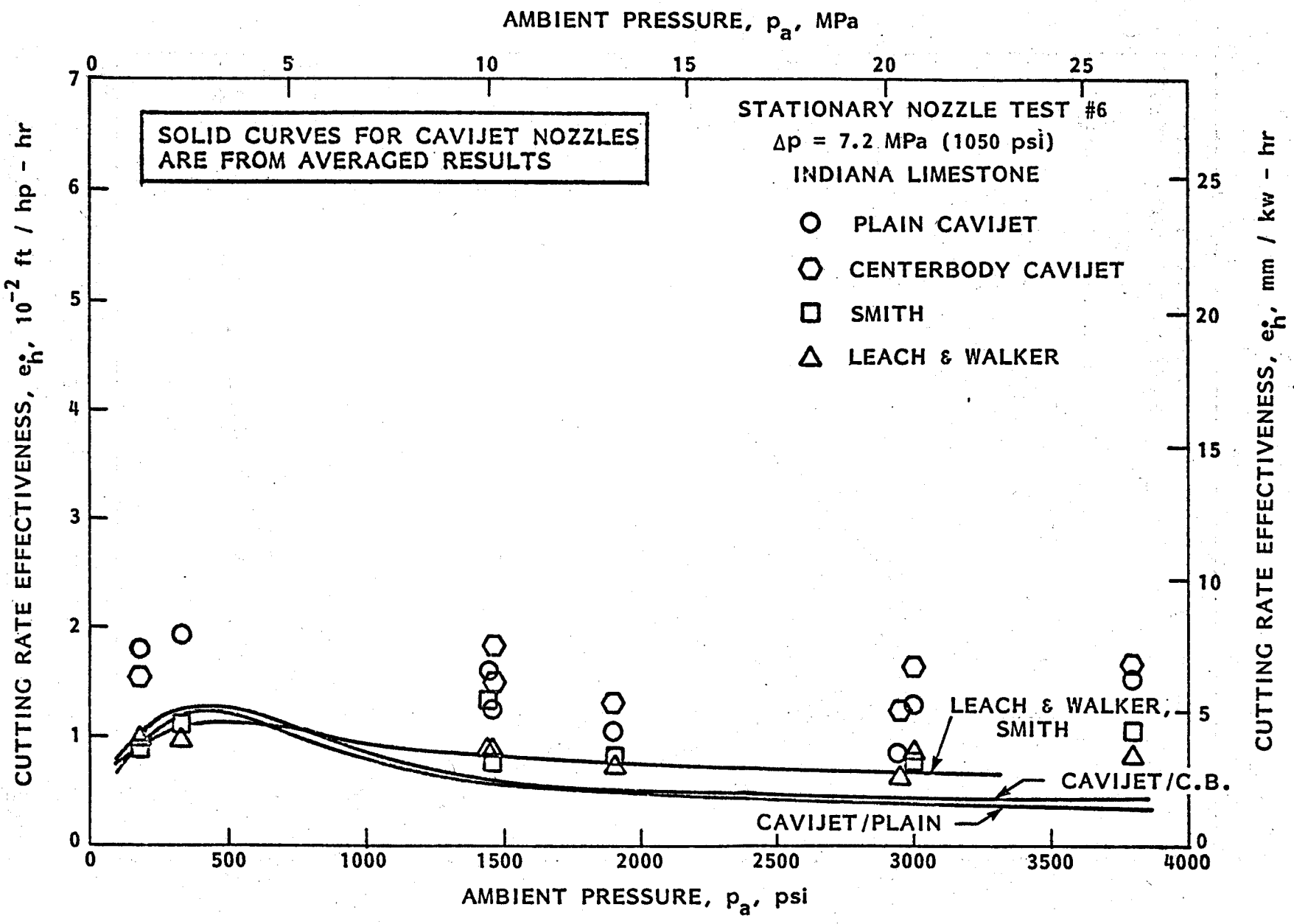

FIGURE A-11 - COMPARISON OF CUTTING RATE EFFECTIVENESSES AT Δp = 7.2 MPa (1050 psi)

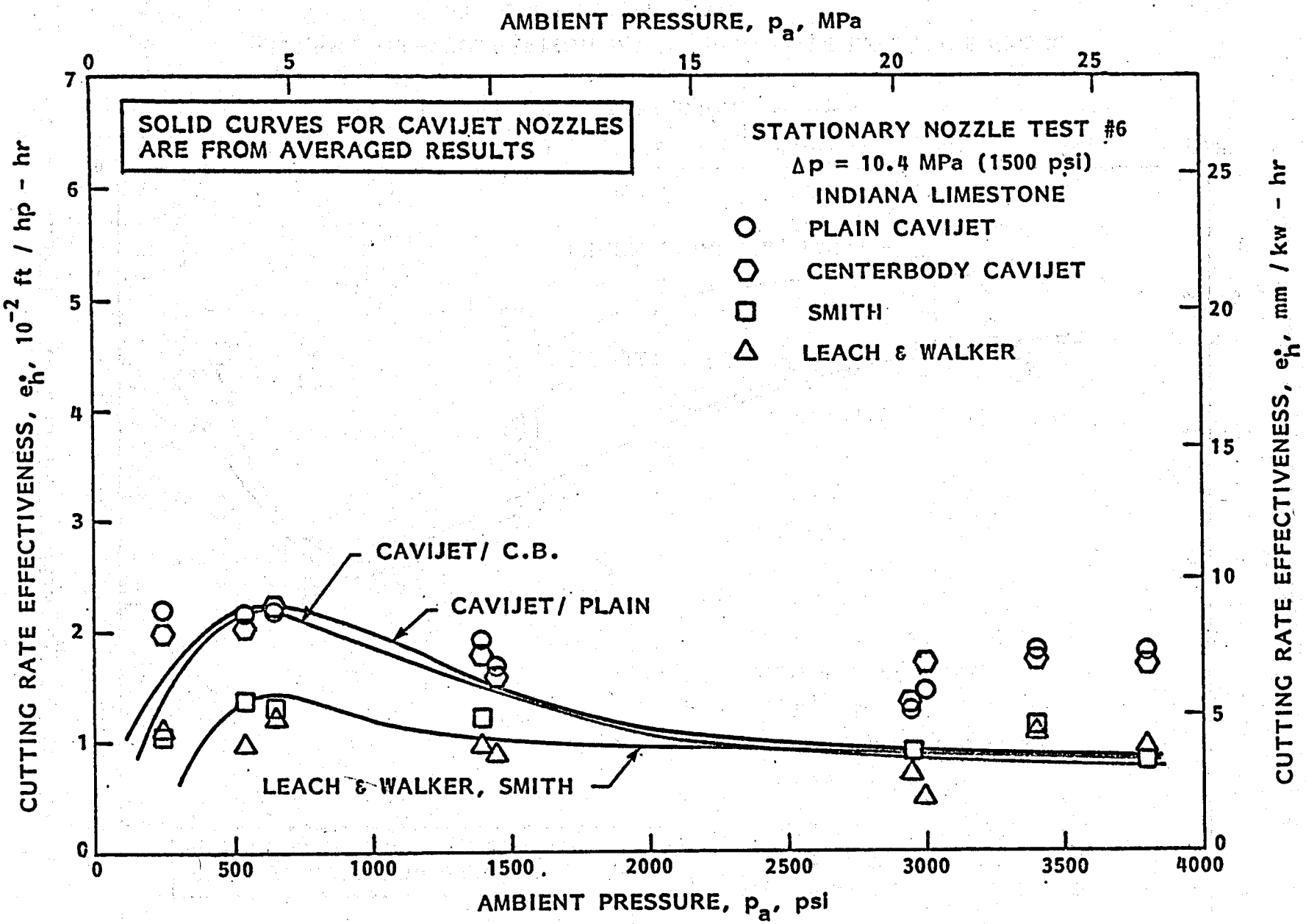

FIGURE A-12 - COMPARISON OF CUTTING RATE EFFECTIVENESSES AT Δp = 10.4 MPa (1500 psi)

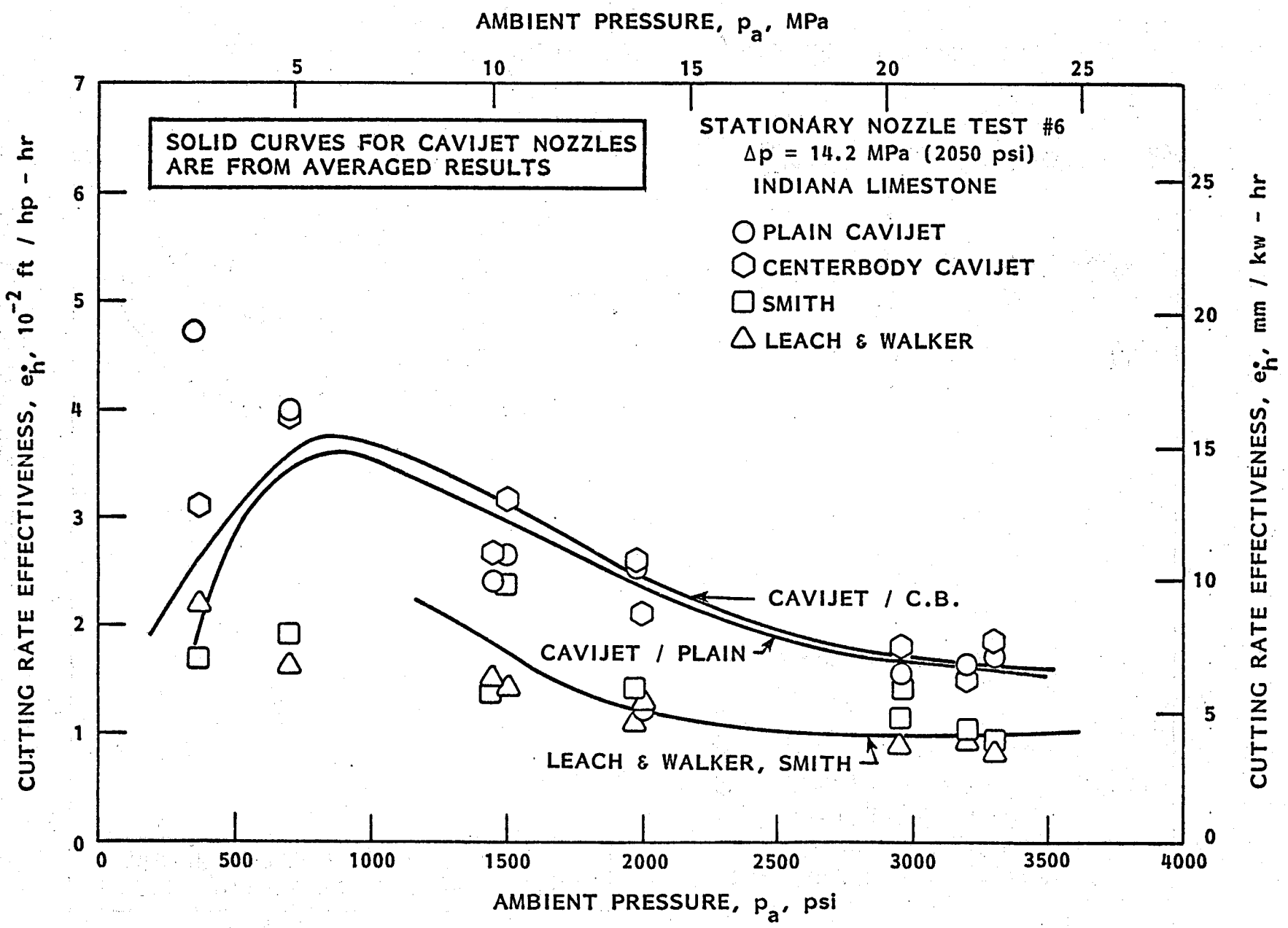

FIGURE A-13 - COMPARISON OF CUTTING RATE EFFECTIVENESSES AT Δp = 14.2 MPa (2050)

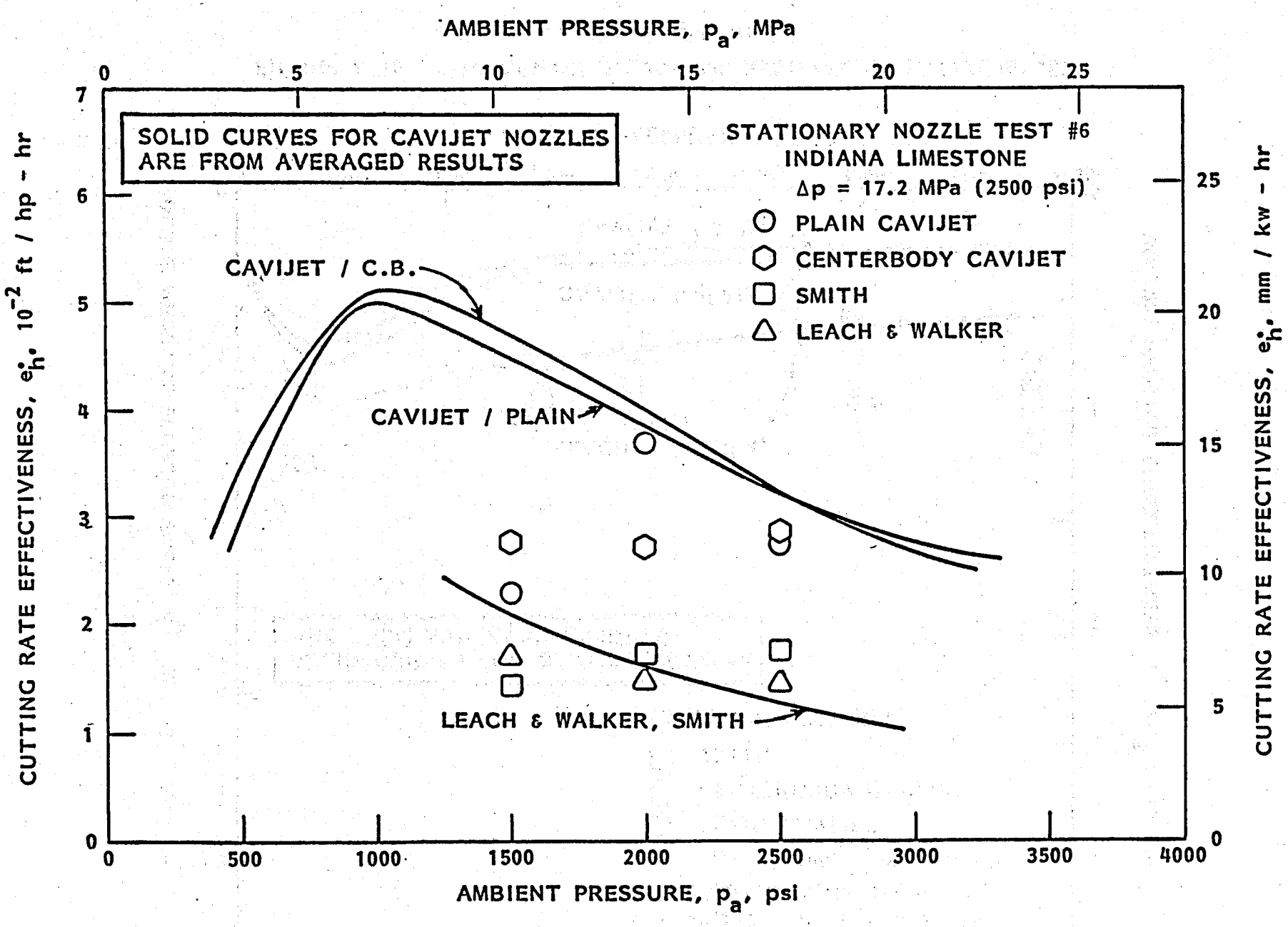

FIGURE A-14 - COMPARISON OF CUTTING RATE EFFECTIVENESSES AT Δp = 17.2 MPa (2500 psi)

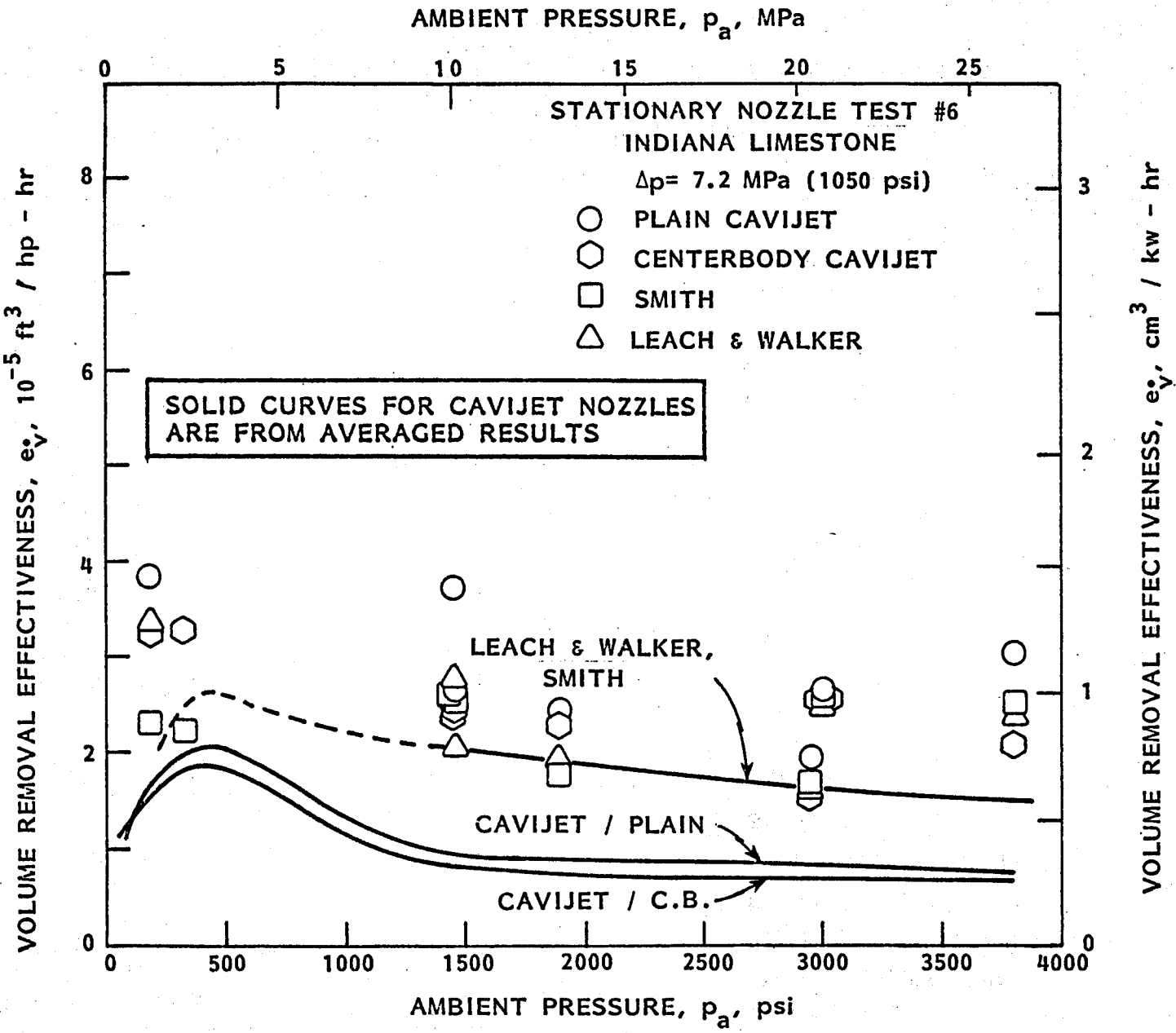

FIGURE A-15 - COMPARISON OF VOLUME REMOVAL EFFECTIVENESSES AT Δp = 7.2 MPa (1050 psi)

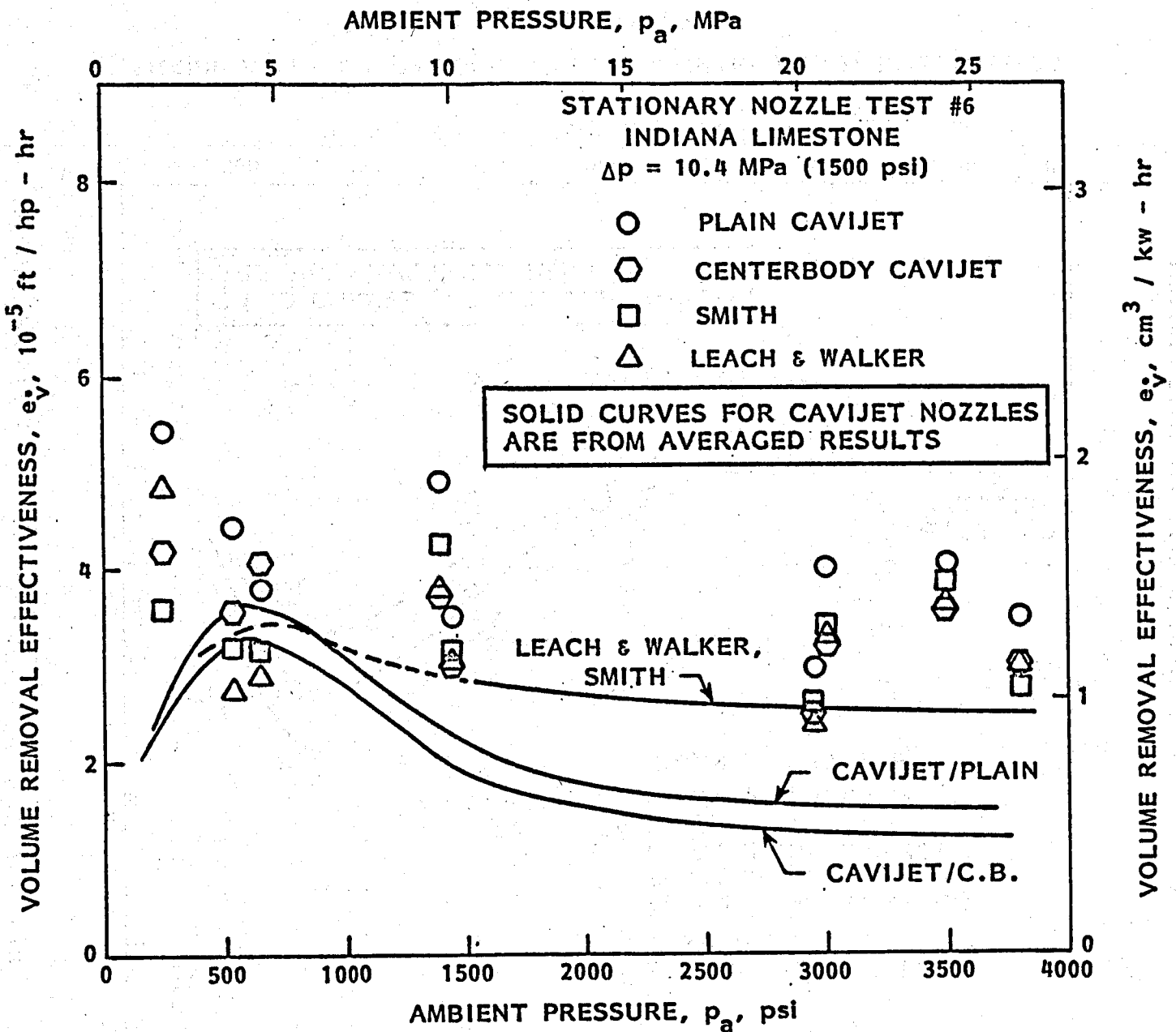

FIGURE A-16 - COMPARISON OF VOLUME REMOVAL EFFECTIVENESSES AT Δp = 10.4 MPa (1500 psi)

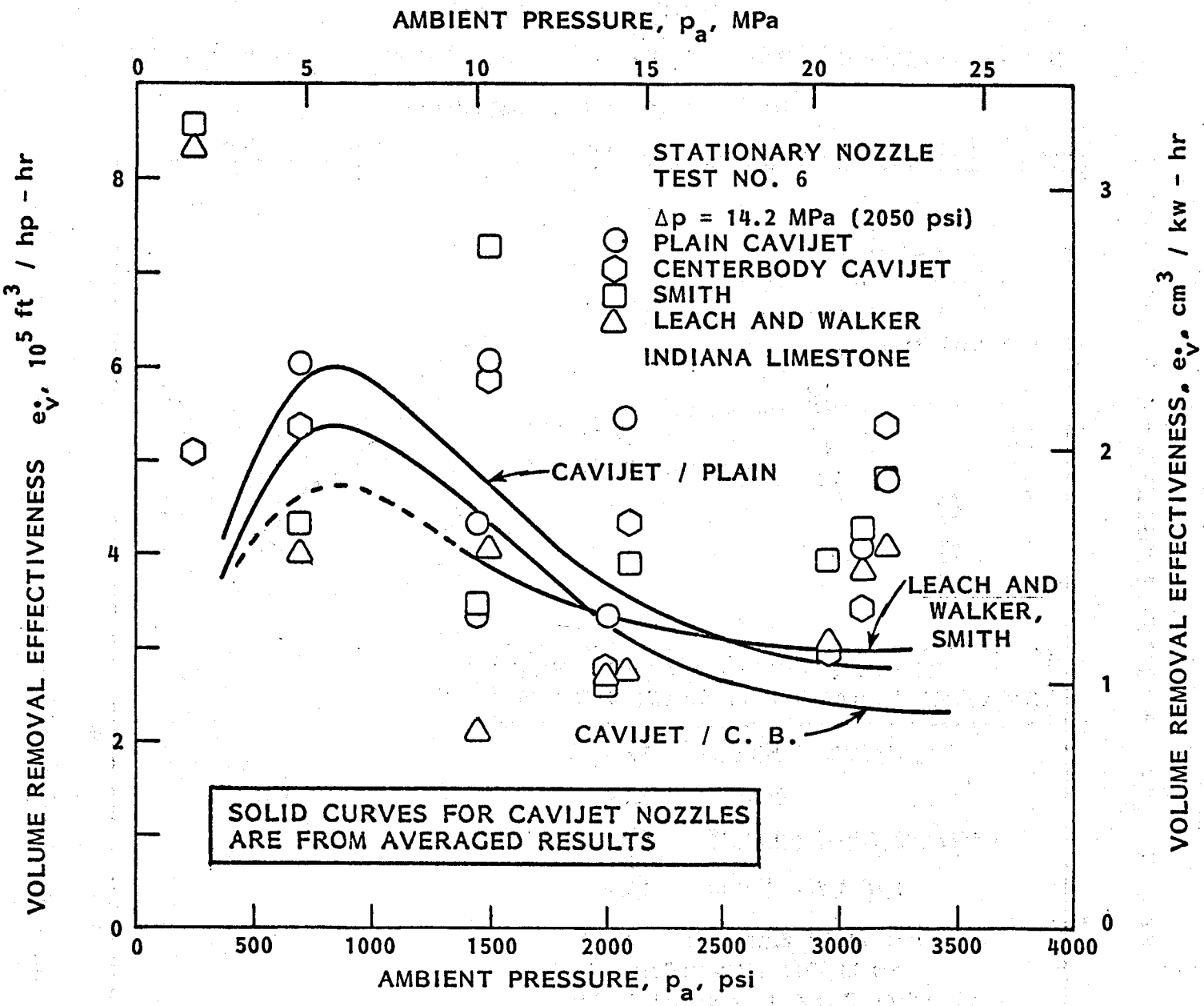

FIGURE A-17 - COMPARISON OF VOLUME REMOVAL EFFECTIVENESSES AT Δp = 14.2 MPa (2050 psi)

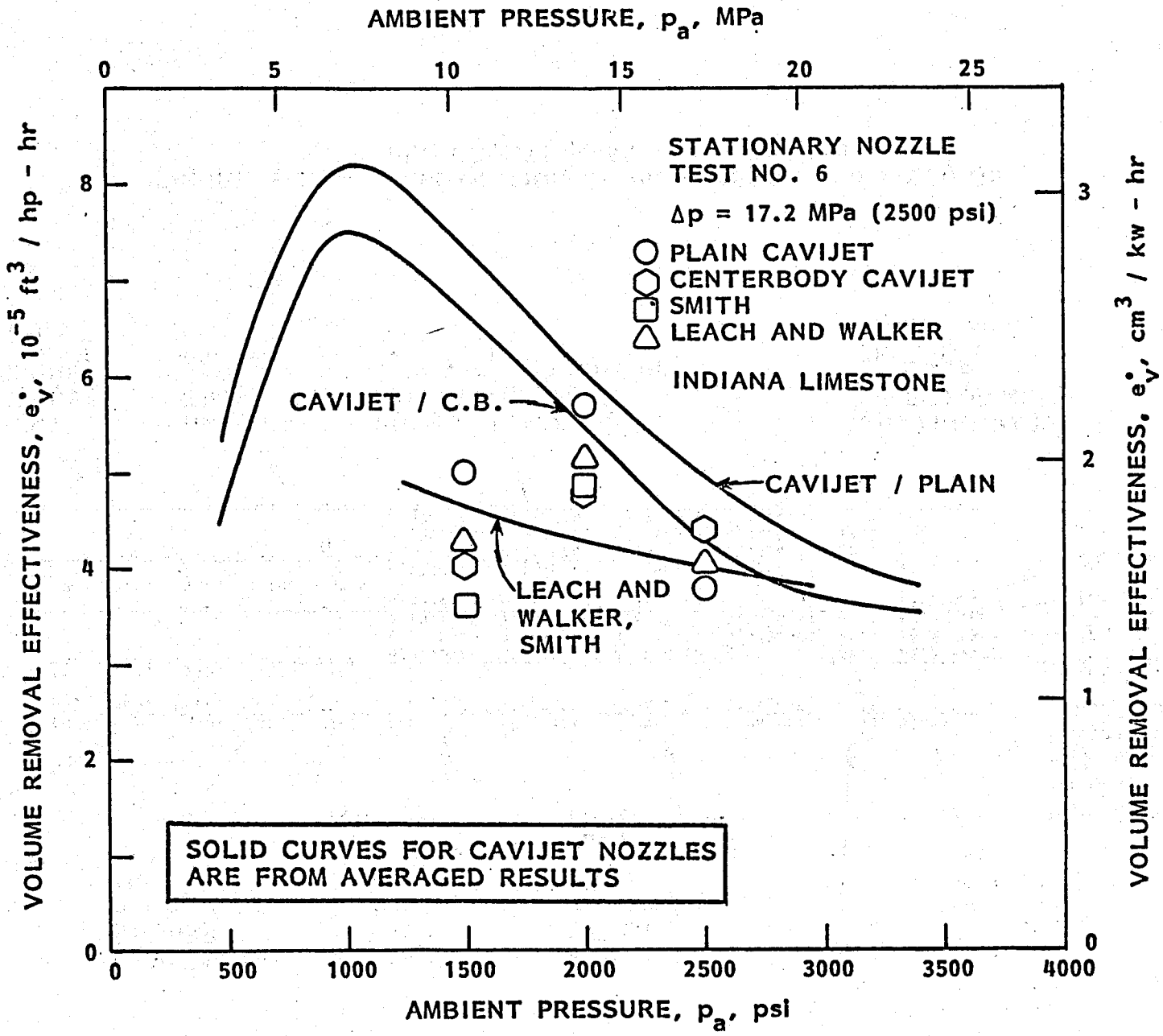

FIGURE A-18 - COMPARISON OF VOLUME REMOVAL EFFECTIVENESSES AT Δp = 17.2 MPa (2500 psi)

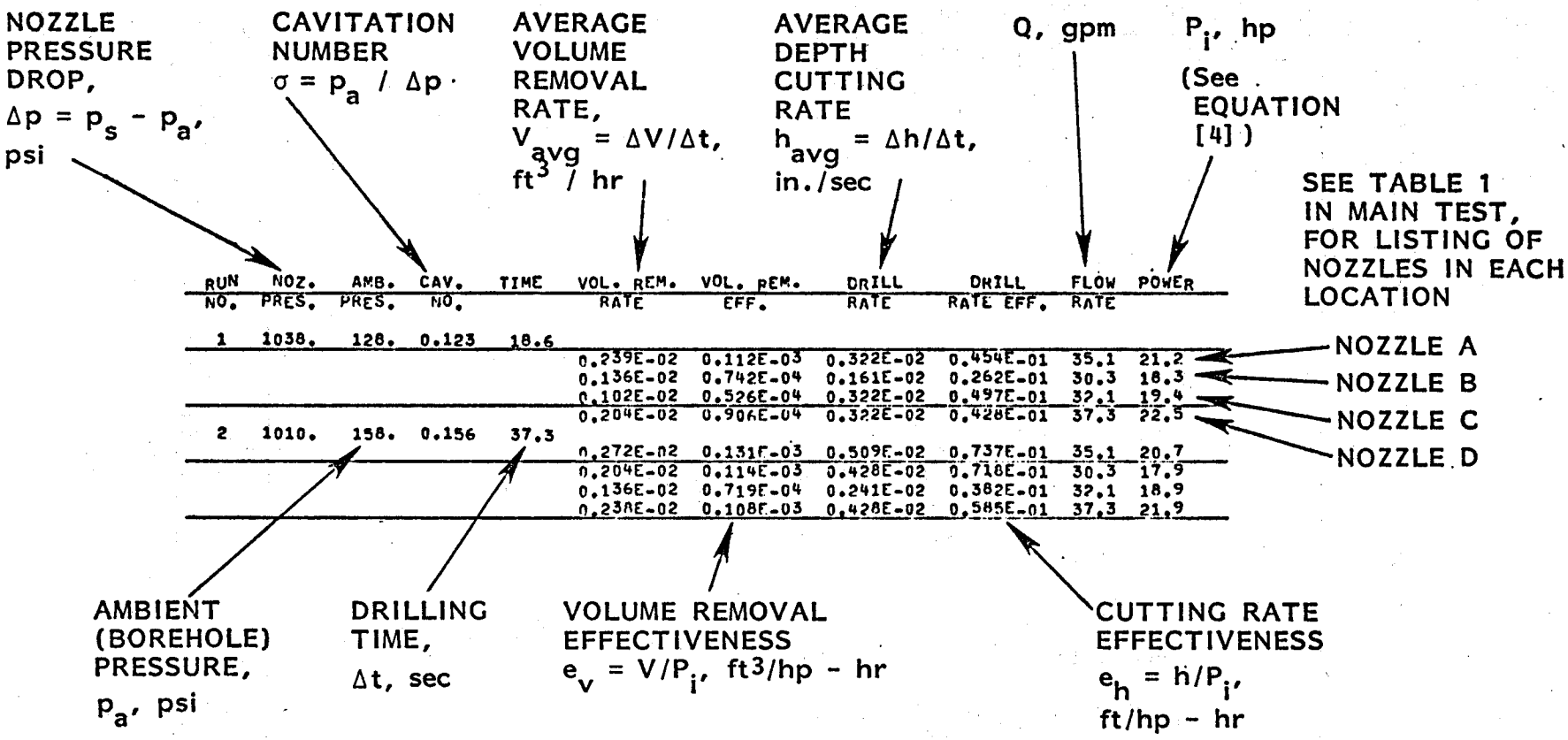

RUN NO.	NOZ. PRES.	AMB. PRES.	CAV. NO.	TIME	VOL. REM. RATE	VOL. REM. EFF.	DRILL RATE	DRILL RATE EFF.	FLOW RATE	POWER
1	1038.	128.	0.123	18.6						
					0.239E-02	0.112E-03	0.322E-02	0.454E-01	35.1	21.2
					0.136E-02	0.742E-04	0.161E-02	0.262E-01	30.3	18.3
					0.102E-02	0.526E-04	0.322E-02	0.497E-01	32.1	19.4
					0.204E-02	0.906E-04	0.322E-02	0.428E-01	37.3	22.5
2	1010.	158.	0.156	37.3						
					0.272E-02	0.131E-03	0.509E-02	0.737E-01	35.1	20.7
					0.204E-02	0.114E-03	0.428E-02	0.718E-01	30.3	17.9
					0.136E-02	0.719E-04	0.241E-02	0.382E-01	32.1	18.9
					0.238E-02	0.108E-03	0.428E-02	0.585E-01	37.3	21.9

FIGURE A-20 - EXPLANATION OF PROCESSED DATA LISTINGS FROM STATIONARY-NOZZLE TESTS

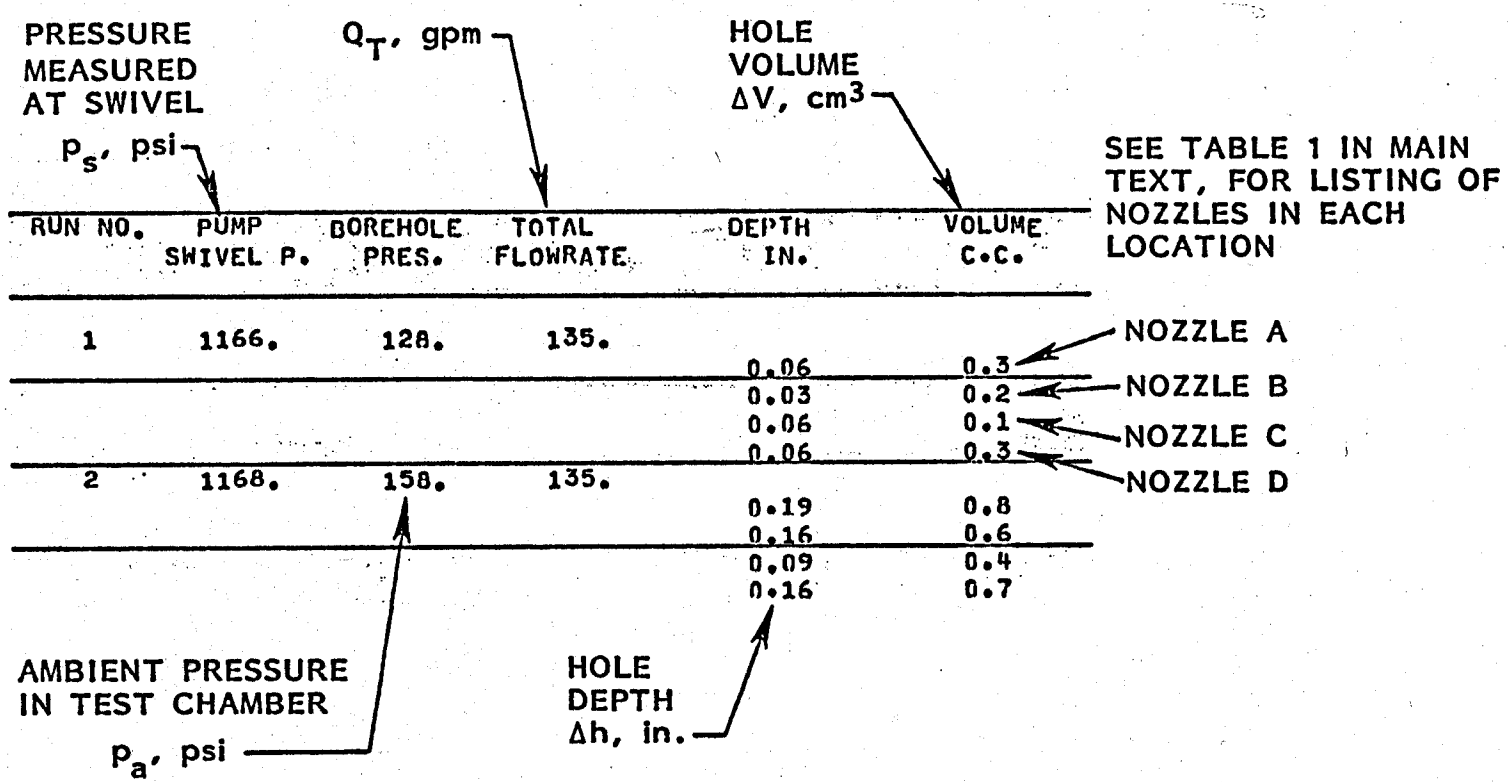

FIGURE A-19 - EXPLANATION OF RAW DATA LISTINGS FROM STATIONARY-NOZZLE TESTS

RAW DATA FOR STATIONARY - NOZZLE
TEST NO 1

RUN NO.	PUMP SWIVEL P.	BORCHOLE PRES.	TOTAL FLOWRATE	DEPTH IN.	VOLUME C.C.
1	1166.	128.	135.		
				0.06	0.3
				0.03	0.2
				0.06	0.1
				0.06	0.3
2	1168.	158.	135.		
				0.19	0.8
				0.16	0.6
				0.09	0.4
				0.16	0.7
3	1190.	147.	135.		
				0.19	1.0
				0.16	0.8
				0.12	1.0
				0.22	1.3
4	2150.	460.	285.		
				0.06	0.1
				0.06	0.0
				0.03	0.0
				0.06	0.0
5	1621.	628.	217.		
				0.09	0.2
				0.06	0.2
				0.06	0.2
				0.06	0.3
6	1596.	629.	264.		
				0.12	0.4
				0.12	0.3
				0.16	0.4
				0.12	0.6
7	1597.	625.	262.		
				0.19	1.0
				0.19	0.8
				0.19	0.5
				0.16	0.6
8	2065.	1107.	260.		
				0.16	0.2
				0.19	0.2
				0.09	0.2
				0.12	0.3
9	2060.	1081.	245.		
				0.22	0.8
				0.19	0.6
				0.12	0.3
				0.12	0.3
10	2058.	1077.	230.		
				0.12	0.7
				0.19	1.0
				0.09	0.4
				0.12	0.3
11	3125.	1250.	330.		
				0.19	0.4

TEST NO 1 (concluded)

				0.25	0.4
				0.16	0.3
				0.12	0.3
12	3125.	1250.	330.		
				0.31	1.4
				0.34	1.8
				0.22	1.3
				0.25	1.2

PROCESSED DATA FOR STATIONARY-NOZZLE TEST NO 1

UNITS
PRESSURE=PSI
TIME=SECOND
VOLUME REMOVAL RATE=FT**3/HR
VOLUME REMOVAL EFF.=FT**3/HR-HP
DRILLING RATE=IN/SEC
DRILLING RATE EFF.=FT/HR-HP
FLOW RATE=GPM
POWER=HP

RUN NO.	NOZ. PRES.	AMB. PRES.	CAV. NO.	TIME	VOL. REM. RATE	VOL. REM. EFF.	DRILL RATE	DRILL RATE EFF.	FLOW RATE	POWER
1	1038.	128.	0.123	18.6						
					0.239E-02	0.112E-03	0.322E-02	0.454E-01	35.1	21.2
					0.136E-02	0.742E-04	0.161E-02	0.262E-01	30.3	18.3
					0.102E-02	0.526E-04	0.322E-02	0.497E-01	32.1	19.4
					0.204E-02	0.906E-04	0.322E-02	0.428E-01	37.3	22.5
2	1010.	158.	0.156	37.3						
					0.272E-02	0.131E-03	0.509E-02	0.737E-01	35.1	20.7
					0.204E-02	0.114E-03	0.428E-02	0.718E-01	30.3	17.9
					0.136E-02	0.719E-04	0.241E-02	0.382E-01	32.1	18.9
					0.238E-02	0.108E-03	0.428E-02	0.585E-01	37.3	21.9
3	1043.	147.	0.140	51.3						
					0.247E-02	0.115E-03	0.370E-02	0.519E-01	35.1	21.3
					0.198E-02	0.107E-03	0.311E-02	0.506E-01	30.3	18.4
					0.247E-02	0.126E-03	0.233E-02	0.358E-01	32.1	19.5
					0.321E-02	0.141E-03	0.428E-02	0.566E-01	37.3	22.7
4	1690.	460.	0.272	2.4						
					0.529E-02	0.723E-04	0.250E-01	0.102E 00	74.2	73.1
					0.370E-02	0.585E-04	0.250E-01	0.110E 00	64.1	63.2
					0.264E-02	0.395E-04	0.125E-01	0.560E-01	67.8	66.8
					0.264E-02	0.340E-04	0.250E-01	0.965E-01	78.7	77.6
5	993.	628.	0.632	21.6						
					0.147E-02	0.448E-04	0.416E-02	0.380E-01	56.6	32.8
					0.117E-02	0.414E-04	0.277E-02	0.293E-01	48.9	28.3
					0.117E-02	0.392E-04	0.277E-02	0.277E-01	51.7	29.9
					0.176E-02	0.506E-04	0.277E-02	0.239E-01	60.1	34.8
6	967.	629.	0.650	45.3						
					0.112E-02	0.289E-04	0.264E-02	0.204E-01	68.7	38.7
					0.841E-03	0.250E-04	0.264E-02	0.237E-01	59.4	33.5
					0.112E-02	0.316E-04	0.353E-02	0.298E-01	62.8	35.4
					0.168E-02	0.408E-04	0.264E-02	0.193E-01	72.9	41.1
7	972.	625.	0.643	60.0						
					0.211E-02	0.547E-04	0.316E-02	0.245E-01	68.2	38.6
					0.169E-02	0.506E-04	0.316E-02	0.284E-01	58.9	33.4
					0.105E-02	0.299E-04	0.316E-02	0.268E-01	62.3	35.3
					0.127E-02	0.309E-04	0.266E-02	0.194E-01	72.4	41.0
8	958.	1107.	1.155	27.2						
					0.116E-02	0.300E-04	0.588E-02	0.466E-01	67.7	37.8
					0.116E-02	0.357E-04	0.698E-02	0.640E-01	58.5	32.7
					0.934E-03	0.270E-04	0.330E-02	0.286E-01	61.9	34.5

TEST NO 1 (concluded)

					0.140E-02	0.348E-04	0.441E-02	0.329E-01	71.8	40.1
9	979.	1081.	1.104	60.0						
					0.169E-02	0.464E-04	0.366E-02	0.301E-01	63.8	36.4
					0.127E-02	0.403E-04	0.316E-02	0.301E-01	55.1	31.4
					0.635E-03	0.190E-04	0.199E-02	0.180E-01	58.3	33.3
					0.635E-03	0.164E-04	0.199E-02	0.155E-01	67.7	38.6
10	981.	1077.	1.097	77.0						
					0.115E-02	0.336E-04	0.155E-02	0.136E-01	59.9	34.2
					0.164E-02	0.556E-04	0.246E-02	0.249E-01	51.7	29.6
					0.659E-03	0.210E-04	0.116E-02	0.111E-01	54.7	31.3
					0.494E-03	0.136E-04	0.155E-02	0.128E-01	63.5	36.3
11	1875.	1250.	0.666	12.0						
					0.423E-02	0.450E-04	0.158E-01	0.505E-01	85.9	94.0
					0.423E-02	0.521E-04	0.208E-01	0.769E-01	74.2	81.2
					0.317E-02	0.369E-04	0.133E-01	0.465E-01	78.5	85.9
					0.317E-02	0.318E-04	0.999E-02	0.300E-01	91.2	99.7
12	1875.	1250.	0.666	12.0						
					0.148E-01	0.157E-03	0.258E-01	0.824E-01	85.9	94.0
					0.190E-01	0.234E-03	0.263E-01	0.104E 00	74.2	81.2
					0.137E-01	0.160E-03	0.183E-01	0.640E-01	78.5	85.9
					0.127E-01	0.127E-03	0.208E-01	0.626E-01	91.2	99.7

RAW DATA FOR
STATIONARY-NOZZLE
TEST NO 2

RUN NO.	PUMP SWIVEL P.	BOREHOLE PRES.	TOTAL FLOWRATE	DEPTH IN.	VOLUME C.C.
1	1150.	187.	135.		
				0.25	1.6
				0.19	0.6
				0.13	0.4
				0.19	1.0
2	1766.	295.	170.		
				0.44	2.4
				0.38	1.2
				0.25	1.0
				0.38	1.3
3	2290.	353.	194.		
				0.38	2.0
				0.25	1.1
				0.13	0.4
				0.17	0.5
4	2893.	387.	225.		
				0.19	1.6
				0.13	0.7
				0.10	0.6
				0.13	1.0
5	1440.	430.	145.		
				0.81	6.2
				0.47	3.8
				0.38	2.1
				0.73	4.4
6	3417.	482.	238.		
				0.75	0.0*
				0.73	0.0*
				0.50	0.0*
				0.88	0.0*
7	4403.	616.	248.		
				1.00	0.0*
				1.00	7.3
				0.50	3.2
				0.44	3.4

* CRACK THROUGH HOLE

PROCESSED DATA FOR STATIONARY-NOZZLE TEST NO 2

UNITS
PRESSURE=PSI
TIME=SECOND
VOLUME REMOVAL RATE=FT**3/HR
VOLUME REMOVAL EFF.=FT**3/HR-HP
DRILLING RATE=IN/SEC
DRILLING RATE EFF.=FT/HR-HP
FLOW RATE=GPM
POWER=HP

RUN NO.	NOZ. PRES.	AMB. PRES.	CAV. NO.	TIME	VOL. REM. RATE	VOL. REM. EFF.	DRILL RATE	DRILL RATE EFF.	FLOW RATE	POWER
1	963.	187.	0.194	215.0						
					0.945E-03	0.472E-04	0.116E-02	0.174E-01	35.6	20.0
					0.354E-03	0.205E-04	0.883E-03	0.153E-01	30.7	17.2
					0.236E-03	0.136E-04	0.604E-03	0.104E-01	30.7	17.2
					0.590E-03	0.278E-04	0.863E-03	0.124E-01	37.8	21.2
2	1471.	295.	0.200	68.0						
					0.448E-02	0.116E-03	0.647E-02	0.504E-01	44.8	38.4
					0.224E-02	0.674E-04	0.558E-02	0.504E-01	38.7	33.2
					0.186E-02	0.561E-04	0.367E-02	0.331E-01	38.7	33.2
					0.242E-02	0.594E-04	0.558E-02	0.410E-01	47.6	40.8
3	1937.	353.	0.182	29.0						
					0.876E-02	0.151E-03	0.131E-01	0.679E-01	51.1	57.8
					0.481E-02	0.964E-04	0.862E-02	0.517E-01	44.2	49.9
					0.175E-02	0.350E-04	0.448E-02	0.269E-01	44.2	49.9
					0.219E-02	0.356E-04	0.586E-02	0.286E-01	54.3	61.3
4	2506.	387.	0.154	15.2						
					0.133E-01	0.154E-03	0.125E-01	0.432E-01	59.3	86.7
					0.585E-02	0.780E-04	0.855E-02	0.342E-01	51.3	74.9
					0.501E-02	0.668E-04	0.657E-02	0.263E-01	51.3	74.9
					0.835E-02	0.907E-04	0.855E-02	0.278E-01	63.0	92.1
5	1010.	430.	0.425	247.0						
					0.318E-02	0.141E-03	0.327E-02	0.436E-01	38.2	22.5
					0.195E-02	0.100E-03	0.190E-02	0.293E-01	33.0	19.4
					0.108E-02	0.554E-04	0.153E-02	0.236E-01	33.0	19.4
					0.226E-02	0.945E-04	0.295E-02	0.370E-01	40.6	23.9
6	2935.	482.	0.164	90.5						
					0.000E 00	0.000E 00	0.828E-02	0.231E-01	62.8	107.5
					0.000E 00	0.000E 00	0.806E-02	0.260E-01	54.2	92.8
					0.000E 00	0.000E 00	0.552E-02	0.178E-01	54.2	92.8
					0.000E 00	0.000E 00	0.972E-02	0.255E-01	66.6	114.1
7	3787.	616.	0.162	167.0						
					0.000E 00	0.000E 00	0.598E-02	0.124E-01	65.4	144.5
					0.555E-02	0.444E-04	0.598E-02	0.143E-01	56.5	124.9
					0.243E-02	0.194E-04	0.299E-02	0.719E-02	56.5	124.9
					0.258E-02	0.168E-04	0.263E-02	0.515E-02	69.4	153.4

RAW DATA FOR
STATIONARY-NOZZLE
TEST NO 3

Note: Runs 1 to 5 were with water

RUN NO.	PUMP SWIVEL P.	BOREHOLE PRES.	TOTAL FLOWRATE	DEPTH IN.	VOLUME C.C.
1	1136.	137.	154.		
				0.03	0.2
				0.03	0.1
				0.00	0.0
				0.00	0.0
2	1714.	269.	192.		
				0.06	0.4
				0.06	0.2
				0.00	0.0
				0.00	0.0
3	2326.	291.	230.		
				0.19	1.3
				0.16	1.0
				0.12	0.2
				0.12	0.4
4	2975.	365.	260.		
				0.12	1.0
				0.16	2.4
				0.06	0.4
				0.12	0.4
5	3447.	452.	278.		
				0.56	5.2
				0.50	7.6
				0.31	2.8
				0.19	1.8
6	1116.	227.	175.		
				0.31	1.4
				0.19	2.3
				0.25	1.4
				0.22	1.0
7	1727.	306.	210.		
				0.16	1.2
				0.12	2.4
				0.19	0.7
				0.25	0.8
8	2313.	370.	238.		
				0.19	0.8
				0.19	2.0
				0.22	0.6
				0.19	0.6
9	2865.	445.	260.		
				0.12	1.1
				0.16	0.9
				0.09	0.5
				0.09	0.6
10	1432.	499.	176.		
				0.28	1.2
				0.22	1.6
				0.22	0.6
				0.19	0.6
11	3298.	535.	280.		
				0.44	1.7

TEST NO. 3 (continued)

				0.47	4.1
				0.31	1.8
				0.28	1.8
12	1576.	705.	186.		
				0.31	1.7
				0.19	2.4
				0.19	1.2
				0.25	0.8
13	2062.	681.	218.		
				0.31	1.6
				0.19	2.0
				0.19	1.0
				0.19	1.0
14	2784.	905.	253.		
				0.19	1.2
				0.16	1.4
				0.12	0.8
				0.16	0.7
15	2392.	985.	228.		
				0.25	1.9
				0.25	2.2
				0.31	1.2
				0.25	1.4
16	1964.	1094.	200.		
				0.31	1.8
				0.19	3.4
				0.25	1.2
				0.28	1.6
17	3497.	1085.	288.		
				0.16	0.7
				0.12	1.2
				0.09	0.4
				0.09	0.5
18	4196.	1293.	315.		
				0.25	1.0
				0.16	1.1
				0.19	0.8
				0.19	0.7
19	3956.	1591.	296.		
				0.31	1.6
				0.12	1.4
				0.19	0.8
				0.19	1.0
20	2981.	1582.	247.		
				0.44	1.4
				0.38	5.2
				0.31	1.0
				0.38	1.8
21	2482.	1583.	215.		
				0.38	3.2
				0.44	5.4
				0.25	1.6
				0.38	1.5
22	4827.	1928.	325.		
				0.25	1.0
				0.12	1.6
				0.16	0.6
				0.19	0.5
23	4441.	2118.	307.		
				0.47	1.2
				0.38	4.6

TEST NO 3 (concluded)

				0.28	1.5
				0.38	1.7
24	3734.	2335.	268.		
				0.56	3.1
				0.44	6.4
				0.38	2.6
				0.50	2.4
25	4973.	2572.	320.		
				0.31	1.5
				0.25	3.1
				0.38	1.1
				0.25	1.1
26	5265.	2713.	340.		
				0.25	1.4
				0.25	3.0
				0.31	1.2
				0.25	1.3
27	4972.	3086.	313.		
				0.38	1.8
				0.38	7.6
				0.38	2.0
				0.34	2.2
28	3227.	1334.	292.		
				0.22	0.7
				0.19	1.2
				0.19	1.0
				0.22	1.0
29	4750.	1643.	367.		
				0.25	1.5
				0.28	2.4
				0.25	0.8
				0.31	1.2
30	3018.	2077.	253.		
				0.50	2.4
				0.38	7.4
				0.38	2.4
				0.41	2.2
31	4566.	2094.	368.		
				0.12	0.5
				0.09	1.1
				0.16	0.5
				0.16	0.6
32	4501.	3129.	315.		
				0.56	3.4
				0.50	13.0
				0.53	3.4
				0.59	3.0
33	5132.	3612.	303.		
				0.50	2.0
				0.50	10.0
				0.50	2.5
				0.50	2.5
34	5075.	3848.	308.		
				0.50	3.2
				0.41	11.2
				0.47	2.8
				0.62	2.9

PROCESSED DATA FOR STATIONARY-NOZZLE TEST NO 3

Note: Runs 1 to 5 were with water

UNITS
PRESSURE=PSI
TIME=SECOND
VOLUME REMOVAL RATE=FT**3/HR
VOLUME REMOVAL EFF.=FT**3/HR-HP
DRILLING RATE=IN/SEC
DRILLING RATE EFF.=FT/HR-HP
FLOW RATE=GPM
POWER=HP

RUN NO.	NOZ. PRES.	AMB. PRES.	CAV. NO.	TIME	VOL. REM. RATE	VOL. REM. EFF.	DRILL RATE	DRILL RATE EFF.	FLOW RATE	POWER
1	999.	137.	0.137	210.0						
					0.120E-03	0.610E-05	0.142E-03	0.216E-02	34.0	19.8
					0.604E-04	0.187E-05	0.142E-03	0.132E-02	55.4	32.2
					0.000E 00	0.000E 00	0.000E 00	0.000E 00	34.0	19.8
					0.000E 00	0.000E 00	0.000E 00	0.000E 00	30.5	17.8
2	1445.	269.	0.186	67.2						
					0.756E-03	0.211E-04	0.892E-03	0.749E-02	42.3	35.7
					0.378E-03	0.649E-05	0.892E-03	0.459E-02	69.1	58.2
					0.000E 00	0.000E 00	0.000E 00	0.000E 00	42.3	35.7
					0.000E 00	0.000E 00	0.000E 00	0.000E 00	38.1	32.1
3	2035.	291.	0.142	29.1						
					0.567E-02	0.941E-04	0.652E-02	0.324E-01	50.7	60.2
					0.436E-02	0.444E-04	0.549E-02	0.167E-01	82.7	98.2
					0.873E-03	0.144E-04	0.412E-02	0.205E-01	50.7	60.2
					0.174E-02	0.322E-04	0.412E-02	0.228E-01	45.6	54.1
4	2610.	365.	0.139	11.2						
					0.113E-01	0.129E-03	0.107E-01	0.367E-01	57.4	87.3
					0.272E-01	0.191E-03	0.142E-01	0.300E-01	93.5	142.4
					0.510E-02	0.584E-04	0.535E-02	0.183E-01	57.4	87.3
					0.453E-02	0.577E-04	0.107E-01	0.409E-01	51.6	78.5
5	2995.	452.	0.150	47.0						
					0.140E-01	0.131E-03	0.119E-01	0.333E-01	61.3	107.2
					0.205E-01	0.117E-03	0.106E-01	0.182E-01	100.0	174.7
					0.756E-02	0.705E-04	0.659E-02	0.184E-01	61.3	107.2
					0.486E-02	0.504E-04	0.404E-02	0.125E-01	55.1	96.4
6	889.	227.	0.255	210.5						
					0.844E-03	0.425E-04	0.147E-02	0.222E-01	38.3	19.8
					0.138E-02	0.777E-04	0.902E-03	0.151E-01	34.4	17.8
					0.844E-03	0.425E-04	0.116E-02	0.179E-01	38.3	19.8
					0.603E-03	0.182E-04	0.104E-02	0.946E-02	63.9	33.1
7	1421.	306.	0.215	67.2						
					0.226E-02	0.591E-04	0.238E-02	0.186E-01	46.2	38.3
					0.453E-02	0.131E-03	0.178E-02	0.155E-01	41.5	34.4
					0.132E-02	0.345E-04	0.282E-02	0.221E-01	46.2	38.3
					0.151E-02	0.240E-04	0.372E-02	0.177E-01	75.9	62.9
8	1943.	370.	0.190	29.8						
					0.341E-02	0.574E-04	0.637E-02	0.322E-01	52.3	59.3
					0.852E-02	0.159E-03	0.637E-02	0.358E-01	47.0	53.3
					0.255E-02	0.430E-04	0.738E-02	0.372E-01	52.3	59.3

TEST NO 3 (continued)

					0.255E-02	0.262E-04	0.637E-02	0.195E-01	86.1	97.6
9	2420.	445.	0.183	19.7						
					0.709E-02	0.878E-04	0.609E-02	0.226E-01	57.2	80.7
					0.580E-02	0.799E-04	0.812E-02	0.335E-01	51.4	72.5
					0.322E-02	0.399E-04	0.456E-02	0.169E-01	57.2	80.7
					0.386E-02	0.291E-04	0.456E-02	0.103E-01	94.1	132.9
10	933.	499.	0.534	182.6						
					0.634E-03	0.392E-04	0.153E-02	0.216E-01	39.0	21.2
					0.111E-02	0.582E-04	0.120E-02	0.189E-01	35.1	19.1
					0.417E-03	0.196E-04	0.120E-02	0.169E-01	39.0	21.2
					0.417E-03	0.122E-04	0.104E-02	0.914E-02	62.7	34.1
11	2763.	535.	0.193	48.0						
					0.449E-02	0.462E-04	0.916E-02	0.282E-01	60.3	97.2
					0.108E-01	0.124E-03	0.979E-02	0.336E-01	54.2	87.3
					0.476E-02	0.489E-04	0.645E-02	0.199E-01	60.3	97.2
					0.476E-02	0.281E-04	0.583E-02	0.103E-01	105.1	169.4
12	871.	705.	0.809	241.6						
					0.893E-03	0.462E-04	0.128E-02	0.199E-01	38.0	19.3
					0.126E-02	0.727E-04	0.786E-03	0.135E-01	34.1	17.3
					0.630E-03	0.326E-04	0.786E-03	0.122E-01	38.0	19.3
					0.420E-03	0.109E-04	0.103E-02	0.805E-02	75.8	38.5
13	1381.	681.	0.493	78.7						
					0.258E-02	0.701E-04	0.393E-02	0.320E-01	45.7	36.8
					0.322E-02	0.975E-04	0.241E-02	0.218E-01	41.0	33.0
					0.161E-02	0.438E-04	0.241E-02	0.196E-01	45.7	36.8
					0.161E-02	0.234E-04	0.241E-02	0.105E-01	85.5	68.8
14	1879.	905.	0.481	31.7						
					0.480E-02	0.848E-04	0.599E-02	0.317E-01	51.7	56.6
					0.561E-02	0.110E-03	0.504E-02	0.297E-01	46.4	50.9
					0.320E-02	0.565E-04	0.378E-02	0.200E-01	51.7	56.6
					0.280E-02	0.248E-04	0.504E-02	0.133E-01	103.1	113.0
15	1407.	985.	0.700	91.1						
					0.264E-02	0.700E-04	0.274E-02	0.217E-01	46.0	37.7
					0.306E-02	0.903E-04	0.274E-02	0.242E-01	41.3	33.9
					0.167E-02	0.442E-04	0.340E-02	0.270E-01	46.0	37.7
					0.195E-02	0.251E-04	0.274E-02	0.106E-01	94.5	77.5
16	870.	1094.	1.257	240.3						
					0.951E-03	0.493E-04	0.129E-02	0.200E-01	37.9	19.2
					0.179E-02	0.103E-03	0.790E-03	0.136E-01	34.1	17.3
					0.634E-03	0.328E-04	0.104E-02	0.161E-01	37.9	19.2
					0.845E-03	0.185E-04	0.116E-02	0.766E-02	89.8	45.6
17	2412.	1085.	0.449	11.9						
					0.747E-02	0.929E-04	0.134E-01	0.501E-01	57.1	80.3
					0.128E-01	0.177E-03	0.100E-01	0.418E-01	51.3	72.2
					0.427E-02	0.531E-04	0.756E-02	0.282E-01	57.1	80.3
					0.533E-02	0.309E-04	0.756E-02	0.131E-01	122.3	172.2
18	2903.	1293.	0.445	11.8						
					0.107E-01	0.103E-03	0.211E-01	0.610E-01	61.5	104.1
					0.118E-01	0.126E-03	0.135E-01	0.434E-01	55.2	93.6
					0.861E-02	0.826E-04	0.161E-01	0.463E-01	61.5	104.1
					0.753E-02	0.325E-04	0.161E-01	0.208E-01	136.6	231.4
19	2365.	1591.	0.672	23.5						
					0.864E-02	0.110E-03	0.131E-01	0.506E-01	56.6	78.1
					0.756E-02	0.107E-03	0.510E-02	0.218E-01	50.9	70.2
					0.432E-02	0.553E-04	0.808E-02	0.310E-01	56.6	78.1
					0.540E-02	0.297E-04	0.808E-02	0.133E-01	131.6	181.6
20	1399.	1582.	1.130	133.3						
					0.133E-02	0.355E-04	0.330E-02	0.264E-01	45.9	37.4
					0.495E-02	0.147E-03	0.285E-02	0.253E-01	41.2	33.6
					0.953E-03	0.254E-04	0.232E-02	0.186E-01	45.9	37.4
					0.171E-02	0.184E-04	0.285E-02	0.920E-02	113.8	92.8

TEST NO 3 (continued)

21	899.	1583.	1.760	301.9						
					0.134E-02	0.666E-04	0.125E-02	0.187E-01	38.4	20.1
					0.227E-02	0.125E-03	0.145E-02	0.241E-01	34.5	18.1
					0.673E-03	0.333E-04	0.828E-03	0.123E-01	38.4	20.1
					0.631E-03	0.116E-04	0.125E-02	0.696E-02	103.4	54.2
22	2899.	1928.	0.665	12.2						
					0.104E-01	0.100E-03	0.204E-01	0.591E-01	61.4	103.9
					0.166E-01	0.178E-03	0.983E-02	0.315E-01	55.2	93.4
					0.624E-02	0.600E-04	0.131E-01	0.378E-01	61.4	103.9
					0.572E-02	0.230E-04	0.155E-01	0.188E-01	146.7	248.1
23	2323.	2118.	0.911	63.9						
					0.238E-02	0.312E-04	0.735E-02	0.289E-01	56.2	76.2
					0.914E-02	0.133E-03	0.594E-02	0.260E-01	50.5	68.5
					0.298E-02	0.391E-04	0.438E-02	0.172E-01	56.2	76.2
					0.337E-02	0.173E-04	0.594E-02	0.915E-02	143.8	194.9
24	1399.	2335.	1.669	180.5						
					0.218E-02	0.581E-04	0.310E-02	0.246E-01	45.9	37.4
					0.450E-02	0.133E-03	0.243E-02	0.217E-01	41.2	33.6
					0.182E-02	0.488E-04	0.210E-02	0.168E-01	45.9	37.4
					0.168E-02	0.153E-04	0.277E-02	0.755E-02	134.8	110.0
25	2401.	2572.	1.071	31.2						
					0.610E-02	0.764E-04	0.993E-02	0.373E-01	57.0	79.8
					0.126E-01	0.175E-03	0.801E-02	0.334E-01	51.2	71.7
					0.447E-02	0.560E-04	0.121E-01	0.457E-01	57.0	79.8
					0.447E-02	0.206E-04	0.801E-02	0.110E-01	154.6	216.6
26	2552.	2713.	1.063	31.2						
					0.570E-02	0.655E-04	0.801E-02	0.276E-01	58.4	86.9
					0.122E-01	0.156E-03	0.801E-02	0.307E-01	52.5	78.1
					0.488E-02	0.561E-04	0.993E-02	0.342E-01	58.4	86.9
					0.529E-02	0.208E-04	0.801E-02	0.946E-02	170.6	253.9
27	1886.	3086.	1.636	90.6						
					0.252E-02	0.443E-04	0.419E-02	0.220E-01	51.7	56.9
					0.106E-01	0.208E-03	0.419E-02	0.245E-01	46.5	51.1
					0.280E-02	0.492E-04	0.419E-02	0.220E-01	51.7	56.9
					0.308E-02	0.172E-04	0.375E-02	0.628E-02	162.9	179.2
28	1893.	1334.	0.704	31.3						
					0.284E-02	0.496E-04	0.702E-02	0.368E-01	51.8	57.2
					0.487E-02	0.946E-04	0.607E-02	0.353E-01	46.5	51.4
					0.405E-02	0.708E-04	0.607E-02	0.318E-01	51.8	57.2
					0.405E-02	0.259E-04	0.702E-02	0.134E-01	141.6	156.4
29	3107.	1643.	0.528	11.7						
					0.162E-01	0.142E-03	0.213E-01	0.559E-01	63.2	114.5
					0.260E-01	0.253E-03	0.239E-01	0.697E-01	56.8	102.9
					0.868E-02	0.758E-04	0.213E-01	0.559E-01	63.2	114.5
					0.130E-01	0.391E-04	0.264E-01	0.238E-01	183.7	333.0
30	941.	2077.	2.207	361.0						
					0.844E-03	0.392E-04	0.138E-02	0.193E-01	39.2	21.5
					0.260E-02	0.134E-03	0.105E-02	0.163E-01	35.2	19.3
					0.844E-03	0.392E-04	0.105E-02	0.146E-01	39.2	21.5
					0.774E-03	0.101E-04	0.113E-02	0.445E-02	139.3	76.4
31	2472.	2094.	0.847	11.0						
					0.577E-02	0.694E-04	0.109E-01	0.393E-01	57.6	83.1
					0.127E-01	0.169E-03	0.818E-02	0.328E-01	51.8	74.7
					0.577E-02	0.694E-04	0.145E-01	0.524E-01	57.6	83.1
					0.692E-02	0.239E-04	0.145E-01	0.150E-01	200.7	289.4
32	1372.	3129.	2.280	240.5						
					0.179E-02	0.492E-04	0.232E-02	0.191E-01	45.5	36.4
					0.686E-02	0.209E-03	0.207E-02	0.190E-01	40.9	32.7
					0.179E-02	0.492E-04	0.220E-02	0.181E-01	45.5	36.4
					0.158E-02	0.108E-04	0.245E-02	0.502E-02	182.8	146.3
33	1520.	3612.	2.376	241.2						

TEST NO 3 (concluded)

				0.105E-02	0.250E-04	0.207E-02	0.147E-01	47.4	42.1
				0.526E-02	0.139E-03	0.207E-02	0.164E-01	42.6	37.8
				0.131E-02	0.312E-04	0.207E-02	0.147E-01	47.4	42.1
				0.131E-02	0.898E-05	0.207E-02	0.424E-02	165.3	146.5
34	1227.	3848.	3.136	322.4					
				0.126E-02	0.404E-04	0.155E-02	0.149E-01	43.5	31.2
				0.441E-02	0.157E-03	0.127E-02	0.136E-01	89.1	28.0
				0.110E-02	0.353E-04	0.145E-02	0.140E-01	43.5	31.2
				0.114E-02	0.879E-05	0.192E-02	0.443E-02	181.6	129.9

RAW DATA FOR STATIONARY-NOZZLE TEST NO 4

RUN NO.	PUMP SWIVEL P.	BOREHOLE PRES.	TOTAL FLOWRATE	DEPTH IN.	VOLUME C.C.
1	1175.	140.	135.		
				0.50	4.4
				0.57	2.6
				0.55	4.3
				0.66	2.9
2	1380.	200.	148.		
				0.43	2.2
				0.39	2.2
				0.41	2.7
				0.42	1.7
3	2250.	300.	190.		
				0.43	2.9
				0.37	2.3
				0.33	2.2
				0.32	1.3
4	1400.	365.	135.		
				0.53	3.2
				0.47	2.0
				0.46	2.5
				0.52	2.3
5	2850.	370.	225.		
				0.42	2.9
				0.38	2.2
				0.34	2.2
				0.43	2.1
6	2500.	390.	195.		
				0.36	2.1
				0.35	2.0
				0.27	2.1
				0.37	1.8
7	3250.	395.	230.		
				0.84	7.8
				0.67	6.0
				0.68	5.8
				0.62	4.8
8	2000.	560.	160.		
				0.33	1.9
				0.38	1.6
				0.32	1.9
				0.31	1.5
9	3650.	600.	230.		
				0.74	4.7
				0.83	4.3
				0.65	4.9
				0.79	4.3
10	3100.	660.	218.		
				0.37	1.3
				0.38	1.8
				0.35	2.0
				0.27	1.4
11	2800.	720.	195.		
				0.36	2.3

TEST NO 4 (continued)

				0.39	1.7
				0.35	2.2
				0.34	1.7
12	1730.	740.	137.		
				0.49	3.0
				0.42	1.7
				0.42	2.9
				0.48	2.1
13	2300.	750.	168.		
				0.45	2.0
				0.51	2.0
				0.57	1.9
				0.65	2.2
14	4100.	760.	245.		
				0.60	0.0*
				0.47	2.6
				0.57	2.9
				0.54	1.5
15	3350.	900.	220.		
				0.67	3.8
				0.47	2.4
				0.44	2.8
				0.52	2.0
16	2020.	1010.	138.		
				0.28	1.6
				0.25	0.9
				0.21	1.0
				0.27	0.8
17	2500.	1000.	170.		
				0.35	2.0
				0.33	1.6
				0.30	1.7
				0.32	1.7
18	2950.	1010.	193.		
				0.83	4.8
				0.70	3.8
				0.57	4.5
				0.73	3.5
19	4000.	1010.	235.		
				0.84	5.1
				0.73	4.0
				0.72	4.6
				0.83	4.3
20	4300.	1290.	240.		
				0.55	4.0
				0.47	2.3
				0.44	2.5
				0.54	2.5
21	2500.	1480.	140.		
				0.22	1.2
				0.22	1.0
				0.19	1.0
				0.16	0.6
22	3050.	1500.	170.		
				0.42	2.0
				0.34	1.8
				0.31	1.8
				0.38	1.5
23	3500.	1550.	195.		
				0.56	3.6
				0.53	2.8

TEST NO 4 (continued)

				0.48	2.5
				0.52	2.7
24	3950.	1530.	218.		
				0.40	2.8
				0.42	2.2
				0.32	1.5
				0.33	1.3
25	4450.	1530.	240.		
				1.19	8.8
				1.11	7.2
				1.06	7.5
				1.14	7.0
26	5000.	1940.	232.		
				0.72	5.3
				0.87	5.6
				0.86	5.5
				0.87	4.6
27	3000.	2000.	130.		
				0.62	3.1
				0.46	2.0
				0.48	2.6
				0.57	2.5
28	4000.	2050.	195.		
				0.59	3.7
				0.52	3.1
				0.56	3.6
				0.99	3.0
29	4450.	2010.	215.		
				1.30	10.8
				1.08	8.3
				1.05	6.9
				0.92	5.7
30	5300.	2300.	233.		
				0.82	6.1
				0.93	5.2
				0.88	5.8
				0.87	4.6
31	4950.	2500.	215.		
				1.08	6.4
				0.87	4.8
				0.65	6.6
				0.74	4.7
32	5400.	2950.	217.		
				0.87	5.0
				0.68	3.7
				0.61	3.2
				0.73	3.2
33	3950.	3010.	127.		
				0.27	1.6
				0.27	1.6
				0.27	1.5
				0.31	1.5
34	4400.	3000.	160.		
				0.55	3.6
				0.55	3.0
				0.40	2.7
				0.53	2.7
35	5250.	3300.	191.		
				0.63	3.8
				0.59	3.0
				0.62	3.8

TEST NO 4 (concluded)

				0.58	2.8
36	5230.	3950.	155.		
				1.30	14.0
				1.16	12.0
				1.23	14.1
				1.20	12.9

* CRACK THROUGH HOLE

PROCESSED DATA FOR STATIONARY-NOZZLE TEST NO 4

UNITS
PRESSURE=PSI
TIME=SECOND
VOLUME REMOVAL RATE=FT**3/HR
VOLUME REMOVAL EFF.=FT**3/HR-HP
DRILLING RATE=IN/SEC
DRILLING RATE EFF.=FT/HR-HP
FLOW RATE=GPM
POWER=HP

RUN NO.	NOZ. PRES.	AMB. PRES.	CAV. NO.	TIME	VOL. REM. RATE	VOL. REM. EFF.	DRILL RATE	DRILL RATE EFF.	FLOW RATE	POWER
1	1035.	140.	0.135	301.0						
					0.185E-02	0.894E-04	0.166E-02	0.240E-01	34.3	20.7
					0.109E-02	0.528E-04	0.189E-02	0.273E-01	34.3	20.7
					0.181E-02	0.823E-04	0.182E-02	0.248E-01	36.5	22.0
					0.122E-02	0.682E-04	0.219E-02	0.366E-01	29.7	17.9
2	1180.	200.	0.169	122.0						
					0.229E-02	0.882E-04	0.352E-02	0.407E-01	37.6	25.9
					0.229E-02	0.8[illegible]2E-04	0.319E-02	0.369E-01	37.6	25.9
					0.281E-02	0.102E-03	0.336E-02	0.365E-01	40.0	27.5
					0.177E-02	0.789E-04	0.344E-02	0.460E-01	32.5	22.4
3	1950.	300.	0.153	33.0						
					0.111E-01	0.202E-03	0.130E-01	0.710E-01	48.3	55.0
					0.885E-02	0.160E-03	0.112E-01	0.611E-01	48.3	55.0
					0.846E-02	0.144E-03	0.999E-02	0.513E-01	51.3	58.4
					0.500E-02	0.105E-03	0.969E-02	0.611E-01	41.8	47.5
4	1035.	365.	0.352	211.0						
					0.192E-02	0.928E-04	0.251E-02	0.363E-01	34.3	20.7
					0.120E-02	0.580E-04	0.222E-02	0.321E-01	34.3	20.7
					0.150E-02	0.682E-04	0.218E-02	0.296E-01	36.5	22.0
					0.138E-02	0.771E-04	0.246E-02	0.412E-01	29.7	17.9
5	2480.	370.	0.149	16.8						
					0.219E-01	0.264E-03	0.250E-01	0.904E-01	57.3	82.9
					0.166E-01	0.200E-03	0.226E-01	0.818E-01	57.3	82.9
					0.166E-01	0.188E-03	0.202E-01	0.689E-01	60.8	88.0
					0.158E-01	0.221E-03	0.255E-01	0.107E 00	49.5	71.6
6	2110.	390.	0.184	31.2						
					0.855E-02	0.139E-03	0.115E-01	0.566E-01	49.6	61.1
					0.814E-02	0.133E-03	0.112E-01	0.550E-01	49.6	61.1
					0.855E-02	0.131E-03	0.865E-02	0.599E-01	52.7	64.9
					0.732E-02	0.138E-03	0.118E-01	0.673E-01	42.9	52.8
7	2855.	395.	0.138	43.2						
					0.229E-01	0.235E-03	0.194E-01	0.597E-01	58.5	97.5
					0.176E-01	0.180E-03	0.155E-01	0.476E-01	58.5	97.5
					0.170E-01	0.164E-03	0.157E-01	0.455E-01	62.2	103.6
					0.141E-01	0.167E-03	0.143E-01	0.510E-01	50.6	84.3
8	1440.	560.	0.388	81.3						
					0.296E-02	0.867E-04	0.405E-02	0.355E-01	40.7	34.2
					0.250E-02	0.730E-04	0.467E-02	0.409E-01	40.7	34.2
					0.296E-02	0.816E-04	0.393E-02	0.324E-01	43.2	36.3

TEST NO 4 (continued)

					0.234E-02	0.792E-04	0.381E-02	0.386E-01	35.2	29.5
9	3050.	600.	0.196	46.2						
					0.129E-01	0.124E-03	0.160E-01	0.461E-01	58.5	104.2
					0.118E-01	0.113E-03	0.179E-01	0.517E-01	58.5	104.2
					0.134E-01	0.121E-03	0.140E-01	0.381E-01	62.2	110.6
					0.118E-01	0.131E-03	0.170E-01	0.569E-01	50.6	90.8
10	2440.	660.	0.270	21.4						
					0.771E-02	0.976E-04	0.172E-01	0.656E-01	55.5	79.0
					0.106E-01	0.135E-03	0.177E-01	0.674E-01	55.5	79.0
					0.118E-01	0.141E-03	0.163E-01	0.584E-01	58.9	83.9
					0.831E-02	0.121E-03	0.126E-01	0.554E-01	47.9	68.2
11	2080.	720.	0.346	36.2						
					0.807E-02	0.133E-03	0.994E-02	0.495E-01	49.6	60.2
					0.596E-02	0.990E-04	0.107E-01	0.536E-01	49.6	60.2
					0.772E-02	0.120E-03	0.966E-02	0.453E-01	52.7	63.9
					0.596E-02	0.114E-03	0.939E-02	0.541E-01	42.9	52.0
12	990.	740.	0.747	242.8						
					0.156E-02	0.778E-04	0.201E-02	0.300E-01	34.8	20.1
					0.889E-03	0.441E-04	0.172E-02	0.257E-01	34.8	20.1
					0.151E-02	0.709E-04	0.172E-02	0.242E-01	37.0	21.4
					0.109E-02	0.630E-04	0.197E-02	0.340E-01	30.1	17.4
13	1550.	750.	0.483	91.5						
					0.277E-02	0.717E-04	0.491E-02	0.381E-01	42.7	38.6
					0.277E-02	0.717E-04	0.557E-02	0.432E-01	42.7	38.6
					0.263E-02	0.642E-04	0.622E-02	0.454E-01	45.4	41.0
					0.305E-02	0.913E-04	0.710E-02	0.637E-01	36.9	33.4
14	3340.	760.	0.227	15.0						
					0.000E 00	0.000E 00	0.399E-01	0.987E-01	62.4	121.5
					0.220E-01	0.181E-03	0.313E-01	0.773E-01	62.4	121.5
					0.245E-01	0.190E-03	0.380E-01	0.882E-01	66.2	129.1
					0.127E-01	0.120E-03	0.359E-01	0.102E 00	53.9	105.0
15	2450.	900.	0.367	18.8						
					0.256E-01	0.320E-03	0.356E-01	0.133E 00	56.0	80.0
					0.162E-01	0.202E-03	0.250E-01	0.936E-01	56.0	80.0
					0.189E-01	0.222E-03	0.234E-01	0.825E-01	59.5	85.0
					0.135E-01	0.195E-03	0.276E-01	0.119E 00	48.4	69.1
16	1010.	1010.	1.000	242.2						
					0.839E-03	0.405E-04	0.115E-02	0.167E-01	35.1	20.7
					0.472E-03	0.227E-04	0.103E-02	0.149E-01	35.1	20.7
					0.524E-03	0.238E-04	0.867E-03	0.118E-01	37.3	21.9
					0.419E-03	0.234E-04	0.111E-02	0.186E-01	30.3	17.8
17	1500.	1000.	0.666	105.5						
					0.240E-02	0.635E-04	0.331E-02	0.262E-01	43.2	37.8
					0.192E-02	0.508E-04	0.312E-02	0.247E-01	43.2	37.8
					0.204E-02	0.508E-04	0.284E-02	0.212E-01	45.9	40.2
					0.204E-02	0.625E-04	0.303E-02	0.277E-01	37.4	32.7
18	1940.	1010.	0.520	46.0						
					0.132E-01	0.238E-03	0.180E-01	0.973E-01	49.1	55.6
					0.104E-01	0.188E-03	0.152E-01	0.820E-01	49.1	55.6
					0.124E-01	0.210E-03	0.123E-01	0.629E-01	52.2	59.0
					0.966E-02	0.201E-03	0.158E-01	0.990E-01	42.4	48.0
19	2990.	1010.	0.337	16.4						
					0.395E-01	0.378E-03	0.512E-01	0.147E 00	59.8	104.3
					0.309E-01	0.296E-03	0.445E-01	0.127E 00	59.8	104.3
					0.356E-01	0.321E-03	0.439E-01	0.118E 00	63.5	110.8
					0.333E-01	0.369E-03	0.506E-01	0.168E 00	51.7	90.2
20	3010.	1290.	0.428	16.8						
					0.302E-01	0.281E-03	0.327E-01	0.915E-01	61.1	107.3
					0.173E-01	0.162E-03	0.279E-01	0.782E-01	61.1	107.3
					0.189E-01	0.165E-03	0.261E-01	0.689E-01	64.9	113.5
					0.189E-01	0.203E-03	0.321E-01	0.103E 00	52.8	92.7

TEST NO 4 (continued)

21	1020.	1480.	1.450	301.6						
					0.505E-03	0.238E-04	0.729E-03	0.103E-01	35.6	21.2
					0.421E-03	0.198E-04	0.729E-03	0.103E-01	35.6	21.2
					0.421E-03	0.186E-04	0.629E-03	0.838E-02	37.8	22.5
					0.252E-03	0.137E-04	0.530E-03	0.868E-02	30.8	18.3
22	1550.	1500.	0.967	136.1						
					0.186E-02	0.476E-04	0.308E-02	0.236E-01	43.2	39.1
					0.168E-02	0.429E-04	0.249E-02	0.191E-01	43.2	39.1
					0.168E-02	0.404E-04	0.227E-02	0.164E-01	45.9	41.5
					0.140E-02	0.413E-04	0.279E-02	0.247E-01	37.4	33.8
23	1950.	1550.	0.794	45.7						
					0.100E-01	0.177E-03	0.122E-01	0.650E-01	49.6	56.4
					0.778E-02	0.137E-03	0.115E-01	0.615E-01	49.6	56.4
					0.694E-02	0.115E-03	0.105E-01	0.525E-01	52.7	59.9
					0.750E-02	0.153E-03	0.113E-01	0.699E-01	42.9	48.8
24	2420.	1530.	0.632	31.4						
					0.113E-01	0.144E-03	0.127E-01	0.487E-01	55.5	78.3
					0.890E-02	0.113E-03	0.133E-01	0.511E-01	55.5	78.3
					0.606E-02	0.729E-04	0.101F-01	0.367E-01	58.9	83.2
					0.525E-02	0.776E-04	0.105E-01	0.465E-01	47.9	67.7
25	2920.	1530.	0.523	17.0						
					0.657E-01	0.631E-03	0.699E-01	0.201E 00	61.1	104.1
					0.538E-01	0.516E-03	0.652E-01	0.188E 00	61.1	104.1
					0.560E-01	0.506E-03	0.623E-01	0.169E 00	64.9	110.5
					0.523E-01	0.581E-03	0.670E-01	0.223E 00	52.8	89.9
26	3060.	1940.	0.633	26.7						
					0.252E-01	0.239E-03	0.269E-01	0.767E-01	59.0	105.4
					0.266E-01	0.252E-03	0.325E-01	0.926E-01	59.0	105.4
					0.261E-01	0.233E-03	0.322E-01	0.862E-01	62.7	112.0
					0.218E-01	0.240E-03	0.325E-01	0.107E 00	51.0	91.1
27	1000.	2000.	2.000	301.3						
					0.130E-02	0.676E-04	0.205E-02	0.319E-01	33.1	19.3
					0.843E-03	0.436E-04	0.152E-02	0.237E-01	33.1	19.3
					0.109E-02	0.534E-04	0.159E-02	0.253E-01	35.1	20.5
					0.105E-02	0.631E-04	0.189E-02	0.340E-01	28.6	16.6
28	1950.	2050.	1.051	61.1						
					0.769E-02	0.136E-03	0.965E-02	0.512E-01	49.6	56.4
					0.644E-02	0.114E-03	0.851E-02	0.451E-01	49.6	56.4
					0.748E-02	0.124E-03	0.916E-02	0.458E-01	52.7	59.9
					0.623E-02	0.127E-03	0.162E-01	0.995E-01	42.9	48.8
29	2440.	2010.	0.823	46.0						
					0.298E-01	0.382E-03	0.282E-01	0.108E 00	54.7	77.9
					0.229E-01	0.294E-03	0.234E-01	0.903E-01	54.7	77.9
					0.190E-01	0.230E-03	0.228E-01	0.827E-01	58.1	82.7
					0.157E-01	0.233E-03	0.199E-01	0.890E-01	47.3	67.3
30	3000.	2300.	0.766	41.0						
					0.189E-01	0.182E-03	0.199E-01	0.577E-01	59.3	103.8
					0.161E-01	0.155E-03	0.226E-01	0.655E-01	59.3	103.8
					0.179E-01	0.162E-03	0.214E-01	0.583E-01	63.0	110.2
					0.142E-01	0.158E-03	0.212E-01	0.709E-01	51.2	89.7
31	2450.	2500.	1.020	39.8						
					0.204E-01	0.261E-03	0.271E-01	0.104E 00	54.7	78.2
					0.153E-01	0.195E-03	0.218E-01	0.837E-01	54.7	78.2
					0.210E-01	0.253E-03	0.163E-01	0.589E-01	58.1	83.1
					0.150E-01	0.221E-03	0.185E-01	0.824E-01	47.3	67.6
32	2450.	2950.	1.204	51.0						
					0.124E-01	0.157E-03	0.170E-01	0.647E-01	55.2	78.9
					0.921E-02	0.116E-03	0.133E-01	0.506E-01	55.2	78.9
					0.797E-02	0.950E-04	0.119E-01	0.427E-01	58.6	83.8
					0.797E-02	0.116E-03	0.143E-01	0.629E-01	47.7	68.2
33	940.	3010.	3.202	300.2						

TEST NO 4 (concluded)

					0.677E-03	0.381E-04	0.899E-03	0.152E-01	32.3	17.7
					0.677E-03	0.381E-04	0.899E-03	0.152E-01	32.3	17.7
					0.634E-03	0.336E-04	0.899E-03	0.143E-01	34.3	18.8
					0.634E-03	0.414E-04	0.103E-02	0.202E-01	27.9	15.3
34	1400.	3000.	2.142	211.3						
					0.216E-02	0.650E-04	0.260E-02	0.234E-01	40.7	33.2
					0.180E-02	0.541E-04	0.260E-02	0.234E-01	40.7	33.2
					0.162E-02	0.459E-04	0.189E-02	0.160E-01	43.2	35.3
					0.162E-02	0.564E-04	0.250E-02	0.261E-01	35.2	28.7
35	1950.	3300.	1.692	211.0						
					0.228E-02	0.413E-04	0.298E-02	0.161E-01	48.6	55.3
					0.180E-02	0.326E-04	0.279E-02	0.151E-01	48.6	55.3
					0.228E-02	0.389E-04	0.293E-02	0.150E-01	51.6	58.7
					0.168E-02	0.352E-04	0.274E-02	0.172E-01	42.0	47.8
36	1280.	3950.	3.085	301.8						
					0.589E-02	0.199E-03	0.430E-02	0.438E-01	39.4	29.4
					0.505E-02	0.171E-03	0.384E-02	0.391E-01	39.4	29.4
					0.593E-02	0.189E-03	0.407E-02	0.390E-01	41.9	31.3
					0.542E-02	0.213E-03	0.397E-02	0.468E-01	34.1	25.4

RAW DATA FOR STATIONARY-NOZZLE TEST NO 5

RUN NO.	PUMP SWIVEL P.	BOREHOLE PRES.	TOTAL FLOWRATE	DEPTH IN.	VOLUME C.C.
1	1200.	120.	124.		
				0.48	2.4
				0.40	1.9
				0.38	2.2
				0.40	1.9
2	1370.	200.	140.		
				0.36	2.3
				0.36	1.6
				0.28	1.9
				0.32	1.5
3	2380.	300.	187.		
				0.39	2.5
				0.33	1.5
				0.29	1.8
				0.33	1.6
4	1400.	320.	130.		
				0.39	1.6
				0.27	1.1
				0.30	1.1
				0.24	1.3
5	2850.	380.	205.		
				0.37	1.8
				0.28	1.3
				0.31	1.6
				0.22	1.0
6	2450.	390.	185.		
				0.25	1.7
				0.15	1.1
				0.23	1.1
				0.16	1.0
7	3650.	430.	230.		
				0.71	3.1
				0.50	3.9
				0.58	4.7
				0.48	3.1
8	2100.	530.	160.		
				0.31	1.8
				0.27	1.1
				0.31	1.5
				0.27	1.1
9	3200.	650.	210.		
				0.34	1.8
				0.36	1.0
				0.35	1.6
				0.28	0.9
10	2750.	700.	193.		
				0.35	1.7
				0.18	0.9
				0.24	1.3
				0.26	1.1
11	1800.	750.	135.		
				0.45	2.3

TEST NO 5 (concluded)

				0.32	1.6
				0.31	1.4
				0.33	1.4
12	2250.	760.	160.		
				0.38	2.3
				0.26	1.0
				0.25	0.8
				0.27	0.6
13	3400.	900.	205.		
				0.22	0.9
				0.18	0.5
				0.15	0.7
				0.17	0.5
14	2000.	980.	134.		
				0.42	2.8
				0.49	1.9
				0.43	2.3
				0.37	2.0
15	2550.	1000.	160.		
				0.45	2.6
				0.41	1.8
				0.38	2.7
				0.46	1.8
16	3137.	1020.	192.		
				0.28	1.7
				0.36	1.2
				0.25	1.2
				0.25	1.0
17	4229.	1070.	235.		
				0.31	2.0
				0.35	1.1
				0.23	1.7
				0.21	1.1
18	4510.	1200.	240.		
				0.34	1.9
				0.28	1.2
				0.28	1.6
				0.22	1.2
19	3773.	1500.	195.		
				0.81	6.8
				0.65	3.9
				1.01	7.1
				0.96	5.3
20	4602.	1500.	225.		
				0.73	5.6
				0.87	4.6
				0.89	5.8
				0.78	4.5
21	5292.	1500.	255.		
				0.70	4.3
				0.60	3.7
				0.69	4.4
				0.59	3.0
22	6090.	1480.	275.		
				0.75	6.4
				0.82	4.3
				0.73	5.1
				0.67	4.4

PROCESSED DATA FOR STATIONARY-NOZZLE TEST NO 5

UNITS
PRESSURE=PSI
TIME=SECOND
VOLUME REMOVAL RATE=FT**3/HR
VOLUME REMOVAL EFF.=FT**3/HR-HP
DRILLING RATE=IN/SEC
DRILLING RATE EFF.=FT/HR-HP
FLOW RATE=GPM
POWER=HP

RUN NO.	NOZ. PRES.	AMB. PRES.	CAV. NO.	TIME	VOL. REM. RATE	VOL. REM. EFF.	DRILL RATE	DRILL RATE EFF.	FLOW RATE	POWER
1	1080.	120.	0.111	302.0						
					0.100E-02	0.481E-04	0.158E-02	0.227E-01	33.2	20.9
					0.799E-03	0.441E-04	0.132E-02	0.219E-01	28.7	18.1
					0.925E-03	0.441E-04	0.125E-02	0.180E-01	33.2	20.9
					0.799E-03	0.441E-04	0.132E-02	0.219E-01	28.7	18.1
2	1170.	200.	0.170	150.5						
					0.194E-02	0.757E-04	0.239E-02	0.280E-01	37.5	25.6
					0.135E-02	0.609E-04	0.239E-02	0.324E-01	32.4	22.1
					0.160E-02	0.625E-04	0.186E-02	0.217E-01	37.5	25.6
					0.126E-02	0.571E-04	0.212E-02	0.288E-01	32.4	22.1
3	2080.	300.	0.144	45.8						
					0.693E-02	0.113E-03	0.851E-02	0.419E-01	50.1	60.8
					0.416E-02	0.791E-04	0.720E-02	0.411E-01	43.3	52.5
					0.499E-02	0.820E-04	0.633E-02	0.312E-01	50.1	60.8
					0.443E-02	0.843E-04	0.720E-02	0.411E-01	43.3	52.5
4	1080.	320.	0.296	151.3						
					0.134E-02	0.611E-04	0.257E-02	0.352E-01	54.8	21.9
					0.923E-03	0.486E-04	0.178E-02	0.282E-01	30.1	18.9
					0.923E-03	0.420E-04	0.198E-02	0.270E-01	34.8	21.9
					0.109E-02	0.574E-04	0.158E-02	0.250E-01	30.1	18.9
5	2470.	380.	0.153	21.6						
					0.105E-01	0.133E-03	0.171E-01	0.648E-01	54.9	79.2
					0.764E-02	0.111E-03	0.129E-01	0.568E-01	47.5	68.4
					0.941E-02	0.118E-03	0.143E-01	0.543E-01	54.9	79.2
					0.588E-02	0.859E-04	0.101E-01	0.446E-01	47.5	68.4
6	2060.	390.	0.189	31.0						
					0.696E-02	0.116E-03	0.806E-02	0.405E-01	49.6	59.6
					0.450E-02	0.874E-04	0.483E-02	0.281E-01	42.8	51.5
					0.450E-02	0.756E-04	0.741E-02	0.373E-01	49.6	59.6
					0.409E-02	0.795E-04	0.516E-02	0.300E-01	42.8	51.5
7	3220.	430.	0.133	30.2						
					0.130E-01	0.112E-03	0.235E-01	0.608E-01	61.6	115.8
					0.164E-01	0.163E-03	0.165E-01	0.496E-01	53.3	100.1
					0.197E-01	0.170E-03	0.192E-01	0.497E-01	61.6	115.8
					0.130E-01	0.130E-03	0.158E-01	0.476E-01	53.3	100.1
8	1570.	530.	0.337	92.0						
					0.248E-02	0.632E-04	0.336E-02	0.257E-01	42.9	39.2
					0.151E-02	0.447E-04	0.293E-02	0.259E-01	37.0	33.9
					0.207E-02	0.527E-04	0.336E-02	0.257E-01	42.9	39.2

TEST NO 5 (continued)

					0.151E-02	0.447E-04	0.293E-02	0.259E-01	37.0	33.9
9	2550.	650.	0.254	26.8						
					0.853E-02	0.101E-03	0.126E-01	0.454E-01	56.3	83.7
					0.474E-02	0.654E-04	0.134E-01	0.556E-01	48.6	72.4
					0.758E-02	0.905E-04	0.130E-01	0.467E-01	56.3	83.7
					0.426E-02	0.589E-04	0.104E-01	0.432E-01	48.6	72.4
10	2050.	700.	0.341	36.5						
					0.591E-02	0.955E-04	0.958E-02	0.464E-01	51.7	61.8
					0.313E-02	0.585E-04	0.493E-02	0.276E-01	44.7	53.4
					0.452E-02	0.730E-04	0.657E-02	0.316E-01	51.7	61.8
					0.382E-02	0.715E-04	0.712E-02	0.399E-01	44.7	53.4
11	1050.	750.	0.714	212.0						
					0.137E-02	0.621E-04	0.212E-02	0.287E-01	36.2	22.1
					0.958E-03	0.500E-04	0.150E-02	0.236E-01	31.2	19.1
					0.838E-03	0.376E-04	0.146E-02	0.197E-01	36.2	22.1
					0.838E-03	0.437E-04	0.155E-02	0.243E-01	31.2	19.1
12	1490.	760.	0.510	91.5						
					0.319E-02	0.856E-04	0.415E-02	0.334E-01	42.9	37.2
					0.138E-02	0.430E-04	0.284E-02	0.264E-01	37.0	32.2
					0.111E-02	0.297E-04	0.273E-02	0.219E-01	42.9	37.2
					0.833E-03	0.258E-04	0.295E-02	0.274E-01	37.0	32.2
13	2500.	900.	0.360	10.8						
					0.105E-01	0.132E-03	0.203E-01	0.762E-01	54.9	80.1
					0.588E-02	0.848E-04	0.166E-01	0.721E-01	47.5	69.2
					0.823E-02	0.102E-03	0.138E-01	0.519E-01	54.9	80.1
					0.588E-02	0.848E-04	0.157E-01	0.681E-01	47.5	69.2
14	1020.	980.	0.960	240.3						
					0.148E-02	0.692E-04	0.174E-02	0.245E-01	35.9	21.3
					0.100E-02	0.543E-04	0.203E-02	0.331E-01	31.0	18.4
					0.121E-02	0.568E-04	0.178E-02	0.251E-01	35.9	21.3
					0.105E-02	0.572E-04	0.153E-02	0.249E-01	31.0	18.4
15	1550.	1000.	0.645	105.6						
					0.312E-02	0.806E-04	0.426E-02	0.329E-01	42.9	38.7
					0.216E-02	0.645E-04	0.388E-02	0.347E-01	37.0	33.5
					0.324E-02	0.837E-04	0.359E-02	0.278E-01	42.9	38.7
					0.216E-02	0.645E-04	0.435E-02	0.389E-01	37.0	33.5
16	2117.	1020.	0.481	31.0						
					0.696E-02	0.109E-03	0.903E-02	0.426E-01	51.4	63.5
					0.491E-02	0.894E-04	0.116E-01	0.633E-01	44.5	54.9
					0.491E-02	0.773E-04	0.806E-02	0.380E-01	51.4	63.5
					0.409E-02	0.745E-04	0.806E-02	0.440E-01	44.5	54.9
17	3159.	1070.	0.338	11.3						
					0.224E-01	0.193E-03	0.274E-01	0.708E-01	63.0	116.1
					0.123E-01	0.123E-03	0.309E-01	0.925E-01	54.4	100.3
					0.191E-01	0.164E-03	0.203E-01	0.525E-01	63.0	116.1
					0.123E-01	0.123E-03	0.185E-01	0.555E-01	54.4	100.3
18	3310.	1200.	0.362	12.4						
					0.194E-01	0.156E-03	0.274E-01	0.661E-01	64.3	124.2
					0.122E-01	0.114E-03	0.225E-01	0.630E-01	55.6	107.4
					0.163E-01	0.131E-03	0.225E-01	0.545E-01	64.3	124.2
					0.122E-01	0.114E-03	0.177E-01	0.495E-01	55.6	107.4
19	2273.	1500.	0.659	303.0						
					0.285E-02	0.411E-04	0.267E-02	0.115E-01	52.2	69.3
					0.163E-02	0.272E-04	0.214E-02	0.107E-01	45.2	59.9
					0.297E-02	0.429E-04	0.333E-02	0.144E-01	52.2	69.3
					0.222E-02	0.370E-04	0.316E-02	0.158E-01	45.2	59.9
20	3102.	1500.	0.483	136.7						
					0.520E-02	0.476E-04	0.534E-02	0.146E-01	60.3	109.1
					0.427E-02	0.452E-04	0.636E-02	0.202E-01	52.1	94.3
					0.538E-02	0.493E-04	0.651E-02	0.178E-01	60.3	109.1
					0.418E-02	0.443E-04	0.570E-02	0.181E-01	52.1	94.3

TEST NO 5 (concluded)

21	3792.	1500.	0.395	41.0						
					0.133E-01	0.880E-04	0.170E-01	0.338E-01	68.3	151.2
					0.114E-01	0.876E-04	0.146E-01	0.335E-01	59.1	130.7
					0.136E-01	0.901E-04	0.168E-01	0.333E-01	68.3	151.2
					0.929E-02	0.710E-04	0.143E-01	0.330E-01	59.1	130.7
22	4610.	1480.	0.321	36.8						
					0.220E-01	0.111E-03	0.203E-01	0.308E-01	73.7	198.3
					0.148E-01	0.865E-04	0.222E-01	0.389E-01	63.7	171.4
					0.176E-01	0.887E-04	0.198E-01	0.300E-01	73.7	198.3
					0.151E-01	0.886E-04	0.182E-01	0.318E-01	63.7	171.4

RAW DATA FOR STATIONARY-NOZZLE TEST NO 6

RUN NO.	PUMP SWIVEL P.	BOREHOLE PRES.	TOTAL FLOWRATE	DEPTH IN.	VOLUME C.C.
1	2550.	1460.	195.		
				0.32	1.6
				0.37	2.0
				0.27	2.1
				0.33	1.3
2	3000.	1450.	230.		
				0.32	1.6
				0.28	2.2
				0.25	2.0
				0.27	1.2
3	3500.	1450.	260.		
				0.21	0.9
				0.20	0.7
				0.18	1.0
				0.20	0.6
4	4000.	1500.	290.		
				0.25	1.3
				0.30	1.8
				0.22	1.3
				0.26	0.9
5	4000.	2000.	255.		
				0.15	1.0
				0.26	1.3
				0.22	1.1
				0.23	0.7
6	4500.	2000.	295.		
				0.30	1.1
				0.19	1.6
				0.19	1.3
				0.19	0.8
7	5000.	2500.	295.		
				0.21	0.7
				0.18	1.2
				0.19	1.0
				0.19	0.7
8	5450.	2750.	300.		
				0.20	0.9
				0.19	1.3
				0.16	1.1
				0.22	0.8
9	4000.	3000.	185.		
				0.29	1.4
				0.31	2.1
				0.25	1.9
				0.32	1.2
10	4500.	3000.	225.		
				0.35	2.3
				0.40	3.1
				0.37	2.7
				0.36	1.6
11	5000.	2950.	265.		
				0.35	0.0*

TEST NO 6 (continued)

				0.34	2.7
				0.45	3.0
				0.36	1.4
12	5400.	3200.	275.		
				0.48	3.3
				0.44	4.5
				0.42	4.6
				0.38	3.2
13	5000.	3500.	230.		
				0.42	2.2
				0.41	3.2
				0.36	2.9
				0.35	1.7
14	4900.	3800.	198.		
				0.32	1.5
				0.28	1.9
				0.31	1.7
				0.30	0.9
15	5300.	3800.	225.		
				0.44	2.0
				0.37	2.8
				0.27	2.2
				0.36	1.5
16	THIS RUN WAS NOT MADE				
17	1150.	180.	180.		
				0.38	1.9
				0.32	2.7
				0.27	1.6
				0.28	1.4
18	1800.	250.	225.		
				0.46	2.7
				0.38	3.9
				0.32	2.5
				0.36	1.8
19	2350.	350.	260.		
				0.40	2.4
				0.30	2.7
				0.20	2.4
				0.23	0.9
20	1350.	330.	193.		
				0.32	0.0*
				0.26	0.0*
				0.25	1.2
				0.28	1.1
21	2100.	540.	231.		
				0.33	1.6
				0.24	1.6
				0.29	1.6
				0.27	1.1
22	2600.	700.	265.		
				0.27	1.3
				0.24	1.4
				0.24	1.3
				0.23	1.0
23	2150.	650.	230.		
				0.32	1.3
				0.29	1.6

TEST NO 6 (concluded)

				0.26	1.5
				0.28	1.2
24	2450.	1450.	190.		
				0.38	2.0
				0.33	2.4
				0.42	1.9
				0.36	1.1
25	3000.	1400.	240.		
				0.40	2.4
				0.32	3.0
				0.35	2.9
				0.32	1.6
26	3500.	1500.	262.		
				0.23	1.2
				0.19	1.3
				0.28	2.0
				0.23	1.0
27	3000.	1900.	195.		
				0.27	1.5
				0.30	1.9
				0.28	1.5
				0.29	1.2
28	4000.	1980.	255.		
				0.32	1.6
				0.22	1.3
				0.24	1.6
				0.28	1.1
29	4000.	2950.	190.		
				0.20	1.1
				0.26	1.5
				0.23	1.3
				0.26	0.8
30	4500.	2950.	230.		
				0.33	1.8
				0.29	2.4
				0.32	2.2
				0.30	1.3
31	5000.	2950.	265.		
				0.37	2.2
				0.35	3.3
				0.36	3.2
				0.36	1.6
32	5500.	3300.	270.		
				0.50	0.0*
				0.37	0.0*
				0.37	0.0*
				0.46	0.0*

* CRACK THROUGH HOLE

PROCESSED DATA FOR STATIONARY-NOZZLE TEST NO 6

UNITS
PRESSURE=PSI
TIME=SECOND
VOLUME REMOVAL RATE=FT**3/HR
VOLUME REMOVAL EFF.=FT**3/HR-HP
DRILLING RATE=IN/SEC
DRILLING RATE EFF.=FT/HR-HP
FLOW RATE=GPM
POWER=HP

RUN NO.	NOZ. PRES.	AMB. PRES.	CAV. NO.	TIME	VOL. REM. RATE	VOL. REM. EFF.	DRILL RATE	DRILL RATE EFF.	FLOW RATE	POWER
1	1090.	1460.	1.339	301.0						
					0.675E-03	0.265E-04	0.106E-02	0.125E-01	40.0	25.4
					0.844E-03	0.205E-04	0.122E-02	0.897E-02	64.6	41.0
					0.886E-03	0.250E-04	0.897E-03	0.759E-02	55.7	35.4
					0.548E-03	0.249E-04	0.109E-02	0.149E-01	34.6	22.0
2	1550.	1450.	0.935	135.0						
					0.150E-02	0.352E-04	0.237E-02	0.166E-01	47.2	42.7
					0.207E-02	0.300E-04	0.207E-02	0.903E-02	76.1	68.8
					0.188E-02	0.316E-04	0.185E-02	0.934E-02	65.7	59.4
					0.112E-02	0.305E-04	0.199E-02	0.162E-01	40.8	36.9
3	2050.	1450.	0.707	41.2						
					0.277E-02	0.434E-04	0.509E-02	0.239E-01	53.4	63.8
					0.215E-02	0.209E-04	0.485E-02	0.141E-01	86.1	103.0
					0.308E-02	0.347E-04	0.436E-02	0.147E-01	74.3	88.8
					0.185E-02	0.335E-04	0.485E-02	0.263E-01	46.1	55.1
4	2500.	1500.	0.600	38.0						
					0.434E-02	0.500E-04	0.657E-02	0.227E-01	59.5	86.8
					0.601E-02	0.429E-04	0.789E-02	0.169E-01	96.0	140.1
					0.434E-02	0.359E-04	0.578E-02	0.143E-01	82.8	120.8
					0.300E-02	0.400E-04	0.684E-02	0.273E-01	51.4	75.0
5	2000.	2000.	1.000	61.9						
					0.205E-02	0.335E-04	0.242E-02	0.118E-01	52.3	61.1
					0.266E-02	0.270E-04	0.420E-02	0.127E-01	84.4	98.5
					0.225E-02	0.265E-04	0.355E-02	0.125E-01	72.8	85.0
					0.143E-02	0.272E-04	0.371E-02	0.211E-01	45.2	52.8
6	2500.	2000.	0.800	27.7						
					0.504E-02	0.570E-04	0.108E-01	0.367E-01	60.5	88.3
					0.733E-02	0.514E-04	0.685E-02	0.144E-01	97.7	142.5
					0.596E-02	0.484E-04	0.685E-02	0.167E-01	84.3	122.9
					0.366E-02	0.480E-04	0.685E-02	0.269E-01	52.3	76.3
7	2500.	2500.	1.000	26.4						
					0.336E-02	0.381E-04	0.795E-02	0.270E-01	60.5	88.3
					0.577E-02	0.405E-04	0.681E-02	0.143E-01	97.7	142.5
					0.481E-02	0.391E-04	0.719E-02	0.175E-01	84.3	122.9
					0.336E-02	0.441E-04	0.719E-02	0.282E-01	52.3	76.3
8	2700.	2750.	1.018	27.0						
					0.423E-02	0.436E-04	0.740E-02	0.228E-01	61.6	97.0
					0.611E-02	0.390E-04	0.703E-02	0.134E-01	99.3	156.5
					0.517E-02	0.383E-04	0.592E-02	0.141E-01	85.7	135.0

TEST NO 6 (continued)

					0.376E-02	0.448E-04	0.814E-02	0.291E-01	53.2	83.8
9	1000.	3000.	3.000	300.3						
					0.592E-03	0.267E-04	0.965E-03	0.130E-01	37.9	22.1
					0.888E-03	0.248E-04	0.103E-02	0.866E-02	61.2	35.7
					0.803E-03	0.260E-04	0.832E-03	0.809E-02	52.8	30.8
					0.507E-03	0.265E-04	0.106E-02	0.166E-01	32.8	19.1
10	1500.	3000.	2.000	180.0						
					0.162E-02	0.401E-04	0.194E-02	0.144E-01	46.2	40.4
					0.218E-02	0.335E-04	0.222E-02	0.102E-01	74.5	65.2
					0.190E-02	0.338E-04	0.205E-02	0.109E-01	64.3	56.2
					0.112E-02	0.323E-04	0.199E-02	0.171E-01	39.9	34.9
11	2050.	2950.	1.439	106.0						
					0.000E 00	0.000E 00	0.330E-02	0.152E-01	54.4	65.0
					0.323E-02	0.308E-04	0.320E-02	0.916E-02	87.7	104.9
					0.359E-02	0.396E-04	0.424E-02	0.140E-01	75.7	90.5
					0.167E-02	0.298E-04	0.339E-02	0.181E-01	47.0	56.2
12	2200.	3200.	1.454	120.7						
					0.347E-02	0.479E-04	0.397E-02	0.164E-01	56.4	72.4
					0.473E-02	0.405E-04	0.364E-02	0.935E-02	91.1	116.9
					0.484E-02	0.480E-04	0.347E-02	0.103E-01	78.5	100.8
					0.336E-02	0.537E-04	0.314E-02	0.150E-01	48.8	62.6
13	1500.	3500.	2.333	166.7						
					0.167E-02	0.405E-04	0.251E-02	0.182E-01	47.2	41.3
					0.243E-02	0.365E-04	0.245E-02	0.110E-01	76.1	66.6
					0.220E-02	0.384E-04	0.215E-02	0.112E-01	65.7	57.5
					0.129E-02	0.362E-04	0.209E-02	0.176E-01	40.8	35.7
14	1100.	3800.	3.454	240.3						
					0.792E-03	0.303E-04	0.133E-02	0.153E-01	40.6	26.0
					0.100E-02	0.238E-04	0.116E-02	0.850E-02	65.5	42.0
					0.898E-03	0.247E-04	0.129E-02	0.106E-01	56.5	36.3
					0.475E-03	0.210E-04	0.124E-02	0.166E-01	35.1	22.5
15	1500.	3800.	2.533	180.0						
					0.141E-02	0.349E-04	0.244E-02	0.181E-01	46.2	40.4
					0.197E-02	0.302E-04	0.205E-02	0.945E-02	74.5	65.2
					0.155E-02	0.275E-04	0.150E-02	0.799E-02	64.3	56.2
					0.105E-02	0.302E-04	0.199E-02	0.171E-01	39.9	34.9
16	0.	0.*******		0.0						
					0.600E 34	0.170E 39	0.170E 39	0.170E 39	0.0	0.0
					0.600E 34	0.170E 39	0.170E 39	0.170E 39	0.0	0.0
					0.600E 34	0.170E 39	0.170E 39	0.170E 39	0.0	0.0
					0.600E 34	0.170E 39	0.170E 39	0.170E 39	0.0	0.0
17	970.	180.	0.185	301.0						
					0.801E-03	0.383E-04	0.126E-02	0.181E-01	36.9	20.9
					0.113E-02	0.337E-04	0.106E-02	0.945E-02	59.6	33.7
					0.675E-03	0.231E-04	0.897E-03	0.924E-02	51.4	29.1
					0.590E-03	0.326E-04	0.930E-03	0.154E-01	31.9	18.0
18	1550.	250.	0.161	150.7						
					0.227E-02	0.544E-04	0.305E-02	0.219E-01	46.2	41.7
					0.328E-02	0.487E-04	0.252E-02	0.112E-01	74.5	67.3
					0.210E-02	0.362E-04	0.212E-02	0.109E-01	64.3	58.1
					0.151E-02	0.420E-04	0.238E-02	0.198E-01	39.9	36.1
19	2000.	350.	0.175	41.0						
					0.743E-02	0.119E-03	0.975E-02	0.469E-01	53.4	62.3
					0.836E-02	0.832E-04	0.731E-02	0.218E-01	86.1	100.4
					0.743E-02	0.857E-04	0.487E-02	0.168E-01	74.3	86.6
					0.278E-02	0.517E-04	0.560E-02	0.312E-01	46.1	53.8
20	1020.	330.	0.323	210.2						
					0.000E 00	0.000E 00	0.152E-02	0.193E-01	39.6	23.5
					0.000E 00	0.000E 00	0.123E-02	0.975E-02	63.9	38.0
					0.725E-03	0.220E-04	0.118E-02	0.108E-01	55.1	32.8
					0.664E-03	0.326E-04	0.133E-02	0.196E-01	34.2	20.3

TEST NO 6 (concluded)

21	1560.	540.	0.346	105.7						
					0.192E-02	0.445E-04	0.312E-02	0.216E-01	47.4	43.1
					0.192E-02	0.276E-04	0.227E-02	0.978E-02	76.5	69.6
					0.192E-02	0.320E-04	0.274E-02	0.137E-01	66.0	60.0
					0.132E-02	0.354E-04	0.255E-02	0.205E-01	41.0	37.3
22	1900.	700.	0.368	45.5						
					0.362E-02	0.601E-04	0.593E-02	0.295E-01	54.4	60.3
					0.390E-02	0.401E-04	0.527E-02	0.162E-01	87.7	97.2
					0.362E-02	0.432E-04	0.527E-02	0.188E-01	75.7	83.9
					0.279E-02	0.535E-04	0.505E-02	0.290E-01	47.0	52.1
23	1500.	650.	0.433	105.0						
					0.157E-02	0.380E-04	0.304E-02	0.221E-01	47.2	41.3
					0.193E-02	0.290E-04	0.276E-02	0.124E-01	76.1	66.6
					0.101E-02	0.315E-04	0.247E-02	0.129E-01	65.7	57.5
					0.145E-02	0.406E-04	0.266E-02	0.223E-01	40.8	35.7
24	1000.	1450.	1.450	300.0						
					0.846E-03	0.372E-04	0.126E-02	0.166E-01	39.0	22.7
					0.101E-02	0.276E-04	0.109E-02	0.898E-02	62.9	36.7
					0.804E-03	0.254E-04	0.139E-02	0.132E-01	54.3	31.6
					0.465E-03	0.236E-04	0.120E-02	0.183E-01	33.7	19.6
25	1600.	1400.	0.875	135.5						
					0.225E-02	0.489E-04	0.295E-02	0.192E-01	49.2	46.0
					0.281E-02	0.379E-04	0.236E-02	0.954E-02	79.5	74.2
					0.271E-02	0.424E-04	0.258E-02	0.121E-01	68.5	64.0
					0.150E-02	0.377E-04	0.236E-02	0.178E-01	42.5	39.7
26	2000.	1500.	0.750	40.0						
					0.381E-02	0.607E-04	0.575E-02	0.274E-01	53.8	62.7
					0.412E-02	0.407E-04	0.475E-02	0.140E-01	86.8	101.2
					0.635E-02	0.727E-04	0.700E-02	0.240E-01	74.8	87.3
					0.317E-02	0.585E-04	0.575E-02	0.317E-01	46.5	54.2
27	1100.	1900.	1.727	300.0						
					0.635E-03	0.247E-04	0.899E-03	0.105E-01	40.0	25.6
					0.804E-03	0.194E-04	0.999E-03	0.723E-02	64.6	41.4
					0.635E-03	0.177E-04	0.933E-03	0.783E-02	55.7	35.7
					0.508E-03	0.220E-04	0.966E-03	0.130E-01	34.6	22.2
28	2020.	1980.	0.980	60.3						
					0.337E-02	0.546E-04	0.530E-02	0.257E-01	52.3	61.7
					0.273E-02	0.275E-04	0.364E-02	0.109E-01	84.4	99.5
					0.337E-02	0.392E-04	0.398E-02	0.139E-01	72.8	85.8
					0.231E-02	0.434E-04	0.464E-02	0.261E-01	45.2	53.3
29	1050.	2950.	2.809	300.1						
					0.465E-03	0.194E-04	0.666E-03	0.836E-02	39.0	23.9
					0.634E-03	0.164E-04	0.866E-03	0.674E-02	62.9	38.5
					0.550E-03	0.165E-04	0.766E-03	0.691E-02	54.3	33.2
					0.338E-03	0.163E-04	0.866E-03	0.125E-01	33.7	20.6
30	1550.	2950.	1.903	180.2						
					0.126E-02	0.297E-04	0.183E-02	0.126E-01	47.2	42.7
					0.169E-02	0.245E-04	0.160E-02	0.700E-02	76.1	68.8
					0.155E-02	0.260E-04	0.177E-02	0.896E-02	65.7	59.4
					0.916E-03	0.248E-04	0.166E-02	0.135E-01	40.8	36.9
31	2050.	2950.	1.439	105.0						
					0.266E-02	0.408E-04	0.352E-02	0.162E-01	54.4	65.0
					0.399E-02	0.380E-04	0.333E-02	0.952E-02	87.7	104.9
					0.387E-02	0.427E-04	0.342E-02	0.113E-01	75.7	90.5
					0.193E-02	0.344E-04	0.342E-02	0.182E-01	47.0	56.2
32	2200.	3300.	1.500	120.2						
					0.000E 00	0.000E 00	0.415E-02	0.175E-01	55.4	71.1
					0.000E 00	0.000E 00	0.307E-02	0.804E-02	89.4	114.7
					0.000E 00	0.000E 00	0.307E-02	0.932E-02	77.1	99.0
					0.000E 00	0.000E 00	0.382E-02	0.186E-01	47.9	61.5

APPENDIX B

RESULTS FROM STATIONARY-NOZZLE AND SLOT CUTTING TESTS AT HYDRONAUTICS

Table B-1

Stationary-Nozzle Tests on Indiana Limestone

CAVIJET® Nozzle Size and Type: 6.2 mm (0.244 in.), Carbide, Plain, Submerged
Standoff: 2.1 cm (0.812 in.)
Rock Type: Indiana Limestone—Parallel to Bedding Plane
Mud Weight: 1.1 gm/cm³ (9.3 lbs/gal) nominal

Run No.	Cumulative Time	Mean Depth h		Hole Diameter d		Volume Removed V	
	sec.	mm	in.	mm	in.	cm^3	10^{-1} $in.^3$
Nozzle Pressure: 10.3 MPa (1.50 ksi), Ambient Pressure: 4.14 MPa (0.60 ksi), σ = 0.40							
10CIa	20	3.3	0.13	19	0.75	0.40	0.24
10CIb	40	5.1	0.20	22	0.88	1.2	0.73
10CIc	60	6.9	0.27	22	0.88	1.7	1.0
10CId	80	7.9	0.31	25	1.0	2.2	1.3
10CIe	100	9.7	0.38	25	1.0	2.6	1.6
10CIf	120	11	0.42	25	1.0	3.1	1.9
10CIg	140	12	0.47	25	1.0	3.5	2.1
10CIIa	65	8.4	0.33	22	0.88	1.8	1.1
11AIa	65	7.9	0.31	22	0.88	1.8	1.1
11AIb	130	11	0.44	24	0.94	2.9	1.8
11AIIa*	20	4.8	0.19	16	0.63	0.70	0.43
11AIIb*	40	8.6	0.34	19	0.75	1.4	0.85
11AIIc*	80	13	0.50	19	0.75	2.6	1.6
11AIIIa	20	4.3	0.17	18	0.69	0.70	0.43
11AIIIb*	40	7.1	0.28	18	0.69	1.3	0.79
11AIIIc*	60	9.1	0.36	18	0.69	2.0	1.2
11CIa	20	3.6	0.14	19	0.75	0.70	0.43
11CIIa	40	5.1	0.20	19	0.75	1.1	0.67
11CIIIa*	80	9.9	0.39	19	0.75	2.0	1.2
11CIVa	130	13	0.50	22	0.88	3.4	2.1
Nozzle Pressure: 6.90 MPa (1.00 ksi), Ambient Pressure: 5.17 MPa (0.75 ksi), σ = 0.75							
10DIa	60	3.6	0.14	19	0.75	0.60	0.37
10DIIa	120	5.8	0.23	21	0.81	1.4	0.85
10DIIIa	180	8.6	0.34	21	0.81	2.0	1.2
10DIVa	240	10	0.41	22	0.88	2.9	1.8
11DIa	60	4.8	0.19	19	0.75	0.90	0.55
11DIIa	116	6.9	0.27	21	0.81	1.6	0.98
11DIIIa	180	8.4	0.33	19	0.75	1.9	1.2
11DIVa	240	10	0.41	22	0.88	2.6	1.6
Nozzle Pressure: 8.28 MPa (1.20 ksi), Ambient Pressure: 3.31 MPa (0.48 ksi) σ = 0.40							
17AIa	30	1.9	0.075	19	0.75	0.40	0.24
17AIIa	120	6.6	0.26	22	0.88	1.6	0.98
17AIIIa	180	8.1	0.32	24	0.94	2.2	1.3
17AIVa*	240	11	0.44	21	0.81	2.8	1.7
17AVa	30	2.0	0.080	19	0.75	0.40	0.24
Nozzle Pressure: 12.4 MPa (1.80 ksi), Ambient Pressure: 2.07 MPa (0.30 ksi), σ = 0.17							
11BIa	12	2.0	0.078	25	1.0	0.75	0.46
11BIIa	100	15	0.58	28	1.1	4.5	2.7
11BIIIa	160	18	0.69	28	1.1	6.1	3.7
11BIVa	200	20	0.77	28	1.1	7.0	4.3
11BVa	60	8.9	0.35	25	1.0	3.0	1.8

*"Gully Erosion": deep, anamolous slot away from main hole.

Table B-2

Stationary-Nozzle Tests on Berea Sandstone

CAVIJET® Nozzle Size and Type: 6.2 mm (0.244 in.), Carbide, Plain, Submerged
Standoff: 2.1 cm (0.812 in.)
Rock Type: Berea Sandstone—Parallel to Bedding Plane
Mud Weight: 1.1 gm/cm^3 (9.3 lbs/gal) nominal

Run No.	Cumulative Time	Mean Depth h		Hole Diameter d		Volume Removed V	
	sec.	mm	in.	mm	in.	cm^3	10^{-1} in.^{3}
Nozzle Pressure: 12.4 MPa (1.80 ksi), Ambient Pressure: 2.07 MPa (0.30 ksi), σ = 0.17							
16DIa	12	0.43	0.017	25	1.0	0.20	0.12
16DIIa	60	4.6	0.18	25	1.0	2.2	1.3
16DIIIa	160	7.1	0.28	33	1.3	2.8	1.7
16DIVa	200	11	0.43	30	1.2	4.1	2.5
16DVa	100	6.4	0.25	30	1.2	2.8	1.7

Table B-4

Slot Cutting Tests on Indiana Limestone with Mud

CAVIJET® Nozzle Size and Type: 6.2 mm (0.244 in.), Carbide, Plain, Submerged
Standoff: 2.1 cm (0.812 in.)
Rock Type: Indiana Limestone—Parallel to Bedding Plane
Mud Weight: 1.1 gm/cm³ (9.3 lbs/gal) nominal
Each Run: <1 Revolution

Run No.	Translation Velocity, v		Mean Depth h'		Mean Width w		Volume Removal Rate, $\dot{V}$		Volume Removal Effectiveness, $e_{\dot{V}}$	
	cm/sec	in/sec	mm	in.	mm	in.	10^{-1} cm³/sec	10^{-3} in³/sec	10^{+1} cm³/kw-hr	10^{-1} in.³/hp-hr
Nozzle Pressure: 12.4 MPa (1.80 ksi), Ambient Pressure: 1.38 MPa (0.20 ksi), σ = 0.11.										
6C	2.5	1.0	0.38	0.015	16	0.63	1.2	7.5	1.2	5.4
Nozzle Pressure: 12.1 MPa (1.75 ksi), Ambient Pressure: 2.41 MPa (0.35 ksi), σ = 0.20										
6A	2.5	1.0	0.36	0.014	14	0.56	1.0	6.1	1.0	4.6
Nozzle Pressure: 11.7 MPa (1.70 ksi), Ambient Pressure: 2.41 MPa (0.35 ksi), σ = 0.21										
6B	2.5	1.0	0.33	0.013	16	0.63	1.0	6.4	1.1	5.0
Nozzle Pressure: 10.3 MPa (1.50 ksi), Ambient Pressure: 4.14 MPa (0.60 ksi), σ = 0.40.										
9A	0.64	0.25	0.81	0.032	16	0.63	0.66	4.0	0.81	3.7
9B	0.64	0.25	0.84	0.033	16	0.63	0.67	4.1	0.84	3.8
9C	1.3	0.50	0.58	0.023	14	0.56	0.82	5.0	1.0	4.7
10B	1.3	0.50	0.53	0.021	16	0.63	0.87	5.3	1.1	5.0
10A	1.9	0.75	0.46	0.018	14	0.56	0.97	5.9	1.2	5.5
9D	1.9	0.75	0.43	0.017	14	0.56	0.92	5.6	1.2	5.3
Nozzle Pressure: 12.4 MPa (1.80 ksi), Ambient Pressure: 2.07 MPa (0.30 ksi), σ = 0.17.										
8D	0.64	0.25	1.1	0.042	18	0.69	0.97	5.9	0.92	4.2
7D	0.64	0.25	1.2	0.046	19	0.75	1.2	7.2	1.1	5.1
8A	0.64	0.25	1.1	0.045	18	0.69	1.0	6.3	0.99	4.5
7B	1.3	0.50	0.76	0.030	16	0.63	1.2	7.5	1.2	5.4
8B	1.3	0.50	0.71	0.028	16	0.63	1.1	7.0	1.1	5.0
7A	2.5	1.0	0.46	0.018	16	0.63	1.5	8.9	1.4	6.4
8C	2.5	1.0	0.48	0.019	14	0.56	1.4	8.3	1.3	5.9
17B*	0.64	0.25	1.1	0.045	19	0.75	1.1	7.0	1.1	5.0
18A*	0.64	0.25	1.2	0.046	19	0.75	1.2	7.2	1.1	5.1
18B**	0.64	0.25	1.1	0.042	19	0.75	1.1	6.6	1.0	4.7
Nozzle Pressure: 11.7 MPa (1.70 ksi), Ambient Pressure: 2.07 MPa (0.30 ksi), σ = 0.18.										
17C**	0.64	0.25	0.91	0.036	19	0.75	0.92	5.6	0.97	4.4
7C	0.64	0.25	0.97	0.038	18	0.69	0.87	5.3	0.92	4.2

*Mud Weight: 1.3 gm/cm³ (10.5 lbs/gal) nominal.

**Mud Weight: 1.4 gm/cm³ (11.9 lbs/gal) nominal.

Table B-3

Stationary-Nozzle Tests on Georgia Granite

CAVIJET® Nozzle Size and Type: 6.2 mm (0.244 in.) Carbide, Plain, Submerged
Standoff: 2.1 cm (0.812 in.)
Rock Type: Georgia Granite—Parallel to Bedding Plane
Mud Weight: 1.1 gm/cm^3 (9.3 lbs/gal) nominal

Run No.	Cumulative Time	Mean Depth* h		Hole Diameter* d		Volume Removed V	
	sec.	mm	in.	mm	in.	cm^3	10^{-1} in.^{3}
Nozzle Pressure: 12.4 MPa (1.80 ksi), Ambient Pressure: 2.07 MPa (0.30 ksi), σ=0.17							
12AIa	75	0.48	0.019	13	0.50	0.13	0.079
12DIa	75	0.43	0.017	13	0.50	0.14	0.085
13CIa	120	1.3	0.052	13	0.50	0.24	0.15
13CIIa	360	2.8	0.11	16	0.63	0.80	0.49
13CIIIa	240	1.9	0.075	13	0.50	0.55	0.34
13CIVa	480	3.3	0.13	16	0.63	1.0	0.61
14AIa	60	0.33	0.013	12	0.47	0.10	0.061
14AIIa	120	0.76	0.030	13	0.50	0.15	0.092
14AIIIa	240	1.3	0.050	13	0.50	0.50	0.31
14AIVa	60	0.33	0.013	12	0.47	0.11	0.067
14AVa	360	1.7	0.068	13	0.50	0.53	0.32

*These measurements are only for central holes; outer ring erosion not included.

Table B-5

Slot Cutting Tests on Indiana Limestone, with Water

CAVIJET Nozzle Size and Type: 6.2 mm (0.244 in.), Carbide, Plain, Submerged
Standoff: 2.1 cm (0.812 in.), or noted
Rock Type: Indiana Limestone - Parallel to Bedding Plane, except as noted
Each Run: < 1 Revolution, unless noted

Run No.	Translation Velocity, v		Mean Depth h'		Mean Width w		Volume Removal Rate, $\dot{V}$		Volume Removal Effectiveness, $e_{\dot{V}}$	
	cm/sec	in/sec	mm	in.	mm	in.	10^{-1} $\frac{cm^3}{sec}$	10^{-3} $\frac{in^3}{sec}$	10^{+1} $\frac{cm^3}{kw\text{-}hr}$	10^{-1} $\frac{in.^3}{hp\text{-}hr}$
Nozzle Pressure: 6.90 MPa (1.00 ksi), Ambient Pressure: 3.45 MPa (0.50 ksi), σ=0.50										
1A[b]	16.	6.3	SPECIMEN HAD LIFTED OFF SPINDLE							
Nozzle Pressure: 10.3 MPa (1.50 ksi), Ambient Pressure: 3.45 MPa (0.50 ksi), σ=0.33										
1B[b]	16.	6.3	SAME PROBLEM AS RUN 1A							
1C[c]	16.	6.3	HEAVY PEAKING - NO MEASUREMENTS TAKEN							
1D[d]	16.	6.3	0.79	0.031	13.	0.50	12.	73.	15.	69.
Nozzle Pressure: 10.3 MPa (1.50 ksi), Ambient Pressure: 4.14 MPa (0.60 ksi), σ=0.40										
4A[a]	1.3	0.50	0.51	0.020	14.	0.56	0.72	4.4	0.90	4.1
Nozzle Pressure: 12.1 MPa (1.75 ksi), Ambient Pressure: 2.41 MPa (0.35 ksi), σ=0.20										
4D	0.64	0.25	0.56	0.022	16.	0.63	0.46	2.8	0.46	2.1
4C	1.3	0.50	0.46	0.018	16.	0.63	0.74	4.5	0.75	3.4
4B[a]	1.3	0.50	0.76	0.030	16.	0.63	1.2	7.5	1.2	5.6
Nozzle Pressure: 12.8 MPa (1.85 ksi), Ambient Pressure: 1.72 MPa (0.25 ksi), σ=0.14										
4E	0.64	0.25	2.5	0.10	25.	1.0	3.6	22.	3.3	15.
Nozzle Pressure: 12.4 MPa (1.80 ksi), Ambient Pressure: 2.07 MPa (0.30 ksi), σ=0.17										
4F	0.64	0.25	1.0	0.040	19.	0.75	1.0	6.3	0.99	4.5

a - Normal to bedding plane
b - Nozzle standoff was: 9.21 cm (3.63 in.)
c - Specimen made approximately 10 revolutions (20 sec. total time)
d - Specimen made approximately 20 revolutions (40 sec. total time)

Table B-6

Slot Cutting Tests on Berea Sandstone with Mud

CAVIJET® Nozzle Size and Type: 6.2 mm (0.244 in.), Carbide, Plain, Submerged
Standoff: 2.1 cm (0.812 in.)
Rock Type: Berea Sandstone—Parallel to Bedding Plane, except as noted
Mud Weight: 1.1 gm/cm^3 (9.3 lbs/gal) nominal
Each Run: <1 Revolution

Run No.	Translation Velocity, v		Mean Depth h'		Mean Width w		Volume Removal Rate, $\dot{V}$		Volume Removal Effectiveness, $e_{\dot{V}}$	
	cm/sec	in/sec	mm	in.	mm	in.	10^{-1} $\frac{cm^3}{sec}$	10^{-3} $\frac{in^3}{sec}$	10^{+1} $\frac{cm^3}{kw\text{-}hr}$	10^{-1} $\frac{in.^3}{hp\text{-}hr}$
Nozzle Pressure: 10.3 MPa (1.50 ksi), Ambient Pressure: 4.14 MPa (0.60 ksi) σ = 0.40.										
15B	0.64	0.25	0.23	0.009	19	0.75	0.23	1.4	0.29	1.3
15A	1.3	0.50	0.15	0.006	19	0.75	0.31	1.9	0.40	1.8
Nozzle Pressure: 12.4 MPa (1.80 ksi), Ambient Pressure: 2.07 MPa (0.30 ksi), σ = 0.17.										
15C	0.64	0.25	0.48	0.019	21	0.81	0.54	3.3	0.53	2.4
5C	0.64	0.25	0.53	0.021	19	0.75	0.54	3.3	0.53	2.4
16A	0.64	0.25	0.74	0.029	19	0.75	0.74	4.5	0.70	3.2
15E*	2.5	1.0	0.74	0.029	21	0.81	3.3	20.	3.1	14.

*Normal to Bedding Plane.

Table B-7

Slot Cutting Tests on Berea Sandstone, with Water

CAVIJET Nozzle Size and Type: 6.2 mm (0.244 in.), Carbide, Plain, Submerged
Standoff: 2.1 cm (0.812 in.)
Rock Type: Berea Sandstone - Parallel to Bedding Plane, except as noted
Each Run: < 1 revolution

Run No.	Translation Velocity, v		Mean Depth h'		Mean Width w		Volume Removal Rate, $\dot{V}$		Volume Removal Effectiveness, $e_{\dot{V}}$	
	cm/sec	in/sec	mm	in.	mm	in.	10^{-1} $\frac{cm^3}{sec}$	10^{-3} $\frac{in^3}{sec}$	10^{+1} $\frac{cm^3}{kw\text{-}hr}$	10^{-1} $\frac{in.^3}{hp\text{-}hr}$
Nozzle Pressure: 10.3 MPa (1.50 ksi), Ambient Pressure: 4.14 MPa (0.60 ksi) σ=0.40										
3E	1.3	0.50	2.8	0.11	18	0.69	5.1	31.	6.4	29.
3D	2.5	1.0	2.8	0.11	18	0.69	10.	61.	12.	57.
3F	2.5	1.0	2.3	0.090	16.	0.63	7.4	45.	9.2	42.
3C	3.8	1.5	1.9	0.075	16.	0.63	9.2	56.	12.	53.
2C	3.8	1.5	1.4	0.055	13.	0.50	5.1	31.	6.4	29.
2D	3.8	1.5	2.2	0.085	13.	0.50	7.9	48.	9.9	45.
2E	3.8	1.5	1.5	0.060	13.	0.50	5.6	34.	7.0	32.
2B[a]	7.6	3.0	6.1	0.24	22.	0.88	87.	530.	109.	495.
3A[a]	7.6	3.0	4.6	0.18	22.	0.88	65.	394.	81.	368.
3B[a]	15.	6.0	3.3	0.13	22.	0.88	95.	581.	119.	543.
2A[a]	15.	6.0	1.8	0.070	18.	0.69	39.	236.	49.	221.
Nozzle Pressure: 12.4 MPa (1.80 ksi), Ambient Pressure: 2.07 MPa (0.30 ksi), σ=0.17										
5A[a]	2.5	1.0	17.	0.65	19.	0.75	67.	406.	64.	290.
Nozzle Pressure: 11.4 MPa (1.65 ksi), Ambient Pressure: 2.41 MPa (0.35 ksi), σ=0.21										
5B[a]	2.5	1.0	14.	0.57	22.	0.88	70.	428.	76.	348.

a - Normal to Bedding Plane

Table B-8

Slot Cutting Tests on Georgia Granite

CAVIJET Nozzle Size and Type: 6.2 mm (0.244 in.) Carbide, Plain, Submerged
Standoff: 2.1 cm (0.812 in.)
Rock Type: Georgia Granite - Parallel to Bedding Plane
Mud Weight: 1.1 gm/cm^3 (9.3 lbs/gal.) nominal
Each Run: Approximately 10 revolutions

Run No.	Translation Velocity, v		Mean Depth h'		Mean Width w		Volume Removal Rate, $\dot{V}$		Volume Removal Effectiveness, $e_{\dot{V}}$	
	cm/sec	in/sec	mm	in.	mm	in.	10^{-1} $\frac{cm^3}{sec}$	10^{-3} $\frac{in.^3}{sec}$	10^{+1} $\frac{cm^3}{kw\text{-}hr}$	10^{-1} $\frac{in.^3}{hp\text{-}hr}$
Nozzle Pressure: 12.4 MPa (1.80 ksi), Ambient Pressure: 2.07 MPa (0.30 ksi), σ=0.17										
12B	0.64	0.25	0.28	0.011	13.	0.50	0.16	1.0	0.16	0.71
13A	0.64	0.25	0.30	0.012	13.	0.50	0.18	1.1	0.17	0.79

Table B-9

Properties of Mud* Used in Stationary-Nozzle and Slot-Cutting Tests at HYDRONAUTICS

Density			Apparent Viscosity			Plastic Viscosity			Yield Point			Mean Gel		Temperature
gm/cm^3 (lb/gal)			Centipoise			Centipoise			kPa (lb/100 ft^2)			kPa (lb/100 ft^2)		°C
Typical	Min	Max	Typical	Min	Max	Typical	Min	Max	Typical	Min	Max	Initial	10 Minute	(°F)
1.1 (9.3)	1.10 9.19	1.12 9.34	12	9	19	10	7	15	29 (6)	14 (3)	48 (10)	5 (1)	43 (9)	28-46 (83-115)
1.3 (10.5)	1.3 (10.5)	1.3 (10.5)	18	18	18	14	14	14	38 (8)	38 (8)	38 (8)	12 (2.5)	81 (17)	31 (88)
1.4 (11.9)	1.4 (11.9)	1.4 (11.9)	24.5	24	25	16	16	16	81 (17)	81 (17)	81 (17)	53 (11)	192 (40)	32 (90)

*Water-based mud, with barite (NL/Baroid: Marine BAROID®) weighting additive, and bentonite (NL/Baroid: Marine AQUAGEL®) as the viscosity additive.

APPENDIX C

RESULTS FROM DRILL BIT TESTS AT DRL

TABLE C-1

DRILL BIT TEST RESULTS FOR COLTON SANDSTONE:
SMITH TOOL COMPANY NOZZLES

Rock type: Colton sandstone
Nozzle: Smith Tool Company, 6.4 mm (0.25 in.) diameter
Series: 3rd, Test: #3
Bit: 20 cm (7-7/8 in.) dia., two cone, Smith Tool Company, Type A-1
Bit weight: 44.5 kN (10000 lb) (Nominal)
Standoff distance: 1.6 cm (0.62 in.)

RUN NO.	SWIVEL PRESSURE		AMBIENT PRESSURE		NOZZLE PRESSURE		TOTAL FLOW RATE		RATE OF PENETRATION		MUD TEMP	BIT WEIGHT		NOZZLE FLOW RATE		POWER		DRILLING RATE EFFECTIVENESS	
	MPa	psi	MPa	psi	MPa	psi	m^3/min	gpm	m/hr	ft/hr	°C	kN	lb	m^3/min	gpm	kw	hp	mm/kw-hr	10^{-2} ft/hp-hr
1	16.3	2370	3.2	470	13.1	1900	0.95	250	2.3	7.4	28	45.3	10,200	0.54	143	118	159	19.2	4.7
2	16.4	2380	3.2	470	13.2	1900	0.95	250	2.5	8.2	29	45.3	10,200	0.54	143	119	159	20.8	5.1
3	17.6	2550	4.4	640	13.2	1910	0.98	260	1.8	5.8	29	45.7	10,300	0.55	145	120	162	14.7	3.6
4	19.0	2750	6.6	960	12.4	1790	0.98	260	1.8	5.8	31	43.5	9,800	0.53	139	108	146	16.3	4.0
5	25.9	3750	13.6	1980	12.3	1780	1.06	280	1.5	5.0	32	45.7	10,300	0.52	138	107	144	14.3	3.5
6	32.9	4770	20.3	2940	12.6	1830	1.12	300	2.3	7.6	35	45.3	10,200	0.53	140	111	149	20.8	5.1
7	20.3	2940	3.5	500	16.9	2440	1.16	280	2.9	9.4	38	49.7	11,200	0.60	160	170	227	16.7	4.1
8	22.0	3200	6.3	910	15.8	2280	1.19	290	2.3	7.6	39	45.7	10,300	0.59	156	155	208	14.7	3.6
9	23.9	3460	6.8	980	17.1	2480	1.14	300	2.0	6.4	40	45.3	10,200	0.61	161	174	233	11.4	2.8
10	30.4	4400	13.8	2000	16.6	2400	1.28	310	1.4	4.7	41	44.5	10,000	0.58	154	161	216	9.0	2.2
11	37.9	5490	20.5	2980	17.4	2510	1.36	330	1.5	4.8	45	46.2	10,400	0.60	158	172	231	8.6	2.1
12	11.9	1720	3.4	500	8.4	1220	0.80	220	2.3	7.4	48	45.3	10,200	0.46	122	65	87	34.7	8.5
13	13.0	1890	4.4	630	8.7	1260	0.84	220	2.0	6.4	48	44.0	9,900	0.44	117	64	85	30.6	7.5
15	22.4	3240	13.6	1970	8.8	1270	0.94	250	1.6	5.2	49	46.2	10,400	0.47	124	68	92	23.3	5.7
16	28.8	4180	20.4	2960	8.4	1210	0.99	260	1.3	4.2	50	46.6	10,500	0.47	124	65	87	19.6	4.8

TABLE C-2

DRILL BIT TEST RESULTS FOR COLTON SANDSTONE:
PLAIN CAVIJET NOZZLE

Rock Type: Colton sandstone
Nozzle: Plain CAVIJET, 6.4 mm (0.25 in.) diameter
Series: 3rd, Test: #4
Bit: 20 cm (7-7/8 in.) two cone, Smith Tool Co., Type A-1
Bit Weight: 44.5 kN (10000 lb) (Nominal)
Standoff distance: 1.6 cm (0.62 in.)

RUN NO.	SWIVEL PRESSURE		AMBIENT PRESSURE		NOZZLE PRESSURE		TOTAL FLOW RATE		RATE OF PENETRATION		MUD TEMP	BIT WEIGHT		NOZZLE FLOW RATE		POWER		DRILLING RATE EFFECTIVENESS	
	MPa	psi	MPa	psi	MPa	psi	m^3/min	gpm	m/hr	ft/hr	°C	kN	lb	m^3/min	gpm	kw	hp	mm/kw-hr	10^{-2} ft/hp-hr
1	16.2	2350	3.5	510	12.7	1840	0.91	240	1.4	4.6	46	46.2	10,400	0.38	102	86	109	17.2	4.2
2	16.3	2360	3.6	510	12.7	1850	0.91	240	1.4	4.7	47	44.8	10,100	0.38	102	82	110	17.6	4.3
3	17.3	2510	4.6	670	12.7	1840	0.93	250	1.5	4.8	47	44.7	10,050	0.40	106	85	114	17.2	4.2
4	19.1	2770	7.1	1030	12.0	1740	0.96	250	1.3	4.2	48	45.3	10,200	0.38	99	75	101	17.2	4.2
5	26.4	3820	13.9	2020	12.4	1800	1.10	290	1.3	4.2	50	45.7	10,300	0.39	104	81	109	15.5	3.8
6	33.3	4830	21.0	3050	12.3	1780	1.15	300	1.5	4.8	54	46.6	10,500	0.39	102	79	106	18.4	4.5
7	19.6	2850	3.8	540	15.9	2300	1.01	270	1.9	6.3	56	44.5	10,000	0.42	112	112	151	17.2	4.2
8	22.8	3310	6.2	900	16.6	2410	1.07	280	1.7	5.7	57	44.5	10,000	0.43	113	118	158	14.7	3.6
9	23.6	3420	7.0	1010	16.6	2400	1.09	290	2.2	7.2	58	43.5	9,800	0.42	112	117	157	18.8	4.6
10	30.4	4400	14.0	2020	16.4	2380	1.22	320	2.0	6.4	60	47.1	10,500	0.43	114	118	158	16.3	4.0
11	37.7	5470	21.1	3060	16.7	2420	1.29	340	1.9	6.2	62	45.7	10,300	0.43	115	121	162	15.5	3.8
12	11.2	1620	3.4	500	7.8	1130	0.77	200	1.8	5.8	64	48.8	11,000	0.32	86	42	56	42.1	10.3
13	13.0	1890	4.1	600	8.9	1300	0.80	210	1.8	5.9	61	44.5	10,000	0.33	88	50	67	35.9	8.8
14	15.5	2250	6.8	990	8.7	1260	0.87	230	2.0	6.4	61	44.5	10,000	0.34	90	49	66	39.6	9.7
15	22.5	3260	13.8	2000	8.7	1270	0.93	240	1.6	5.2	62	44.5	10,000	0.33	87	48	64	33.1	8.1
16	30.4	4410	20.7	3000	9.7	1410	1.02	270	1.5	4.8	63	43.5	9,800	0.34	91	56	75	26.1	6.4

TABLE C-3

DRILL BIT TEST RESULTS FOR COLTON SANDSTONE:
PLAIN CAVIJET NOZZLES

Rock type: Colton sandstone
Nozzle: Plain CAVIJET, 6.4 mm (0.25 in.) diameter
Series: 3rd, Test: #5
Bit: 20 cm (7-7/8 in.) two cone, Smith Tool Co., Type A-1
Bit weight: 44.5 kN (10000 lb) (Nominal)
Standoff distance: 1.6 cm (0.62 in.)

RUN NO.	SWIVEL PRESSURE		AMBIENT PRESSURE		NOZZLE PRESSURE		TOTAL FLOW RATE		RATE OF PENETRATION		MUD TEMP	BIT WEIGHT		NOZZLE FLOW RATE		POWER		DRILLING RATE EFFECTIVENESS	
	MPa	psi	MPa	psi	MPa	psi	m^3/min	gpm	m/hr	ft/hr	°C	kN	lb	m^3/min	gpm	kw	hp	mm/ kw-hr	10^{-2} ft/ hp-hr
1	15.9	2310	3.4	500	12.5	1810	0.92	240	1.9	6.2	58	45.7	10,300	0.38	101	80	107	23.7	5.8
2	22.8	3320	3.5	500	12.5	1820	0.94	250	2.3	7.4	58	46.2	10,400	0.38	101	80	108	24.5	6.9
3	15.9	2310	4.4	640	11.5	1670	0.92	240	2.1	7.0	59	45.7	10,300	0.37	98	71	95	29.8	7.3
4	18.6	2700	6.8	990	11.8	1710	0.99	260	2.0	6.4	59	47.1	10,600	0.38	99	74	99	26.6	6.5
5	25.3	3670	13.6	1960	11.8	1700	1.09	290	1.7	5.5	60	46.2	10,400	0.38	100	74	100	22.5	5.5
6	32.5	4720	20.8	3010	11.8	1700	1.14	300	2.2	7.1	62	45.7	10,300	0.37	98	73	98	29.8	7.3
7	19.2	2790	3.4	490	15.8	2300	1.02	270	2.7	8.9	65	47.5	10,700	0.42	112	112	150	24.1	5.9
8	23.7	3440	5.9	860	17.8	2580	1.14	300	2.5	8.2	65	46.2	10,400	0.86	115	130	174	19.2	4.7
9	22.7	3290	6.9	1000	15.8	2290	1.09	290	2.0	6.5	66	45.7	10,300	0.45	118	118	158	16.8	4.1
10	29.7	4310	13.9	2010	15.9	2300	1.22	320	1.6	5.3	68	45.3	10,200	0.42	112	112	150	14.3	3.5
11	36.2	5250	20.7	3000	15.5	2250	1.26	330	1.5	4.9	70	46.2	10,400	0.41	109	107	143	13.9	3.4
12	18.0	2610	3.4	500	14.6	2110	0.99	260	2.8	9.2	71	46.6	10,500	0.41	108	99	133	28.2	6.9
13	12.6	1820	4.6	670	7.8	1140	0.81	220	1.6	5.4	72	47.5	10,700	0.33	86	43	57	38.4	9.4
15	21.7	3140	18.6	2020	7.7	1120	0.94	250	1.3	4.2	72	47.1	10,600	0.32	86	42	56	30.6	7.5
16	28.1	4070	20.5	2980	7.6	1090	0.99	260	1.2	3.9	73	47.1	10,600	0.32	85	41	54	29.4	7.2

TABLE C-4

DRILL BIT TEST RESULTS FOR INDIANA LIMESTONE:
SMITH TOOL COMPANY NOZZLES

Rock type: Indiana Limestone
Nozzle: Smith Tool Company, 6.4 mm (0.25 in.) diameter
Series: 4th, Test: #1
Bit: 20 cm (7-7/8 in.) two cone, Smith Tool Co., Type A-1
Bit weight: 22.2 kN (5,000 lb) (nominal)
Standoff distance: 1.6 cm (0.62 in.)

RUN NO.	SWIVEL PRESSURE		AMBIENT PRESSURE		NOZZLE PRESSURE		TOTAL FLOW RATE		RATE OF PENETRATION		MUD TEMP	BIT WEIGHT		NOZZLE FLOW RATE		POWER		DRILLING RATE EFFECTIVENESS	
	MPa	psi	MPa	psi	MPa	psi	m^3/min	gpm	m/hr	ft/hr	°C	kN	lb	m^3/min	gpm	kw	hp	mm/kw-hr	10^{-2} ft/hp-hr
1	11.9	1730	3.5	500	8.4	1220	0.73	190	2.0	6.6	31	22.2	5000	0.50	132	70	94	28.7	7.0
2	11.9	1730	3.5	500	8.4	1220	0.73	190	2.3	7.4	32	22.2	5000	0.50	132	70	94	32.2	7.9
3	13.0	1880	4.5	650	8.5	1230	0.73	190	2.1	7.0	33	22.2	5000	0.50	132	71	95	30.1	7.4
4	15.3	2210	6.9	990	8.4	1220	0.76	200	1.5	5.0	35	22.2	5000	0.50	132	70	93	21.8	5.4
5	22.1	3200	13.6	1970	8.5	1230	0.79	210	0.5	1.5	37	22.2	5000	0.50	132	71	95	6.4	1.6
6	28.8	4170	20.6	2980	8.2	1190	0.76	200	0.2	0.8	41	22.2	5000	0.47	123	64	85	3.8	0.9
7	15.8	2290	3.2	460	12.6	1830	0.88	230	5.0	16.4	43	22.2	5000	0.60	158	126	168	39.8	9.7
8	17.2	2480	4.6	660	12.6	1820	0.88	230	4.0	13.2	44	22.2	5000	0.60	159	127	170	31.7	7.8
9	19.5	2820	7.1	1020	12.4	1800	0.89	240	3.2	10.6	46	22.2	5000	0.59	157	123	165	26.3	6.4
10	26.8	3890	14.1	2040	12.8	1850	0.95	250	2.8	9.1	49	22.2	5000	0.60	158	127	171	21.8	5.3
11	33.5	4860	20.9	3020	12.6	1830	0.98	260	4.6	15.0	56	22.2	5000	0.60	158	126	169	36.2	8.9
12	19.8	2870	3.4	500	16.3	2370	0.98	260	7.5	24.6	56	22.2	5000	0.68	180	185	248	40.5	9.9
13	22.5	3270	5.8	840	16.7	2420	1.05	280	6.6	21.8	59	22.2	5000	0.70	185	162	217	34.0	8.3
14	25.6	3710	6.8	980	16.7	2420	1.05	280	7.5	24.7	60	22.2	5000	0.70	185	196	262	38.5	9.4
15	30.2	4380	13.8	2000	16.4	2370	1.09	290	7.2	23.7	64	22.2	5000	0.69	181	187	250	38.6	9.5

TABLE C-5

DRILL BIT TEST RESULTS FOR INDIANA LIMESTONE:
SMITH TOOL COMPANY NOZZLES

Rock type: Indiana Limestone
Nozzle: Smith Tool Company, 6.4 mm (0.25 in.) diameter
Series: 4th, Test: #2
Bit: 20 cm (7-7/8 in.) two cone, Smith Tool Co., Type A-1
Bit weight: 22.2 kN (5000 lbs)(nominal)
Standoff distance: 3.8 cm (1.5 in.)

RUN NO.	SWIVEL PRESSURE		AMBIENT PRESSURE		NOZZLE PRESSURE		TOTAL FLOW RATE		RATE OF PENETRATION		MUD TEMP	BIT WEIGHT		NOZZLE FLOW RATE		POWER		DRILLING RATE EFFECTIVENESS	
	MPa	psi	MPa	psi	MPa	psi	m^3/min	gpm	m/hr	ft/hr	°C	kN	lb	m^3/min	gpm	kw	hp	mm/ kw-hr	10^{-2} ft/ hp-hr
1	12.5	1820	3.7	530	8.8	1280	0.69	183	1.4	4.5	33	22.2	5000	0.47	124	69	93	19.8	4.8
2	11.8	1710	3.6	520	8.2	1200	0.67	178	1.5	4.9	35	22.2	5000	0.46	121	63	84	28.6	7.0
3	13.0	1890	4.5	660	8.5	1230	0.70	185	1.6	5.3	35	22.2	5000	0.47	124	66	89	24.4	5.9
4	15.1	2190	7.0	1020	8.1	1170	0.70	185	1.0	3.4	36	22.2	5000	0.46	120	61	82	17.0	4.2
5	22.0	3190	13.8	2000	8.2	1180	0.76	201	0.4	1.2	38	22.2	5000	0.47	124	64	85	5.7	1.4
6	28.9	4190	20.8	3010	8.2	1180	0.76	202	0.4	1.3	42	22.2	5000	0.45	120	62	82	6.4	1.6
7	16.0	2320	3.4	490	12.6	1830	0.83	220	3.3	10.9	40	22.2	5000	0.57	150	119	160	27.9	6.8
8	17.0	2460	4.6	670	12.4	1800	0.84	221	3.3	10.7	41	22.2	5000	0.56	148	115	155	28.3	6.9
9	19.3	2790	7.0	1020	12.2	1780	0.86	226	2.5	8.3	43	22.2	5000	0.56	147	113	152	22.3	5.5
10	26.2	3800	14.0	2030	12.2	1760	0.90	238	1.4	4.5	46	22.2	5000	0.55	146	112	151	12.2	3.0
11	33.1	4800	20.7	3000	12.4	1800	0.95	251	0.9	3.1	50	22.2	5000	0.56	148	117	156	8.1	2.0
12	19.8	2880	3.6	520	16.2	2350	0.94	248	6.2	20.2	51	22.2	5000	0.64	168	172	231	35.7	8.7
13	22.3	3230	6.1	880	16.2	2350	0.98	259	6.1	19.9	52	15.5	3500	0.64	170	174	233	34.9	8.6
14	23.5	3400	6.9	1000	16.6	2400	1.00	264	7.6	24.9	54	15.5	3500	0.67	177	179	240	42.4	10.4
15	30.3	4390	14.1	2040	16.2	2360	1.04	275	5.7	18.7	57	15.5	3500	0.64	169	173	232	32.9	8.0
16	37.4	5420	20.7	3000	16.7	2420	1.10	290	7.1	23.3	62	22.2	5000	0.65	172	181	242	39.3	9.6

TABLE C-6
DRILL BIT TEST RESULTS FOR INDIANA LIMESTONE:
PLAIN CAVIJET NOZZLES

Rock type: Indiana Limestone
Nozzle: Plain CAVIJET, 6.4 mm (0.25 in.) diameter
Series: 4th, Test: #3
Bit: 20 cm. (7-7/8 in.) two cone, Smith Tool Co., Type A-1
Bit weight: 22.2 kN (5000 lbs)(nominal)
Standoff distance: 1.6 cm (0.62 in.)

RUN NO.	SWIVEL PRESSURE		AMBIENT PRESSURE		NOZZLE PRESSURE		TOTAL FLOW RATE		RATE OF PENETRATION		MUD TEMP	BIT WEIGHT		NOZZLE FLOW RATE		POWER		DRILLING RATE EFFECTIVENESS	
	MPa	psi	MPa	psi	MPa	psi	m^3/min	gpm	m/hr	ft/hr	°C	kN	lb	m^3/min	gpm	kw	hp	mm/kw-hr	10^{-2} ft/hp-hr
1	12.2	1770	3.6	520	8.6	1240	0.54	144	1.8	5.9	34	20.0	4500	0.32	86	46	62	38.8	9.5
2	12.1	1760	3.6	520	8.5	1240	0.54	144	1.9	6.2	36	20.0	4500	0.32	86	46	62	41.0	10.0
3	12.7	1840	4.4	640	8.3	1200	0.54	144	1.6	5.4	37	20.0	4500	0.32	84	44	59	37.3	9.1
4	15.1	2190	6.9	1010	8.2	1180	0.57	150	0.6	1.8	38	22.2	5000	0.32	84	43	58	12.7	3.1
5	22.2	3220	13.7	1980	8.6	1240	0.63	167	0.2	0.8	41	22.2	5000	0.33	88	47	64	5.2	1.3
6	29.3	4240	20.6	2980	8.7	1260	0.64	170	0.2	0.6	44	22.2	5000	0.32	85	47	63	3.9	1.0
7	15.7	2280	3.4	490	12.4	1790	0.64	169	5.0	16.5	43	20.0	4500	0.38	101	79	106	63.7	15.6
8	17.1	2480	4.4	640	12.7	1840	0.66	174	2.5	8.3	44	22.2	5000	0.38	102	82	109	31.0	7.6
9	19.7	2860	7.0	1020	12.7	1840	0.69	182	2.3	7.4	46	22.2	5000	0.38	102	82	109	27.7	6.8
10	25.9	3750	13.5	1960	12.4	1790	0.73	193	1.1	3.7	48	20.0	4500	0.38	101	79	106	14.3	3.5
11	33.4	4850	20.9	3030	12.6	1820	0.78	207	1.0	3.4	52	22.2	5000	0.39	103	82	109	12.7	3.1
12	20.0	2900	3.4	500	16.6	2400	0.75	199	6.2	20.3	51	22.2	5000	0.45	119	87	117	49.8	12.2
13	22.6	3280	6.1	880	16.6	2400	0.78	205	5.6	18.4	52	22.2	5000	0.44	116	121	163	46.2	11.3
14	23.5	3410	7.1	1020	16.5	2380	0.79	208	5.8	19.2	53	20.0	4500	0.44	116	121	162	48.5	11.9
15	30.4	4400	13.8	2010	16.5	2400	0.83	220	5.2	17.1	56	20.0	4500	0.44	115	120	161	43.3	10.6
16	37.2	5390	20.7	3000	16.6	2400	0.88	232	4.2	13.7	59	22.2	5000	0.44	116	121	162	34.6	8.5
17	33.4	4840	20.7	3000	12.7	1840	0.80	212	4.4	14.3	60	22.2	5000	0.40	106	85	113	51.5	12.6
18	33.1	4800	20.5	2970	12.6	1830	0.81	214	4.0	13.2	65	22.2	5000	0.40	107	85	114	47.3	11.6
19	36.3	5260	24.3	3520	12.0	1740	0.82	216	3.6	11.8	64	22.2	5000	0.40	105	80	107	45.3	11.1

TABLE C-7

DRILL BIT TEST RESULTS FOR INDIANA LIMESTONE:
CENTERBODY CAVIJET NOZZLES

Rock type: Indiana Limestone
Nozzle: 3.2 mm (0.12 in.) Centerbody CAVIJET, 6.4 mm (0.25 in.) diameter
Series 4th, Test: #4
Bit: 20 cm (7-7/8 in.) two cone, Smith Tool Co., Type A-1
Bit weight: 22.2 kN (5000 lbs)(nominal)
Standoff distance: 1.6 cm (0.62 in.)

RUN NO.	SWIVEL PRESSURE		AMBIENT PRESSURE		NOZZLE PRESSURE		TOTAL FLOW RATE		RATE OF PENETRATION		MUD TEMP	BIT WEIGHT		NOZZLE FLOW RATE		POWER		DRILLING RATE EFFECTIVENESS	
	MPa	psi	MPa	psi	MPa	psi	m^3/min	gpm	m/hr	ft/hr	°C	kN	lb	m^3/min	gpm	kw	hp	mm/kw-hr	10^{-2} ft/hp-hr
1	11.8	1710	3.5	510	8.3	1200	0.46	122	1.7	5.5	36	22.2	5000	0.25	65	34	46	49.3	12.1
2	11.9	1720	3.5	510	8.3	1210	0.46	122	1.5	5.0	38	22.2	5000	0.25	65	34	46	44.6	10.9
3	12.8	1860	4.1	600	8.0	1160	0.47	124	1.0	3.3	38	20.0	4500	0.24	64	32	43	31.4	7.7
4	15.2	2210	7.2	1040	8.1	1170	0.49	130	0.3	1.0	39	20.0	4500	0.24	64	32	43	9.4	2.3
5	22.6	3270	14.0	2020	8.6	1250	0.56	147	0.2	0.7	42	22.2	5000	0.25	67	37	49	5.84	1.4
6	29.0	4210	20.5	2970	8.5	1240	0.59	155	0.4	1.3	45	22.2	5000	0.26	68	37	49	10.8	2.6
7	33.2	4810	24.5	3550	8.7	1260	0.57	151	0.8	2.8	48	22.2	5000	0.24	64	35	47	24.3	5.9
8	37.5	5440	28.1	4070	9.4	1360	0.59	157	1.4	4.5	50	22.2	5000	0.25	65	39	52	35.5	8.7
9	16.0	2330	3.6	510	12.5	1810	0.56	148	5.9	19.4	47	22.2	5000	0.30	79	62	83	95.0	23.3
10	16.9	2450	4.6	670	12.3	1780	0.56	149	4.8	15.8	48	22.2	5000	0.29	77	59	79	81.3	19.9
11	19.6	2840	7.4	1070	12.2	1770	0.59	155	3.2	10.6	49	22.2	5000	0.29	76	58	78	55.2	13.5
12	19.6	2840	14.2	2050	12.3	1790	0.64	170	2.4	7.9	51	20.0	4500	0.29	78	60	81	39.8	9.7
13	33.0	4780	21.2	3070	11.8	1710	0.68	179	4.0	13.1	54	20.0	4500	0.30	78	58	78	68.7	16.8
14	37.1	5380	24.9	3620	12.2	1760	0.71	187	4.4	14.5	57	20.0	4500	0.30	79	61	82	72.7	17.8
15	20.4	2960	3.8	550	16.6	2410	0.65	172	6.0	19.7	56	24.4	5500	0.34	91	95	127	63.2	15.5
16	22.4	3240	6.2	890	16.2	2350	0.66	175	4.5	14.7	57	20.0	4500	0.33	87	89	119	50.4	12.3
17	23.5	3400	7.1	1020	16.4	2380	0.68	179	4.4	14.6	58	20.0	4500	0.33	88	91	122	48.9	12.0
18	30.4	4400	14.2	2060	16.2	2350	0.73	192	4.0	13.0	61	22.2	5000	0.33	88	90	120	44.2	10.8
19	37.3	5410	20.8	3010	16.6	2400	0.77	204	3.6	11.7	65	20.0	4500	0.34	89	93	125	38.3	9.4
20	33.6	4860	21.0	3050	12.5	1820	0.71	187	3.7	12.0	65	22.2	5000	0.31	83	66	88	53.9	13.2
21	36.9	5340	24.3	3520	12.6	1820	0.73	194	3.5	11.6	68	22.2	5000	0.31	82	64	86	56.7	13.9

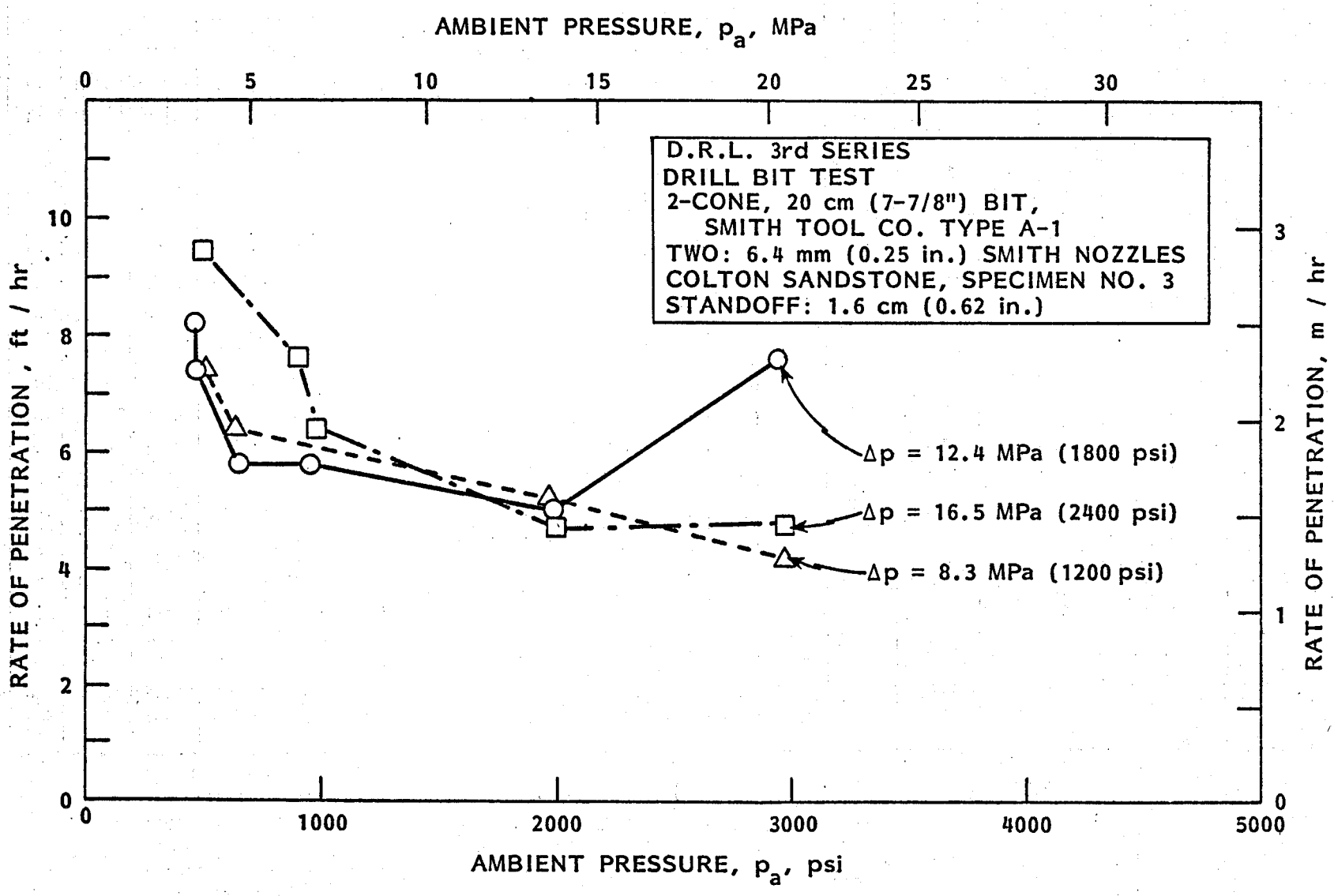

FIGURE C-1 - DRILL BIT TESTS IN COLTON SANDSTONE, SMITH NOZZLES

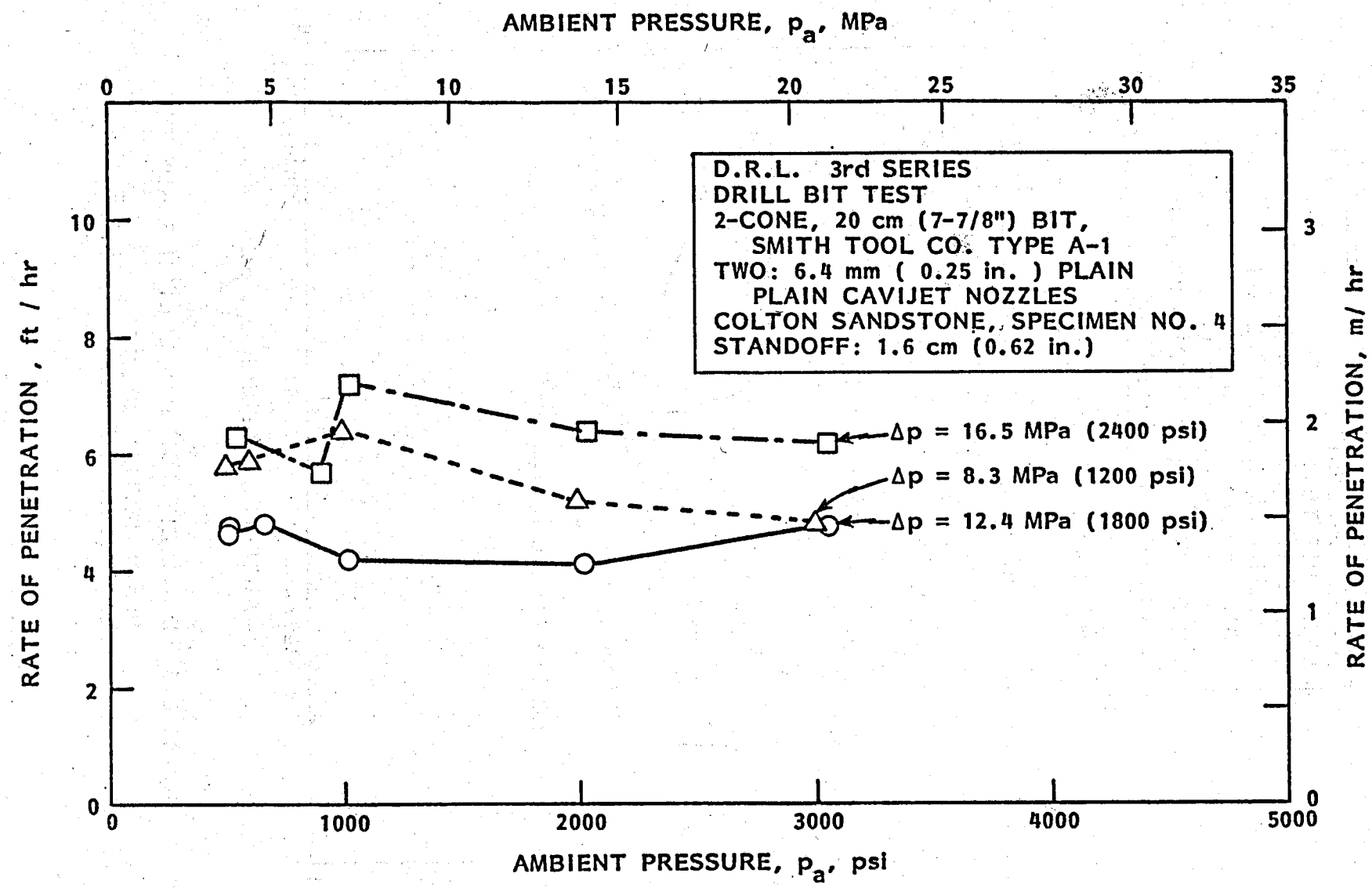

FIGURE C-2 - DRILL BIT TESTS IN COLTON SANDSTONE, PLAIN CAVIJET® NOZZLES

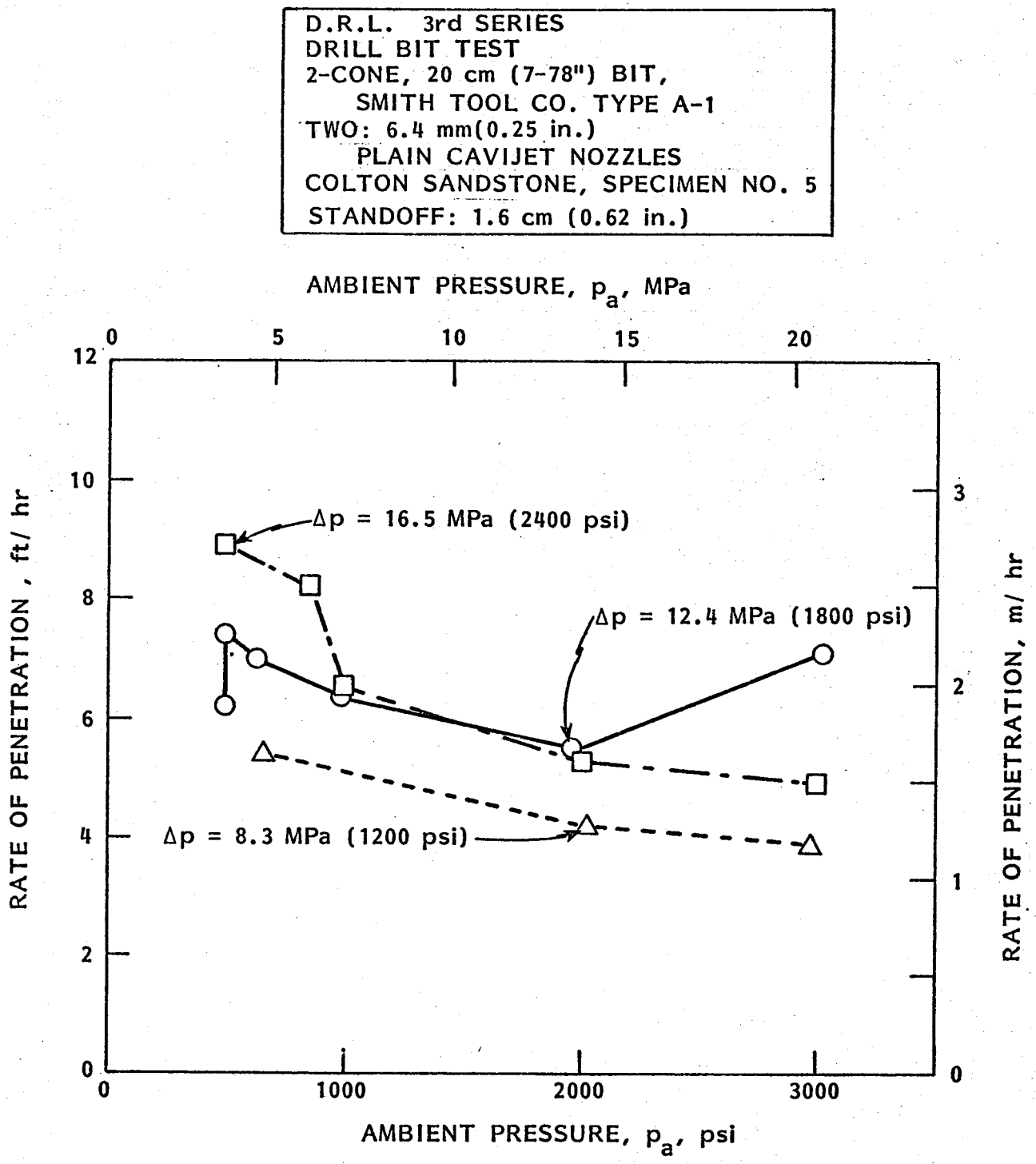

FIGURE C-3 - DRILL BIT TESTS IN COLTON SANDSTONE, PLAIN CAVIJET® NOZZLES

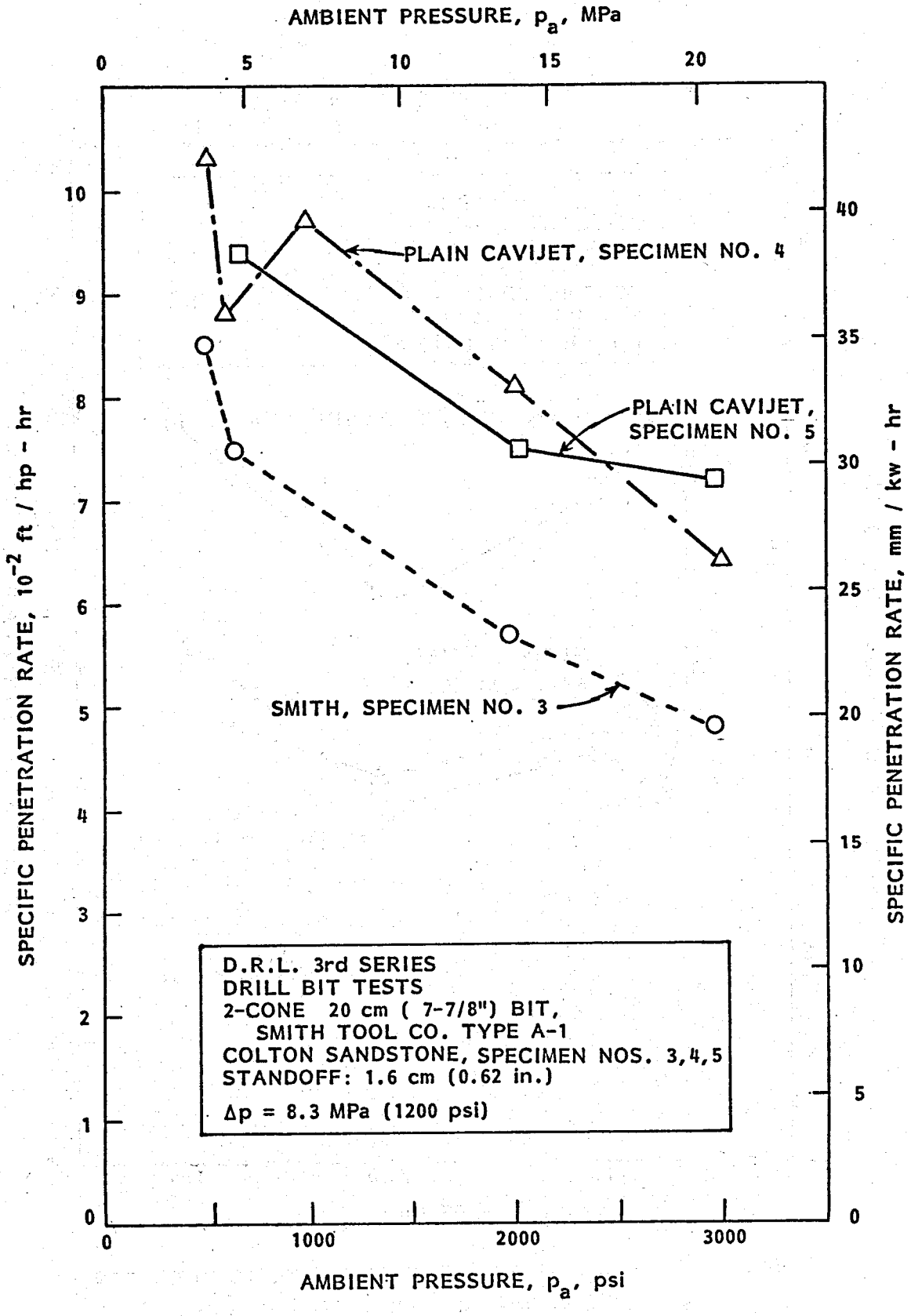

FIGURE C-4 - COMPARISON OF DRILL BIT TESTS IN COLTON SANDSTONE, Δp = 8.3 MPa (1200 psi)

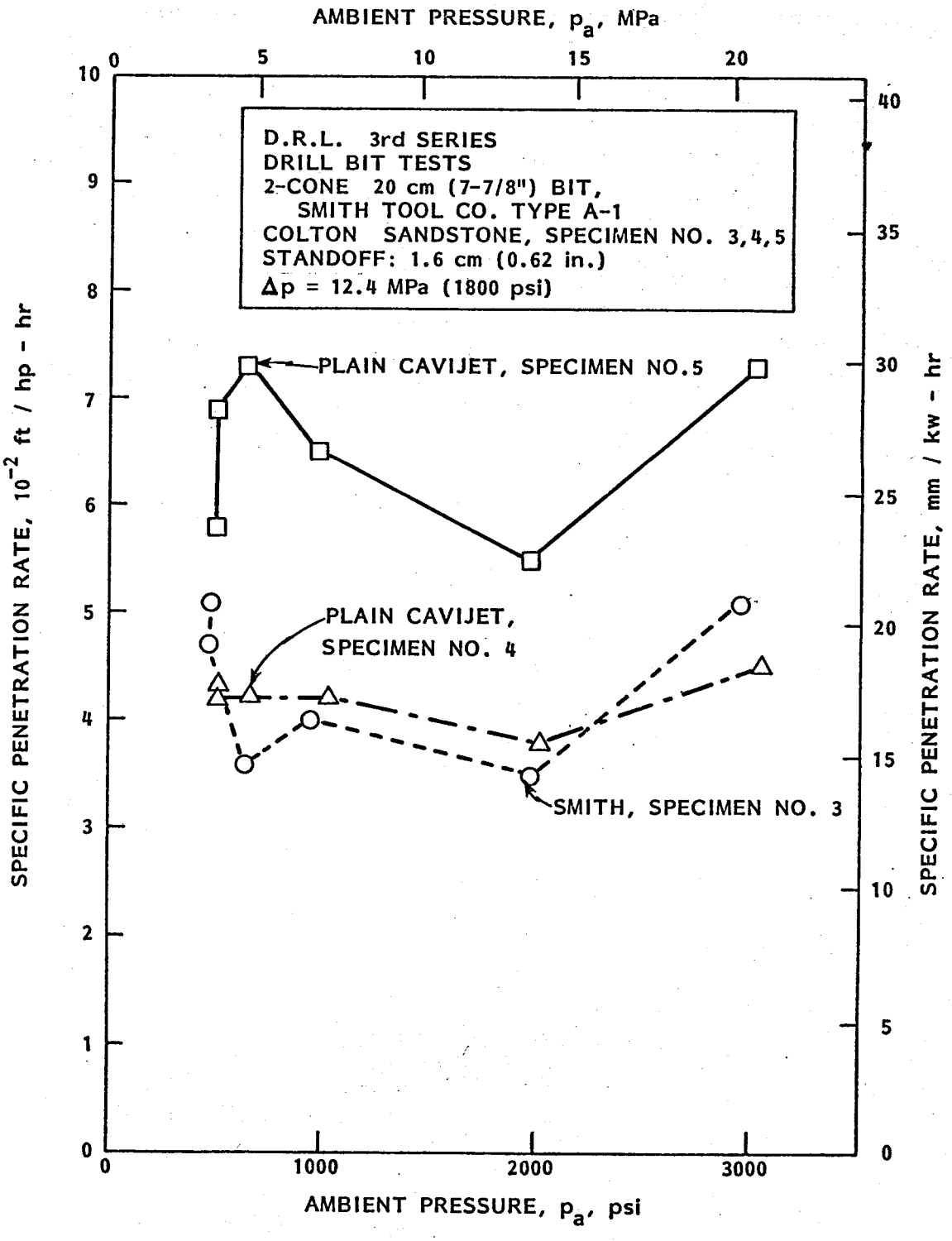

FIGURE C-5 - COMPARISON OF DRILL BIT TESTS IN COLTON SANDSTONE, Δp = 12.4 MPa (1800 psi)

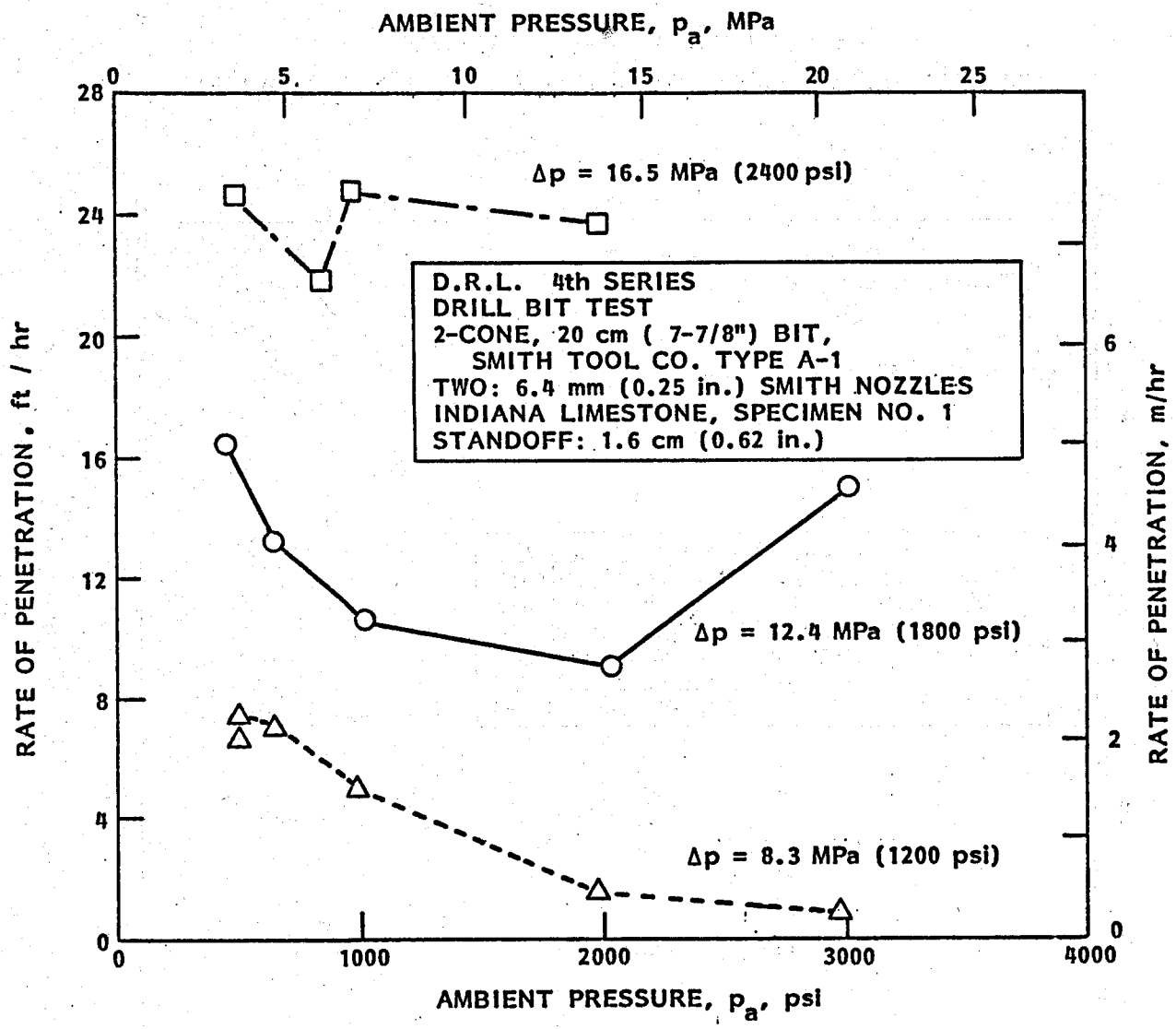

FIGURE C-6 - DRILL BIT TESTS IN INDIANA LIMESTONE, SMITH NOZZLES, STANDOFF: 1.6 cm (0.62 in)

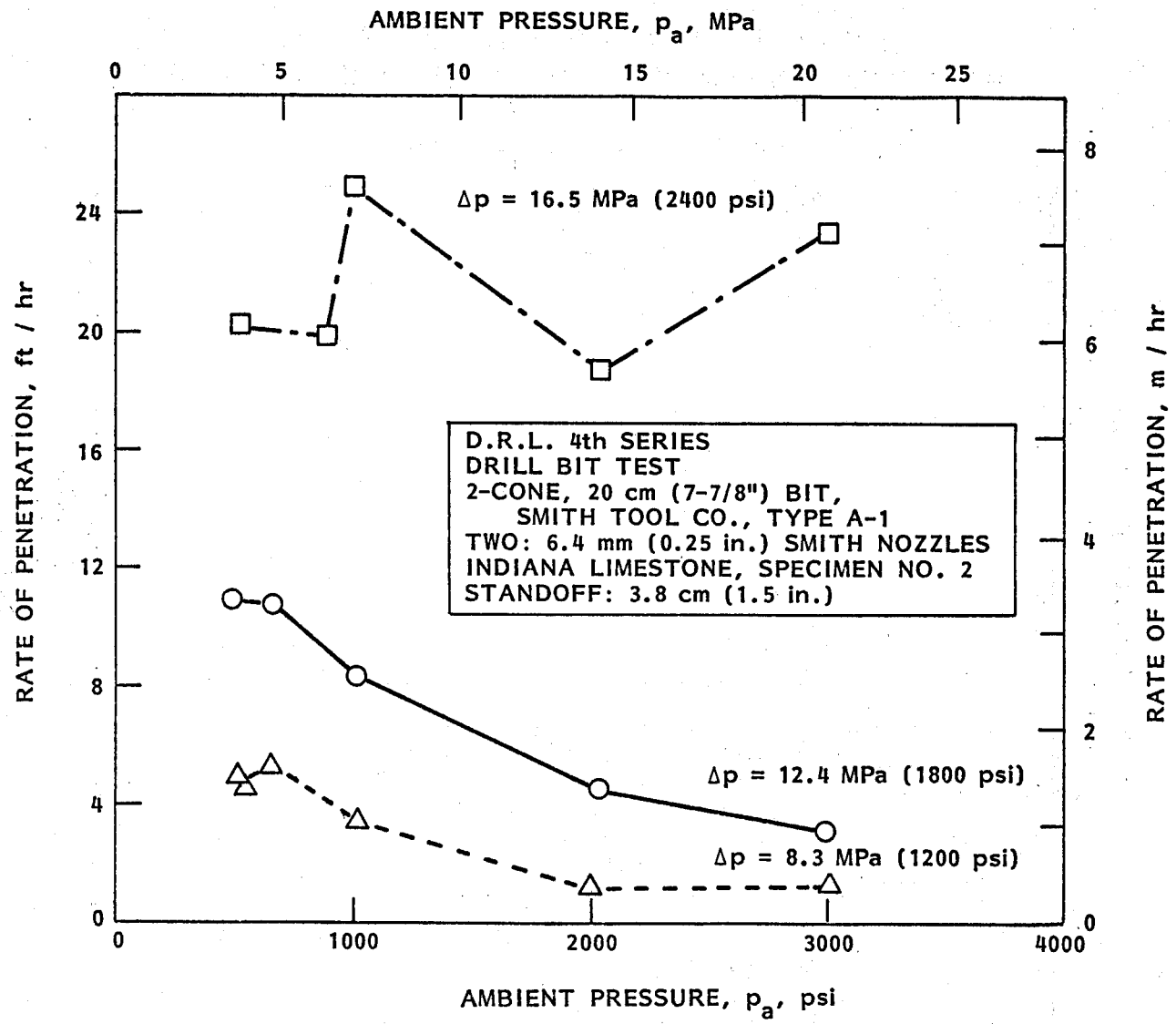

FIGURE C-7 - DRILL BIT TESTS IN INDIANA LIMESTONE, SMITH NOZZLES, STANDOFF: 3.8 cm (1.5 in)

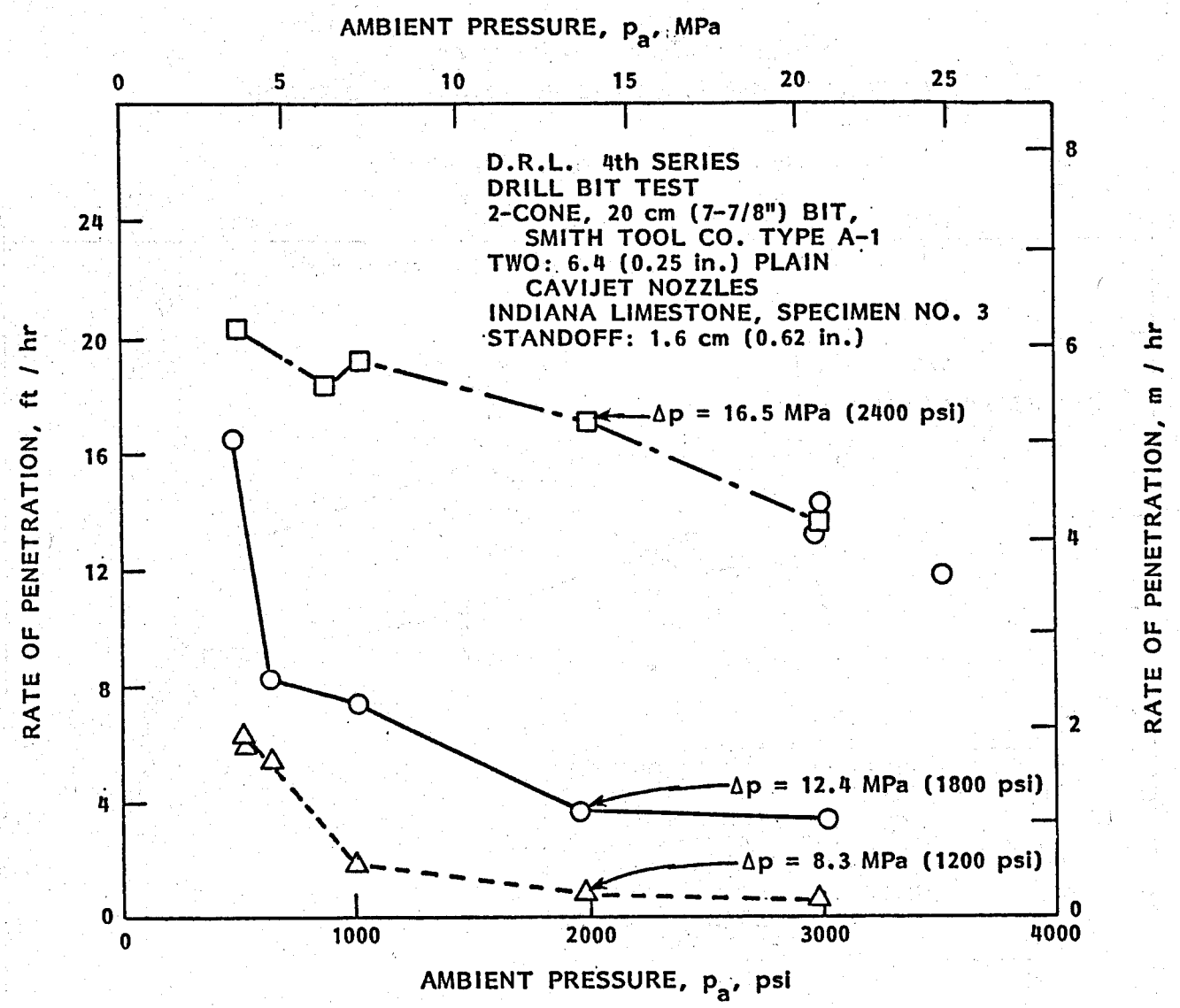

FIGURE C-8 - DRILL BIT TESTS IN INDIANA LIMESTONE, PLAIN CAVIJET® NOZZLES

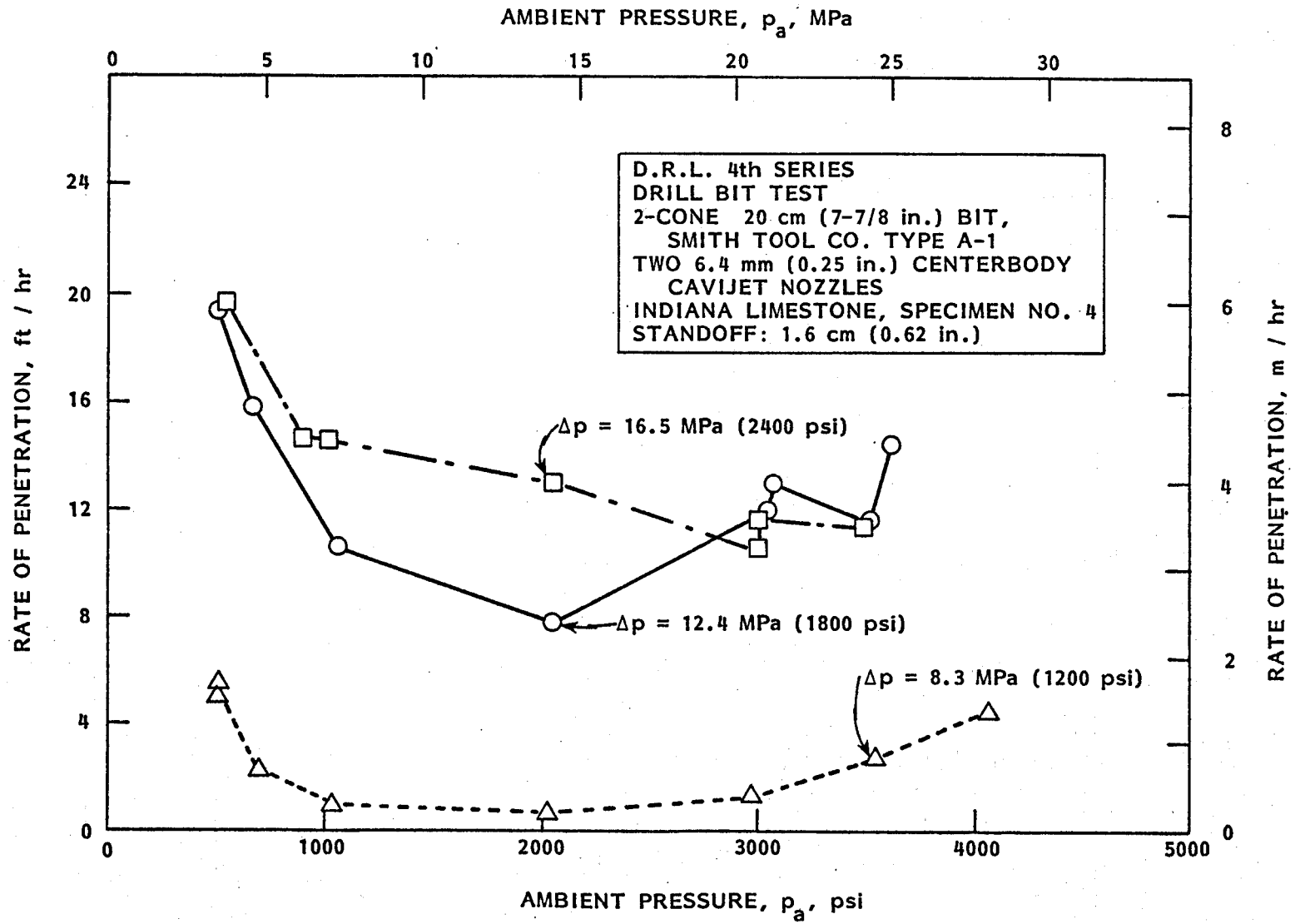

FIGURE C-9 - DRILL BIT TESTS IN INDIANA LIMESTONE, CENTERBODY CAVIJET® NOZZLES

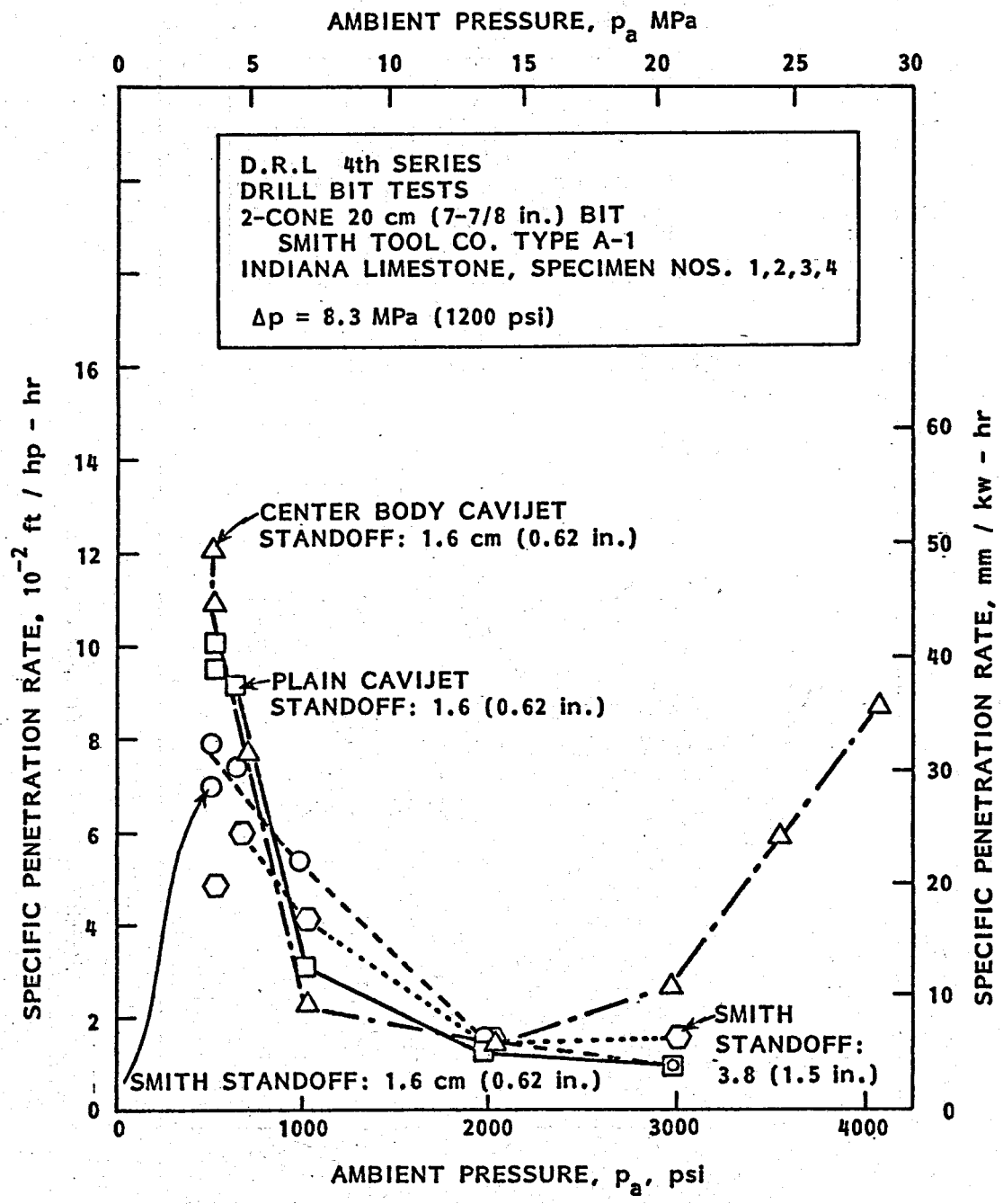

FIGURE C-10 - COMPARISON OF DRILL BIT TESTS IN INDIANA LIMESTONE, Δp = 8.3 MPa (1200 psi)

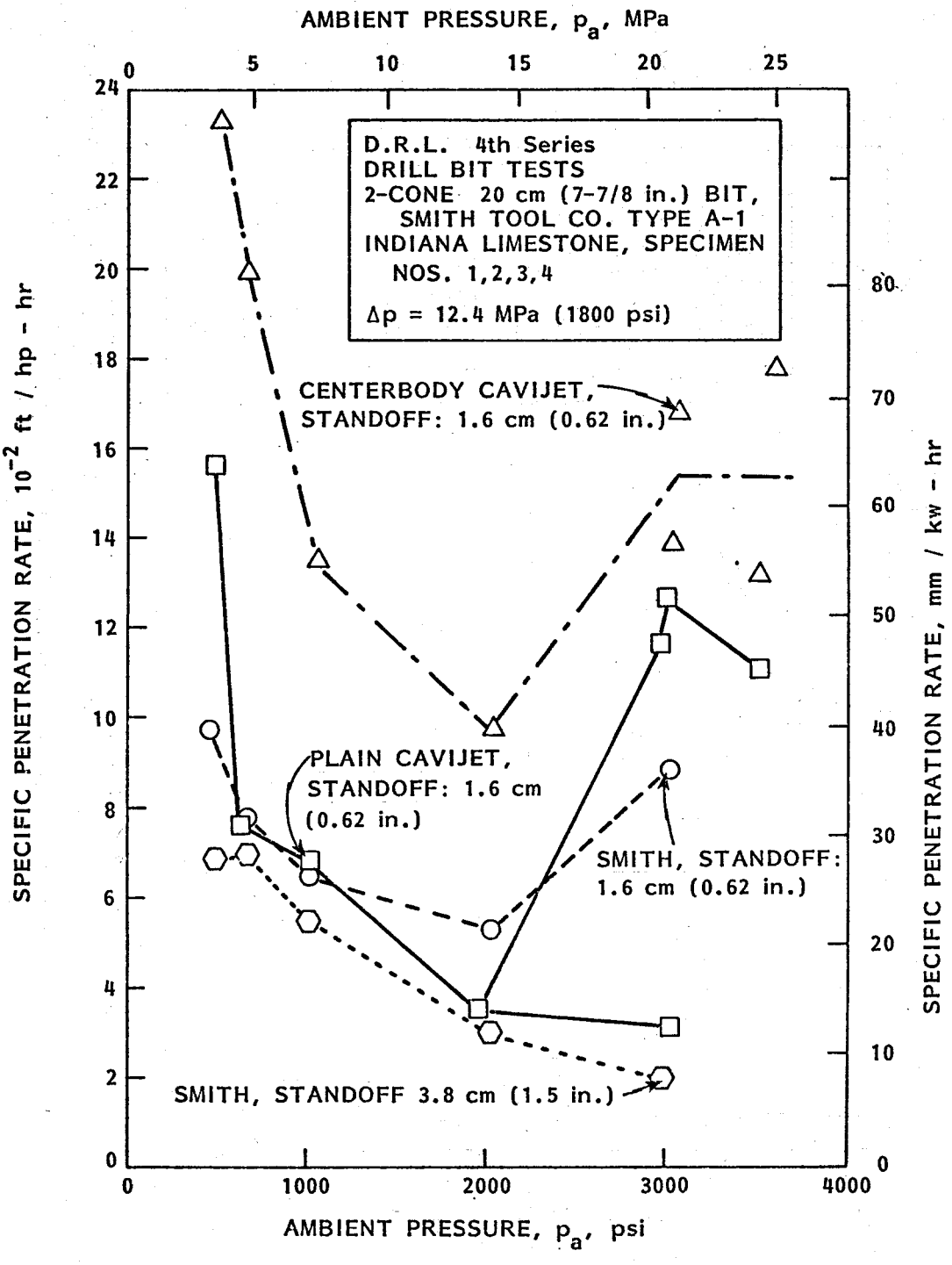

FIGURE C-11 - COMPARISON OF DRILL BIT TESTS IN INDIANA LIMESTONE, Δp = 12.4 MPa (1800 psi)

DISTRIBUTION:
TID-4500-R66-UC-66c (675)

Amoco Production Company
Research Center
P.O. Box 591
Tulsa, Oklahoma 74102
Attn: B. Wilder

Department of Energy (10)
Division of Geothermal Energy
Mail Station 3344
12th & Penn, NW
Federal Building
Washington, D.C. 20461
Attn: C. McFarland
C. Carwile (2)
M. Skalka
A. Jelacic
R. Toms
R. R. Reeber
J. Salisbury
R. Black
M. Scheve

Department of Energy (5)
Office of Oil, Gas, and Shale Technology
Mail Station D107
Washington, D.C. 20545
Attn: J. Smith
M. Adams
B. Dibona
D. Duke
A. Sikri

Dresser Industries, Inc.
P.O. Box 24647
Dallas, Texas 75224
Attn: J. W. Langford

Dyna-Drill
P.O. Box C-19576
Irvine, California 92713
Attn: Larry Diamond

DISTRIBUTION (Continued)

Halliburton
Drawer 1413
Duncan, Oklahoma 73533
Attn: Dwight Smith

Hydronautics, Incorporated (20)
7210 Pindell School Road
Laurel, MD 20810
Attn: A. F. Conn
V. E. Johnson, Jr.
H. L. Liu
G. S. Frederick

Loffland Brothers Company
P.O. Box 2847
Tulsa, Oklahoma 74101
Attn: H. E. Mallory

Los Alamos National Scientific Laboratory
Mail Stop 570
Los Alamos, New Mexico 87545
Attn: John C. Rowley

Mobil Research and Development Corporation
Field Research Laboratory
P.O. Box 900
Dallas, Texas 75221
Attn: W. Gravley

NL Baroid Petroleum Services
City Centre Building, Suite 365W
6400 Uptown Boulevard
Albuquerque, New Mexico 87110
Attn: Gene Polk

NL Petroleum Services
P.O. Box 1473
Houston, Texas 77001
Attn: J. Fontenot

Otis
P.O. Box 34380
Dallas, Texas 75243
Attn: W. D. Rumbaugh

DISTRIBUTION (Continued)

Phillips Petroleum Company
P.O. Box 239
Salt Lake City, Utah 84110
Attn: Earl Hoff

Smith Tool Company
P.O. Box C-19511
Irvine, California 92713
Attn: J. Vincent

Texas A&M University
College Station, Texas 77843
Attn: M. Friedman
Dept. of Geology

Union Geothermal Division
Union Oil Company of California
Union Oil Center
Los Angeles, California 90017
Attn: D. E. Pyle

Shell Oil Co.
Two Shell Plaza
P.O. Box 2099
Houston, Texas 77001
Attn: W. E. Bingman

400 C. Winter
1000 G. A. Fowler
1100 C. D. Broyles
1130 H. E. Viney
2000 E. D. Reed
2300 J. C. King
2320 K. Gillespie
2325 R. E. Fox
2328 J. H. Barnette
2500 J. C. Crawford
2513 W. B. Leslie
4000 A. Narath
4200 G. Yonas
4300 R. L. Peurifoy, Jr.
4400 A. W. Snyder
4443 P. Yarrington
4500 E. H. Beckner

DISTRIBUTION (Continued)

4700 J. H. Scott
4710 G. E. Brandvold
4720 J. H. Scott (acting)
4740 R. K. Traeger
4741 J. R. Kelsey
4741 C. C. Carson
4743 H. C. Hardee
4750 V. L. Dugan
4751 J. R. Tillerson
4751 D. A. Glowka (25)
4752 H. M. Dodd
4754 A. F. Veneruso
5000 J. K. Galt
5510 D. B. Hayes
5512 D. F. McVey
5512 A. Ortega
5530 W. Herrmann
5532 B. M. Butcher
5533 J. M. McGlaun
5600 D. B. Shuster
5620 M. M. Newsom
5800 R. S. Claassen
5810 R. G. Kepler
5812 C. J. M. Northrup, Jr.
5812 B. T. Kenna
5813 P. B. Rand
5830 M. J. Davis
5832 R. W. Rohde
5832 R. J. Salzbrenner
5833 J. L. Jellison
5836 J. L. Ledman
5840 N. J. Magnani
3141 L. J. Erickson (5)
3151 W. L. Garner (3)
8214 M. A. Pound

☆U.S. GOVERNMENT PRINTING OFFICE: 1981-0-777-023/586